



**FATİH UNIVERSITY**

The Graduate School of Sciences and Engineering

Doctor of Philosophy in  
Physics

**DENSITY FUNCTIONAL THEORY STUDIES ON  
MOLECULAR STRUCTURES & VIBRATIONAL  
SPECTRA OF TRANSITION METAL COMPLEXES  
OF ANILINE DERIVATIVES**

by

**Tayyibe BARDAKÇI**

**June 2015**



**DENSITY FUNCTIONAL THEORY STUDIES ON MOLECULAR  
STRUCTURES & VIBRATIONAL SPECTRA OF TRANSITION  
METAL COMPLEXES OF ANILINE DERIVATIVES**

by

Tayyibe BARDAKÇI

A thesis submitted to

the Graduate School of Sciences and Engineering

of

Fatih University

in partial fulfillment of the requirements for the degree of

Doctor of Philosophy

in

Physics

June 2015  
Istanbul, Turkey

## APPROVAL PAGE

This is to certify that I have read this thesis written by Tayyibe BARDAKÇI and that in my opinion it is fully adequate, in scope and quality, as a thesis for the degree of Doctor of Philosophy in Physics.

---

Prof. Mustafa KUMRU  
Thesis Supervisor

I certify that this thesis satisfies all the requirements as a thesis for the degree of Doctor of Philosophy in Physics.

---

Prof. Mustafa KUMRU  
Head of Department

Examining Committee Members

Prof. Mustafa KUMRU

---

Assoc. Prof. Ahmet ALTUN

---

Assoc. Prof. Mehmet KARABACAK

---

Prof. Ahmet ATAÇ

---

Assoc. Prof. Levent SARI

---

It is approved that this thesis has been written in compliance with the formatting rules laid down by the Graduate School of Sciences and Engineering.

---

Prof. Nurullah ARSLAN  
Director

June 2015

# DENSITY FUNCTIONAL THEORY STUDIES ON MOLECULAR STRUCTURES & VIBRATIONAL SPECTRA OF TRANSITION METAL COMPLEXES OF ANILINE DERIVATIVES

Tayyibe BARDAKÇI

Ph.D. Thesis – Physics  
June 2015

Thesis Supervisor: Prof. Mustafa KUMRU

## ABSTRACT

In recent years, Density Functional Theory (DFT) has become a promising choice for investigating the molecular properties of transition metal complexes. This thesis analyzes computational studies on transition metal complexes of aniline derivatives (p-toluidine and m-toluidine) using DFT. A literature review on transition metal complexes and related DFT studies is presented in the first chapter, whereas an introduction to the theory behind DFT is explained in the second chapter. Chapter 3 mentions the choice of B3LYP/def2-TZVP level for calculations using Gaussian 03 program. Optimized molecular structures, charge, spin distributions and also vibrational frequencies of Mn, Co, Ni, Cu, Zn, Cd, and Hg bromide complexes, and Ni, Zn, and Cd iodide complexes of p-toluidine and m-toluidine are provided in a detailed manner in chapter 4. Stable complex geometries have been obtained considering each accessible spin state. Charge distribution analysis for the title compounds have been performed by means of Mulliken, NBO and APT methods, and physically most meaningful method for our compounds is explained. The vibrational band assignments are determined based on the computational results expressed in terms of internal coordinates with percent potential energy distributions (PED). The effects of the ligands on the vibrational modes of the metal complexes upon coordination are also elucidated. And finally significant outcomes of this study are summarized in chapter 5.

**Keywords:** Density Functional Theory, def2-TZVP, Transition Metal Complex, Molecular Structure, Charge and Spin Distribution, Vibrational Frequency.

# YOĞUNLUK FONKSİYONEL TEORİ İLE ANILIN TÜREVLERİ GEÇİŞ METAL KOMPLEKSLERİNİN MOLEKÜLER YAPISI VE TİTREŞİM SPEKTRUMLARININ İNCELENMESİ

Tayyibe BARDAKÇI

Doktora Tezi – Fizik  
Haziran 2015

Tez Danışmanı: Prof. Dr. Mustafa KUMRU

## ÖZ

Son yıllarda, geçiş metal komplekslerinin moleküler özelliklerini incelemek için Yoğunluk Fonksiyonel Teorisi (DFT) umut verici bir tercih haline gelmiştir. Bu tezde DFT metodu kullanılarak anilin türevleri (p-toluidin ve m-toluidin) geçiş metal komplekslerinin bilgisayara dayalı hesaplamaları analiz edilmiştir. Geçiş metal kompleksleri ve ilgili DFT çalışmalarının literatür taraması ilk bölümde verilirken, DFT'nin anlaşılması için gerekli olan teorik bilgi de ikinci bölümde anlatılmıştır. Üçüncü bölüm, Gaussian 03 programı kullanılarak yapılan hesaplamalarda B3LYP/def2-TZVP seviyesinin tercihine değinir. P-toluidin ve m-toluidinin Mn, Co, Ni, Cu, Zn, Cd, ve Hg brom ve Ni, Zn ve Cd iyot komplekslerinin optimize edilmiş molekül yapıları, yük ve spin dağılımları, ve ayrıca titreşim frekansları detaylı olarak dördüncü bölümde verilmiştir. Komplekslerin kararlı geometrileri, ulaşılabilen her spin seviyesi dikkate alınarak elde edilmiştir. Yük dağılımı analizinde Mulliken, NBO ve APT yöntemleri kullanılmış olup, bizim moleküllerimiz için fiziksel olarak en anlamlı sonuç veren yöntem belirlenmiştir. Hesaplamaların sonucunda, titreşimsel band atalamaları iç kordinatlar türünden ifade edilip, % potensiyel enerji dağılımlarıyla (PED) birlikte verilmiştir. Ayrıca, ligandların, metal komplekslerinin titreşim modları üzerine etkisi izah edilmiştir. Ve son olarak bu çalışmanın önemli sonuçları beşinci bölümde özetlenmiştir.

**Anahtar Kelimeler:** Yoğunluk Fonksiyonel Teorisi, def2-TZVP, Geçiş Metal Kompleksi, Moleküler Yapı, Yük ve Spin Dağılımı, Titreşim Frekansı.

To my family

## **ACKNOWLEDGEMENT**

I express sincere appreciation to my supervisor Prof. Mustafa Kumru for his guidance throughout the research. His academic experience and consistent direction provided me with the inspiration to undertake and expand upon the research of this study. I am also thankful to Assoc. Prof. Ahmet Altun, for his being accessible all the time and always answering my questions with patience and understanding. I would like to give my gratitude to Assoc. Prof. Levent Sarı for his support and help throughout my studies. I would like to thank all the members of the physics department for their memorable and warm friendships. I am also grateful to my friends for their moral support, continuous friendship and for being there to listen whenever I needed. Last but not least, a very special thanks goes to my family for their understanding, motivation and patience. Without their support, none of this work would have been possible.

## TABLE OF CONTENTS

ABSTRACT.....	iii
ÖZ .....	iv
DEDICATION.....	v
ACKNOWLEDGMENT .....	vi
TABLE OF CONTENTS.....	vii
LIST OF TABLES .....	x
LIST OF FIGURES .....	xii
LIST OF ABBREVIATIONS.....	xiv
CHAPTER 1 INTRODUCTION .....	1
1.1 Transition Metal Complexes. ....	2
1.2 Background.....	3
1.3 Motivation and Objectives.....	7
1.4 Dissertation Outline.....	8
CHAPTER 2 THEORY .....	10
2.1 Introductory Theory.....	10
2.1.1 The Schrödinger Equation.....	10
2.1.2 The Born-Oppenheimer Approximation .....	11
2.1.4 Variational Principle .....	13
2.2 The Hartree-Fock Approximation. ....	13
2.3 Density Functional Theory. ....	18
2.3.1 Thomas-Fermi Model.....	18
2.3.2 The Hohenberg-Kohn Theorems.....	19
2.3.3 The Kohn-Sham Approach .....	21
2.3.4 Exchange Correlation Energy Functionals.....	23
2.3.4.1 Local Density Approximation .....	23
2.3.4.2 Local Spin Density Approximation.....	24



2.3.4.3	Generalized Gradient Approximation .....	24
2.3.4.4	Hybrid Functionals .....	25
2.4	Basis Sets .....	25
2.4.1	Types of Basis Sets .....	27
2.4.1.1	Minimal Basis Sets .....	27
2.4.1.2	Zeta Basis Sets .....	27
2.4.1.3	Split-Valance Basis Sets .....	27
2.4.1.4	Pople Basis Sets .....	28
2.4.1.5	Dunning's Correlation-Consistent Basis Sets .....	29
2.4.1.6	Alrichs Def2 Basis Set Family .....	29
2.4.2	Effective Core Potentials (Pseudopotentials) .....	29
2.5	General Considerations .....	30
2.5.1	Geometry Optimization .....	31
2.5.2	Vibrational Frequencies .....	31
2.5.2.1	Infrared Spectroscopy .....	32
2.5.2.2	Raman Spectroscopy .....	32
2.5.2.3	The Mutual Exclusion Principle .....	33
CHAPTER 3	COMPUTATIONS .....	34
3.1	Hardwares and Softwares .....	34
3.1.1	Gaussian Program .....	34
3.1.2	Gabedit .....	35
3.1.3	VEDA .....	35
3.2	Calculation Details .....	35
3.2.1	Geometry Optimization .....	35
3.2.2	Charge and Spin Analysis .....	36
3.2.3	Vibrational Frequency Calculations .....	36
3.2.3.1	Prediction of Raman Intensities .....	37
CHAPTER 4	RESULTS & DISCUSSIONS .....	38
4.1	Molecular Structures .....	38
4.1.1	Molecular Structures of the Free Ligands .....	38
4.1.2	Molecular Structures of the Metal Bromide Complexes of P-toluidine .....	41
4.1.3	Molecular Structures of the Metal Iodide Complexes of P-toluidine .....	44
4.1.4	Molecular Structures of the Metal Bromide Complexes of M-toluidine .....	45
4.1.5	Molecular Structures of the Metal Iodide Complexes of M-toluidine .....	48

4.2	Charge and Spin Distribution.....	50
4.2.1	Charge Distribution of the Free Ligands.....	50
4.2.2	Charge and Spin Distribution of the Metal Bromide Complexes of P-toluidine.....	51
4.2.3	Charge and Spin Distribution of the Metal Iodide Complexes of P-toluidine and M-toluidine.....	54
4.2.4	Charge and Spin Distribution of the Metal Bromide Complexes of M-toluidine.....	56
4.3	Vibrational Frequencies.....	58
4.3.1	Vibrational Frequencies of the Free Ligands.....	58
4.3.2	Vibrational Frequencies of the Metal Bromide Complexes of P-toluidine ...	61
4.3.2.1	3500-2700 cm <sup>-1</sup> Region.....	61
4.3.2.2	1700-600 cm <sup>-1</sup> Region.....	64
4.3.2.3	Below 600 cm <sup>-1</sup> .....	65
4.3.3	Vibrational Frequencies of the Metal Iodide Complexes of P-toluidine.....	80
4.3.3.1	3500-2700 cm <sup>-1</sup> Region.....	81
4.3.3.2	1700-600 cm <sup>-1</sup> Region.....	82
4.3.3.3	Below 600 cm <sup>-1</sup> .....	83
4.3.4	Vibrational Frequencies of the Metal Bromide Complexes of M-toluidine ..	90
4.3.4.1	3500-2700 cm <sup>-1</sup> Region.....	90
4.3.4.2	1700-600 cm <sup>-1</sup> Region.....	93
4.3.4.3	Below 600 cm <sup>-1</sup> .....	94
4.3.5	Vibrational Frequencies of the Metal Iodide Complexes of M-toluidine....	109
4.3.5.1	3500-2700 cm <sup>-1</sup> Region.....	110
4.3.5.2	1700-600 cm <sup>-1</sup> Region.....	111
4.3.5.3	Below 600 cm <sup>-1</sup> .....	112
4.3.6	Comparison Between Computed and Observed Vibrational Frequencies of the Title Compounds.....	119
CHAPTER 5 CONCLUDING REMARKS.....		121
REFERENCES.....		123
APPENDIX A DECLARATION STATEMENT.....		141
CURRICULUM VITAE.....		143

## LIST OF TABLES

### TABLE

4.1	Geometry parameters of p-toluidine and m-toluidine .....	40
4.2	The key geometry parameters around the metal ion of the p-toluidine bromide complexes.....	41
4.3	The key geometry parameters around the metal ion of the p-toluidine iodide complexes.....	45
4.4	The key geometry parameters around the metal ion of the m-toluidine bromide complexes.....	47
4.5	The key geometry parameters around the metal ion of the m-toluidine iodide complexes.....	49
4.6	Experimental and calculated vibrational frequencies (in $\text{cm}^{-1}$ ) and % assignments of p-toluidine .....	59
4.7	Experimental and calculated vibrational frequencies (in $\text{cm}^{-1}$ ) and % assignments of m-toluidine. ....	60
4.8	Experimental and calculated vibrational frequencies (in $\text{cm}^{-1}$ ) of free p-toluidine and $\text{MnBr}_2(\text{p-tol})_2$ . ....	66
4.9	Experimental and calculated vibrational frequencies (in $\text{cm}^{-1}$ ) of free p-toluidine and $\text{CoBr}_2(\text{p-tol})_2$ .....	68
4.10	Experimental and calculated vibrational frequencies (in $\text{cm}^{-1}$ ) of free p-toluidine and $\text{NiBr}_2(\text{p-tol})_2$ .....	70
4.11	Experimental and calculated vibrational frequencies (in $\text{cm}^{-1}$ ) of free p-toluidine and $\text{CuBr}_2(\text{p-tol})_2$ .....	72
4.12	Experimental and calculated vibrational frequencies (in $\text{cm}^{-1}$ ) of free p-toluidine and $\text{ZnBr}_2(\text{p-tol})_2$ .....	74
4.13	Experimental and calculated vibrational frequencies (in $\text{cm}^{-1}$ ) of free p-toluidine and $\text{CdBr}_2(\text{p-tol})_2$ .....	76

4.14	Experimental and calculated vibrational frequencies (in $\text{cm}^{-1}$ ) of free p-toluidine and $\text{HgBr}_2(\text{p-tol})_2$ .....	78
4.15	Experimental and calculated vibrational frequencies (in $\text{cm}^{-1}$ ) of free p-toluidine and $\text{NiI}_2(\text{p-tol})_2$ .....	84
4.16	Experimental and calculated vibrational frequencies (in $\text{cm}^{-1}$ ) of free p-toluidine and $\text{ZnI}_2(\text{p-tol})_2$ .....	86
4.17	Experimental and calculated vibrational frequencies (in $\text{cm}^{-1}$ ) of free p-toluidine and $\text{CdI}_2(\text{p-tol})_2$ .....	88
4.18	Experimental and calculated vibrational frequencies (in $\text{cm}^{-1}$ ) of free m-toluidine and $\text{MnBr}_2(\text{m-tol})_2$ .....	95
4.19	Experimental and calculated vibrational frequencies (in $\text{cm}^{-1}$ ) of free m-toluidine and $\text{CoBr}_2(\text{m-tol})_2$ .....	97
4.20	Experimental and calculated vibrational frequencies (in $\text{cm}^{-1}$ ) of free m-toluidine and $\text{NiBr}_2(\text{m-tol})_2$ .....	99
4.21	Experimental and calculated vibrational frequencies (in $\text{cm}^{-1}$ ) of free m-toluidine and $\text{CuBr}_2(\text{m-tol})_2$ .....	101
4.22	Experimental and calculated vibrational frequencies (in $\text{cm}^{-1}$ ) of free m-toluidine and $\text{ZnBr}_2(\text{m-tol})_2$ .....	103
4.23	Experimental and calculated vibrational frequencies (in $\text{cm}^{-1}$ ) of free m-toluidine and $\text{CdBr}_2(\text{m-tol})_2$ .....	105
4.24	Experimental and calculated vibrational frequencies (in $\text{cm}^{-1}$ ) of free m-toluidine and $\text{HgBr}_2(\text{m-tol})_2$ .....	107
4.25	Experimental and calculated vibrational frequencies (in $\text{cm}^{-1}$ ) of free m-toluidine and $\text{NiI}_2(\text{m-tol})_2$ .....	113
4.26	Experimental and calculated vibrational frequencies (in $\text{cm}^{-1}$ ) of free m-toluidine and $\text{ZnI}_2(\text{m-tol})_2$ .....	115
4.27	Experimental and calculated vibrational frequencies (in $\text{cm}^{-1}$ ) of free m-toluidine and $\text{CdI}_2(\text{m-tol})_2$ .....	117
4.28	The M.A.E and the $R^2$ values for the title complexes .....	119

## LIST OF FIGURES

### FIGURE

1.1	Complex geometries.....	2
1.2	An example for possible spin states of a transition metal complex .....	3
2.1	The representation of the positions of electrons and nuclei .....	11
2.2	Geometry optimization.....	31
4.1	Optimized geometries of p-toluidine and m-toluidine .....	39
4.2	Optimized geometries of the Mn and Ni bromide complexes of p-toluidine in solid phase .....	42
4.3	Optimized geometries of the Co, Zn, Cd, Hg, and Cu bromide complexes of p-toluidine .....	43
4.4	Optimized molecular geometries of the Ni (in solid phase), Zn and Cd iodide complexes of p-toluidine .....	44
4.5	Optimized geometry parameters of Mn and Ni bromide complexes of m-toluidine in solid phase .....	46
4.6	Optimized geometries of Co, and Cu complexes and Zn, Cd and Hg bromide complexes of m-toluidine.....	46
4.7	Optimized geometry parameters of Ni (in solid phase), Zn and Cd complexes.....	48
4.8	Charge distributions of p-toluidine and m-toluidine with Mulliken, NBO, and APT methods .....	51
4.9	Mulliken, NBO, and APT charge distributions of metal bromide complexes of p-toluidine .....	53
4.10	Charge distribution of Ni, Zn, and Cd complexes of p-toluidine and m-toluidine .....	55
4.11	Mulliken, NBO, and APT charge distributions of metal bromide complexes of m-toluidine .....	57
4.12	Theoretical IR spectra of p-toluidine and its bromide complexes.....	62
4.13	Theoretical Raman spectra of p-toluidine and its bromide complexes .....	63

4.14	Theoretical IR spectra of p-toluidine and its iodide complexes .....	80
4.15	Theoretical Raman spectra of p-toluidine and its iodide complexes.....	81
4.16	Theoretical IR spectra of m-toluidine and its bromide complexes .....	89
4.17	Theoretical Raman spectra of m-toluidine and its bromide complexes .....	90
4.18	Theoretical IR spectra of m-toluidine and its ioide complexes.....	109
4.19	Theoretical Raman spectra of m-toluidine and its ioide complexes .....	110

## LIST OF ABBREVIATIONS

APT	Atomic polar tensors
B3LYP	Becke's three-parameter Lee-Yang-Par
DFT	Density Functional Theory
ECP	Effective core potential
GGA	Generalized gradient approximation
GTO	Gaussian type orbitals
HF	Hartree-Fock
IR	Infrared
KS	Kohn-Sham
LDA	Local density approximation
LSDA	Local spin density approximation
NBO	Natural bond orbital
PED	Potential energy distribution
PES	Potential energy surface
SCF	Self-Consistent Field
STO	Slater type orbitals
XC	Exchange correlation

# CHAPTER 1

## INTRODUCTION

Describing how matter behaves has been one of the fundamental goals of quantum mechanics since the beginning of the 1900s and it is possible to understand it in microscopic level by solving time-independent Schrödinger equation. However, it was not easy to solve this equation, particularly for many body systems as Paul Dirac [1] stated in 1929:

*“The fundamental laws necessary for the mathematical treatment of large parts of physics and the whole of chemistry are thus fully known, and the difficulty lies only in the fact that application of these laws leads to equations that are too complex to be solved.”*

Although various approaches to solve the Schrödinger equation have been proposed by physicists and chemists in those years, amazing breakthrough has been provided with the development of the modern computers. Thus, computational studies based on the laws of quantum mechanics have become an important tool to understand the properties of atoms and molecules, and have been the center of attraction for many disciplines. Now with the use of clustered computers, it is also possible to predict accurate results even for large systems. Nevertheless, working theoretically on transition metal containing systems is still challenging and computationally expensive due to the strong correlation effects and open shell configurations of some transition metals [2-4]. In order to obtain reliable results for investigating the transition metal complexes, density functional theory (DFT) has recently become a promising choice [5]. DFT is exact in principle and able to predict the molecular properties of transition metal complexes almost accurate since electron correlation effects are included in DFT [6]. Therefore, taking into account of the accuracy and the computational cost, DFT is become most preferred method for studying transition metal complexes [6-8].



## 1.1 TRANSITION METAL COMPLEXES

In a transition metal complex, a central transition metal atom is coordinated to one or more ligands, which donate electrons from a lone pair electron to the metal orbital via coordinative covalent bonds. The geometry of a transition metal complex is determined by the number of ligands bonded to the metal atom. The number of bonds is also named as coordination number, and this number can be changed according to the electronic configuration and the charge of the metals and the ligands. In Fig. 1.1 some common examples of the transition metal complex geometries are provided.

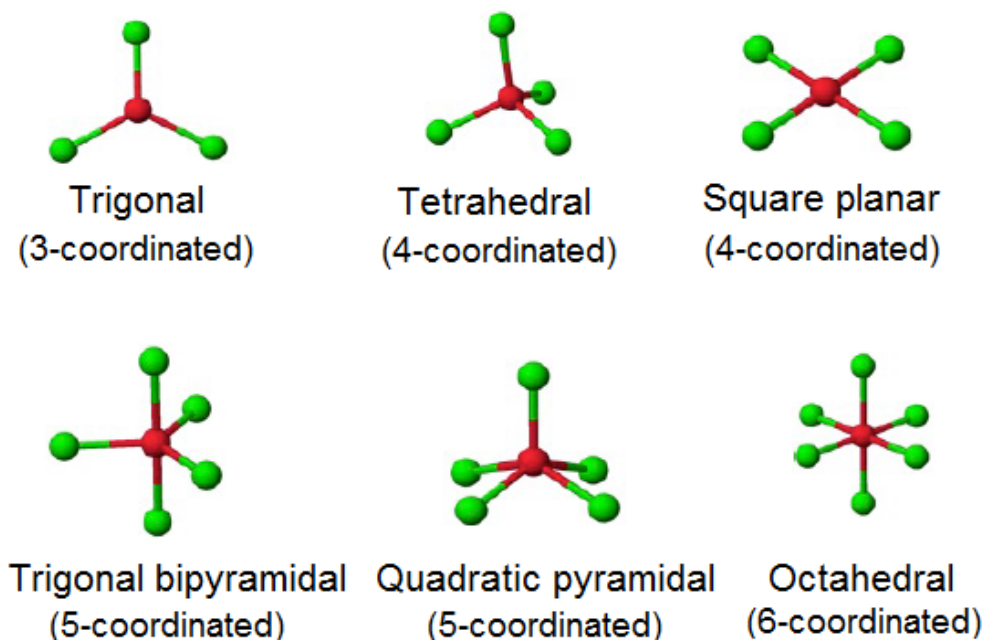


Figure 1.1 Complex geometries [9].

Spin states of transition metal complexes are also important in their classifications. High spin and low spin are the possible spin configurations of the d orbital of a metal atom, and schematic demonstration is given in Fig. 1.2. Generally octahedral complexes have high spin states, but nevertheless calculations are performed considering each accessible spin state. Computations on transition metal complexes can predict stable spin state of a complex accurately, by taking account of the energy differences.

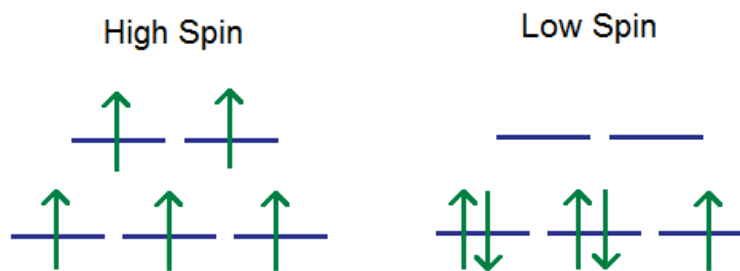


Figure 1.2 An example for possible spin states of a transition metal complex.

In the present study, transition metal complexes are formed using manganese, cobalt, nickel, copper, zinc, cadmium and mercury as metals; and bromine, iodine, p-toluidine and m-toluidine which are electron donors as ligands. Bromine and iodine are the halogens, whereas p-toluidine and the m-toluidine are the aniline derivatives. Aniline and its derivatives have wide range of applications as potential starting materials in some drugs, chemicals, dyes and antioxidants [10-13]. They are also used as diodes and transistors in microelectronic and electro-optical devices [14-16], as well as ligands in coordination chemistry [17-26].

## 1.2 BACKGROUND

Over 100 years ago, Werner described the structure and origin of complex compounds concentrating on the transition metal complexes [27-29]. Since transition metal complexes have an important role in coordination chemistry, his studies have highly affected researches in various disciplines [29,30], and so a great number of studies especially in the fields of biochemistry, analytical chemistry, magnetism, nanotechnology, and medicine have been conducted [31-38].

Besides, various studies have also been carried out on transition metal halide complexes for decades. In 1965, Clark and Williams [39] recorded far-infrared spectra of metal halide complexes of pyridine and some nitrogen donor ligands. In this study they indicated that it is possible to predict the structure of complex, such as tetrahedral or octahedral by determining metal-ligand and metal-halogen stretching vibrations. In the same year Ahuja et al. [40], proposed the UV-Vis and far-infrared spectra of the

aniline complexes of transition metal (II) chlorides, bromides, and iodides. Their purpose was determining the environment around the metal atom in the complexes, and so they reported nickel and manganese complexes have octahedral structure, whereas cobalt complex has a tetrahedral environment. Allan et al. [41] and Brown et al. [42] reported preparation and thermal decomposition of some metal (II) halides in their papers. Beech et al. [43], investigated stoichiometries and spectroscopic properties of  $ML_nX_n$  (M: metal, L: ligand, and X: halogen) types transition metal complexes in 1970. Two years later Coucouvanis et al. [44], prepared nickel (II) and palladium (II) halide complexes and reported their structures and some other properties by recording X-ray, ultraviolet, visible, and near-infrared spectra. In 1973, Brown and Richardson [45] synthesized chromium (III) chloride and bromide complexes with pyridines and tried to predict their structures by thermal decomposition and spectroscopic methods. In the same year Karayannis [46] published a comprehensive review about metal complexes of aromatic amines with a focus on coordination compounds of aromatic amine N-oxides. Structural, thermal and spectroscopic studies of metal (II) halide complexes of morpholine-4-thiocarbonic acid anilide were reported by Venkappayya and Brown [47]. A few years later Engelter et al. studied infrared spectra of metal halide complexes of aniline and its derivatives p-toluidine, o-toluidine and m-toluidine [19,20] providing metal-ligand vibrations in a detail. In the later years, Ahrlund et al. proposed thermodynamics [48], equilibrium and enthalpy measurements [49] of metal halide and pseudo-halide complexes. Akyüz and Davies [18] performed vibrational spectral study of  $MX_2L_3$  types of transition metal halide complexes of aniline in 1982. Synthesis, structural, thermal, magnetic and spectroscopic properties of cobalt, nickel and copper complexes of m-toluidine which is an aniline derivative was reported by Allan and Paton [17]. They found chloride complex of cobalt as tetrahedral geometry, and nickel and copper complexes as octahedral. A similar study with a p-toluidine containing ligand carried out for the cobalt (II) chloride complex by Cseh et al. [50], giving the same tetrahedral result for the cobalt geometry. Different from these, Henderson and Evans provided electrospray mass spectrometric investigation of some transition metal halide complexes in order to observe ionization processes [51]. Altun and Gölcük et al. performed studies on synthesis, structures, thermal, and spectroscopic properties of metal halide complexes of p-toluidine and m-toluidine [21-26]. In the same years Yurdakul et al., synthesized metal halide complexes of isonicotinamide and provided their X-ray powder diffraction patterns and infrared spectra [52]. Wu et al. [53],

prepared metal (II) halide complexes of some ligands including pyridine, and they also provided structures and photoluminescence properties of these complexes. In their study they found different types of halides and coordination geometries of the metal atoms have an important effect on the structure of the related complexes.

With the widespread use of computational chemistry tools, density functional calculations started to support experimental studies of transition metal halide complexes, and thus a large number of studies have been carried out within the past several years. For example, Özel et al.[54, 55], and Yurdakul et al.[56] employed quantum chemical calculations of zinc (II) halide complexes of different quinoline derivatives using B3LYP density functional. Akalın and Akyüz [57] also studied zinc halide complexes with pyridine derivative ligands employing B3LYP/6-311++G(d,p) level of theory. Sabounchei et al. [58], studied mercury (II) halides providing structural and spectral characterization. B3LYP/LanL2MB method has been employed in their theoretical calculations. Erdogdu et al.[59], performed theoretical and experimental investigations on structures and vibrational spectra of bis(4-pyridyl)propane complexes of zinc and mercury halides. They used B3LYP hybrid functional with LANL2DZ and SDD basis sets for their calculations. Similarly Kesan et al. [60], studied metal halide complexes of 1-phenylpiperazine both experimentally and theoretically using same functional and basis set. In addition to experimental studies, B3LYP density functional calculations on metal halide complexes of pyridine-containing ligands provided by Gökçe and Bahçeli [61] and Tyagi et al.[62] In common with previous studies Gökçe and Bahçeli preferred LANL2DZ basis set for the complexes, however Tyagi et al., employed 6-31+g(d,p) basis set for their complexes. Eryürek et al.[63], performed density functional calculations on palladium halide complexes with B3LYP level of theory using mixed basis set, i.e. LANL2DZ for the metal atom, and 6-31++G(d,p) for all other atoms. Özbek et al. [64] prepared platinum complexes and Mansour [65], prepared ruthenium, palladium, and platinum complexes and both performed B3LYP/LANL2DZ level of calculations for the structural and spectral properties of their complexes. In 2013 and 2014 we also provided experimental and density functional studies on copper chloride complexes of m-toluidine and p-toluidine using BVP86 and B3LYP functionals by applying 6-311G+(d,p) basis set [66,67].

In addition to these, several density functional studies have also been performed in order to evaluate the performance of different functionals and basis sets employed in transition metal systems. Furche and Perdew [68] carried out a comprehensive study for some molecular properties of 3d transition metal systems, employing quadruple zeta valance basis set with six different functionals. Riley and Merz also published a DFT study on third row transition metal systems. They evaluated 6-31G\*\* and TZVP basis sets with different functionals for the ionization potentials, heats of formation and other properties of their title complexes, and found the more accurate results with TZVP level[69]. Williams and Wilson [3] performed a study on evaluation of the basis sets on molecular geometries and dissociation energies of transition metal systems. Yang et al. [70], investigated the performance of 6-31+G\*\* + LANL2DZ mixed basis set with GGA, hybrid-GGA, meta-GGA and hybrid-meta-GGA types of functionals on heats of formation and ionization potentials of transition metal containing systems. The assessment of forty four density functionals on enthalpies of formation for 3d transition metal containing molecules carried out by Tekarli et al [71]. Density functional calculations on spin-state energetics of iron complexes for different GGA and hybrid functionals, employing def2-QZVPP basis set performed by Ye and Neese [72]. More recently, Matczak [73] carried out B3LYP density functional calculations on some transition metal containing systems in order to evaluate the performance of various basis sets, finding def2-TZVP prior to others for predicting geometries and harmonic vibrational frequencies.

### 1.3 MOTIVATION AND OBJECTIVES

There has been developing interest in transition metals and their complexes because of their significant roles in coordination chemistry, and their potential applications as drugs, cosmetics [74,75], photosensitizers, photo-initiators of radical reactions [76,77], photo-catalysts, organic solar cells [78], phosphorescent dyes, molecular devices (molelectronics), and also non-linear optical materials [79].

As the transition metals display different oxidation states, they may also interact with the negatively charged molecules, and their complexes can be easily synthesized and characterized [35]. These characteristics of transition metals are caused the

development of metal-based drugs for the treatment of several diseases such as cancer, lymphomas, infection control, diabetes and neurological disorders, etc. [34, 36, 37]. In recent years, especially cancer has become a major cause of death. Prevalence of the cases and costs of the treatment of cancer necessitated the search for new drugs and therapies. Cisplatin is one of those transition metal drugs containing platinum as transition metal and chlorine as halogen. Although cisplatin is a successful example in treatment of various cancers, it also brings some side-effects concomitantly. Therefore, there is a need to search for the new transition metal compounds that exhibit different mechanisms of action and resistance profiles.

Vibrational spectroscopy is one of the most fundamental methods enables the investigation of various types of compounds deeply. Mutually complementary infrared and Raman spectroscopy techniques are powerful vibrational spectroscopic tools giving significant information about the structure and dynamics of complexes. However, it is not easy to interpret experimental spectrum results without computational tools. Electronic structure calculations based on the Schrödinger equation engage in here and give very good results in calculating spectroscopic constants and vibrational frequencies providing determination of band assignments, and comparison of the peaks in the experimental and theoretical spectra. Besides, molecular structures and geometries (e.g. bond lengths and bond angles) which can be partially recorded with X-ray spectroscopy, molecular energies in different spin states, charge and spin density analysis can be performed accurately. Thus, with the use of computational methods, we can predict various molecular properties of the compounds which are not possible to obtain with the available experimental techniques or having high costs while acquiring them experimentally. Since most scientific softwares provide visual animation for the compounds, it is also possible to display optimized molecular structures, and animate vibrational frequencies for each mode. By this means, existing experimental infrared and Raman spectra results can be fully understood.

Additionally, determining the most appropriate functional and basis set for the title transition metal complexes will be useful for researchers investigating similar types of complexes without causing a loss of time. And our ultimate expectation is that the results from this systematic work will be able to serve as a reference for future

theoretical studies on transition metal-based drugs or large systems such as metalloproteins.

## 1.4 DISSERTATION OUTLINE

In this dissertation we perform a systematic density functional theory study with a consistent functional and basis set for the transition metal complexes of aniline derivatives extending the previous experimental works performed by Altun and Gölcük et al. [21-26]. Manganese, cobalt, nickel, copper, zinc, cadmium and mercury are the transition metals of this study, and the bromine and iodide are the halogens used in coordination to metal atoms, together with the aniline derivatives p-toluidine and m-toluidine. To give an outline of this study, brief explanations of the chapters are given below.

**In chapter 2**, theoretical background of the dissertation is provided by focusing on DFT. Since DFT is based on quantum mechanics, we have introduced some basic concepts of quantum mechanics starting from Schrödinger equation. Then Hartree-Fock approach is explained, because it has a conceptual importance as a traditional wavefunction based method, and also understanding it would be helpful in getting a solid grasp of DFT. Thomas-Fermi Model is given as original roots of the DFT, and for the basis of the modern density functional theory, Hohenberg-Kohn and Kohn-Sham approaches are proposed. Brief information on exchange correlation functionals, basis sets and effective core potentials are also given. And finally, general considerations such as geometry optimization and vibrational frequencies (infrared and Raman spectroscopy) are provided at the end of this chapter.

**In chapter 3**, details of the DFT calculations are explained by introducing the hardwares and the softwares used in this study.

**In chapter 4**, the results of computations on optimized geometries, charge and spin distributions and harmonic vibrational frequencies of twenty transition metal complexes are presented and explained in detail. Spin densities of the metal complexes are provided with the Mulliken method, whereas charge distribution analysis is performed by means of the Mulliken, NBO and APT methods. Although

there is large number of experimental and theoretical studies about transition metals in the literature, there is no systematic theoretical study about our title complexes as a whole. Experimental infrared and Raman spectra results of the complexes are taken from previous studies [21-26] and compared with our theoretical results. The vibrational band assignments are determined based on the computational results expressed in terms of internal coordinates with percent potential energy distributions. The detailed theoretical molecular structure and vibrational spectral analyses are also utilized in obtaining the properties of the complexes that are not accessible by experimental data, such as the structure around the metal atoms and the effects of ligands to the coordination.

**In the final chapter**, the results are summarized emphasising on significant points.



## CHAPTER 2

### THEORY

To understand the methods used in this study, and also to analyze the results of calculations obtained via these methods, a comprehension of the theoretical basis is needed. This chapter provides basic theory essential for this thesis.

#### 2.1 INTRODUCTORY THEORY

##### 2.1.1 The Schrödinger Equation

According to the fundamental postulates of quantum mechanics, the state of any system is completely described by a wave function  $\psi$ . So the properties of any time-independent quantum mechanical system can be understood by finding the wave function by solving the Schrödinger equation [80],

$$\hat{H}\psi = E\psi \quad (2.1)$$

here, where  $\hat{H}$  is the Hamiltonian operator, that shows the behavior of a system of interacting  $N$  electrons and  $M$  nuclei in the following form:

$$\hat{H} = -\sum_i^N \frac{1}{2} \nabla_i^2 - \sum_a^M \frac{1}{2M_a} \nabla_a^2 - \sum_{i,a}^{N,M} \frac{Z_a}{|\vec{r}_i - \vec{R}_a|} + \sum_{i \neq j}^N \frac{1}{|\vec{r}_i - \vec{r}_j|} + \sum_{a \neq b}^M \frac{Z_a Z_b}{|\vec{R}_a - \vec{R}_b|} \quad (2.2)$$

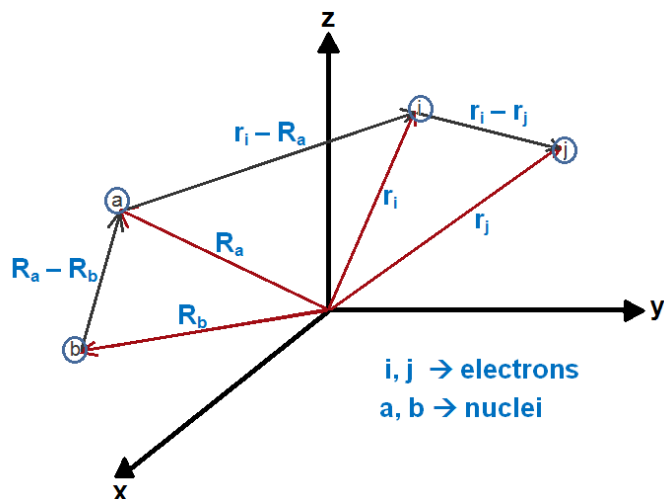


Figure 2.1 The representation of the positions of electrons and nuclei.

where summations over  $i, j$  correspond to electrons, and summations over  $a, b$  correspond to nuclei (see Fig. 2.1). In the equation, first two terms are the kinetic energy contributions from the electrons and the nuclei respectively, and the others are the Coulombic potential energy contributions, which represent the electron–nuclei interaction, electron–electron repulsive interaction, and finally the nuclei–nuclei repulsive interaction respectively. Since, solving the Schrödinger equation analytically even for the  $H_2^+$ , which consists of only three particles, is impossible with this complicated Hamiltonian, doing simplifications via approximations is become indispensable.

### 2.1.2 The Born-Oppenheimer Approximation

The first simplification to the Hamiltonian operator, which plays a vital role in electronic structure calculations, is done by Max Born and J. Robert Oppenheimer [81]. Their motivation behind this approximation is having the great difference in masses of electrons and nuclei. Since nuclei are  $\sim 10^3$  times heavier than electrons, they move more slowly, that is, they can be considered to remain fixed from the point of view of electrons. If we rewrite the Hamiltonian;

$$\hat{H} = \hat{T}_e(\vec{r}) + \hat{T}_N(\vec{R}) + \hat{V}_{eN}(\vec{r}, \vec{R}) + \hat{V}_{ee}(\vec{r}) + \hat{V}_{NN}(\vec{R}) \quad (2.3)$$

one can easily see that second term and last term are directly related with nuclei. Since nuclei are accepted as stationary, kinetic energy of the nuclei can be neglected, and

nuclei–nuclei repulsion can be treated as a constant. Hence, with the remaining terms we get electronic Hamiltonian:

$$\hat{H}_e = -\sum_i^N \frac{1}{2} \nabla_i^2 - \sum_{i,a}^{N,M} \frac{Z_a}{|\vec{r}_i - \vec{R}_a|} + \sum_{i \neq j}^N \frac{1}{|\vec{r}_i - \vec{r}_j|} \quad (2.4)$$

where  $\hat{H}_e$  describes the motion of  $N$  electrons in a fixed environment of  $M$  atomic nuclei. Schrödinger equation with the electronic Hamiltonian becomes:

$$\hat{H}_e \psi_e = E_e \psi_e \quad (2.5)$$

where  $\psi_e$  is the electronic wave function, explicitly depends on electrons positions, and implicitly depends on nuclei positions, as electronic energy,

$$\psi_e = \psi_e(\vec{r} ; \vec{R}_a) \quad E_e = E_e(\vec{R}_a) \quad (2.6)$$

So the total energy can be written as the sum of electronic energy and constant nuclear repulsion. In the same way, the solution to the Schrödinger equation including the nuclear Hamiltonian is,

$$\hat{H}_n \psi_n = E \psi_n \quad (2.7)$$

where  $\psi_n$  is the nuclear wave function depends on the nuclear coordinates, and describes the vibration, rotation and translation of a molecule. On the other hand,  $E$  involves electronic, vibrational, rotational and translational energy.

However, the key problem in understanding the structure of matter is solving the Schrödinger equation for a system of interacting  $N$  electrons in an external field, so we focus on electronic structure problem instead of vibrational, rotational or translation problem. That is, from now on,  $\hat{H}$  refers to electronic Hamiltonian operator unless stated otherwise. Nevertheless, solving the Schrödinger equation with only electronic Hamiltonian is still a difficult task for the systems containing many electrons. For this reason, further approximations have been needed for many-body systems.

### 2.1.3 Variational Principle

The variational principle, which is one of the main algorithms used by computers for the approximate solution of the Schrödinger equation, states that the energy calculated with a trial wave function  $\psi'$  will be an upper bound to the ground state energy [82].

$$E_0 \leq E[\psi'] \text{ where } E[\psi'] = \frac{\langle \psi' | \hat{H} | \psi' \rangle}{\langle \psi' | \psi' \rangle} \quad (2.8)$$

So, if we minimize the  $E[\psi']$  with respect to all acceptable  $N$ -electron wave functions, we can reach the true ground state energy  $E_0$  with true ground state  $\psi_0$ .

$$E_0 = \min_{\psi' \rightarrow N} E[\psi'] = \min_{\psi' \rightarrow N} \langle \psi' | T + V_{NE} + V_{ee} | \psi' \rangle \quad (2.9)$$

where Hamilton operator  $\hat{H}$  explicitly depends on the number of electrons  $N$  and  $V_{ext}$ , because of the kinetic energy and electron-electron repulsion are also determined by  $N$ . So it can be concluded that ground state energy is a functional of the number of electrons  $N$  and the nuclear potential  $V_{ext}$ .

$$E_0 = E[N, V_{ext}] \quad (2.10)$$

## 2.2 THE HARTREE-FOCK APPROXIMATION

After Born-Oppenheimer approximation, many theories including Hartree-Fock were developed in order to solve the electronic Schrödinger equation. Hartree-Fock approximation [83, 84] has a great conceptual importance within the history of quantum chemistry, because of providing a useful starting point to the solution of many-particle system and introducing the concept of self-consistent field.

The first approximation states that the total electronic wave function of many electron systems can be written as a simple product of one-electron wave functions, which is known as a Hartree Product:

$$\psi_{HP} = (\vec{x}_1, \vec{x}_2, \dots, \vec{x}_N) = \chi_i(\vec{x}_1)\chi_j(\vec{x}_2)\dots\chi_k(\vec{x}_N) \quad (2.11)$$

However, in quantum mechanics we know that electrons are all indistinguishable, but in Hartree product electron 1 occupies  $\chi_i$ , electron 2 occupies  $\chi_j$  on the contrary to the antisymmetry principle. So Hartree product does not satisfy the antisymmetry principle, and we need to obtain antisymmetrized wave functions. For this reason, firstly, consider two-electron system occupying the spin orbitals  $\chi_i$  and  $\chi_j$ .

$$\psi_{HP} = (\vec{x}_1, \vec{x}_2) = \chi_i(\vec{x}_1)\chi_j(\vec{x}_2) \quad (2.12)$$

If we interchange the coordinates of electrons, we obtain

$$\psi_{HP} = (\vec{x}_2, \vec{x}_1) = \chi_i(\vec{x}_2)\chi_j(\vec{x}_1) \quad (2.13)$$

and we can also obtain a wave function which takes account of the indistinguishability of electrons and satisfies the antisymmetry principle by writing:

$$\psi(\vec{x}_1, \vec{x}_2) = \frac{1}{\sqrt{2}} \left[ \chi_i(\vec{x}_1)\chi_j(\vec{x}_2) - \chi_i(\vec{x}_2)\chi_j(\vec{x}_1) \right] \quad (2.14)$$

This wave function can be written as a determinant

$$\psi(\vec{x}_1, \vec{x}_2) = \frac{1}{\sqrt{2}} \begin{pmatrix} \chi_i(\vec{x}_1) & \chi_j(\vec{x}_1) \\ \chi_i(\vec{x}_2) & \chi_j(\vec{x}_2) \end{pmatrix} \quad (2.15)$$

and if we generalize it to  $N$  electrons, we obtain a determinant of spin orbitals, which is called a Slater determinant [85].

$$\psi(\vec{x}_1, \vec{x}_2, \dots, \vec{x}_N) = \frac{1}{\sqrt{N!}} \begin{pmatrix} \chi_i(\vec{x}_1) & \dots & \chi_k(\vec{x}_1) \\ \vdots & \ddots & \vdots \\ \chi_i(\vec{x}_N) & \dots & \chi_k(\vec{x}_N) \end{pmatrix} \quad (2.16)$$

here,  $(N!)^{-1/2}$  is a normalization factor; rows represent electrons whereas columns represent spin orbitals.

After determining wave function having the form of a Slater determinant, let's return to the Hamiltonian. In order to obtain a simpler system, one-electron operator  $\hat{h}$  will be defined as:

$$\hat{h}(i) = -\frac{1}{2}\nabla_i^2 - \sum_a \frac{Z_a}{\vec{r}_{ia}} \quad (2.17)$$

and a two electron operator

$$\hat{v}(i, j) = \frac{1}{\vec{r}_{ij}} \quad (2.18)$$

Then full electronic Hamiltonian can be written as

$$\hat{H} = \sum_i \hat{h}(i) + \sum_{i<j} \hat{v}(i, j) + V_{NN} \quad (2.19)$$

In that way, complicated many electron problem is replaced with one-electron problem with average electron-electron repulsion. If we remember the variational principle, which states energy calculated with a trial wave function, will be an upper bound to the true energy:

$$E_{HF} = \int \psi_{HF}^* \hat{H} \psi_{HF} d\tau = \langle \psi_{HF} | \hat{H} | \psi_{HF} \rangle \quad (2.20)$$

which equals to

$$E_{HF} = \langle i | \hat{h} | i \rangle + \frac{1}{2} \sum_{ij} [ii|jj] - [ij|ji] \quad (2.21)$$

where

$$\langle i | \hat{h} | i \rangle = \int \chi_i^*(\vec{x}_1) \hat{h}(\vec{x}_1) \chi_i(\vec{x}_1) d\vec{x}_1 \quad (2.22)$$

and

$$[ij|kl] = \int d\vec{x}_1 \int d\vec{x}_2 \chi_i^*(\vec{x}_1) \chi_j(\vec{x}_1) \frac{1}{r_{12}} \chi_k^*(\vec{x}_2) \chi_l(\vec{x}_2) \quad (2.23)$$

Now, we need to minimize the Hartree-Fock energy with respect to  $\chi_i \rightarrow \chi_i + \delta \chi_i$  in order to obtain the possible minimum energy by using Lagrange's method of undetermined multipliers [86];

$$L[\{\chi_i\}] = E_{HF}[\{\chi_i\}] - \sum_{ij} \varepsilon_{ij} (\langle i|j \rangle) - \delta_{ij} \quad (2.24)$$

where

$$\langle i|j \rangle = \int \chi_i^*(\bar{x}_1) \chi_j(\bar{x}_1) d\bar{x}_1 \quad (2.25)$$

So, by making first variation:

$$\delta L = \delta E_{HF}[\{\chi_i\}] - \sum_{ij} \varepsilon_{ij} \delta \langle i|j \rangle = 0 \quad (2.26)$$

where

$$\delta \langle i|j \rangle = \langle \delta \chi_i | \chi_j \rangle + \langle \chi_i | \delta \chi_j \rangle \quad (2.27)$$

Then, change in the Hartree-Fock part is

$$\begin{aligned} \delta E_{HF} = & \sum_i \langle \delta i | \hat{h} | i \rangle + \langle i | \hat{h} | \delta i \rangle + \frac{1}{2} \sum_{ij} [\delta ii | jj] + [i \delta i | jj] + [ii | \delta jj] + [ii | j \delta j] \\ & - \frac{1}{2} \sum_{ij} [\delta ij | ji] + [i \delta j | ji] + [ij | \delta ji] + [ij | j \delta i] \end{aligned} \quad (2.28)$$

Putting equations 2.27 and 2.28 in equation 2.26 we obtain,

$$\begin{aligned} \delta L = & \sum_i \langle \delta i | \hat{h} | i \rangle + \langle i | \hat{h} | \delta i \rangle + \sum_{ij} [\delta ii | jj] + [i \delta i | jj] - \sum_{ij} [\delta ij | ji] + [i \delta j | ji] \\ & - \sum_{ij} \varepsilon_{ij} (\langle \delta i | j \rangle + \langle i | \delta j \rangle) = 0 \end{aligned} \quad (2.29)$$

In equation 2.29, second terms are complex conjugates of the first terms. So,

$$\delta L = \sum_i \langle \delta i | \hat{h} | i \rangle + \sum_{ij} [\delta ii | jj] - [\delta ij | ji] - \sum_{ij} \varepsilon_{ij} \langle \delta i | j \rangle + \text{Complex Conjugate} = 0 \quad (2.30)$$

Rewriting these terms by remembering equation 2.23,

$$\begin{aligned} \delta L = \sum_i \int d\vec{x}_1 \delta \chi_i^*(\vec{x}_1) & \left[ \hat{h}(\vec{x}_1) \chi_i(\vec{x}_1) + \sum_j \chi_j(\vec{x}_1) \int d\vec{x}_2 \frac{1}{r_{12}} \chi_j^*(\vec{x}_2) \chi_j(\vec{x}_2) \right. \\ & \left. - \chi_j(\vec{x}_1) \int d\vec{x}_2 \frac{1}{r_{12}} \chi_j^*(\vec{x}_2) \chi_i(\vec{x}_2) - \sum_j \varepsilon_{ij} \chi_j(\vec{x}_1) \right] + CC = 0 \end{aligned} \quad (2.31)$$

We finally obtain Hartree-Fock equations with orbitals,

$$\begin{aligned} \hat{h}(\vec{x}_1) \chi_i(\vec{x}_1) + \sum_{j \neq i} \left[ \int d\vec{x}_2 |\chi_j(\vec{x}_2)|^2 \frac{1}{r_{12}} \right] \chi_i(\vec{x}_1) - \sum_{j \neq i} \left[ \int d\vec{x}_2 \chi_j^*(\vec{x}_2) \chi_i(\vec{x}_2) \chi_j(\vec{x}_1) \frac{1}{r_{12}} \right] \chi_j(\vec{x}_1) \\ = \sum \varepsilon_{ij} \chi_j(\vec{x}_1) \end{aligned} \quad (2.32)$$

where  $\varepsilon$  is the energy eigenvalue.

In this equation first term in square brackets is the Coulomb interaction (**J**), whereas second term is the exchange term (**K**) coming from antisymmetry principle. Rewriting with new Coulomb and exchange operators, Hartree-Fock equations become:

$$\left[ \hat{h}(\vec{x}_1) + \sum_{j \neq i} \hat{J}_j(\vec{x}_1) - \sum_{j \neq i} \hat{K}_j(\vec{x}_1) \right] \chi_i(\vec{x}_1) = \sum_j \varepsilon_{ij} \chi_j(\vec{x}_1) \quad (2.33)$$

Since they are eigenvalue equations, we know that, if  $j=i$ , they would be in the same orbital. So we can define a new operator  $\hat{F}$ , which is called the Fock operator:

$$\hat{F}(\vec{x}_1) = \hat{h}(\vec{x}_1) + \sum \hat{J}_j(\vec{x}_1) - \hat{K}_j(\vec{x}_1) \quad (2.34)$$

Hence, Hartree-Fock equations eventually become:

$$\hat{F}(\vec{x}_1) \chi_i(\vec{x}_1) = \varepsilon_i \chi_i(\vec{x}_1) \quad (2.35)$$

Thus, Fock operator ( $\hat{F}$ ) is defined in terms of Coulomb ( $\hat{J}$ ) and exchange ( $\hat{K}$ ) operators, and they are defined in terms of orbital  $\chi$ s. That is, in order to make  $\hat{F}$ , we need  $\chi$ s. So, the starting point is guessing some  $\chi$ s, and this is why it is also called as Self-consistent field (SCF) method.



## 2.3 DENSITY FUNCTIONAL THEORY

Since the wave function  $\psi$  describes all properties of a system, the methods described above are proposed to solve the electronic Schrodinger equation in order to obtain that wave function. Among these methods, especially Hartree–Fock method is widely used today in quantum chemistry. However its neglecting electron correlation effects and having computational difficulties in many-electron systems lead to search for an alternative method, such as density functional theory [8, 87]. The basic idea of DFT is replacing that complicated many-electron wave function (which depends on  $4N$  variables including the spin variable), with a simpler quantity, the electron density  $\rho(\vec{r})$  (which depends on only 3 spatial coordinates) [82, 88, 89]. What underlies behind the reputation of DFT is, it includes electron correlation effects, and its computational effort is significantly low than Hartree–Fock methods. Besides, in transition metal systems the results of DFT are more accurate than traditional methods when compared with experimental data [6,8].

### 2.3.1 Thomas-Fermi Model

Historically, first attempts to use the electron density for the energy, are based on the early works of Thomas and Fermi [90, 91]. They considered the distribution of electrons in an atom statistically as uniform gas, which is composed of non-interacting electrons. In their model, they derived kinetic energy in a very simple way, based on the uniform electron gas and in terms of electron density:

$$T[\rho(\vec{r})] = \frac{3}{10} (3\pi^2)^{2/3} \int \rho^{5/3}(\vec{r}) d\vec{r} \quad (2.36)$$

Although they treated electron-electron and nuclear-electron interactions in a classical way, they expressed total energy completely in terms of the electron density  $\rho(\vec{r})$ .

$$E[\rho(\vec{r})] = \frac{3}{10} (3\pi^2)^{2/3} \int \rho^{5/3}(\vec{r}) d\vec{r} - z \int \frac{\rho(\vec{r})}{r} d\vec{r} + \frac{1}{2} \iint \frac{\rho(\vec{r}_1)\rho(\vec{r}_2)}{r_{12}} d\vec{r}_1 d\vec{r}_2 \quad (2.37)$$

Since this equation neglects exchange and correlation effects, its accuracy for atoms is not high. But, having the original idea for DFT makes Thomas-Fermi model important [92].

### 2.3.2 The Hohenberg-Kohn Theorems

Introduction to the Hohenberg and Kohn (HK) theorems in 1964 [93] provides a basis for the modern density functional theory. The two basic concepts of their paper are introducing electron density as basic variable and employing variational principle in order to find ground state density.

For the first part, we know that for an arbitrary number of electrons, external potential  $v(\vec{r})$  fixes the Hamiltonian, so full many-particle ground state is determined by the number of electrons ( $N$ ) and  $v(\vec{r})$ . And the electron density is employed in the first Hohenberg-Kohn theorem as follows:

*Theorem 1: External potential  $v(\vec{r})$  is a unique functional of  $\rho(\vec{r})$ ; apart from a trivial additive constant.*

which means ground state electron density  $\rho(\vec{r})$  determines the number of electrons, ( $\int \rho(\vec{r}) d\vec{r} = N$ ), ground state wave function, Hamiltonian and all other electronic properties of a system. In order to prove this theorem, assume we have same system having another external potential,  $v'(\vec{r})$ , (which differs from  $v(\vec{r})$  by more than a constant) with a ground state wave function  $\psi'$ , giving the same ground state density  $\rho(\vec{r})$ . Keeping in mind that,  $E_0$  and  $E_0'$  are the ground state energies for the  $\hat{H}$  and  $\hat{H}'$ ;

$$\begin{aligned} E_0 &< \langle \psi' | \hat{H} | \psi' \rangle = \langle \psi' | \hat{H} | \psi' \rangle + \langle \psi' | \hat{H} - \hat{H}' | \psi' \rangle \\ &= E_0' + \int \rho(\vec{r}) [v(\vec{r}) - v'(\vec{r})] d\vec{r} \end{aligned} \quad (2.38)$$

Interchanging primed quantities with the unprimed ones, we obtain,

$$\begin{aligned} E_0' &< \langle \psi | \hat{H}' | \psi \rangle = \langle \psi | \hat{H} | \psi \rangle - \langle \psi | \hat{H} - \hat{H}' | \psi \rangle \\ &= E_0 - \int \rho(\vec{r}) [v(\vec{r}) - v'(\vec{r})] d\vec{r} \end{aligned} \quad (2.39)$$

Adding equations 2.38 and 2.39, we come up with an inconsistent result,

$$E_0 + E_0' < E_0' + E_0 \quad (2.40)$$

which leads us there cannot be any other external potential giving the same ground state density  $\rho(\vec{r})$ , in other words, ground state density uniquely determines external potential with all other properties such as energy of the system.

$$E[\rho(\vec{r})] = T[\rho(\vec{r})] + V_{ee}[\rho(\vec{r})] + V_{Ne}[\rho(\vec{r})] = F[\rho(\vec{r})] + \int \rho(\vec{r}) V_{Ne} d\vec{r} \quad (2.41)$$

where,  $F[\rho(\vec{r})]$  is the Hohenberg-Kohn functional which is a universal functional, completely independent from the system.

In the second Hohenberg-Kohn theorem electron density obeys variational principle, which is stated as:

*Theorem 2: Any trial electron density function  $\rho'(\vec{r})$  satisfying  $\int \rho'(\vec{r}) d\vec{r} = N$  will give an energy higher or equal to the true ground state energy.*

$$E[\rho'(\vec{r})] \geq E[\rho(\vec{r})] \quad (2.42)$$

where  $E[\rho(\vec{r})]$  is the energy functional of the ground state electron density.

From the first Hohenberg-Kohn theorem we know that ground state electron density determines its own external potential  $v(\vec{r})$ , wave function  $\psi$ , and hence its own Hamiltonian  $\hat{H}$ . So, it can be said that, trial electron density function  $\rho'(\vec{r})$  determines its own properties as well, such as  $v'(\vec{r})$ ,  $\psi'$  and  $\hat{H}'$ .

$$\langle \psi' | \hat{H}' | \psi' \rangle = \int \rho'(\vec{r}) v'(\vec{r}) d\vec{r} + F[\rho'(\vec{r})] = E[\rho'(\vec{r})] \geq E[\rho(\vec{r})] \quad (2.43)$$

In brief, electron density determines all properties of a system and the energy of this system achieves its minimum value if and only if the electron density is the true ground state density.

### 2.3.3 The Kohn-Sham Approach

Although Hohenberg-Kohn theorem tells the ground state energy is a functional of ground state density  $\rho(\vec{r})$ , we still do not know how to construct unknown universal functional  $F[\rho(\vec{r})]$  in order to obtain energy functional  $E[\rho(\vec{r})]$ .

$$E[\rho(\vec{r})] = F[\rho(\vec{r})] + \int \rho(\vec{r}) V_{Ne} d\vec{r} \quad (2.44)$$

One year after the proposal of Hohenberg-Kohn theorems, in 1965 Kohn and Sham [94] provided applicability for modern DFT by publishing a paper, in which how to approach to  $F[\rho(\vec{r})]$  is presented. From the previous section we remember that  $F[\rho(\vec{r})]$  contains kinetic energy and electron-electron interactions. If we write this explicitly,

$$F[\rho(\vec{r})] = T_s[\rho(\vec{r})] + J[\rho(\vec{r})] + E_{xc}[\rho(\vec{r})] \quad (2.45)$$

where the r.h.s. of the equation are, respectively, the kinetic energy of the non-interacting system, classical Coulomb interaction, and exchange-correlation energy, which is the sum of the correction to the kinetic energy (because of interacting electrons) and the correction to the nonclassical electron-electron interactions.

In order to compute the kinetic energy to a good accuracy, Kohn and Sham considered a fictitious non-interacting reference system of electrons (having the same density with the real physical system) and introduced orbital expression for the density. So the Eq. (2.45) can be rewritten as:

$$F[\rho(\vec{r})] = \sum_i^N \langle \chi_i | -\frac{1}{2} \nabla_i^2 | \chi_i \rangle + \sum_i^N \langle \chi_i | \frac{1}{2} \frac{\rho(\vec{r}')}{|\vec{r}_i - \vec{r}'|} d\vec{r}' | \chi_i \rangle + E_{xc}[\rho(\vec{r})] \quad (2.46)$$

where  $N$  is the number of electrons and the electron density is,

$$\rho = \sum_i^N \langle \chi_i | \chi_i \rangle \quad (2.47)$$

Since the reference system is composed of non-interacting electrons, its ground state wave function can be represented by a single Slater determinant as in the Hartree-Fock approach.

$$\psi_S = \frac{1}{\sqrt{N!}} \begin{pmatrix} \chi_i(\vec{x}_1) & \dots & \chi_k(\vec{x}_1) \\ \vdots & \ddots & \vdots \\ \chi_i(\vec{x}_N) & \dots & \chi_k(\vec{x}_N) \end{pmatrix} \quad (2.48)$$

Exact electron density can be calculated by finding orbitals  $\chi_i$ 's that minimize the energy functional. These orbitals are determined analogously to the HF theory, and in order not to cause confusion with HF orbitals they are named as Kohn-Sham orbitals or shortly KS orbitals.

$$h_i^{KS} \chi_i = \varepsilon_i \chi_i \quad (2.49)$$

where the one-electron Kohn-Sham operator is defined as

$$h_i^{KS} = -\frac{1}{2} \nabla_i^2 - \sum \frac{z}{|\vec{r}_i - \vec{r}_j|} + \int \frac{\rho(\vec{r}')}{|\vec{r}_i - \vec{r}'|} d\vec{r}' + V_{XC} \quad (2.50)$$

and exchange-correlation potential  $V_{XC}$  is given by the functional derivative,

$$V_{XC} = \frac{\delta E_{XC}}{\delta \rho} \quad (2.51)$$

In order to compute KS orbitals, we need to know density, but at the same time density is determined using the orbitals according to the Eq. (2.47). Thus, in a similar manner with HF theory, an iterative SCF procedure must be followed to solve the problem. This can be achieved by first guessing a starting density using the orbitals. By this way, KS orbitals, and also the Hamiltonian can be constructed. Solving the equation will give new density and this will be used for the next step. At the end, resulting densities will converge, and become self-consistent with the output density that in turn will be used to calculate the energy.

Despite having obvious common features between HF and Kohn-Sham approaches, while KS-DFT in principle exact, HF gives an approximate wave function. That is, if the exchange-correlation functional in KS approach was known, we could calculate the exact energy. However, since the HF approach does not take into account the electron correlation effects, it will remain as an approximation [95]. So, the only problem in KS-DFT is the unknown exchange-correlation energy functional. Many approximations for this functional have been proposed, some of them will be mentioned in the next section [82, 88, 96, 97].

### 2.3.4 Exchange Correlation Energy Functionals

As mentioned in the previous section, the fourth term of Eq. (2.50) is the functional derivative of exchange-correlation energy functional with respect to electron density. If  $E_{xc}[\rho(\vec{r})]$  is known, then  $V_{xc}(\vec{r})$  can be obtained, but the explicit form of the exchange-correlation energy is unavailable. Although, numerous approximations for  $E_{xc}[\rho(\vec{r})]$  have been developed, devising more accurate functionals is still the main problem in DFT [8]. A wide variety of papers have been published merely on developing, improving, testing and comparing the performance of functionals. This is because, the accuracy of the calculations is strongly correlated with the quality of the functionals and the choice of the functional also creates differences between various methods of DFT [89, 98]. In this part, we provide a brief overview for the most common functionals.

#### 2.3.4.1 Local Density Approximation

The Local Density Approximation (LDA) is the simplest approximation for the exchange-correlation energy functional, as suggested by Kohn and Sham [94] is based on the uniform (homogeneous) electron gas. In the LDA approach energy only depends on the density at a particular point, and is given by

$$E_{xc}^{LDA}[\rho(\vec{r})] = \int \rho(\vec{r}) \varepsilon_{xc}[\rho(\vec{r})] d\vec{r} \quad (2.52)$$

where the  $\varepsilon_{xc}$  is the exchange-correlation energy per electron in a uniform electron gas having electron density  $\rho(\vec{r})$ . The advantage of the LDA approach is that the

exchange-correlation functional can be accurately derived using the  $X\alpha$  model of Slater [99] in which, comparatively small correlation part of the exchange-correlation functional is ignored.

$$E_{XC}^{LDA}[\rho(\vec{r})] = E_x^{x\alpha}[\rho(\vec{r})] = -\frac{9}{8} \left( \frac{3}{\pi} \right)^{1/3} \alpha \int \rho(\vec{r})^{4/3} d\vec{r} \quad (2.53)$$

where  $\alpha$  is an empirical value. Although Kohn and Sham uses  $\alpha$  as 2/3 and Slater as 1, values between 1 and 2/3 such as 3/4 give more reasonable results for atoms and molecules [82].

#### 2.3.4.2 Local Spin Density Approximation

The local spin density approximation (LSDA) is an extension of LDA for the systems having one or more unpaired electrons i.e. for the open-shell systems. Introducing  $\rho(\vec{r})^\alpha$  (spin-up) and  $\rho(\vec{r})^\beta$  (spin-down), densities such that  $\rho(\vec{r}) = \rho(\vec{r})^\alpha + \rho(\vec{r})^\beta$ , the energy is given by:

$$E_{XC}^{LSDA}[\rho(\vec{r})^\alpha, \rho(\vec{r})^\beta] = \int [\rho(\vec{r})^\alpha + \rho(\vec{r})^\beta] \varepsilon_{XC}[\rho(\vec{r})^\alpha, \rho(\vec{r})^\beta] d\vec{r} \quad (2.54)$$

As in the LDA, exchange-correlation functional can also be accurately calculated in LSDA and for the systems in which all electrons are paired (i.e. for the closed systems) LSDA will yield same result with LDA [95].

#### 2.3.4.3 Generalized Gradient Approximation

In a real molecular system, the electron density is not uniform on the contrary to LDA approach. This limitation for LDA leads to the development of generalized gradient approximation (GGA), which takes into account the inhomogeneous nature of the electron density. So, GGA does not only depend on electron density, but also on its gradient, since the density is changing locally.

$$E_{XC}^{GGA}[\rho(\vec{r})] = \int \rho(\vec{r}) \varepsilon_{XC}(\rho(\vec{r}), \nabla\rho(\vec{r})) d\vec{r} \quad (2.55)$$

Despite the fact that GGA functionals generally give better results than LDA

especially for the structural parameters, both of them are not successful for the systems having strongly correlated electrons such as transition metal oxides [100]. Functionals proposed by Perdew, Burke and Enzerhof (PBE) [101,102] and Becke and Perdew (BP86) [103,104] can be given as examples for widely used GGAs.

More recently, meta-GGA functionals have been developed to reach the chemical accuracy by employing higher derivatives of the density. The exchange functional of Tao, Perdew, Staroverov, and Scuseria (TPSS) [105] is a popular meta-GGA functional showing good performance on properties such as, thermochemistry, kinetics and noncovalent interactions [106].

#### 2.3.4.4 Hybrid Functionals

Introduction of hybrid functionals is an important breakthrough in the improvement of DFT. Since the previously proposed DFT functionals have self-interaction problem, these new functionals are designed by adding exact Hartree–Fock exchange to the conventional DFT exchange–correlation functionals. The most common hybrid DFT functional is the B3LYP, which is based on Becke’s three-parameter exchange energy functional and Lee, Yang and Parr’s correlation energy functional [107-109]. Its energy functional expression is defined by

$$E_{XC}^{B3LYP} = (1 - A)E_X^{LSDA} + AE_X^{HF} + B\Delta E_X^B + (1 - C)E_C^{LSDA} + CE_C^{LYP} \quad (2.56)$$

where the constants A,B, and C are the empirical parameters, added to the equation in order to improve the accuracy of the functional [96]. B3LYP has proven the most preferred so far because of giving satisfactory results for predicting ground state properties of numerous chemical systems, such as organic compounds or transition metal containing systems [6, 110].

## 2.4 BASIS SETS

Choosing a basis set in electronic structure calculations highly important since it is directly related with the accuracy of the results and computational cost. So, what is a basis set? A basis set, is a set of mathematical functions representing the molecular



orbitals at particular points in space. Two common functions used to describe the orbitals are the Slater Type Orbitals (STO) and the Gaussian Type Orbitals (GTO). Slater type orbitals have the following general form (former in spherical polar coordinates and the latter in Cartesian coordinates),

$$\begin{aligned}\chi_{nlm} &= NY_{l,m}(\theta, \varphi)r^{n-1} \exp(-\zeta r) \\ \chi_{l_x l_y l_z} &= Nx^{l_x} y^{l_y} z^{l_z} \exp(-\zeta r)\end{aligned}\quad (2.57)$$

where  $n$  is the principal, and  $l$  and  $m$  are the angular momentum quantum numbers,  $N$  corresponds to normalization constant, and  $\zeta$  (zeta) is the orbital exponent. Although linear combinations of these functions will behave correctly, since the exponential is dependent on  $r$ , calculations of the integrals would be computationally difficult and this limits the use of STOs. STOs are generally preferred for atomic and diatomic systems when accurate description is needed, or in some DFT methods without exact exchange [89].

Gaussian type orbitals for Cartesian coordinates can be expressed as,

$$\chi_{l_x l_y l_z} = Nx^{l_x} y^{l_y} z^{l_z} \exp(-\zeta r^2) \quad (2.58)$$

where  $N$  is a normalization constant, and  $L = l_x + l_y + l_z$  determines the type of the orbital. For instance, if  $L$  is 0, it is  $s$  orbital, or if  $L$  is 1, it is  $p$  orbital, etc. As seen from the Eq. 2.58, a typical GTO is described by exponential  $r^2$ , which means simple computable functions, and makes it a common choice for the quantum chemists because of being computationally efficient.

On the other hand, most of the basis functions are designed to emphasize on core orbitals, which make big contributions to the total energy of an atom [111], whereas they show very tiny changes in chemical situations, e.g. chemical bonding. Hence, high computational costs on ignoring the chemically important circumstances bring about the construction of contracted basis sets. A linear combination of  $n$  Gaussian orbitals, which are also named as primitive GTOs (PGTO) are formed in order to make contracted GTO (CGTO) functions.

$$\chi(\text{CGTO}) = \sum_i^n c_i \chi_i(\text{PGTO}) \quad (2.59)$$

Primitive GTOs should provide an accurate representation of the atoms and their numbers used in the construction of CGTOs affect the computational cost significantly. Predictably, contracted basis sets are computationally efficient, but at the same time calculated energy with these basis sets would be higher. So, the problem is constructing such a basis set with significant accuracy and low computational cost.

### **2.4.1 Types of Basis Sets**

There are plenty of basis sets available in the quantum chemistry literature for the electronic structure calculations. In order to choose appropriate basis set for our specific calculation, we should also know pros and cons of the other basis sets. A brief description of some common basis sets is given below.

#### ***2.4.1.1 Minimal Basis Sets***

Minimal basis sets are the simplest basis sets in which the smallest number of functions are employed. For example, a minimal basis set for the H [ $1s^1$ ] atom would contain a single  $s$  function whereas it would contain two  $s$  functions and a single  $p$  function (with its three components) for the Ne [ $1s^2 2s^2 2p^6$ ] atom.

#### ***2.4.1.2 Zeta Basis Sets***

Doubling the number of basis functions will lead to us zeta basis sets. The name zeta comes from the exponent of STO/GTO functions, which we have mentioned in equations 2.57 and 2.58. So, for the H atom we would have two  $s$  functions, and for the Ne atom we would have four  $s$  functions and two  $p$  functions in a double zeta (DZ) basis set. It is also possible to have multiple zeta sets, by tripling or quadrupling of all basis functions.

#### ***2.4.1.3 Split-Valance Basis Sets***

Since the chemical bonding occurs between valance electrons, a small modification can be made over the basis functions related to these valance orbitals in an atom. This slight improvement in zeta basis sets will take us a step further, to the splint-valance basis sets. Although DZ or TZ can still be used for split-valance basis sets, they are generally referred as double zeta valance (DZV) or triple zeta valance (TZV) basis sets.

#### 2.4.1.4 Pople Basis Sets

Pople basis sets are one of the most popular contracted basis sets, developed by the Nobel Laureate John Pople and coworkers [112-119]. *STO-nG* and *k-nlmG* type basis sets are the typical examples for Pople basis sets.

In *STO-nG* types basis sets  $n$  corresponds to the number of Gaussian primitive functions (PGTOs), which are fitted to a STO. STO-3G, STO-4G and STO-6G are the widely used of this type basis sets.

In *k-nlmG* style basis set, which is also a split-valance basis set,  $k$  corresponds to the number of PGTOs describing the core orbitals, whereas the  $nlm$  show the number of PGTOs for representing valance orbitals. If the basis set contains only  $nl$ , it means a split-valance, and if it contains three of the  $nlm$  it means a triple split-valance basis set. To set an example for the split-valance basis set, in 3-21G, three PGTOs are used to describe the core electrons, and two PGTOs are used for the inner, and one PGTO is used for the description of the outer part of the valance orbitals. And 6-311G is an example for the three split-valance type basis sets, in which six PGTOs are used for representing the core electrons, and valance orbitals are a contraction of three, one and one PGTOs.

The quality of these mentioned basis sets can be improved by adding diffuse or polarization functions. Diffuse functions are generally added to obtain a better description for the anion geometries and denoted by one plus sign (+) or two plus signs (++). One plus sign means  $s$  and  $p$  diffuse functions are added to heavy atoms, and two plus signs mean  $s$  diffuse function is also added to the light atom, hydrogen. On the other hand, polarization functions are added in order to provide more flexibility and obtained by adding additional higher angular momentum functions, that is  $d$  or higher functions. These functions are commonly denoted by an asterisk \* or (d), and two asterisks \*\* or (d,p). Former refers to single  $d$  polarization function is added to heavy atoms, whereas latter refers to  $d$  function is added to heavy atoms, and  $p$  function is added to hydrogen. For example 6-311G+(d,p) is a three split-valance basis set including  $s$  and  $p$  diffuse functions on heavy atoms, and one  $d$  function on heavy atoms, and one  $p$  function on hydrogen.

#### **2.4.1.5 Dunning's Correlation-Consistent Basis Sets**

The correlation consistent (*cc*) basis sets are designed by Dunning and coworkers [120] in order to recover the correlation energy of the valence orbitals. The *cc* basis sets are optimized using CISD (configuration interaction with all single and double substitutions) wavefunctions. There are various sizes of *cc* basis sets, generally having the name as *cc-pVnZ*, meaning Dunning's correlation-consistent polarized valence *n* zeta basis set, where *n* corresponds to double, triple, quadruple, etc.

If diffuse functions (including small exponents) are added to these energy optimized *cc* basis sets, "aug" prefixes to *cc-pVXZ*, and so the basis set will be denoted by *aug-cc-pVnZ*. If the additional tight functions (with large exponents) are added to the *cc* basis sets in order to enhance core-valence and core-core correlation, the new basis set will be in the *cc-pCVnZ* form [89].

#### **2.4.1.6 Ahlrichs Def2 Basis Set Family**

Ahlrichs and coworkers [121, 122] proposed double, triple and quadruple zeta quality basis sets for the elements Li to Kr, and more recently Weigend and coworkers [123] extended these basis sets to the lanthanides. The abbreviation *def2* is used in order not to cause confusion, since previously in the TURBOMOLE program default basis sets were named as "def-bases" [124]. The *def2* family basis sets are composed of contracted GTOs, and polarization functions, P and PP can also be added to these new basis sets as a suffix, e.g. *def2-TZVPP*. It should not be forgotten that, P is designed for HF and DFT calculations, and PP is designed for post-HF calculations [125]. Although in the *def2* basis set family the quality of the basis sets is improved with the increasing sizes of basis sets (as in the most of the basis set types), each of these new basis sets are developed to give similar accuracy for the elements in the periodic table [124]. The *def2-SV(P)*, *def2-TZVP*, and *def2-QZVP* are the widely used and strongly recommended basis sets of this family.

#### **2.4.2 Effective Core Potentials (Pseudopotentials)**

As it is well known, lower parts of the periodic table contain heavy elements having large number of core electrons, which require a great number of basis functions to describe the corresponding orbitals. However, as it mentioned before chemically or

physically important properties are generally occurred in the valence orbitals, rather than core orbitals. As well as spending much of the computational effort to the less important part, the relativistic effects because of the interaction of the core electrons with the nucleus arise problems. In 1935, Hellmann solved these two problems by introducing the effective core potentials (ECPs) or pseudopotentials [96]. He suggested that core electrons would be replaced with analytical functions (pseudopotentials), which would lead more accurate and efficient description of orbitals. In order to construct these pseudopotentials, firstly valence orbitals should be described with a set of pseudo orbitals, then the core electrons should be replaced by a potential, which is composed of appropriate analytical functions. And finally constituents of this potential should be fitted such that the solutions are compatible with the all-electron wavefunction [89].

## **2.5 GENERAL CONSIDERATIONS**

### **2.5.1 Geometry Optimization**

In the geometry optimization process of DFT calculations, the main purpose is to find the equilibrium structures. In this regard, potential energy surfaces (PES) are important, because they are mathematical functions giving the potential energies of the molecules as a function of their geometries [95]. The potential energy of a molecule depends on the  $3N-6$  internal coordinates, which means it doesn't depend on the translation or rotation of a molecule.

All optimization algorithms (used in computational chemistry packages) try to find the stationary points on the potential energy surface. Minima and the saddle points are among the stationary points and these points can be found at places on the surface, where the gradients with respect to all internal coordinates are zero. However our purpose is to obtain lowest minimum, which is also named as global minimum, demonstrated in Fig. 2.2.

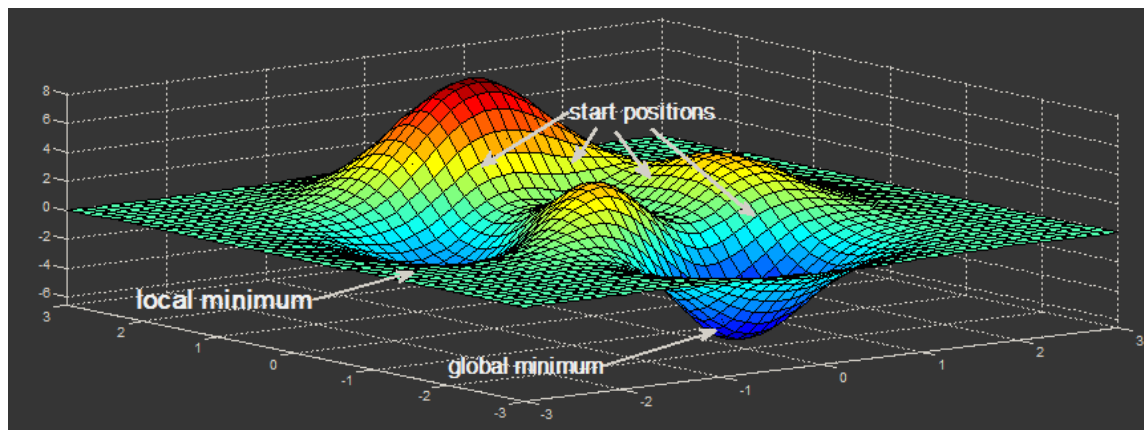


Figure 2.2 Geometry optimization, taken from the Ref. [126].

The global minimum or lowest minimum corresponds to the most stable geometry of the investigated molecule, whereas local minimum corresponds to the lowest point in some part of the potential energy surface. In the geometry optimizations we may also find saddle points, since the geometry optimizations tend to find the stationary points that are close to the initial geometries. At saddle points, gradient, i.e. first derivative of the energy is also zero, but different from the minima points second derivative gives negative eigenvalues. By means of the vibrational frequency calculations, minima or saddle points can be distinguishable. Obtaining non-negative frequencies indicates the minima points, whereas negative (imaginary) frequencies verify the saddle points. The number of imaginary frequencies is also important on the analysis of stationary points; finding one imaginary frequency corresponds to the transition state, and if the number of imaginary frequencies greater than 1, it means higher order saddle points.

### 2.5.2 Vibrational Frequency

As mentioned above, vibrational frequency calculations are also used to characterize the stationary points as minima or saddle points, and also to predict the infrared (IR) and Raman spectra of the molecules. The IR and Raman spectroscopy methods generally give information about the vibrational modes of substances and these substances can also be identified by their IR and Raman spectra. In this part, some basic information about IR and Raman spectroscopies will be provided.

### 2.5.2.1 Infrared Spectroscopy

Infrared (IR) spectroscopy deals with the interaction of energy with a molecule or more specifically, it is the absorption of IR radiation by matter. The IR spectroscopy yields information about the chemical constituents of the compounds and also their molecular structures. Organic, organometallic and polyatomic inorganic molecules can be investigated with this method [127].

In order for a molecule to absorb IR radiation there must be an overall change of the electric dipole moment during that particular vibration. The IR intensity depends on the magnitude of the dipole moment, and if there is no change in dipole moment during the vibration, these modes are called infrared-inactive.

On the electromagnetic spectrum IR region is between  $\sim 12800$ - $10\text{ cm}^{-1}$  wavenumber range and this region is also divided to three sub-regions [128]:

*Near-infrared region:* Mostly, overtones and harmonic vibrations are examined in this region. It is considered to lie between  $12800$ - $4000\text{ cm}^{-1}$ .

*Mid-infrared region:* It is in the  $4000$ - $200\text{ cm}^{-1}$  range. This is most widely used region in molecular spectroscopic studies. Fundamental vibrational modes of the molecules are generally found in this region.

*Far-infrared region:* Extends from  $200\text{ cm}^{-1}$  to  $10\text{ cm}^{-1}$ . It has low energy, generally vibrations of heavy atoms and lattice vibrations are investigated in this region. Since it is adjacent to the microwave region, it may also be used for rotational spectroscopy.

### 2.5.2.2 Raman Spectroscopy

As in the IR Spectroscopy, Raman spectroscopy also provides structural information about molecules, and can be used for the purity analysis of the compounds. However the working mechanism of the Raman method is totally different from the IR, because it is based on the collision of a monochromatic light with a molecule. Since the collision is inelastic, after the collision the scattered light has a different energy than the incident light upon interaction with the molecule [129]. Raman spectroscopy technique

measures this shift in energy, which corresponds to the energy of the vibrational transitions of molecules. Gaseous, liquid and solid samples can be analyzed with this method.

As distinct from the physical principles of IR spectroscopy, in order for Raman scattering to occur there must be a change in the polarizability of the molecule during the vibration. This is because Raman arises from the interaction of the polarizability with the normal modes of vibrations. And there is also a relationship between the polarizability of the atoms and their Raman intensities.

#### ***2.5.2.3 The Mutual Exclusion Principle***

IR and Raman spectroscopy are complementary methods, since one IR inactive mode may be Raman active or vice-versa. This difference in two methods stems from the different symmetry properties of the polarizability and dipole moment operators. The mutual exclusion principle states that no vibrational mode may be active in both IR and Raman spectra, in molecules with a center of symmetry [130].

However, in molecules with different symmetries, some modes may be both IR and Raman active or inactive, separately IR or Raman active. In complex molecules, modes are generally both IR and Raman active, sometimes with strong or weak bands depending on the polarizability or the dipole moment of the molecules [131].



## CHAPTER 3

### COMPUTATIONS

#### 3.1 HARDWARES AND SOFTWARES

All calculations were carried out on Linux server cluster (Clustered 13 HP DL Proliant Servers), which includes high performance computing supercomputer. Our supercomputer is designed to perform parallel computations up to 104 CPUs and 200 GB RAM. Gaussian software package (V. 03) [132] was used to perform quantum chemical calculations, and the geometries and the normal modes of the complexes were visualized by Gaussview [133]. Gabedit [134] was used to simulate vibrational spectra by pure Lorentzian band shapes with a bandwidth (FWHH) of  $10\text{ cm}^{-1}$  by using the scaled computational frequency of each mode and the corresponding calculated IR and Raman intensities. And finally VEDA [135] program was used to analyze potential energy distributions of the vibrational modes.

##### 3.1.1 Gaussian Program

The Gaussian program is based on the fundamental laws of quantum mechanics that is widely used by computational chemists, physicists, biophysicists, and other scientists having various fields. It can predict the energies, molecular geometries, vibrational frequencies and other properties of isolated molecules and reactions in different chemical environments. It includes HF, post HF, and TD-DFT methods as well as DFT. A wide variety of basis sets and effective core potentials can be used with these methods. Gaussview is its very practical and user-friendly graphical interface, which could build and display molecular structures, animate computation results, such as animation of normal modes and monitor and control all Gaussian calculations.

### 3.1.2 Gabedit

Gabedit is a freeware graphical interface that can be adapted to computational chemistry software packages, e.g. Gaussian. Related molecular properties can be processed directly from the output file of the computational chemistry softwares. With Gabedit, it is possible to display UV–visible, infrared, and Raman-computed spectra after a convolution, and it is also possible to display, analyze and animate molecules [134].

### 3.1.3 VEDA

Vibrational energy distribution analysis (VEDA) program is developed to calculate potential energy distribution (PED) contributions for molecules including up to 240 atoms. VEDA reads the Gaussian program output data directly, and to find the PED contributions it proposes an introductory set of local coordinates. The percentage PED results obtained by VEDA and the normal modes animation displayed by Gaussview generally complement each other [136].

## 3.2 CALCULATION DETAILS

Density Functional Theory and B3LYP [107-109] functional have been shown satisfactory for predicting ground-state properties of both organic compounds and transition metal complexes [30, 110, 137-140]. Besides, B3LYP has been proven [73] to give accurate bond lengths and vibrational frequencies with triple- $\zeta$  quality def2-TZVP basis set [124]. Therefore, calculations were performed in the gas phase at the B3LYP/def2-TZVP level, and in the calculations of cadmium, mercury and iodine including complexes, effective core potentials (ECP) were also used within this basis set. Def2-TZVP was downloaded from EMSL Basis Set Library [141] and used with GEN keyword in Gaussian 03 program package.

### 3.2.1 Geometry Optimization

Optimized geometries in the gas phase were obtained for the various possible spin states at DFT/B3LYP level of theory using the def2-TZVP basis set for all the atoms. Since Zn(II), Cd(II), and Hg(II) complexes have closed shell configurations (i.e. all

electrons are paired in spatial orbitals), they have no spin states, so in calculations their multiplicities were determined as 1. In order to determine ground state energies in the open shell complexes, the doublet, quartet and sextet spin state calculations were carried out for Mn(II), Co(II), and Cu(II) complexes, whereas the singlet, triplet, and quintet spin state calculations were performed for the Ni(II) complexes. Ground state energies of the tetracoordinate, pentacoordinate and hexacoordinate form of complexes were determined by considering all possible conformations around the metal ions and the spin states. Since, handling with open-shell complexes is computationally compelling than closed shell complexes, in the spin states except spin ground states, we have generally encountered SCF convergence problems, and re-optimized the complexes by using the checkpoint files of the ground state spin state with the “guess=read” keyword. In some cases the problem continued so we set the SCF convergence criterion to  $10^{-6}$ , which gives the same result with the default convergence criterion ( $10^{-8}$ ) for the optimization and the frequency calculations.

### **3.2.2 Charge and Spin Analysis**

Mulliken charge and spin distributions of the title compounds were obtained from default optimization calculation results. APT charges were also calculated with default vibrational frequency calculations. And as for natural charge distribution, single point energy calculations were performed with “Pop=NBORread” keyword at B3LYP/def2-TZVP level.

### **3.2.3 Vibrational Frequency Calculations**

Vibrational frequency calculations for the ground spin state of the complexes were calculated with the same level of theory calculations on the basis of the optimized geometries. In most complexes, there was no imaginary frequency, which means we have obtained ground state structures. However in Co(II) and Ni(II) complexes we have encountered with imaginary frequency problem. This is because transition metals have degenerate s and d orbitals, especially for the open-shell systems, so SCF convergence is quite compelling [4]. In our case, those imaginary frequencies mean our complexes converged to a saddle point instead of minima points. So we re-optimized our complexes until the ground-state energy was found.

Since the DFT calculations are performed in the gas phase, harmonic vibrational frequencies generally overestimate the experimental frequencies due to the neglect of anharmonicity [142]. General procedure for correcting these discrepancies is scaling the calculated frequencies. Therefore, we have determined scale factors for the vibrational frequencies of the free ligands p-toluidine and m-toluidine, respectively as 0.9771 ( $R^2 = 0.999$ ) and 0.9802 ( $R^2 = 0.999$ ) below the  $1700 \text{ cm}^{-1}$  and 0.9514 ( $R^2 = 0.732$ ) and 0.9465 ( $R^2 = 0.996$ ) above the  $1700 \text{ cm}^{-1}$  at def2-TZVP level and used these scale factors for the computed frequencies of the complexes.

The vibrational spectra of the free ligands and the complexes were simulated by pure Lorentzian band shapes with a bandwidth (FWHH) of  $10 \text{ cm}^{-1}$  and using the scaled computational frequency  $\nu_i$  of each mode  $i$  and the corresponding calculated IR ( $I_{IR}$ ) and Raman ( $I_{Ra}$ ) intensities.

### 3.2.2.1 Prediction of Raman Intensities

Raman intensity of each mode was obtained from its calculated Raman scattering activity ( $S_{Ra}$ ) by taking the laser excitation frequency  $\nu_0$  to be  $9398.5 \text{ cm}^{-1}$  ( $= 1064 \text{ nm}$ ) and using the following well-known formula of the scattering theory [143]:

$$I_{Ra,i} = \frac{f(\nu_0 - \nu_i)^4 S_{Ra,i}}{\nu_i \left[ 1 - \exp\left(-\frac{hc\nu_i}{kT}\right) \right]} \quad (3.1)$$

where  $h$ ,  $c$ , and  $k$  are Planck's constant, speed of light, and Boltzmann's constant;  $f$  is a normalization factor that is common for all peak intensities.

## CHAPTER 4

### RESULTS & DISCUSSIONS

Results of this study are provided and analyzed in this chapter under the three fundamental sections as molecular structures, charge and spin distributions and finally vibrational frequencies.

#### 4.1 MOLECULAR STRUCTURES

Optimized molecular geometries of the ligands p-toluidine and m-toluidine, and the related twenty transition metal complexes have been obtained in the gas phase at B3LYP/def2-TZVP level using Gaussian 03 program package. As mentioned in Chapter 3, ground state energies of the tetracoordinate, pentacoordinate and hexacoordinate form of open-shell complexes have been determined by considering all possible conformations around the metal ions and the spin states (doublet, quartet and sextet for the Mn(II), Co(II), and Cu(II) complexes; singlet, triplet, and quintet for the Ni(II) complex). As far as we know, in the literature there is no available X-ray data or theoretical calculation results for these complexes. Therefore we provide predictions for the molecular structures of the title complexes for the first time.

##### 4.1.1 Molecular Structures of the Free Ligands

Aniline derivatives are generally used as coordination ligands in transition metal complexes [17-26]. The addition of a CH<sub>3</sub> as a substituent group to aniline, results in diversity on structural and vibrational parameters, as well as charge distribution. P-toluidine and m-toluidine are used as the coordination ligands in this study consist of an amino and a methyl groups attached to a planar benzene ring at para- and meta-positions respectively (see Fig. 4.1).

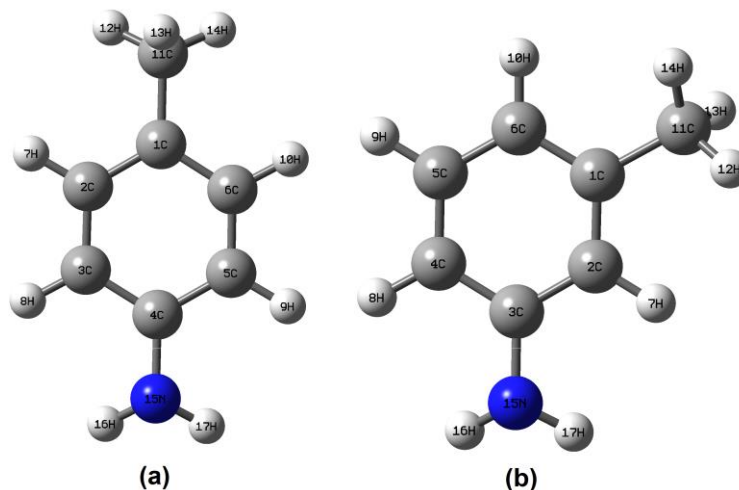


Figure 4.1 Optimized geometry parameters of a) p-toluidine and b) m-toluidine.

Molecular geometries of the p-toluidine and m-toluidine have been previously determined with HF, MP2, BVP86, and B3LYP methods, employing 6-31G (d), 6-31G(d,p), 6-311G+(d,p) basis sets [66, 67, 144, 145]. In this thesis, for the ligands we have employed def2-TZVP basis set at B3LYP level, in order to provide integrity with our title transition metal complexes and compared computed geometry parameters by means of experimental bond lengths and bond angles which are taken from Ref. [146].

Table 4.1 gives the computed geometry parameters of the ligands (p-toluidine and m-toluidine), and also experimental X-ray data of p-toluidine. Since the experimental X-ray data of m-toluidine is not available in the literature, we use geometry parameters of p-toluidine which has similar structure with m-toluidine. According to Table 1, experimental N-H bond length is 1.02 Å, and computed bond lengths are ~1.01 Å both for p-toluidine and m-toluidine being very close to the experimental data. Computed C-N bond length of p-toluidine is a bit longer than from m-toluidine, due to the para position of the substituent group. C-C bond lengths are also close to the experimental bond lengths, varying with a very small difference between two ligands. According to the X-ray data, the bond distance between C and CH<sub>3</sub> is 1.55 Å, whereas it is computationally 1.51 Å in both of the ligands. Computed C-H bond lengths of the ring and methyl group have exactly same values (respectively, 1.08 Å and 1.09 Å) with the experimental result for both of the ligands. Computed bond angles are also in agreement with the experimental data, e.g. the angle

between H-N-H is experimentally 113° and computationally ~112°, whereas the angle between H-C-H in the methyl group is experimentally 109° and computationally ~108° for both of the ligands. C-C-C angles in the rings differ 1-2° in the p-toluidine and m-toluidine due to the position of the CH<sub>3</sub>.

Table 4.1 Geometry parameters of p-toluidine and m-toluidine.

	Exp <sup>a</sup>	B3LYP/def2-TZVP	
		p-toluidine	m-toluidine
<b>Bond Lengths (Å)</b>			
N-H <sup>b</sup>	1.02	1.007	1.008
C-N	1.43	1.397	1.394
C3-C4	1.36	1.398	1.399
C3-C2	1.39	1.388	1.399
C1-C2	1.40	1.395	1.392
C1-C6	1.39	1.395	1.396
C5-C6	1.40	1.388	1.390
C4-C5	1.39	1.398	1.387
C-CH <sub>3</sub>	1.55	1.507	1.507
C-H (Ring) <sup>b</sup>	1.08	1.084	1.084
C-H (Methyl) <sup>b</sup>	1.09	1.092	1.092
<b>Bond Angles (Degree)</b>			
H-N-H	113.0	111.9	112.2
H-C-H (Methyl) <sup>b</sup>	109.5	107.4	107.6
C6-C1-C2	117.8	117.1	118.9
C1-C2-C3	120.5	121.8	121.6
C2-C3-C4	120.5	120.6	118.7
C3-C4-C5	120.3	118.0	119.9
C4-C5-C6	119.2	120.6	120.9
C5-C6-C1	121.5	121.8	119.9

<sup>a</sup>; Experimental X-ray data of p-toluidine [146] <sup>b</sup>; Average Value.

Therefore, calculated bond lengths and bond angles obtained with def2-TZVP basis set are very close to the experimental data, having small values of mean absolute errors (MAE) and linear correlation coefficient (R<sup>2</sup>) values very close to 1, for both of the ligands. For bond lengths, these values are respectively 0.015 and 0.984 for p-toluidine and 0.016 and 0.983 for m-toluidine. However for bond angles MAE and R<sup>2</sup> values are respectively 1.164 and 0.926 for p-toluidine and 1.300 and 0.913 for m-toluidine.

### 4.1.2 Molecular Structures of the Metal Bromide Complexes of P-toluidine

In this section, molecular structures of the Mn(II), Co(II), Ni(II), Cu(II), Zn(II), Cd(II), and Hg(II) bromide complexes of p-toluidine are explained in detail. Optimized molecular structures and the key geometry parameters around the metal atom of the title complexes are given in Fig. 4.2, Fig. 4.3 and Table 4.2, and in the following we will not discuss the species those lie more than 10 kcal/mole above the ground-state-species.

Table 4.2 The key geometry parameters around the metal ion of the p-toluidine bromide complexes.

	Mn comp.	Co comp.	Ni comp.	Cu comp.	Zn comp.	Cd comp.	Hg comp.
<b>Bond Lengths (Å)</b>							
M–Br <sup>a</sup>	2.545 (2.620) <sup>b</sup>	2.386	2.711	2.433	2.364	2.525	2.485
M–L <sup>a</sup>	2.481	2.145	2.186	2.097	2.213	2.500	2.790
C–N <sup>a</sup>	1.405	1.438	1.402	1.439	1.434	1.427	1.412
<b>Bond Angles (Degree)</b>							
L <sub>1</sub> –M–L <sub>2</sub>	167.6	107.9	177.9	179.9	98.36	92.27	85.31
Br–M–Br <sup>a</sup>	120.0	136.5	90.01	179.9	138.4	150.2	164.8
M–N–C <sup>a</sup>	128.3	115.7	127.9	117.3	116.2	114.8	115.6
H–N–H <sup>a</sup>	111.1	108.4	110.0	110.1	108.6	108.0	110.3
<b>Torsion Angles (Degree)</b>							
C–N(L <sub>1</sub> )–M–N(L <sub>2</sub> )	120.8	2.398	-96.52	178.6	179.6	-179.9	-163.8
C–N(L <sub>2</sub> )–M–N(L <sub>1</sub> )	120.3	-171.9	-97.03	1.422	-0.180	-0.001	2.891

<sup>a</sup>; Average Value. <sup>b</sup>; One of the Mn–Br bonds is significantly longer than the other two bonds. Therefore, it is not included in the average and given as a separate value in parentheses.

According to the experimental studies performed by Ahuja, Allen, and Gölcük et al. [24, 40, 41], the magnetic and electronic data suggest polymeric octahedral environments around the Mn and Ni complexes in the solid phase that have the chemical formula of ML<sub>2</sub>Br<sub>2</sub>. This is possible through two bridging bromides in the solid phase for the hexa-coordinate complex. This suggests that the ML<sub>2</sub>Br<sub>2</sub> complexes of the solid phase resemble structurally and electronically more to the isolated [ML<sub>2</sub>Br<sub>4</sub>]<sup>2-</sup> in the gas phase that include all the atoms in the coordination spheres. Therefore, we performed geometry optimizations for the isolated hexa-coordinate



complexes of  $[\text{ML}_2\text{Br}_4]^{-2}$  for  $\text{M} = \text{Mn}$  and  $\text{Ni}$ . However, the optimizations give stationary points only for the hexa-coordiante Ni complex. So we also performed geometry optimization for the penta-coordiante Mn complex of the form  $[\text{ML}_2\text{Br}_3]^{-1}$ . And this time we found stationary points. The lowest energy species of the isolated penta-coordinate Mn complex is a sextet ( $S = 5/2$ ) while that of the isolated hexa-coordiante Ni complex is a triplet ( $S = 1$ ). Hence, the polymeric structures of the Mn and Ni complexes share one and two bromides of the neighboring complex in the solid phase, respectively, as shown in Fig. 4.2a and Fig. 4.2b.

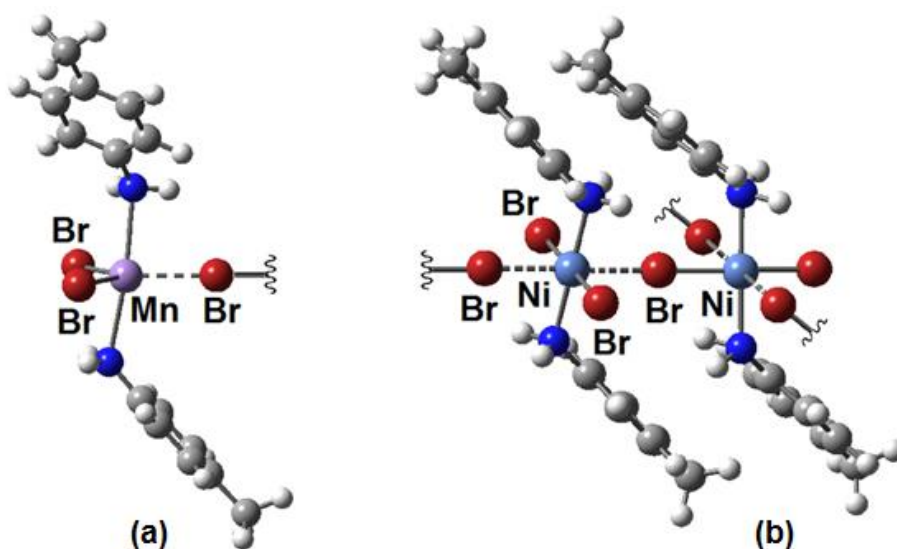


Figure 4.2 Optimized geometries of the Mn and Ni bromide complexes of p-toluidine in solid phase.

For the Co, Zn, Cd, and Hg complexes we have obtained several stable tetrahedral conformers that differ in the orientation of p-toluidine (Fig. 3a). Among those, Conf. 1 is the ground state species and the next lying species (Conf. 2) is only (as an average)  $\sim 5$  kcal/mole above it. For the Cu complex, we have found square planar environment as in the Fig. 4.3b. Since the Co and Cu complexes have open-shell configurations, Co complex is found as quartet ( $S=3/2$ ), and Cu complex is found as doublet ( $S=1/2$ ).

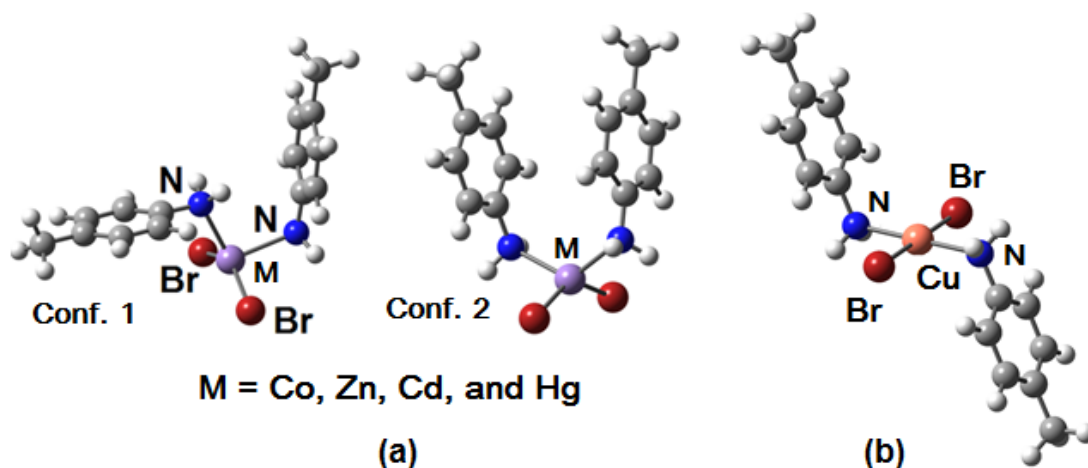


Figure 4.3 Optimized geometries of the Co, Zn, Cd, Hg, and Cu bromide complexes of p-toluidine.

In Co, Cu, Zn, Cd, and Hg complexes, metal-bromine bond lengths lie between 2.36-2.53 Å, and metal-ligand bond lengths are between 2.10-2.79 Å. In Co, Cu, Zn and Cd complexes metal-bromine bond lengths are found to be longer than metal-ligand bond lengths, whereas in Hg complex metal-ligand bond length is found to be longer than metal-bromine bond length. These differences in metal-bromine and metal-ligand bond lengths show that these complexes have distorted geometries. For the free p-toluidine, C-N bond length is 1.397 Å at B3LYP/def2-TZVP level, however in all of the bromide complexes of p-toluidine these bond lengths are found to be longer (having average value 1.422 Å) due to the complexations occur via nitrogen atom of the free ligand.

Although bromine-metal-bromine and ligand-metal-ligand angles have the same value for the Cu complex because of square planar configuration, these angles differ for other complexes. Metal-ligand-carbon angles of Mn and Ni complexes bigger than other complexes due to the penta and hexa-coordinate of these complexes. H-N-H angles are close to each other for all of the complexes. On the other hand complexation affects H-N-H angle causing decrease in the angle from  $\sim 112^\circ$  to  $\sim 109^\circ$  in the complexes when compared with free p-toluidine. C-N-Metal-N dihedral angles also vary according to the geometrical structures of the complexes (see Table 4.2).

### 4.1.3 Molecular Structures of the Metal Iodide Complexes of P-toluidine

In this part, molecular structures of Ni(II), Zn(II), and Cd(II) iodide complexes of p-toluidine are investigated. Optimized geometries have been obtained with same level of calculations (given in Fig. 4.4), and some important parameters around the metal atoms of the complexes are shown in Table 4.3.

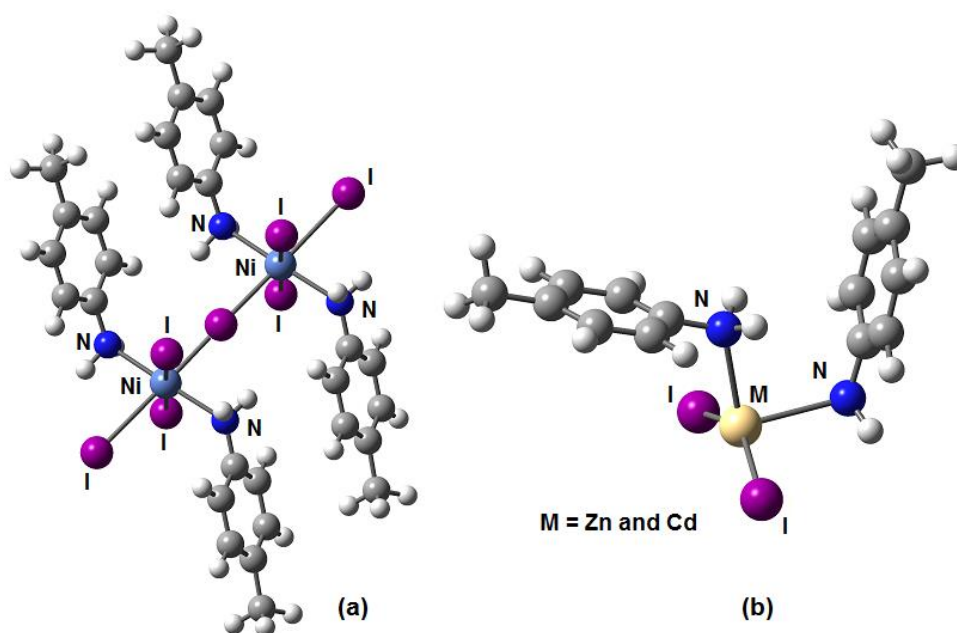


Figure 4.4 Optimized molecular geometries of the Ni (in solid phase), Zn, and Cd iodide complexes of p-toluidine.

For the Ni complex, Ni(II) ion in the complex was found monomeric distorted octahedral in the UV-Vis study performed by Altun et al. [22]. On the other hand Engelter et al. [19] states the polymeric octahedral coordination of Ni(II) complexes according to the color and magnetic moments. Being consistent with the Engelter's results, in our calculations we also predict the structure of Ni complex as distorted polymeric octahedral having nickel-bromine bond length as 2.99 Å and nickel-ligand bond length as 2.16 Å (see Fig. 4.4a). Among singlet, triplet and quintet calculations, the lowest energy species is obtained for triplet having  $S=1$ .

Table 4.3 The key geometry parameters around the metal ion of the p-toluidine iodide complexes.

	Ni comp.	Zn comp.	Cd comp.
<b>Bond Lengths (Å)</b>			
M-I <sup>a</sup>	2.988	2.564	2.712
M-L <sup>a</sup>	2.162	2.223	2.518
C-N <sup>a</sup>	1.414	1.434	1.426
<b>Bond Angles (Degree)</b>			
L <sub>1</sub> -M-L <sub>2</sub>	177.6	97.17	90.60
I-M-I <sup>a</sup>	90.00	136.1	147.8
M-N-C <sup>a</sup>	128.4	116.7	115.5
H-N-H <sup>a</sup>	108.7	108.5	108.9
<b>Torsion Angles (Degree)</b>			
C-N(L <sub>1</sub> )-M-N(L <sub>2</sub> )	-96.36	-180.0	-0.117
C-N(L <sub>2</sub> )-M-N(L <sub>1</sub> )	-99.74	-0.584	-179.9

<sup>a</sup>; Average Value.

The density functional calculations predict the molecular structures of Zn and Cd complexes as distorted tetrahedral, being in agreement with the previous experimental and theoretical study on these complexes [22]. Supporting this information metal-iodine and metal-ligand bond lengths are respectively 2.56 Å and 2.22 Å for Zn complex, and 2.71 Å and 2.52 Å for the Cd complex. Because of the complexation occurred from the nitrogen atom of the free p-toluidine, an increase from 1.397 Å (p-toluidine) to ~1.425 Å (average value for the complexes) is observed in the C-N bond lengths of the complexes.

On the other hand, ligand-metal-ligand and iodine-metal-iodine angles are in parallel with each other in tetrahedral (Zn and Cd) complexes whereas it is quite different in octahedral (Ni) complex. H-N-H angle is ~112° in the free p-toluidine and this angle is decreased to ~109° in complexes, having almost same values for three of the complexes.

#### 4.1.4 Molecular Structures of the Metal Bromide Complexes of M-toluidine

Molecular structures of the Mn(II), Co(II), Ni(II), Cu(II), Zn(II), Cd(II), and Hg(II) bromide complexes of m-toluidine are represented in this part. As in the Mn and Ni bromide complexes of p-toluidine, we have calculated penta- and hexa- coordinate

complexes of  $[\text{ML}_2\text{Br}_3]^{-1}$  and  $[\text{ML}_2\text{Br}_4]^{-2}$  for  $\text{M} = \text{Mn}$  and  $\text{Ni}$ ,  $\text{L} = m\text{-toluidine}$ . And we have obtained stable conformers only for penta-coordinate Mn complex and for hexa-coordinate Ni complex, which mean in the solid phase Mn complex is sharing one of the bromines (Fig. 4.5a), whereas Ni complex is sharing two bromides with the neighbor complex (Fig. 4.5b). Calculations also predict Mn complex as sextet, and Ni complex as triplet for the ground state structures.

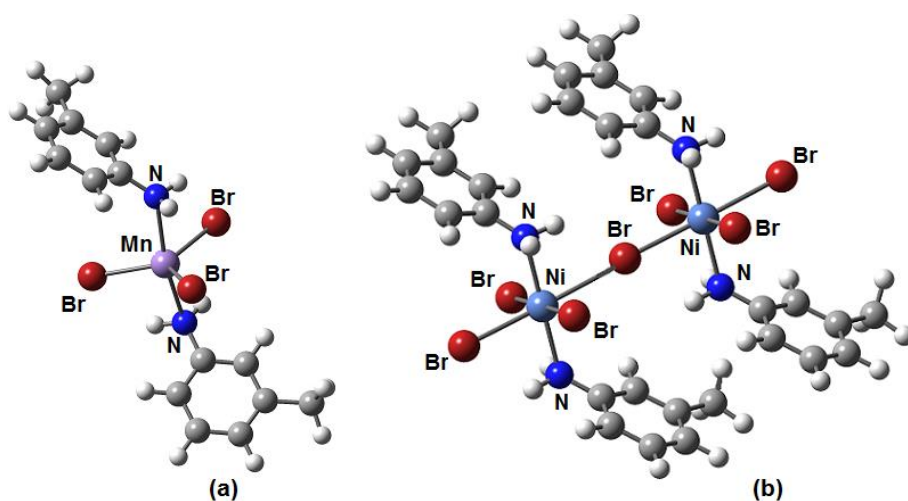


Figure 4.5 Optimized geometry parameters of Mn and Ni bromide complexes of *m*-toluidine in solid phase

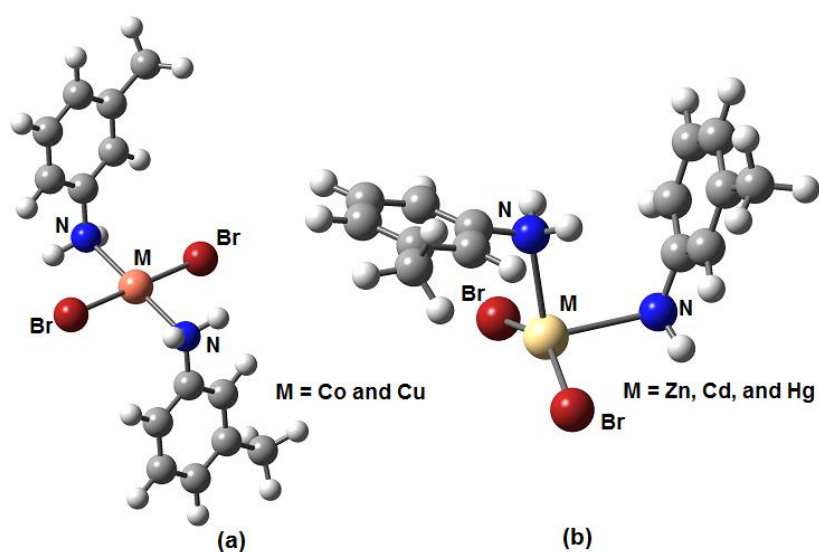


Figure 4.6 Optimized geometries of Co, and Cu complexes and Zn, Cd and Hg bromide complexes of *m*-toluidine.

According to the Fig. 4.6 and Table 4.4, calculations suggest square planar geometries for the Co and Cu complexes, and distorted tetrahedral structures for the Zn, Cd and Hg complexes. Metal-bromine bond lengths of these complexes are longer than the metal-ligand bond lengths except for the Hg complex, having a longer metal-ligand bond length. An increase in the C-N bond length with respect to free ligand (m-toluidine) is also observed for these complexes from 1.394 Å to ~1.423 Å. DFT calculations predict Co complex as doublet, different from the  $\text{CoBr}_2(\text{p-tol})_2$ , and Cu complex as also doublet in parallel with the  $\text{CuBr}_2(\text{p-tol})_2$ . Co and Cu complexes have exactly same values for the ligand-metal-ligand and bromine-metal-bromine angles as  $180^\circ$  (see Fig. 4.6a) and Zn, Cd, and Hg complexes have similar values for these angles and same structures (see Fig. 4.6b). Metal-ligand-carbon angles differ according to the complex geometries. 5- and 6 coordinated complexes have larger metal-ligand-carbon angles than the 4-coordinated structures. Change in H-N-H angles with respect to free m-toluidine is also observed for metal bromide complexes of m-toluidine. This angle changed from  $\sim 112^\circ$  (for m-toluidine) to  $\sim 110^\circ$  (average value for the title complexes). Although dihedral angles are generally different for each of the complexes, Co and Cu complexes have very close values for the C-N-M-N torsion angles.

Table 4.4 The key geometry parameters around the metal ion of the m-toluidine bromide complexes.

	Mn comp.	Co comp.	Ni comp.	Cu comp.	Zn comp.	Cd comp.	Hg comp.
<b>Bond Lengths (Å)</b>							
M-Br <sup>a</sup>	2.543 (2.616) <sup>b</sup>	2.395	2.710	2.432	2.364	2.525	2.484
M-L <sup>a</sup>	2.490	2.018	2.191	2.100	2.214	2.501	2.793
C-N <sup>a</sup>	1.403	1.449	1.401	1.439	1.433	1.426	1.411
<b>Bond Angles (Degree)</b>							
L <sub>1</sub> -M-L <sub>2</sub>	167.8	180.0	179.8	180.0	98.83	92.83	84.52
Br-M-Br <sup>a</sup>	120.0	180.0	90.00	180.0	138.2	149.9	164.6
M-N-C <sup>a</sup>	128.5	117.6	127.8	117.5	116.1	114.8	115.0
H-N-H <sup>a</sup>	111.3	109.0	110.2	110.2	108.7	109.2	110.4
<b>Torsion Angles (Degree)</b>							
C-N(L <sub>1</sub> )-M-N(L <sub>2</sub> )	120.4	92.86	-93.10	94.23	-0.028	2.965	-0.441
C-N(L <sub>2</sub> )-M-N(L <sub>1</sub> )	120.2	87.60	-97.18	86.50	-168.5	-170.6	-172.8

<sup>a</sup>; Average Value. <sup>b</sup>; One of the Mn-Br bonds is significantly longer than the other two bonds as in the  $\text{MnBr}_2(\text{p-tol})_2$ .

#### 4.1.5 Molecular Structures of the Metal Iodide Complexes of *m*-toluidine

In this section molecular structures of Ni(II), Zn(II), and Cd(II) iodide complexes of *m*-toluidine are investigated. For the title complexes, B3LYP/def2-TZVP level calculations predict geometrical structures around the metal atoms similar with the iodide complexes of *p*-toluidine.

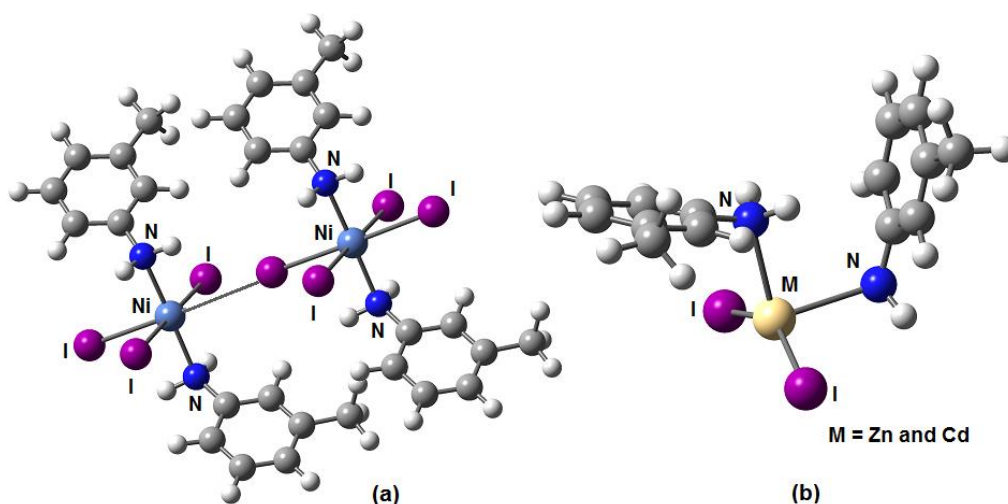


Figure 4.7 Optimized geometry parameters of Ni (in solid phase), Zn and Cd complexes.

Stable conformer for the Ni complex has been obtained only for  $[ML_2I_4]^{-2}$  having metal-iodine bond length as 2.99 Å and metal-ligand bond length as 2.16 Å which suggest distorted octahedral structure around the nickel atom (Fig. 4.7a). DFT calculations also predict Ni complex as triplet ( $S=1$ ).

Since Zn and Cd complexes have closed-shell configurations ( $S=0$ ), calculations have performed with multiplicities as 1. Optimized geometrical structures of Zn and Cd complexes are given in Fig. 4.7b and the key geometry parameters around the metal atoms of all three complexes are provided in Table 4.5. According to the Table 4.5, metal-iodine bond lengths are longer than metal-ligand bond lengths for both Zn and Cd complexes, which supports distorted tetrahedral environment around the metal atom.

Due to coordination occurs via nitrogen atom of the m-toluidine, C-N bond lengths of m-toluidine are increased in the complexes from 1.394 Å to 1.424 Å, H-N-H angles are decreased from ~112° to ~109° consistent with all other complexes. As seen from Table 4.5, bond angles and dihedral angles have very close values for Zn and Cd complexes, supporting the given structure in Fig. 4.7b.

Table 4.5 The key geometry parameters around the metal ion of the m-toluidine iodide complexes.

	Ni comp.	Zn comp.	Cd comp.
<b>Bond Lengths (Å)</b>			
M-I <sup>a</sup>	2.988	2.565	2.712
M-L <sup>a</sup>	2.162	2.221	2.521
C-N <sup>a</sup>	1.414	1.434	1.425
<b>Bond Angles (Degree)</b>			
L <sub>1</sub> -M-L <sub>2</sub>	178.7	97.78	91.21
I-M-I <sup>a</sup>	90.00	136.1	147.5
M-N-C <sup>a</sup>	128.0	116.6	115.0
H-N-H <sup>a</sup>	108.8	108.6	109.2
<b>Torsion Angles (Degree)</b>			
C-N(L <sub>1</sub> )-M- N(L <sub>2</sub> )	-94.89	5.976	4.813
C- N(L <sub>2</sub> )-M- N(L <sub>1</sub> )	-101.8	-170.9	-167.5

<sup>a</sup>; Average Value.



## 4.2 CHARGE AND SPIN DISTRIBUTION

In this section Mulliken, natural bond orbital (NBO), and atomic polar tensor (APT) charge analyses are performed for all compounds including ligands, whereas Mulliken spin analyses is performed only for the complexes having open-shell configurations. Computations of atomic charges and spins are important since they are directly related with the molecular structures and properties of the compounds. However accurate calculations on charge distributions are challenging. Since the default optimization and energy calculations provide the Mulliken charge results, it is one of the traditional and most widely used methods for charge distribution analysis. But at the same time, it is basis set dependent and thus have weaknesses in predicting inaccurate results at some basis sets [147, 148]. Natural charges provided by the NBO method are based on the investigation of the atomic and molecular orbitals and mostly give good results, having no basis set dependency. Apart from these methods APT charges are based on the parametrization of the experimental infrared intensities, and can be directly obtained from default vibrational frequency calculations. If the observed infrared frequencies are consistent with the computed frequencies, mostly APT charge results are also accurate [149]. In order to obtain physically meaningful results on charge distributions of atoms, we apply traditional Mulliken method with the more improved NBO and APT charge analysis methods at B3LYP/def2-TZVP level for our all compounds.

### 4.2.1 Charge Distribution of the Free Ligands

P-toluidine and m-toluidine are the ligands used for coordination in this study. Both of the ligands include amino and methyl groups at different positions, and independent from their positions these CH<sub>3</sub> and NH<sub>2</sub> groups are accepted as the electron donors of the aromatic ring compounds [144].

Mulliken, NBO, and APT charge distributions of the ligands are provided in Fig. 4.8 consistent with the numbering scheme of atoms given in Fig.4.1. Although Mulliken charge distribution is giving unnatural results for most of the basis sets [147, 148], in this study for both of the free ligands we have obtained compatible results with the NBO and APT analyses by using def2-TZVP basis set.

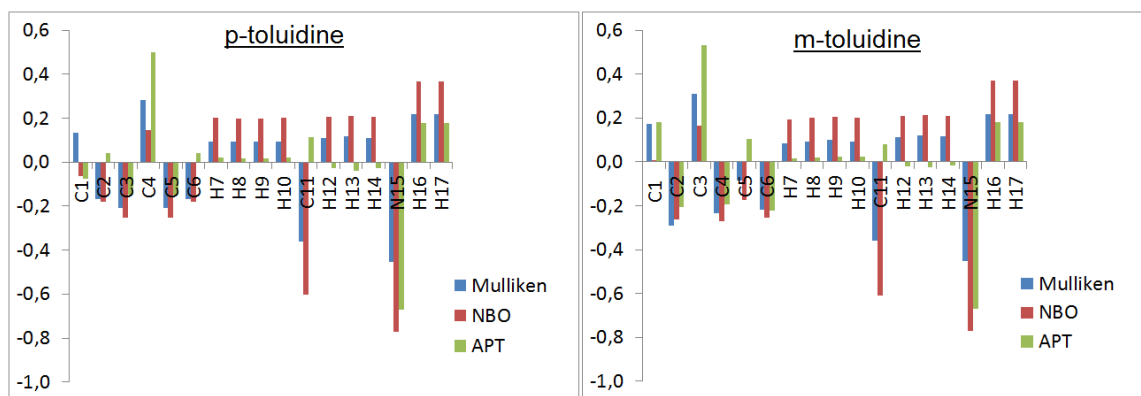


Figure 4.8 Charge distributions of p-toluidine and m-toluidine with Mulliken, NBO, and APT methods.

According to the Fig. 4.8 charge distributions are mostly in agreement with three of the methods, having small differences. Nitrogen atom is found to be most negative in all methods, and C4 of p-toluidine and C3 of m-toluidine which are bonded with nitrogen atom found to have positive charges as expected. C11 atoms of ligands are negative in Mulliken and NBO methods, whereas it is positive in APT method. According to Mulliken and APT analyses, C4 of p-toluidine and C3 of m-toluidine are the most positive, however for NBO hydrogen atoms of the amino group are found to have most positive charges.

#### 4.2.2 Charge and Spin Distribution of the Metal Bromide Complexes of P-toluidine

Charge distribution of the Mn, Ni, Co, Cu, Zn, Cd, and Hg bromide complexes of p-toluidine have been analyzed by means of Mulliken, NBO, and APT methods at B3LYP/def2-TZVP level (see Fig. 4.9). Although Mulliken method is known for giving unnatural results on charges of atoms, in our study for the metal bromide complexes of p-toluidine its results are mostly in agreement with other methods. Unsurprisingly, for the Mn, Ni, Co, Zn and Hg complexes the most positive charges are located on metal atoms, and the most negative charges are located on the nitrogen and bromine atoms in all three methods. On the other hand, in Cu complex, C3 atom is found to have most positive charges instead of Cu atom with the Mulliken method, whereas NBO and APT predicting accurate results. On the contrary in Cd complex, NBO method finds most positive charges on hydrogen atoms instead of cadmium atom, while Mulliken and NBO finds most positive charges on the metal atom as expected.

If we order the quantity of the positive charges found on metals, we see that,

In Mulliken;  $Mn = Cd > Hg > Co = Ni = Zn > Cu$

In NBO;  $Mn > Ni > Zn > Hg > Co > Cu > Cd$

In APT;  $Mn > Ni > Zn > = Cd > Co = Hg > Cu$

Therefore, it can be said that at the B3LYP/def2-TZVP level, prediction of APT charges for all complexes are better than other methods, and except Cu, and Cd complexes all of the three methods predict meaningful charge distribution results on metal bromide complexes of p-toluidine.

As for spin analysis, the ground-state species of the title complexes have pure spin states with almost no spin contamination, indicated from the calculated  $S^2$  values that deviate from the ideal value by less than 0.01. According to possible spin-state calculations Mn complex is found as sextet ( $S=5/2$ ), Ni complex as triplet ( $S=1$ ), Co complex as quartet ( $S=3/2$ ) and finally Cu complex is found as doublet ( $S=1/2$ ). The unpaired spins are mainly located on the metal ions ( $4.81e$  on Mn corresponding to 96%,  $1.56e$  on Ni corresponding to 78%,  $2.66e$  on Co corresponding to 89% and  $0.44e$  on Cu corresponding to 44%). The remaining amount of the spin density is accumulated mostly on Br atoms.

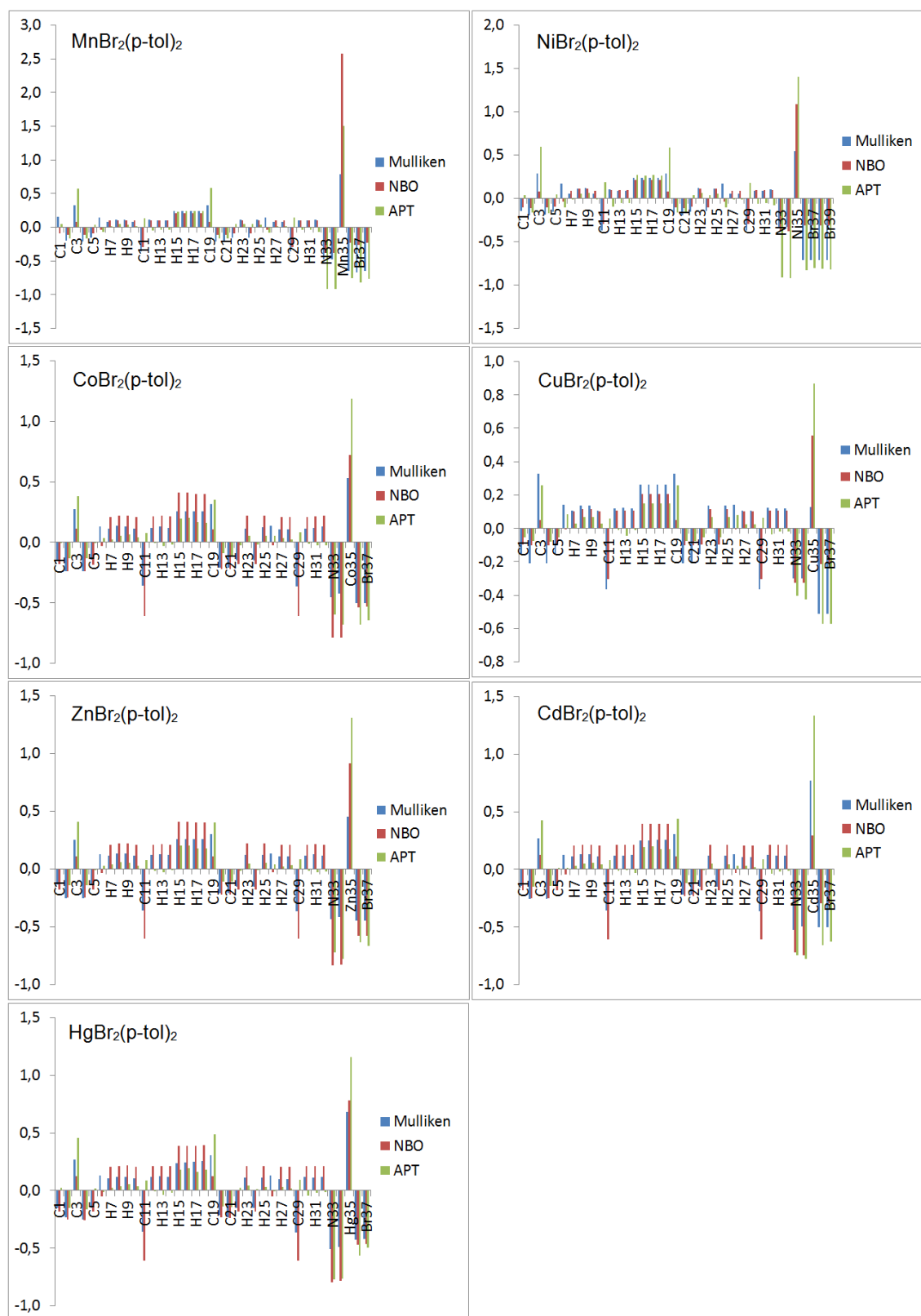


Figure 4.9 Mulliken, NBO, and APT charge distributions of metal bromide complexes of p-toluidine.

### 4.2.3 Charge and Spin Distribution of the Metal Iodide Complexes of P-toluidine and M-toluidine

Mulliken, NBO, and APT charge distributions of the metal (Ni, Zn, and Cd) iodide complexes of p-toluidine and m-toluidine are provided together in Fig. 4.10. Different from the metal bromide complexes, we have obtained inaccurate results for charge distributions of metal iodide complexes in the NBO analysis. The reason for this may be iodine is heavier than bromine, and located in the lower part of the periodic table having large number of core electrons. Since effective core potential (ECP) is used for the iodine containing systems at def2-TZVP level, it may have been affected our natural charge distribution results negatively. In our computations, physically most meaningful results are obtained with APT method. Despite of the shortcomings of Mulliken analysis, results of the Mulliken are also quite well, having accordance with the APT charges. Therefore, for the metal iodide complexes of p-toluidine and m-toluidine NBO charge analysis results are not trustworthy.

The order of positive charges located on metal atoms for p-toluidine and m-toluidine complexes;

Mulliken for p-toluidine and m-toluidine complexes:  $Cd > Ni > Zn$

NBO: As mentioned above, negative charges are found on metals.

APT for p-toluidine complexes:  $Ni > Zn = Cd$ , for m-toluidine complexes  $Ni = Zn = Cd$ .

If we compare p-toluidine and m-toluidine complexes, in APT and Mulliken methods, all hydrogen atoms are found mostly positive and carbon atoms are found negative as in the case of free ligands. We can also observe that most positive charges are located on nickel, zinc and cadmium atoms, and most negative charges are accumulated on nitrogen and iodine atoms as expected.

Since zinc and cadmium complexes have closed shell configurations, spin analysis is only performed for the nickel complexes. Computed  $S^2$  values are found 2.007 for both Ni complexes, which mean there is no spin contamination. The unpaired spins are mostly accumulated on nickel atoms 1.49e on nickel (~74%) and 0.42e on iodine atoms (~21%) in both of the nickel complexes of p-toluidine and m-toluidine.

Ground state Ni complexes also found as triplet having  $S=1$  among singlet, triplet and quintet computations.

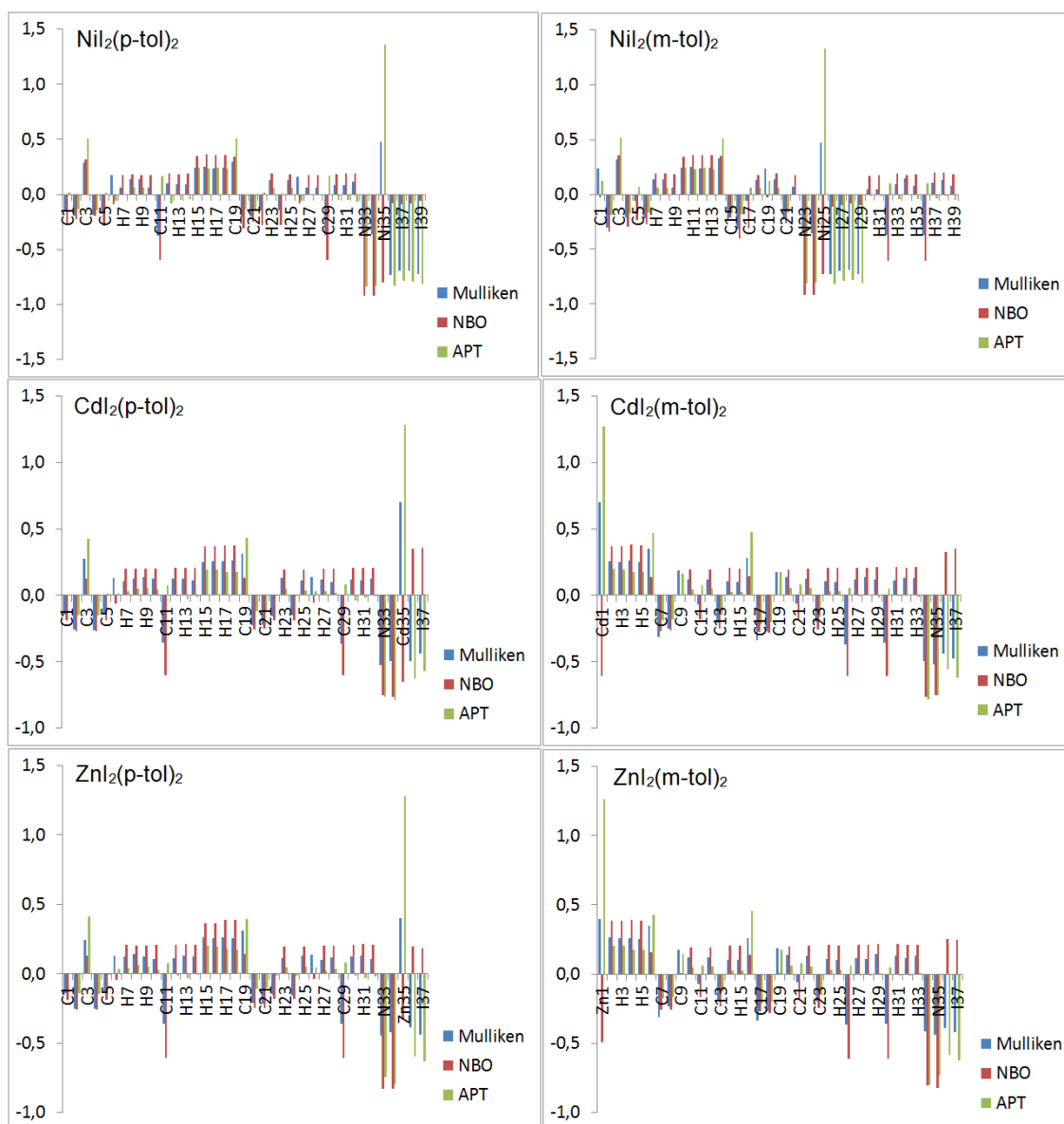


Figure 4.10 Mulliken, NBO, and APT charge distributions of Ni, Zn, and Cd complexes of p-toluidine and m-toluidine.

#### 4.2.4 Charge and Spin Distribution of the Metal Bromide Complexes of M-toluidine

Charge distributions of metal bromide complexes of m-toluidine are provided in Fig. 4.11 by means of Mulliken, NBO and APT methods. As in the case of metal bromide complexes of p-toluidine, APT charges are the physically most meaningful ones among three methods for all of the title complexes. Natural charges obtained with NBO also predict good results, except for Cd and Hg complexes. As it is mentioned above the reason for this may be the usage of ECP potential in cadmium and mercury complexes. Mulliken charge results for Co and Cu complexes are not accurate; having the most positive charges on one of the hydrogen atoms instead of metal atoms.

The positive charges on metal atom of the m-toluidine bromide complexes follow the trends;

In Mulliken:  $Mn = Cd > Hg > Ni = Zn > Co > Cu$

In NBO:  $Hg > Zn > Ni = Cu > Mn > Co > Cd$

In APT:  $Mn > Ni > Zn = Cd > Hg > Cu > Co$

In terms of having physically meaningful results, in all of the complexes most positive charges are found on metal atoms, and most negative charges are found on nitrogen and bromine atoms via APT method. Therefore for our title complexes (both of metal bromide and iodide complexes of p-toluidine and m-toluidine) APT results are more reliable than other two methods.

Low and high spin state calculations are performed for Mn, Ni, Co and Cu bromide complexes of m-toluidine. Computations found Mn complex as sextet having  $S=5/2$ , Ni complex as triplet with  $S=1$ , and Co and Cu complexes as doublet with  $S=1/2$ . The unpaired spins are mostly found on metal atoms as expected (96% are located on Mn atom, 78% on Ni atom, 100% on Co atom and 45% on Cu atom).

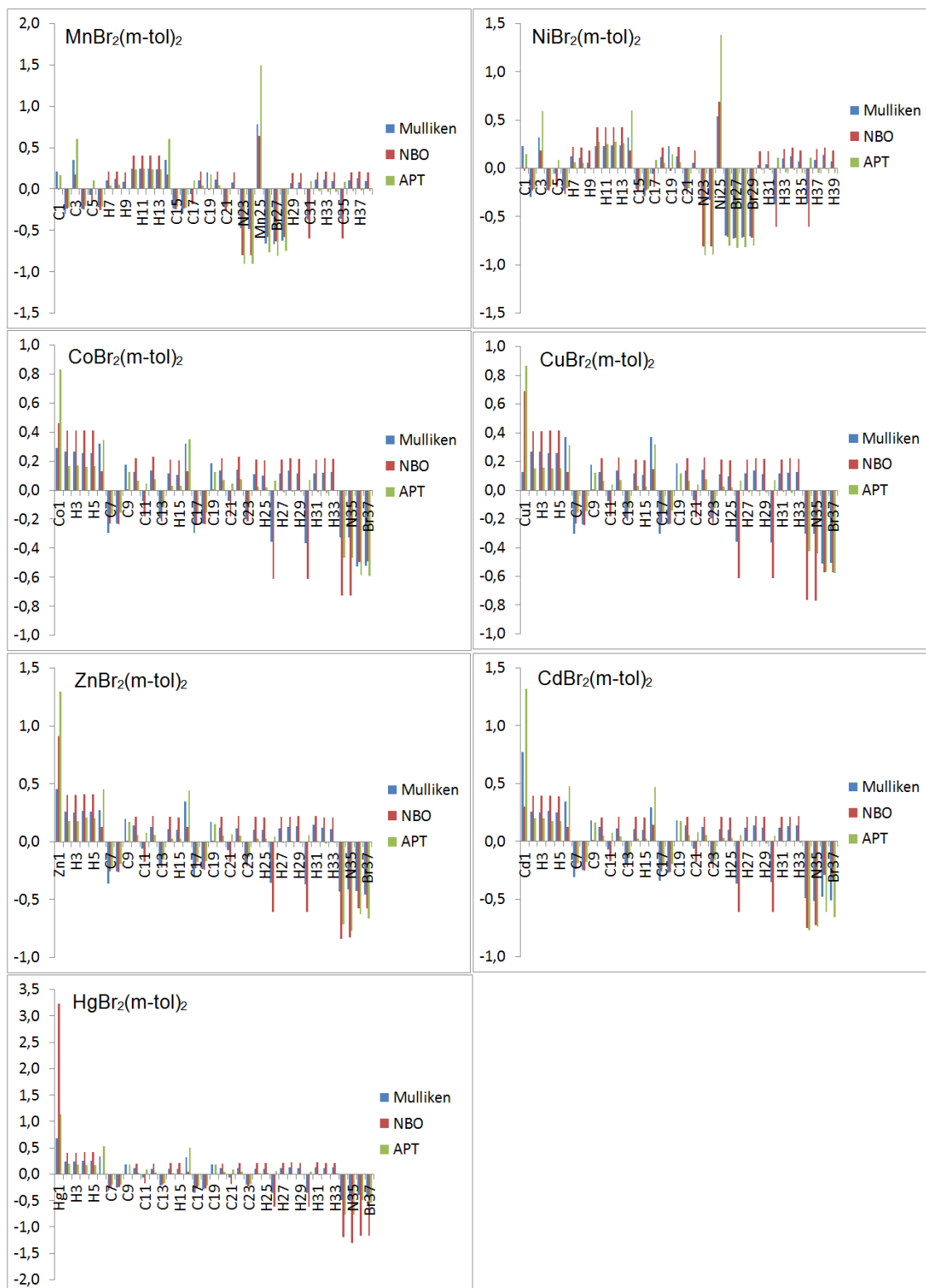


Figure 4.11 Mulliken, NBO, and APT charge distributions of metal bromide complexes of m-toluidine.



### 4.3 VIBRATIONAL FREQUENCIES

Vibrational frequency calculations of the free ligands and related transition metal complexes are obtained from the optimized geometries, and the normal modes have been assigned on the basis of the percent potential energy distribution (PED). All calculations are performed at B3LYP/def2-TZVP level in the gas phase. The absence of imaginary frequencies in the vibrational frequency calculations ensured that we have obtained equilibrium geometries for the corresponding complexes. In this section firstly we provide the vibrational frequencies of the free ligands, then their corresponding complexes by investigating the coordination effects on the modes of the ligands, and metals. In the determination of the vibrational assignments,  $\nu$  stands for stretching,  $\beta$  for in plane deformation,  $\gamma$  for out of plane deformation, and finally  $\tau$  corresponds to the torsional vibrations. Experimental spectra results are obtained from the previous studies [21-26], and our computations are compared with the experimental findings at the end of this section.

#### 4.3.1 Vibrational Frequencies of the Free Ligands

The vibrational frequencies of the ligands p-toluidine and m-toluidine have been already investigated by means of HF, MP2, BVP86, B3LYP, and B3PW91 methods using split-valance Pople basis sets in the previous studies [66,67,144,145]. In this thesis, we extend these calculations with more extensive and accurate def2-TZVP basis set, employed for the complexes using B3LYP. The experimental and theoretical vibrational bands of p-toluidine and m-toluidine are given in Table 4.6 and Table 4.7 with band assignments in terms of the calculated percent contributions of the internal coordinates to each mode. Both of the ligands have 17 atoms, which mean 45 normal modes. Each mode of the ligands are labeled between 1–45 in Tables 4.6 and 4.7, and these labels are then used in the tables of the complexes for relating the modes of free ligands to those for the complexes. Thus we will provide the detailed analysis of vibrational assignments of p-toluidine and m-toluidine with their related complexes in the following sections.

Table 4.6 Experimental and calculated vibrational frequencies (in  $\text{cm}^{-1}$ ) and % assignments of p-toluidine.

		p-toluidine						PED (%) Assignments
Exp.*		B3LYP/def2-TZVP						
No	IR	Ra	Calc.	Scaled	IR Int.	Ra Int.		
1	3416 s	3418 w	3647	3470	13.4	22.6	100 $\nu\text{NH}_2$ (asym.)	
2	3333 s	3337 w	3552	3379	16.3	80.8	100 $\nu\text{NH}_2$ (sym.)	
3	3056 w	3054 s	3171	3017	0.4	160	99 $\nu\text{CH}$	
4	3020m	3032 s	3168	3014	40.2	0.1	96 $\nu\text{CH}$	
5	3008 m	3013 s	3152	2999	1.1	64.7	96 $\nu\text{CH}$	
6			3152	2999	28.6	2.3	99 $\nu\text{CH}$	
7	2912 m	2917 s	3097	2946	18.2	36.5	97 $\nu\text{CH}_3$ (asym.)	
8	2859 m	2861m	3070	2921	21.8	52.9	97 $\nu\text{CH}_3$ (asym.)	
9	2737 w	2738 w	3019	2872	45.4	173	98 $\nu\text{CH}_3$ (sym.)	
10	1621 vs	1617 s	1667	1629	109.8	134.5	44 $\nu\text{CC}$ ; 26 $\beta\text{NH}_2$ (sciss.); 15 $\beta\text{CH}$	
11			1654	1616	12.7	11.8	59 $\beta\text{NH}_2$ (sciss.); 21 $\nu\text{CC}$ ; 11 $\beta\text{CH}$	
12	1582 s	1581 m	1621	1584	3.1	2.5	63 $\nu\text{CC}$ ; 12 $\beta\text{CH}$ ; 15 $\beta\text{NH}_2$ (rock.); 10 $\beta\text{CCH}_3$	
13	1514 vs		1555	1519	100.8	0.7	51 $\beta\text{CH}$ ; 11 $\nu\text{CC}$ ; 15 $\beta\text{CCC}$	
14			1501	1467	8.4	16.7	64 $\beta\text{CH}_3$ ; 14 $\beta\text{CCH}_3$ ; 10 $\beta\text{CH}$	
15			1488	1454	6.1	36.4	74 $\beta\text{CH}_3$ ; 22 $\beta\text{CCH}_3$	
16	1441 s		1463	1429	0.3	2.9	37 $\nu\text{CC}$ ; 26 $\beta\text{CH}$ ; 14 $\beta\text{CH}_3$ ; 12 $\beta\text{NH}_2$ (rock.)	
17		1380 m	1417	1385	0	65	93 $\beta\text{CH}_3$	
18	1324 m	1324 w	1359	1328	1	2	69 $\beta\text{CH}$ ; 20 $\beta\text{NH}_2$ (rock.); 10 $\beta\text{CCC}$	
19		1281 m	1333	1302	7.4	7.8	66 $\nu\text{CC}$ ; 17 $\beta\text{NH}_2$ (rock.); 15 $\beta\text{CCH}_3$	
20	1267 vs	1271 m	1301	1271	75.5	45.9	47 $\nu\text{CN}$ ; 21 $\nu\text{CC}$ ; 16 $\beta\text{CH}$ ; 14 $\beta\text{CCC}$	
21		1218 m	1235	1207	0.2	60.5	71 $\nu\text{CC}$ ; 15 $\beta\text{CH}$	
22	1176 s	1179 m	1207	1179	8.1	24.9	76 $\beta\text{CH}$ ; 10 $\nu\text{CC}$	
23	1120 s		1153	1127	10.2	1.1	58 $\beta\text{CH}$ ; 20 $\beta\text{NH}_2$ (rock.); 18 $\nu\text{CC}$	
24	1074 m		1092	1067	1.8	8.7	57 $\beta\text{NH}_2$ (rock.); 19 $\beta\text{CCH}_3$ ; 11 $\nu\text{CC}$ ; 11 $\beta\text{CCC}$	
25	1044 m		1064	1040	8.4	10.4	70 $\gamma\text{CCH}_3$ ; 18 $\gamma\text{CH}_3$ ; 10 $\gamma\text{CH}$	
26	983 w		1034	1010	0.2	0.9	73 $\beta\text{CCC}$ ; 10 $\beta\text{CH}$	
27	953 w		1002	979	0	3.7	42 $\beta\text{CCH}_3$ ; 18 $\beta\text{CH}_3$ ; 18 $\beta\text{CNH}_2$ ; 14 $\nu\text{CC}$	
28			933	912	0	0.3	82 $\gamma\text{CH}$ ; 11 $\gamma\text{CCC}$	
29	931 w		931	910	0.2	3.8	84 $\gamma\text{CH}$ ; 14 $\gamma\text{CCC}$	
30		844 s	854	834	2.1	259.9	42 $\nu\text{CC}$ ; 27 $\nu\text{CN}$ ; 20 $\beta\text{CCC}$	
31	812 vs		830	811	58.5	21.4	67 $\gamma\text{CH}$ ; 19 $\gamma\text{CCH}_3+\gamma\text{CNH}_2$	
32			821	802	0.2	0.3	92 $\gamma\text{CH}$	
33	720 m		752	735	0.3	5.4	45 $\beta\text{CCC}$ ; 30 $\nu\text{CC}$ ; 24 $\nu\text{CN}$	
34			724	707	1.6	5.9	70 $\gamma\text{CCC}+\gamma\text{NH}_2$ (wag.); 22 $\gamma\text{CCH}_3$	
35		645 s	661	646	0.1	50.5	71 $\beta\text{CCC}$ ; 12 $\beta\text{CNH}_2$	
36			591	577	279.7	57.6	82 $\gamma\text{NH}_2$ (wag.); 10 $\gamma\text{CCH}_3$	
37	504 vs		510	498	75	9.5	80 $\gamma\text{CCC} + \gamma\text{NH}_2$ (wag.)	
38	470	466 s	470	459	3.6	119.6	60 $\beta\text{CCC}$ ; 40 $\nu\text{CC}+\nu\text{CN}$	
39		409 w	420	410	0.1	2.9	79 $\gamma\text{CCC}$ ; 12 $\gamma\text{CH}$	
40			410	401	0	6.7	80 $\beta\text{CCH}_3+\beta\text{CNH}_2$ ; 20 $\beta\text{CCC}$	
41		335 m	323	316	2	54.8	75 $\gamma\text{CNH}_2+ \gamma\text{CCH}_3$ ; 18 $\gamma\text{CCC}$	
42			300	293	0.1	0.3	91 $\beta\text{CCH}_3+\beta\text{CNH}_2$ (twist.)	
43			278	272	20.2	8.9	96 $\gamma\text{NH}_2$ (twist)	
44		121 vs	140	137	4.2	18.5	72 $\gamma\text{CNH}_2+ \gamma\text{CCH}_3$ ; 21 $\gamma\text{CCC}$	
45			20	20	0.4	3057.8	90 $\gamma\text{CH}_3$ (torsion)	

\*Experimental data is taken from Ref. [144].

Table 4.7 Experimental and calculated vibrational frequencies (in  $\text{cm}^{-1}$ ) and % assignments of m-toluidine.

m-toluidine							
No	Exp.*		B3LYP/def2-TZVP		PED (%) Assignments		
	IR	Ra	Calc.	Scaled	IR Int.	Ra Int.	
1	3435 s		3652	3457	14.07	21.922	100 $\nu\text{NH}_2$ (asym.)
2	3354 s	3353 m,br	3556	3366	17.13	75.131	100 $\nu\text{NH}_2$
3	3034 m	3046s	3184	3014	16.81	114.27	87 $\nu\text{CH}$
4	3015 m,sh	3012 s	3169	2999	20.45	34.893	96 $\nu\text{CH}$
5			3158	2989	4.94	38.868	89 $\nu\text{CH}$
6	2975 m,sh	2974 m	3147	2979	19.99	43.032	95 $\nu\text{CH}$
7	2946 m,sh		3104	2938	16.38	34.173	99 $\nu\text{CH}_3$ (asym.)
8	2919 m	2919 s	3078	2913	19.04	46.751	99 $\nu\text{CH}_3$ (asym.)
9	2857 w	2857 m,sh	3026	2864	29.79	137.96	99 $\nu\text{CH}_3$
10	1622 vs		1661	1629	152.69	46.515	77 $\beta\text{NH}_2$ (sciss.); 20 $\nu\text{CC}$
11			1649	1617	40.05	27.272	67 $\nu\text{CC}$ ; 33 $\beta\text{NH}_2$ (sciss.)
12	1591 vs	1590 m	1630	1598	24.03	17.912	64 $\nu\text{CC}$ ; 15 $\beta\text{NH}_2$ (rock.); 12 $\beta\text{CH}_3$
13			1533	1503	34.77	2.9257	44 $\beta\text{CH}$ ; 33 $\nu\text{CC}$ ; 11 $\beta\text{NH}_2$ (rock.); 10 $\beta\text{CH}_3$
14	1493 vs	1493 w	1510	1480	27.08	5.0802	62 $\beta\text{CH}_3$ ; 20 $\nu\text{CC}$ ; 14 $\beta\text{NH}_2$
15	1469 s		1490	1461	6.39	27.125	80 $\beta\text{CH}_3$ ; 17 $\beta\text{CCH}_3$
16	1443 m,sh	1447 w,br	1473	1444	0.86	15.096	50 $\beta\text{CH}_3$ ; 34 $\beta\text{CH}$ ; 13 $\beta\text{NH}_2$
17	1381 w	1378 m	1415	1387	0.71	36.125	92 $\beta\text{CH}_3$
18			1354	1327	3.72	2.2505	62 $\beta\text{CH}$ ; 21 $\nu\text{CC}$
19	1314 m	1313 m,sh	1342	1315	11.28	7.7718	47 $\nu\text{CC}$ ; 20 $\beta\text{CNH}_2$ ; 16 $\beta\text{CH}$ ; 14 $\beta\text{CCH}_3$
20	1293 s	1293 m	1319	1292	44.75	51.364	39 $\nu\text{CN}$ ; 22 $\nu\text{CC}$ ; 26 $\beta\text{CCC}$
21	1170 s	1166 m	1195	1171	12.6	5.63	57 $\beta\text{CH}$ ; 27 $\nu\text{CC}$ ; 14 $\nu\text{CN}$
22			1194	1170	6.59	9.4732	75 $\beta\text{CH}$ ; 12 $\nu\text{CC}$
23		1106 w	1133	1111	1.89	16.283	46 $\beta\text{NH}_2$ (rock.); 38 $\nu\text{CC}$ ; 16 $\beta\text{CH}$
24	1077 w	1075 w	1094	1072	1.49	4.9732	47 $\beta\text{NH}_2$ (rock.); 25 $\nu\text{CC}$ ; 15 $\beta\text{CCH}_3$
25	1038 w		1061	1040	7.42	8.7615	70 $\gamma\text{CCH}_3$ ; 17 $\gamma\text{CH}_3$ ; 13 $\gamma\text{CH}$
26			1021	1001	3.54	1.3697	47 $\beta\text{CCH}_3$ ; 27 $\beta\text{CNH}_2$ ; 20 $\beta\text{CCC}$
27	996 m	996 vs	1014	994	1.97	183.28	68 $\nu\text{CC}$ ; 31 $\beta\text{CCC}$
28	965 vw		946	927	5.97	3.786	36 $\beta\text{CCC}$ ; 30 $\beta\text{CH}$ ; 23 $\nu\text{CN}$ ; 20 $\nu\text{CC}$
29	926 m	928 vw	943	924	0.03	0.1654	78 $\gamma\text{CH}$ ; 21 $\gamma\text{CCC}$
30	870 m		875	858	14.64	2.9537	79 $\gamma\text{CH}$ ; 16 $\gamma\text{CCC}$
31	855 m		856	839	2.32	0.7636	87 $\gamma\text{CH}$ ; 12 $\gamma\text{CCC}$
32	775 vs	784 w	782	766	44.59	2.0319	72 $\gamma\text{CH}$ ; 12 $\gamma\text{CCC}$
33		738 s	749	734	0.14	143.35	41 $\beta\text{CCC}$ ; 31 $\nu\text{CC}$ ; 27 $\nu\text{CN}$ (breath.)
34	691 vs		705	691	16.44	1.7699	52 $\gamma\text{CCC}$ ; 28 $\gamma\text{CH}$ ; 10 $\gamma\text{CNH}_2$ (wag.)
35			600	588	121.93	28.073	53 $\gamma\text{NH}_2$ (wag.); 33 $\gamma\text{CCC}$ ; 14 $\gamma\text{CCH}_3$
36	557 m		559	548	61.89	117.69	41 $\gamma\text{CNH}_2$ ; 32 $\gamma\text{CCH}_3$ ; 26 $\gamma\text{CCC}$
37	538 m	543 m	539	528	134.42	11.679	35 $\beta\text{NH}_2$ (wag.); 25 $\nu\text{CC}$ ; 23 $\nu\text{CN}$ ; 17 $\beta\text{CCC}$
38		518 m	526	515	0.83	59.127	64 $\beta\text{CCC}$ ; 22 $\nu\text{CC}$
39		431 w	449	440	12.62	2.2736	71 $\gamma\text{CCC}$ ; 16 $\gamma\text{CH}$
40			431	422	0.75	4.8369	78 $\beta\text{CCH}_3 + \beta\text{CNH}_2$ ; 20 $\beta\text{CCC}$
41		294 m	304	298	14.48	15.049	82 $\beta\text{NH}_2$ (twist.); 11 $\beta\text{CCC}$
42		234 m	289	284	4.93	30.031	87 $\beta\text{CCH}_3 + \beta\text{NH}_2$ (twist.)
43		218 m	223	219	2.97	56.012	88 $\gamma\text{CCC} + \gamma\text{NH}_2$ (twist.)
44			204	200	6.29	81.13	53 $\gamma\text{CCH}_3$ ; 31 $\gamma\text{CCC}$ ; 16 $\gamma\text{CNH}_2$
45			27	26	0.1	1981	99 $\gamma\text{CH}_3$ (torsion)

\*Experimental data is taken from Ref. [145].

### 4.3.2 Vibrational Frequencies of the Metal Bromide Complexes of P-toluidine

In this section vibrations and corresponding band assignments of Mn, Co, Ni, Cu, Zn, Cd and Hg bromide complexes of p-toluidine are provided. Theoretical vibrational spectra of the title compounds with respect to infrared and Raman intensities are given in Figures 4.12 and 4.13, whereas experimental and theoretical vibrational frequencies with the PED analysis of each complex are given in Tables 4.8-4.14. In order to investigate vibrational assignments deeply, we will analyze following three spectral regions: 3500-2700  $\text{cm}^{-1}$ , 1700-600  $\text{cm}^{-1}$ , and below 600  $\text{cm}^{-1}$ .

#### 4.3.2.1 3500-2700 $\text{cm}^{-1}$ Region

Characteristic vibrations of this region are N-H stretching vibrations of amino group and C-H stretching vibrations of methyl group and benzene ring. PED (%) contributions of these vibrations are above 85% for all the complexes. As an evidence of complex formation between metal (II) bromide and the ligand (p-toluidine), some modes originating from ligand show substantial shifts in the spectra of complexes. Amino group frequencies of the p-toluidine are generally more affected from the coordination, which shows the complex formation occurs via nitrogen atom of the free ligand [17-26]. The N-H bond strength weakens upon coordination and the  $\nu_{\text{NH}}$  asymmetric and symmetric stretching bands shift to lower frequencies because of complexation by 123 and 95  $\text{cm}^{-1}$  for  $\text{MnBr}_2(\text{p-tol})_2$ , 140 and 107  $\text{cm}^{-1}$  for  $\text{CoBr}_2(\text{p-tol})_2$ , and 85 and 93  $\text{cm}^{-1}$  for  $\text{NiBr}_2(\text{p-tol})_2$ , 130 and 107  $\text{cm}^{-1}$  for  $\text{CuBr}_2(\text{p-tol})_2$ , 130 and 97  $\text{cm}^{-1}$  for  $\text{ZnBr}_2(\text{p-tol})_2$ , 115 and 82  $\text{cm}^{-1}$  for  $\text{CdBr}_2(\text{p-tol})_2$ , and 116 and 90  $\text{cm}^{-1}$  for  $\text{HgBr}_2(\text{p-tol})_2$ , respectively.

C-H stretching vibrations in the aromatic benzene rings generally occur in the ~3100-3000  $\text{cm}^{-1}$  region [150-153]. Confirming this information in our compounds these vibrations are between 3056-3000  $\text{cm}^{-1}$  in both p-toluidine and its related complexes. In line with the previous experimental and theoretical studies [22,25,26,144], in this study C-H stretching vibrations of methyl group are observed between 2912-2737  $\text{cm}^{-1}$  in p-toluidine, and these vibrations are also observed in the 2921-2730  $\text{cm}^{-1}$  region in the complexes, being parallel with the free ligand. Therefore, we can say that C-H stretching vibrations of the benzene rings and methyl groups are not affected or affected very little due to the complexation.

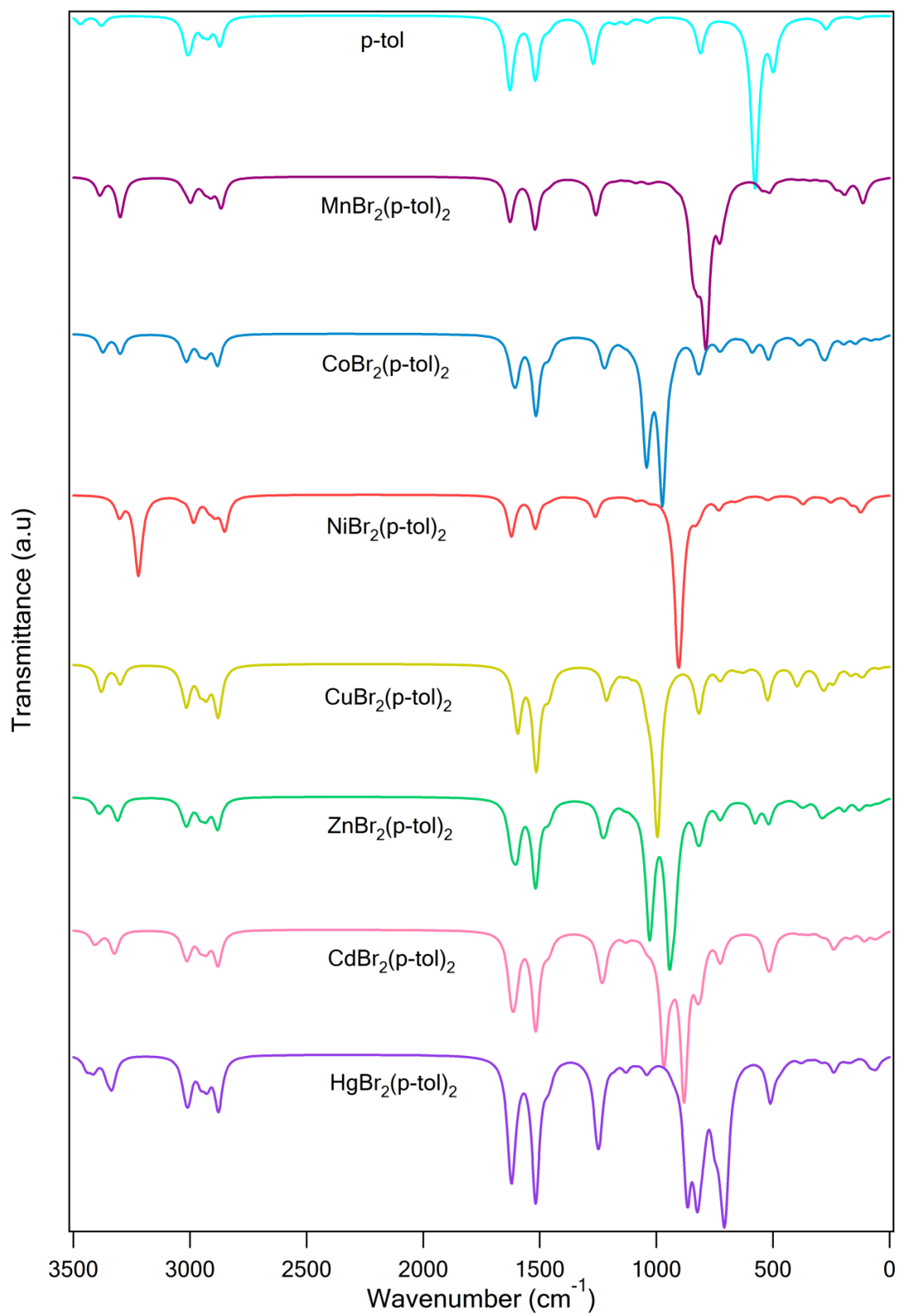


Figure 4.12 Theoretical IR spectra of p-toluidine and its bromide complexes.

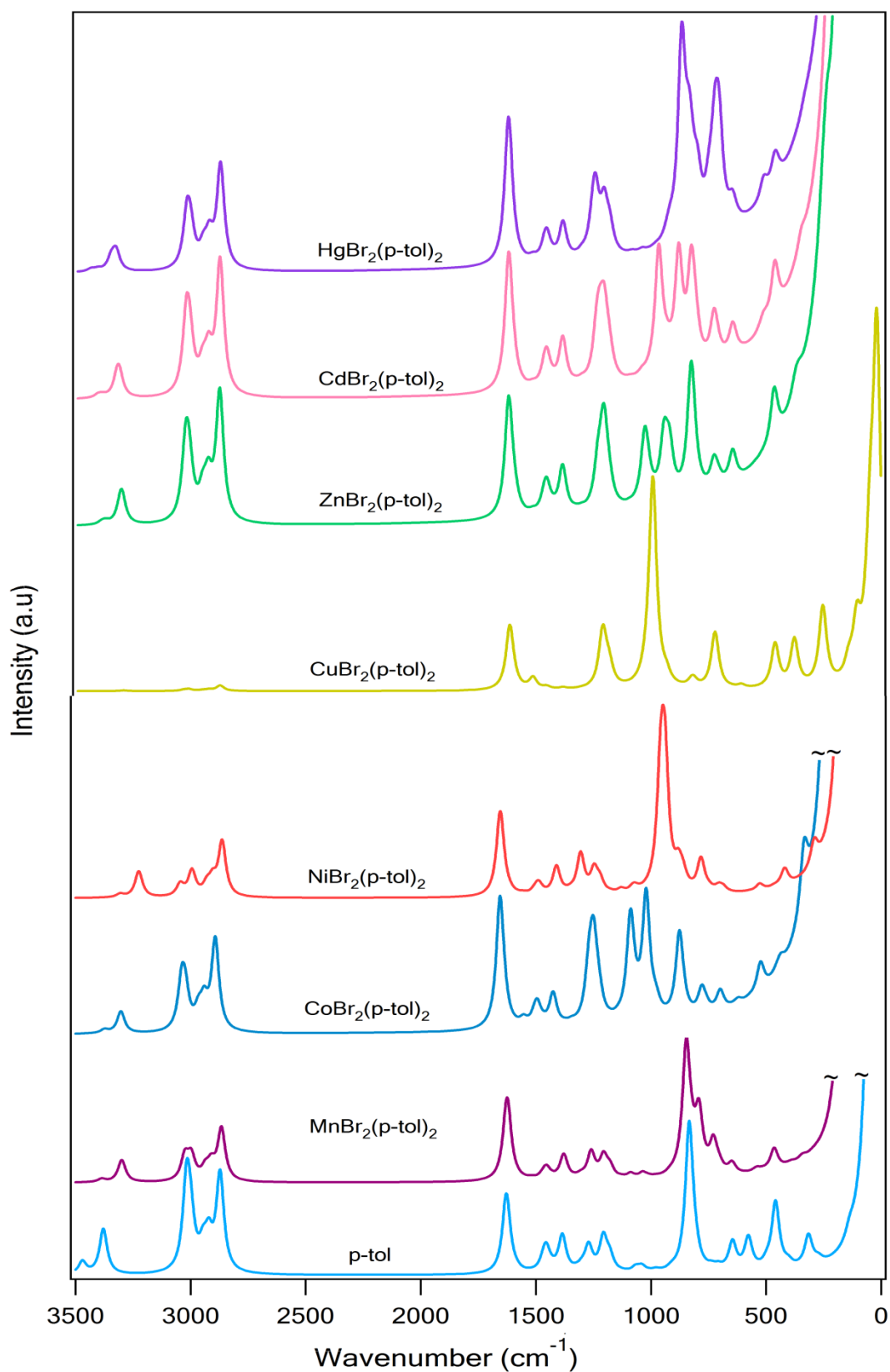


Figure 4.13 Theoretical Raman spectra of p-toluidine and its bromide complexes.

#### 4.3.2.2 1700-600 $\text{cm}^{-1}$ Region

As mentioned above, since the complex formation occurs via nitrogen atom of the free ligand, in this spectral region remarkable changes are observed in the  $\text{NH}_2$  scissoring, rocking, wagging and twisting modes. For example  $\text{NH}_2$  scissoring modes of free p-toluidine generally shift to lower frequencies in complexes, whereas wagging and twisting modes shift to quite higher frequencies as in the literature [18-26]. The average downward shift in  $\text{NH}_2$  scissoring modes of complexes with respect to free p-toluidine is  $27 \text{ cm}^{-1}$ . According to our PED (%) analysis,  $\text{NH}_2$  wagging and twisting modes were not observed in the experimental data of p-toluidine [144], but these modes and dramatic shifts related to these modes are observed easily in the computations. DFT calculations predict wagging mode at  $577 \text{ cm}^{-1}$  (scaled def2-TZVP) in free p-toluidine, whereas this mode is found at  $792 \text{ cm}^{-1}$  for Mn,  $1045 \text{ cm}^{-1}$  for Co,  $909 \text{ cm}^{-1}$  for Ni,  $995 \text{ cm}^{-1}$  for Cu,  $1029 \text{ cm}^{-1}$  for Zn,  $968 \text{ cm}^{-1}$  for Cd and  $868 \text{ cm}^{-1}$  for Hg complexes. According to Akyüz and Davies [18] hybridization effects on nitrogen atom may cause this shift upon coordination. As seen from the wavenumbers, the place of this mode is also changed with respect to the metal atom of the complexes. Similarly, twisting mode is determined at  $272 \text{ cm}^{-1}$  for p-toluidine, and it is also found to be in higher wavenumbers in the Mn, Co, Ni, Cu, Zn, Cd, and Hg complexes respectively at  $548 \text{ cm}^{-1}$ ,  $589 \text{ cm}^{-1}$ ,  $640 \text{ cm}^{-1}$ ,  $626 \text{ cm}^{-1}$ ,  $577 \text{ cm}^{-1}$ ,  $529 \text{ cm}^{-1}$ , and  $474 \text{ cm}^{-1}$ .

Consistent with the present calculations and previous assignments on p-toluidine and other related molecules [144, 151,154], the band observed at  $1267 \text{ cm}^{-1}$  (IR) /  $1271 \text{ cm}^{-1}$  (Ra) is  $\nu\text{CN}$  stretching for free p-toluidine. However this mode is also affected by complexation and has been observed in lower frequencies in the complexes. For instance for the Mn complex it is observed at  $1243 \text{ cm}^{-1}$  (IR) /  $1237 \text{ cm}^{-1}$  (Ra), for the Ni complex  $1250 \text{ cm}^{-1}$  (IR) /  $1242 \text{ cm}^{-1}$  (Ra), and for the Cd complex  $1237 \text{ cm}^{-1}$  (IR) /  $1236 \text{ cm}^{-1}$  (Ra).

In the literature in plane and out of plane C-H vibrations are found approximately between  $1440 - 1066 \text{ cm}^{-1}$  and  $1013-717 \text{ cm}^{-1}$  regions [155-158]. In our PED(%) calculations in plane C-H vibrations found generally coupled with C-C ring stretchings and C-N stretching vibrations, as in the literature and found in the  $\sim 1500-1100 \text{ cm}^{-1}$  range for our all compounds, and mostly are not affected from complexation except  $\text{NH}_2$  bending vibrations also contributed these modes. Out of plane C-H vibrations are

also found in mentioned range as 950-800  $\text{cm}^{-1}$  with strong PEDs. In a similar manner, methyl group e.g.  $\beta\text{CH}_3$  vibrations are found at  $\sim 1385 \text{ cm}^{-1}$  (theoretical) both for free ligand and its related complexes.

#### 4.3.2.3 Below 600 $\text{cm}^{-1}$

Although significant bands of this region are metal-ligand and metal-halogen stretching vibrations in transition metal complexes [52,60,61,63,66,67], some ligand vibrations such as, in/out of plane CCC,  $\text{CNH}_2$  or  $\text{CCH}_3$  bending and  $\text{CH}_3$  torsion vibrations are also observed.

The metal-ligand bands that appear in the far IR region are characteristics of the local structure around metal ions [18-26]. In the experimental only study performed by Gölcük et al. [26], these bands were assigned between 360-400  $\text{cm}^{-1}$  for the Zn, Cd, and Hg bromide complexes of p-toluidine, whereas in our study, these vibrations found in lower wavenumbers. The  $\nu(\text{M-N})$  stretching vibrations appear at 217  $\text{cm}^{-1}$  (medium IR) / 220  $\text{cm}^{-1}$  (weak Raman) for the Mn complex, at 247  $\text{cm}^{-1}$  (strong IR) for the Co complex, at 273  $\text{cm}^{-1}$  (medium IR) / 155  $\text{cm}^{-1}$  (medium Raman) for the Ni complex, at 207  $\text{cm}^{-1}$  (medium IR) for the Cu complex, at 228  $\text{cm}^{-1}$  (medium IR) for the Zn complex, at 139  $\text{cm}^{-1}$  (medium Raman) for the Cd complex, and at 196  $\text{cm}^{-1}$  (medium Raman) for the Hg complex.

The  $\nu(\text{M-Br})$  stretching vibrations appear at 255  $\text{cm}^{-1}$  (strong IR) for the Mn complex, at 217  $\text{cm}^{-1}$  (weak IR) / 213  $\text{cm}^{-1}$  (strong Raman) and at 208  $\text{cm}^{-1}$  (strong IR) / 211  $\text{cm}^{-1}$  (very strong Raman) for the Co complex, at 136  $\text{cm}^{-1}$  (medium Raman) for the Ni complex, at 221  $\text{cm}^{-1}$  (medium IR) / 222  $\text{cm}^{-1}$  (very weak Raman) for the Cu complex, at 246  $\text{cm}^{-1}$  (strong IR) and at 207  $\text{cm}^{-1}$  (strong IR) / 204  $\text{cm}^{-1}$  (strong Raman) for the Zn complex, at 245  $\text{cm}^{-1}$  (strong IR) / 246  $\text{cm}^{-1}$  (strong Raman) for the Cd complex, and finally at 241  $\text{cm}^{-1}$  (medium IR) for the Hg complex. Generally wavenumbers below 100  $\text{cm}^{-1}$  are not observed in the experimental-only studies, but present computations predict these wavenumbers mostly as torsional  $\tau\text{CNMN}$  or out of plane ligand-metal-ligand bending vibrations.



Table 4.8 Experimental and calculated vibrational frequencies (in  $\text{cm}^{-1}$ ) of free p-toluidine and  $\text{MnBr}_2(\text{p-tol})_2$ .

p-toluidine					$\text{MnBr}_2(\text{p-tol})_2$						PED (%) Assignments
Exp*		B3LYP/def2-TZVP		Exp**		B3LYP/def2-TZVP					
No	IR	Ra	Calc.	Scaled	IR	Ra	Calc.	Scaled	Calc.	Scaled	
1	3416 s	3418 w	3647	3470	3293 s		3560	3387	3559	3386	99/100 $\nu\text{NH}_2$ (asym.)
2	3333 s	3337 w	3552	3379	3238 vs	3244 s	3468	3299	3467	3299	98 $\nu\text{NH}_2$
3	3056 w	3054 s	3171	3017	3054 vw	3054 s	3179	3025	3179	3025	78/82 $\nu\text{CH}$
4	3020m,sh	3032 s	3168	3014	3031 m	3030 s	3177	3023	3177	3023	85/84 $\nu\text{CH}$ (asym.)
5	3008 m	3013 s	3152	2999		3011 s	3151	2998	3151	2998	82/87 $\nu\text{CH}$
6			3152	2999			3149	2996	3149	2996	91 $\nu\text{CH}$
7	2912 m	2917 s	3097	2946	2920 m	2916 m	3086	2936	3086	2936	93/98 $\nu\text{CH}_3$ (asym.)
8	2859 m	2861m	3070	2921	2868 w	2863 m	3059	2910	3059	2910	96/93 $\nu\text{CH}_3$ (asym.)
9	2737 w	2738 w	3019	2872	2731 vw		3012	2866	3012	2866	98/96 $\nu\text{CH}_3$
10	1621 vs	1617 s	1667	1629	1596 s		1659	1621	1659	1621	50/39 $\beta\text{NH}_2$ (sciss.); 41/49 $\nu\text{CC}$
11			1654	1616	1619 s	1621 s	1667	1629	1666	1628	55/57 $\beta\text{NH}_2$ (sciss.); 29 $\nu\text{CC}$
12	1582 s,sh	1581 m	1621	1584	1573 s	1575 m,sh	1625	1588	1624	1587	61/59 $\nu\text{CC}$ ; 12 $\beta\text{CH}$ ; 10/11 $\beta\text{NH}_2$ (rock.); 10 $\beta\text{CCH}_3$
13	1514 vs		1555	1519	1518 vs	1519 m	1556	1520	1556	1520	56/57 $\beta\text{CH}$ ; 12/0 $\nu\text{CC}$ ; 14/17 $\beta\text{CCC}$
14			1501	1467			1502	1468	1502	1468	64 $\beta\text{CH}_3$ ; 15 $\beta\text{CH}$
15			1488	1454	1458 w	1451 w	1487	1453	1487	1453	72/73 $\beta\text{CH}_3$ ; 22 $\beta\text{CH}$
16	1441 s		1463	1429		1440 w,br	1465	1431	1465	1431	25/40 $\nu\text{CC}$ ; 27/20 $\beta\text{CH}$
17		1380 m	1417	1385	1374 w	1380 s	1411	1379	1411	1379	93/92 $\beta\text{CH}_3$
18	1324 m	1324 w	1359	1328	1317 m	1324 m	1362	1331	1362	1331	63/60 $\beta\text{CH}$ ; 12 $\nu\text{CC}$
19		1281 m	1333	1302	1294 m	1295 w	1336	1305	1336	1305	56/43 $\nu\text{CC}$ ; 13/19 $\beta\text{CH}$
20	1267 vs	1271 m	1301	1271	1243 vs	1237 m	1290	1260	1289	1259	52/56 $\nu\text{CN}$ ; 17 $\beta\text{CH}$
21		1218 m	1235	1207		1216	1234	1206	1234	1206	66/64 $\nu\text{CC}$ ; 10/0 $\beta\text{CH}$
22	1176 s	1179 m	1207	1179	1205 m	1204 s	1206	1178	1206	1178	66/75 $\beta\text{CH}$ ; 17 $\nu\text{CC}$
23	1120 s		1153	1127	1160 m	1183 s	1159	1132	1157	1131	48/49 $\beta\text{CH}$ ; 25/24 $\beta\text{NH}_2$ (rock.); 11/15 $\nu\text{CC}$
24	1074 m		1092	1067	1100 s,sh		1115	1089	1114	1088	26/30 $\beta\text{NH}_2$ (rock.); 17 $\nu\text{CC}$ ; 11/15 $\beta\text{CH}$ ; 10/11 $\beta\text{CCC}$
25	1044 m		1064	1040	1065 vs	1065 s	1060	1036	1060	1036	61 $\gamma\text{CCH}_3$ ; 18 $\gamma\text{CH}$
26	983 w		1034	1010	998 m	1016	1038	1014	1038	1014	84 $\beta\text{CCC}$
27	953 w		1002	979	956 w	950 vw	1002	979	1002	979	62/63 $\beta\text{CCH}_3$ ; 16/18 $\beta\text{CH}_3$
28			933	912			937	916	936	915	86/84 $\gamma\text{CH}$

Table 4.8 cont.

p-toluidine					MnBr <sub>2</sub> (p-tol) <sub>2</sub>					PED (%) Assignments	
No	Exp*		B3LYP/def2-TZVP		IR	Exp**		B3LYP/def2-TZVP			
	IR	Ra	Calc.	Scaled		Ra	Calc.	Scaled	Calc.		Scaled
29	931 w		931	910	936 w		931	910	931	910	90/91 $\gamma$ CH
30		844 s	854	834	836 m	837 s	867	847	864	844	69/65 $\nu$ CC+ $\nu$ CN; 30 $\beta$ CCC
31	812 vs		830	811	812 vs	806 vs	843	824	841	822	70 $\gamma$ CH; 30 $\gamma$ CNH <sub>2</sub> + $\gamma$ CH <sub>3</sub>
32			821	802			833	814	833	814	82/86 $\gamma$ CH
33	720 m		752	735	739 s	743 w	746	729	744	727	41/38 $\nu$ CN; 18/23 $\beta$ CCC; 25/27 $\nu$ CC
34			724	707	702 s	702 vw	720	704	720	704	61/60 $\gamma$ CCC; 39 $\gamma$ CH
35		645 s	661	646	661 s	660 s	663	648	663	648	72/75 $\beta$ CCC; 13 $\beta$ CNH <sub>2</sub>
36			591	577			811	792	805	787	48/47 $\gamma$ NH <sub>2</sub> (wag.); 45/47 $\gamma$ CH
37	504 vs		510	498	510 vs	521 w	526	514	526	514	71/63 $\gamma$ CCC; 25/30 $\gamma$ NH <sub>2</sub> (wag.)
38	470	466 s	470	459	466 s	474 s	476	465	476	465	63/55 $\nu$ CC+ $\nu$ CN; 26/31 $\beta$ CCC
39		409 w	420	410	406 m	405 m	420	410	420	410	81/82 $\gamma$ CCC
40			410	401	361 m	365	400	391	399	390	80/83 $\beta$ CCH <sub>3</sub> + $\beta$ CNH <sub>2</sub> ; 18/14 $\beta$ CCC
41		335 m	323	316	300 s	307s	351	343	350	342	40/20 $\gamma$ CCC; 30/41 $\gamma$ CCH <sub>3</sub> ; 30/39 $\gamma$ CNH <sub>2</sub>
42			300	293	278 w	260 m	301	294	300	293	84/82 $\beta$ CCH <sub>3</sub> + $\beta$ CNH <sub>2</sub>
43			278	272	566 s	556 m	561	548	552	539	84/80 $\gamma$ NH <sub>2</sub> (twist.)
					255 s		234	229			80 $\nu$ MBr; 18 $\gamma$ CCH <sub>3</sub>
					217 m	220 w	208	203			78 $\nu$ MN; 20/16 $\gamma$ CCH <sub>3</sub>
44		121 vs	140	137			197	192	194	190	75/68 $\gamma$ CNH <sub>2</sub> + $\gamma$ CCH <sub>3</sub> ; 15/27 $\gamma$ NMBr
							139	136			81 $\nu$ MBr; 18 $\gamma$ CCH <sub>3</sub>
							117	114			82 $\nu$ MN
							93	91	93	91	87/89 $\tau$ CNMN
							90	88	81	79	79/81 $\gamma$ NMBr; 15 $\gamma$ CCH <sub>3</sub>
							75	73			47 $\gamma$ NMBr; 24 $\gamma$ CCH <sub>3</sub> ; 20 $\tau$ CNMN
							67	65			70 $\gamma$ NMBr; 20 $\nu$ MBr
							43	42	42	41	65/58 $\gamma$ NMBr; 25/31 $\gamma$ BrMBr
							36	35	33	32	63/62 $\tau$ CCNM; 24 $\tau$ CCCN
45			20	20			29	28	16	16	92 $\gamma$ CH <sub>3</sub> (torsion)
							26	25	14	14	81/65 $\tau$ CNMN; 0/35 $\gamma$ CH <sub>3</sub> (torsion)
							20	20	13	13	90 $\tau$ CNMN

\*Experimental data is taken from Ref. [144], \*\*Experimental data is taken from Ref. [159].

Table 4.9 Experimental and calculated vibrational frequencies (in  $\text{cm}^{-1}$ ) of free p-toluidine and  $\text{CoBr}_2(\text{p-tol})_2$ .

p-toluidine					CoBr <sub>2</sub> (p-tol) <sub>2</sub>						PED (%) Assignments
No	Exp.*		B3LYP/def2-TZVP		IR	Exp.**		B3LYP/def2-TZVP			
	IR	Ra	Calc.	Scaled		Ra	Calc.	Scaled	Calc.	Scaled	
1	3416 s	3418 w	3647	3470	3276 s		3548	3376	3540	3368	100 $\nu\text{NH}_2$ (asym.)
2	3333 s	3337 w	3552	3379	3226 vs	3227 m	3468	3299	3468	3299	100 $\nu\text{NH}_2$
3	3056 w	3054 s	3171	3017	3054 vw	3057 s	3187	3032	3185	3030	91/88 $\nu\text{CH}$
4	3020 m,sh	3032 s	3168	3014	3031 m	3032 m	3182	3027	3179	3025	96/95 $\nu\text{CH}$ (asym.)
5	3008 m	3013 s	3152	2999		3012 m	3169	3015	3168	3014	93/92 $\nu\text{CH}$
6			3152	2999			3165	3011	3165	3011	93/94 $\nu\text{CH}$
7	2912 m	2917 s	3097	2946	2925 m	2924 s	3107	2956	3107	2956	98/97 $\nu\text{CH}_3$ (asym.)
8	2859 m	2861 m	3070	2921	2864 vw	2860 w	3081	2931	3080	2930	98/99 $\nu\text{CH}_3$ (asym.)
9	2737 w	2738 w	3019	2872		2722 w	3029	2882	3028	2881	95/99 $\nu\text{CH}_3$
10	1621 vs	1617 s	1667	1629		1595 m	1650	1612	1638	1600	77/45 $\beta\text{NH}_2$ (sciss.); 17/24 $\beta\text{CNH}_2$
11			1654	1616	1612w,sh	1612 s	1659	1621	1659	1621	54/61 $\nu\text{CC}$ ; 26/22 $\beta\text{NH}_2$ (sciss.); 25 $\beta\text{CH}$
12	1582 s,sh	1581 m	1621	1584	1578 vs	1576 w	1636	1599	1630	1593	36/38 $\nu\text{CC}$ ; 25/22 $\beta\text{CH}$ ; 30/28 $\beta\text{CCC}$
13	1514 vs		1555	1519	1512 vs		1553	1517	1552	1516	58/52 $\beta\text{CH}$ ; 25/20 $\nu\text{CC}$ ; 12 $\beta\text{NH}_2$
14			1501	1467			1501	1467	1500	1466	56/57 $\beta\text{CH}_3$ ; 18/12 $\beta\text{CH}$ ; 11/15 $\nu\text{CC}$
15			1488	1454	1455 w		1489	1455	1489	1455	65/66 $\beta\text{CH}_3$ ; 19/20 $\beta\text{CH}$
16	1441 s		1463	1429	1430 vw		1463	1429	1462	1429	24/29 $\nu\text{CC}$ ; 26 $\beta\text{CH}$ ; 22/19 $\beta\text{CH}_3$ ; 20/21 $\beta\text{CNH}_2$
17		1380 m	1417	1385	1380 vw	1379 m	1418	1386	1418	1386	89/93 $\beta\text{CH}_3$
18	1324 m	1324 w	1359	1328		1327vw	1366	1335	1364	1333	42/48 $\beta\text{CH}$ ; 32 $\beta\text{NH}_2$ ; 20/16 $\nu\text{CC}$
19		1281 m	1333	1302		1292vw	1337	1306	1334	1303	47/50 $\nu\text{CC}$ ; 19/11 $\beta\text{CH}$ ; 11/14 $\beta\text{CCC}$
20	1267 vs	1271 m	1301	1271	1238 m		1257	1228	1243	1215	61/58 $\nu\text{CC}+\text{CN}$ ; 22 $\beta\text{CH}$
21		1218 m	1235	1207	1222 s	1215	1233	1205	1233	1205	60/51 $\nu\text{CC}$ ; 10 $\beta\text{CH}$ ; 15 $\nu\text{CN}$
22	1176 s	1179 m	1207	1179		1217 w	1211	1183	1210	1182	74/72 $\beta\text{CH}$ ; 20/22 $\nu\text{CC}$
23	1120 s		1153	1127		1181 m	1167	1140	1161	1134	34/47 $\beta\text{CH}$ ; 36/30 $\beta\text{NH}_2$ (rock.); 21/16 $\nu\text{CC}$
24	1074 m		1092	1067			1130	1104	1124	1098	46/45 $\beta\text{NH}_2$ (rock.); 27/18 $\beta\text{CH}$ ; 17/20 $\nu\text{CC}$
25	1044 m		1064	1040			1066	1042	1064	1040	51/37 $\gamma\text{CCH}_3$ ; 15/12 $\gamma\text{CH}_3$ ; 0/21 $\gamma\text{CH}$
26	983 w		1034	1010			1040	1016	1039	1015	55/62 $\beta\text{CCC}$ ; 12 $\beta\text{CH}$
27	953 w		1002	979	960vw,sh		1008	985	1006	983	52/46 $\beta\text{CCH}_3$ ; 17/23 $\beta\text{CH}_3$
28			933	912			967	945	847	828	84 $\gamma\text{CH}$

Table 4.9 cont.

		p-toluidine		CoBr <sub>2</sub> (p-tol) <sub>2</sub>							
Exp.*		B3LYP/def2-TZVP		Exp.**		B3LYP/def2-TZVP				PED (%) Assignments	
No	IR	Ra	Calc.	Scaled	IR	Ra	Calc.	Scaled	Calc.		Scaled
29	931 w		931	910	932 vw		953	931	953	931	73/70 $\gamma$ CH; 20 $\gamma$ CCH <sub>3</sub>
30		844 s	854	834	841 s	837 s	846	827	845	826	71/75 $\nu$ CC+CN; 11 $\beta$ CCC
31	812 vs		830	811	810 vs	813 s	836	817	826	807	69/56 $\gamma$ CH; 14 $\gamma$ CCH <sub>3</sub> ; 6/7 $\gamma$ CNH <sub>2</sub>
32			821	802	806 vs	809 m	835	816	944	922	76/79 $\gamma$ CH; 21 $\gamma$ CCC
33	720 m		752	735	741 s	739 w	746	729	742	725	35/37 $\beta$ CCC; 25 $\nu$ CC; 34/38 $\nu$ CN
34			724	707	707 m	705 w	728	711	722	705	44/42 $\gamma$ CCC; 30/31 $\gamma$ CNH <sub>2</sub> ; 26 $\gamma$ CCH <sub>3</sub>
35		645 s	661	646	649 s	645 m	661	646	661	646	69/72 $\beta$ CCC; 18/16 $\beta$ NH <sub>2</sub>
36			591	577	1070vs	1080vs	1069	1045	997	974	54 $\gamma$ NH <sub>2</sub> (wag.); 20 $\gamma$ CH; 18 $\gamma$ CCC
37	504 vs		510	498	507 s	524 m	533	521	528	516	67/70 $\gamma$ CCC+ $\gamma$ CNH <sub>2</sub> ; 30 $\gamma$ CH
38	470	466 s	470	459	472 m	472 vs	480	469	478	467	57/52 $\beta$ CCC; 21 $\nu$ CN; 20 $\nu$ CC
39		409 w	420	410	420 s	421 m	420	410	419	409	87/88 $\gamma$ CCC
40			410	401	394 m	395 w	394	385	386	377	82/75 $\beta$ CNH <sub>2</sub> + $\beta$ CCH <sub>3</sub> ; 17/23 $\beta$ CCC
41		335 m	323	316	303 s	299 vs	400	391	386	377	29/30 $\gamma$ CNH <sub>2</sub> ; 19/20 $\gamma$ CCH <sub>3</sub> ; 25/20 $\gamma$ CCC; 13/10 $\nu$ MN
42			300	293	277 vw		299	292	292	285	75/78 $\beta$ CNH <sub>2</sub> + $\beta$ CCH <sub>3</sub> ; 11 $\nu$ MBr
43			278	272	634 s	635 m	603	589	580	567	87/89 $\gamma$ NH <sub>2</sub> (twist.)
					247 s		282	276	272	266	67/60 $\nu$ MN; 17/15 $\gamma$ CCH <sub>3</sub>
					217 w	213 s	277	271			78 $\nu$ MBr; 12 $\beta$ CCC
					208 s	211 vs	201	196			85 $\nu$ MBr; 12 $\gamma$ CCH <sub>3</sub>
44		121 vs	140	137			149	146			40 $\gamma$ CNH <sub>2</sub> ; 38 $\gamma$ CCH <sub>3</sub> ; 15 $\gamma$ NMN
							127	124	88	86	55/57 $\gamma$ NMBr; 20 $\gamma$ CNH <sub>2</sub> ; 17/15 $\gamma$ CCH <sub>3</sub>
							83	81	80	78	40 $\tau$ CNMN; 51/32 $\gamma$ NMBr
							65	64			75 $\tau$ CNMN
							48	47			52 $\gamma$ BrMBr; 39 $\gamma$ NMBr
							42	41			52 $\tau$ CCNM; 39 $\gamma$ NMBr
							37	36	37	36	84/75 $\tau$ CCNM
45			20	20			31	30			80 $\gamma$ CH <sub>3</sub> (torsion)
							18	18	15	15	81/84 $\tau$ CNMN
							11	11			87 $\tau$ CNMN

\*Experimental data is taken from Ref. [144], \*\*Experimental data is taken from Ref. [159].

Table 4.10 Experimental and calculated vibrational frequencies (in  $\text{cm}^{-1}$ ) of free p-toluidine and  $\text{NiBr}_2(\text{p-tol})_2$ .

p-toluidine				$\text{NiBr}_2(\text{p-tol})_2$										
Exp.*		B3LYP/def2-TZVP		Exp.**		B3LYP/def2-TZVP		B3LYP/def2-TZVP		PED (%) Assignments				
IR	Ra	Calc.	Scaled	IR	Ra	Calc.	Scaled	Calc.	Scaled					
1	3416 s	3418 w	3647	3470	3311 m	3312 s	3472	3303	3471	3302	95/96 $\nu\text{NH}_2$ (asym.)			
2	3333 s	3337 w	3552	3379	3240 s	3232 vs	3386	3221	3384	3220	95 $\nu\text{NH}_2$			
3	3056 w	3054 s	3171	3017	3065 vw	3057 vs	3192	3037	3192	3037	91/90 $\nu\text{CH}$			
4	3020m	3032 s	3168	3014	3032 w	3038 s,sh	3190	3035	3190	3035	95/88 $\nu\text{CH}$			
5	3008 m	3013 s	3152	2999	3008 w	3014 s	3138	2985	3138	2985	90/89 $\nu\text{CH}$ (asym.)			
6			3152	2999			3136	2984	3136	2984	87/86 $\nu\text{CH}$			
7	2912 m	2917 s	3097	2946	2911 m	2915 vs	3068	2919	3068	2919	95/96 $\nu\text{CH}_3$ (asym.)			
8	2859 m	2861m	3070	2921	2857 m	2864 vs	3041	2893	3041	2893	91/89 $\nu\text{CH}_3$ (asym.)			
9	2737 w	2738 w	3019	2872	2721 w	2735 w	2997	2851	2997	2851	87 $\nu\text{CH}_3$			
10	1621 vs	1617 s	1667	1629	1569 vs		1654	1616	1653	1615	31/46 $\beta\text{NH}_2$ (sciss.); 38/21 $\nu\text{CC}$ ; 13 $\beta\text{CH}$			
11			1654	1616	1615 s	1616 vs	1660	1622	1659	1621	57/38 $\beta\text{NH}_2$ (sciss.); 30/39 $\nu\text{CC}$ ; 11 $\beta\text{CH}$			
12	1582 s	1581 m	1621	1584			1620	1583	1619	1582	54/51 $\nu\text{CC}$ ; 22/19 $\beta\text{CH}$ ; 13/12 $\beta\text{CNH}_2$			
13	1514 vs		1555	1519	1516 vs	1518 w	1556	1520	1555	1519	54/56 $\beta\text{CH}$ ; 15 $\nu\text{CC}$ ; 10 $\nu\text{CC}+\nu\text{CN}$ ; 10 $\beta\text{CCC}$			
14			1501	1467			1501	1467	1501	1467	64/63 $\beta\text{CH}_3$ ; 15/16 $\beta\text{CH}$			
15			1488	1454	1451m,br	1449 w	1484	1450	1484	1450	73 $\beta\text{CH}_3$ ; 14 $\beta\text{CH}$			
16	1441 s		1463	1429			1464	1430	1464	1430	38/32 $\nu\text{CC}$ ; 25/24 $\beta\text{CH}$ ; 10 $\beta\text{CNH}_2$			
17		1380 m	1417	1385	1379 w	1377 m	1403	1371	1403	1371	89/90 $\beta\text{CH}_3$			
18	1324 m	1324 w	1359	1328	1326 vw	1327 w	1360	1329	1360	1329	54/59 $\beta\text{CH}$ ; 18/15 $\nu\text{CC}$ ; 19/17 $\beta\text{CNH}_2$			
19		1281 m	1333	1302	1296 w	1293 w	1339	1308	1339	1308	53/56 $\nu\text{CC}$ ; 29/24 $\beta\text{CH}$ ; 17/16 $\beta\text{CNH}_2$			
20	1267 vs	1271 m	1301	1271	1250 s	1242 s	1294	1264	1292	1262	57/60 $\nu\text{CC}+\nu\text{CN}$ ; 39/36 $\beta\text{CH}$			
21		1218 m	1235	1207	1235 s	1222 vs	1232	1204	1232	1204	63/62 $\nu\text{CC}$ ; 17 $\beta\text{CH}$			
22	1176 s	1179 m	1207	1179	1207 w,sh	1207 vs	1206	1178	1206	1178	74/75 $\beta\text{CH}$ ; 17 $\nu\text{CC}$			
23	1120 s		1153	1127	1180 m	1179 s	1158	1131	1157	1131	57/65 $\beta\text{CH}$ ; 20 $\beta\text{NH}_2$ (rock.); 13/12 $\nu\text{CC}$			
24	1074 m		1092	1067	1116 w,sh	1123 w	1112	1087	1110	1085	45/54 $\beta\text{NH}_2$ (rock.); 25/21 $\beta\text{CH}$ ; 20 $\beta\text{CCC}$			
25	1044 m		1064	1040	1062 vs	1070 w	1055	1031	1055	1031	65/64 $\gamma\text{CCH}_3$ ; 20 $\gamma\text{CCC}$ ; 15/14 $\gamma\text{CH}$			
26	983 w		1034	1010	1038	1046 vs	1039	1015	1039	1015	51/54 $\beta\text{CCC}$ ; 30/26 $\beta\text{CH}$ ; 18 $\beta\text{CCH}_3$			
27	953 w		1002	979	998 s	1000 s	998	975	998	975	48/47 $\beta\text{CCH}_3$ ; 22 $\beta\text{CCC}$ ; 30 $\beta\text{CNH}_2$			
28			933	912			920	899	920	899	77/78 $\gamma\text{CH}$ ; 12/14 $\gamma\text{CCC}$			
29	931 w		931	910		930 vw	916	895	912	891	47/38 $\gamma\text{CH}$ ; 35 $\gamma\text{CCC}$ ; 12/10 $\gamma\text{CNH}_2$			

Table 4.10 cont.

p-toluidine				NiBr <sub>2</sub> (p-tol) <sub>2</sub>							
Exp.*		B3LYP/def2-TZVP		Exp.**		B3LYP/def2-TZVP				PED (%) Assignments	
IR	Ra	Calc.	Scaled	IR	Ra	Calc.	Scaled	Calc.	Scaled		
30		844 s	854	834	835 m	830 vs	850	831	850	831	63/58 $\nu$ CC+ $\nu$ CN; 13 $\beta$ CCC
31	812 vs		830	811	810 vs	810 m	832	813	830	811	59/62 $\gamma$ CH; 28/25 $\gamma$ CCC; 10 $\gamma$ CNH <sub>2</sub>
32			821	802			822	803	822	803	83/84 $\gamma$ CH
33	720 m		752	735	733 s	742 m	749	732	748	731	40/46 $\nu$ CC+ $\nu$ CN; 15/12 $\beta$ CCC
34			724	707	705 s	709 vw	710	694	710	694	31/15 $\gamma$ CCC; 16/35 $\gamma$ CCH <sub>3</sub> ; 17/15 $\gamma$ CNH <sub>2</sub>
35		645 s	661	646	647 s	650 vw	677	661	667	652	47/56 $\beta$ CCC; 39/30 $\beta$ CNH <sub>2</sub>
36			591	577	938 s		930	909	928	907	40/45 $\gamma$ NH <sub>2</sub> (wag.); 32/30 $\gamma$ CCH <sub>3</sub> ; 25 $\gamma$ CCC
37	504 vs		510	498	523 vs	518 vw	534	522	532	520	41/40 $\gamma$ CH; 33/31 $\gamma$ CCC; 11/14 $\gamma$ CNH <sub>2</sub>
38	470	466 s	470	459	476 m	476 m	484	473	482	471	54/60 $\nu$ CC+ $\nu$ CN; 22/18 $\beta$ CCC
39		409 w	420	410	412 m	410 m	422	412	422	412	81/84 $\gamma$ CCC
40			410	401	386 m	386 m	406	397	406	397	74/77 $\beta$ CCH <sub>3</sub> + $\beta$ CNH <sub>2</sub> ; 22 $\beta$ CCC
41		335 m	323	316	308 s	315 w	379	371	369	361	33 $\gamma$ CCH <sub>3</sub> ; 24/16 $\gamma$ CNH <sub>2</sub> ; 16/20 $\gamma$ CCC; 17/12 $\nu$ MN
42			300	293	297 s	285 vs	304	297	304	297	82/87 $\beta$ CCH <sub>3</sub> + $\beta$ CNH <sub>2</sub> (twist.)
43			278	272	607 vs	610 m	655	640	647	632	94/90 $\gamma$ NH <sub>2</sub> (twist.)
					273 m,sh		257	252			72 $\nu$ MN; 22 $\gamma$ CCH <sub>3</sub>
44		121 vs	140	137	234 m		235	230			42 $\gamma$ CNH <sub>2</sub> ; 40 $\gamma$ CCH <sub>3</sub> ; 11 $\nu$ MN
						155 m	168	164			67 $\nu$ MN; 10 $\gamma$ CNH <sub>2</sub> ; 10 $\gamma$ CCH <sub>3</sub>
						136 m	129	126			78 $\nu$ MBr; 22 $\gamma$ CCH <sub>3</sub>
							127	124	123	120	61/59 $\nu$ MBr; 29/32 $\gamma$ NMBr
							117	114			42 $\gamma$ NMBr; 30 $\gamma$ NMN
							115	112	108	106	73/75 $\tau$ CNMN; 25 $\gamma$ NMBr
							92	90	90	88	45/50 $\tau$ CNMN; 21/25 $\gamma$ CCH <sub>3</sub> ; 24/19 $\gamma$ CNH <sub>2</sub>
							78	76	72	70	63/66 $\tau$ CNMN; 24/36 $\gamma$ NMBr
							69	67			55 $\gamma$ NMBr; 30 $\nu$ MN
							62	61	57	56	40/70 $\nu$ MBr; 40/30 $\beta$ NMBr
45			20	20			47	46	45	44	95/90 $\gamma$ CH <sub>3</sub> (torsion)
							44	43			57 $\tau$ CCNM; 36 $\gamma$ CCH <sub>3</sub>
							41	40			70 $\tau$ CCNM; 22 $\gamma$ NMBr
							40	39	35	34	61/65 $\gamma$ NMBr; 27/30 $\tau$ CNMN
							23	22	20	20	87/80 $\tau$ CNMN
							15	15			92 $\tau$ CNMN

\*Experimental data is taken from Ref. [144], \*\*Experimental data is taken from Ref. [159].

Table 4.11 Experimental and calculated vibrational frequencies (in  $\text{cm}^{-1}$ ) of free p-toluidine and  $\text{CuBr}_2(\text{p-tol})_2$ .

p-toluidine					$\text{CuBr}_2(\text{p-tol})_2$						
Exp.*			B3LYP/def2-TZVP		Exp.**		B3LYP/def2-TZVP				PED (%) Assignments
No	IR	Ra	Calc.	Scaled	IR	Ra	Calc.	Scaled	Calc.	Scaled	
1	3416 s	3418 w	3647	3470	3286 s		3553	3380	3553	3380	100 $\nu\text{NH}_2$ (asym.)
2	3333 s	3337 w	3552	3379	3226 s		3468	3299	3468	3299	100 $\nu\text{NH}_2$
3	3056 w	3054 s	3171	3017	3056 w	3053 w	3194	3039	3194	3039	96 $\nu\text{CH}$
4	3020m, sh	3032 s	3168	3014			3193	3038	3193	3038	99 $\nu\text{CH}$ (asym.)
5	3008 m	3013 s	3152	2999			3169	3015	3169	3015	99/98 $\nu\text{CH}$
6			3152	2999	3006 w		3169	3015	3169	3015	98 $\nu\text{CH}$
7	2912 m	2917 s	3097	2946	2916 m	2916 w	3107	2956	3107	2956	97 $\nu\text{CH}_3$ (asym.)
8	2859 m	2861m	3070	2921	2857 w		3079	2929	3079	2929	96/98 $\nu\text{CH}_3$ (asym.)
9	2737 w	2738 w	3019	2872			3026	2879	3026	2879	98/96 $\nu\text{CH}_3$
10	1621 vs	1617 s	1667	1629	1592s	1597 m	1634	1597	1632	1595	80/82 $\beta\text{NH}_2$ (sciss.)
11			1654	1616			1656	1618	1655	1617	41/55 $\nu\text{CC}$ ; 23 $\beta\text{CH}$ ; 20/18 $\beta\text{CCC}$
12	1582 s, sh	1581 m	1621	1584	1562 s	1577 w	1632	1595	1632	1595	42/44 $\nu\text{CC}$ ; 20 $\beta\text{CNH}_2$ ; 17/15 $\beta\text{CCH}_3$ ; 12 $\beta\text{CH}$
13	1514 vs		1555	1519	1508 s	1519 w,sh	1552	1516	1551	1515	59/57 $\beta\text{CH}$ ; 16 $\nu\text{CC}$ ; 20/21 $\beta\text{CCC}$
14			1501	1467			1500	1466	1500	1466	62 $\beta\text{CH}_3$ ; 24/22 $\beta\text{CH}$
15			1488	1454		1445 m	1489	1455	1489	1455	75 $\beta\text{CH}_3$ ; 21 $\beta\text{CCH}_3$
16	1441 s		1463	1429	1440 w		1464	1430	1464	1430	41 $\nu\text{CC}$ ; 32 $\beta\text{CH}$ ; 12/14 $\beta\text{CH}_3$ ; 12/13 $\beta\text{NH}_2$
17		1380 m	1417	1385	1347 w	1355 w	1417	1385	1417	1385	94 $\beta\text{CH}_3$
18	1324 m	1324 w	1359	1328	1322 w		1368	1337	1368	1337	64/60 $\beta\text{CH}$ ; 22/24 $\beta\text{NH}_2$ ; 12 $\nu\text{CC}$
19		1281 m	1333	1302			1338	1307	1337	1306	48/50 $\nu\text{CC}$ ; 20 $\beta\text{CH}$ ; 14/12 $\beta\text{NH}_2$ ; 16/15 $\beta\text{CCH}_3$
20	1267 vs	1271 m	1301	1271	1238 w	1239 w	1242	1214	1242	1214	42 $\nu\text{CN}$ ; 36/33 $\nu\text{CC}$ ; 20 $\beta\text{CH}$
21		1218 m	1235	1207	1216 m	1216 w	1234	1206	1234	1206	56/54 $\nu\text{CC}$ ; 24 $\beta\text{CH}$ ; 16/18 $\nu\text{CN}$
22	1176 s	1179 m	1207	1179			1211	1183	1211	1183	78 $\beta\text{CH}$ ; 16 $\nu\text{CC}$
23	1120 s		1153	1127	1144 w	1145 m	1168	1141	1167	1140	44 $\beta\text{CH}$ ; 30/26 $\beta\text{CNH}_2$ ; 15 $\nu\text{CC}$
24	1074 m		1092	1067	1094 vs	1093 m	1132	1106	1131	1105	38/40 $\beta\text{NH}_2$ (rock.); 18/16 $\nu\text{CC}$ ; 18 $\beta\text{CH}$ ; 12 $\beta\text{CCC}$
25	1044 m		1064	1040	1041 w		1066	1042	1065	1041	76/78 $\gamma\text{CCH}_3$ ; 17 $\gamma\text{CH}$
26	983 w		1034	1010			1042	1018	1042	1018	72 $\beta\text{CCC}$ ; 22/24 $\beta\text{CH}$
27	953 w		1002	979			1008	985	1008	985	56 $\beta\text{CCH}_3$ ; 20 $\beta\text{CH}_3$ ; 16 $\beta\text{CH}$
28			933	912			965	943	964	942	82 $\gamma\text{CH}$ ; 12/10 $\gamma\text{CCC}$

Table 4.11 cont.

p-toluidine					CuBr <sub>2</sub> (p-tol) <sub>2</sub>						
Exp.*		B3LYP/def2-TZVP		Exp.**		B3LYP/def2-TZVP				PED (%) Assignments	
No	IR	Ra	Calc.	Scaled	IR	Ra	Calc.	Scaled	Calc.		Scaled
29	931 w		931	910	934 w		956	934	956	934	74 $\gamma$ CH; 13/12 $\gamma$ CNH <sub>2</sub> ; 12/11 $\gamma$ CCH <sub>3</sub>
30		844 s	854	834		877 w	845	826	843	824	68 $\nu$ CC+ $\nu$ CN; 32 $\beta$ CCC
31	812 vs		830	811	812 vs		834	815	833	814	68 $\gamma$ CH; 22 $\gamma$ CNH <sub>2</sub> + $\gamma$ CH <sub>3</sub>
32			821	802			844	825	843	824	86 $\gamma$ CH
33	720 m		752	735	738 m	739 w,sh	744	727	740	723	38/36 $\nu$ CN; 33 $\beta$ CCC; 25/27 $\nu$ CC
34			724	707			726	709	726	709	66 $\gamma$ CCC; 26 $\gamma$ CCH <sub>3</sub>
35		645 s	661	646			669	654	665	650	40 $\beta$ CCC; 45/46 $\beta$ CNH <sub>2</sub>
36			591	577			1018	995	1017	994	84 $\gamma$ NH <sub>2</sub> (wag.)
37	504 vs		510	498	537 w		535	523	532	520	80/82 $\gamma$ CCC+ $\gamma$ CNH <sub>2</sub> (wag.)
38	470	466 s	470	459	487 m	480 vw	478	467	472	461	56/58 $\nu$ CN+ $\nu$ CC; 39/36 $\beta$ CCC
39		409 w	420	410	443 m		420	410	420	410	78 $\gamma$ CCC; 20 $\gamma$ CH
40			410	401	383 m	382 vw	394	385	390	381	76 $\beta$ CCH <sub>3</sub> + $\beta$ CNH <sub>2</sub> ; 22/20 $\beta$ CCC
41		335 m	323	316	332 s		407	398	386	377	66 $\gamma$ CCH <sub>3</sub> + $\gamma$ CNH <sub>2</sub> ; 30/31 $\gamma$ CCC
42			300	293	297 s	296 m	304	297	298	291	82 $\beta$ CCH <sub>3</sub> + $\beta$ CNH <sub>2</sub>
43			278	272	635 m	633 w,sh	641	626	622	608	87/88 $\gamma$ NH <sub>2</sub> (twist.)
44		121 vs	140	137	244 m	251 vw	286	279	259	253	74/80 $\gamma$ CCH <sub>3</sub> + $\gamma$ CNH <sub>2</sub> ; 10/0 $\nu$ MN
					221 m	222 vw	246	240			78 $\nu$ MBr; 20 $\beta$ CNH <sub>2</sub>
					207 m		170	166			76 $\nu$ MN; 26 $\gamma$ CCH <sub>3</sub> + $\gamma$ CNH <sub>2</sub>
							144	141			80 $\nu$ MBr; 18 $\gamma$ CCH <sub>3</sub> + $\gamma$ CNH <sub>2</sub>
							130	127	120	117	80/76 $\tau$ CNMN
							118	115	107	105	58 $\gamma$ NMBr; 20 $\nu$ MN; 18 $\gamma$ CNH <sub>2</sub> + $\gamma$ CCH <sub>3</sub>
							106	104			60 $\gamma$ NMN; 25 $\tau$ CCNM; 15 $\gamma$ CCH <sub>3</sub>
							65	64	51	50	42/44 $\tau$ CCCN; 26/20 $\tau$ CCNM; 24/14 $\gamma$ NMBr
							47	46	46	45	80/66 $\tau$ CNMN; 16/30 $\gamma$ NMBr
45			20	20			20	20	15	15	94/88 $\gamma$ CH <sub>3</sub> (torsion)
							18	18	16	16	64/66 $\tau$ CNMN; 24/18 $\gamma$ CCH <sub>3</sub>
							4	4			70 $\tau$ CNMN; 24 $\gamma$ NMN

\*Experimental data is taken from Ref. [144], \*\*Experimental data is taken from Ref. [25].



Table 4.12 Experimental and calculated vibrational frequencies (in  $\text{cm}^{-1}$ ) of free p-toluidine and  $\text{ZnBr}_2(\text{p-tol})_2$ .

p-toluidine					$\text{ZnBr}_2(\text{p-tol})_2$						
Exp.*		B3LYP/def2-TZVP			Exp.**		B3LYP/def2-TZVP				PED (%) Assignments
No	IR	Ra	Calc.	Scaled	IR	Ra	Calc.	Scaled	Calc.	Scaled	
1	3416 s	3418 w	3647	3470	3286 s	3286 w	3566	3393	3549	3377	100 $\nu\text{NH}_2$ (asym.)
2	3333 s	3337 w	3552	3379	3236 vs	3237 s	3482	3313	3476	3307	100 $\nu\text{NH}_2$
3	3056 w	3054 s	3171	3017	3056 vw	3057 s	3186	3031	3181	3027	87/99 $\nu\text{CH}$
4	3020m, sh	3032 s	3168	3014	3034 w	3035 s	3183	3029	3179	3024	89/99 $\nu\text{CH}$ (asym.)
5	3008 m	3013 s	3152	2999	3014 w	3011 s	3168	3014	3165	3011	88/98 $\nu\text{CH}$
6			3152	2999			3167	3013	3164	3011	91/98 $\nu\text{CH}$
7	2912 m	2917 s	3097	2946	2920 m	2924 s	3108	2956	3106	2955	98/92 $\nu\text{CH}_3$ (asym.)
8	2859 m	2861m	3070	2921	2862 w	2862 m	3081	2931	3080	2930	98/92 $\nu\text{CH}_3$ (asym.)
9	2737 w	2738 w	3019	2872	2733 vw	2734 w	3029	2881	3029	2881	87/91 $\nu\text{CH}_3$
10	1621 vs	1617 s	1667	1629		1596 s	1654	1616	1636	1598	67/73 $\beta\text{NH}_2$ (sciss.); 14/17 $\beta\text{CNH}_2$ ; 10 $\nu\text{CC}$
11			1654	1616		1615 s	1661	1623	1660	1622	55/53 $\nu\text{CC}$ ; 21/20 $\beta\text{CH}$ ; 17/11 $\beta\text{NH}_2$
12	1582 s, sh	1581 m	1621	1584	1577 s	1577 m,sh	1636	1599	1630	1593	48/52 $\nu\text{CC}$ ; 23 $\beta\text{CCC}$ ; 15/12 $\beta\text{CH}$ ; 17/15 $\beta\text{NH}_2$
13	1514 vs		1555	1519	1513 vs	1511 vw	1554	1518	1553	1518	60/58 $\beta\text{CH}$ ; 17 $\beta\text{CCC}$ ; 16/18 $\nu\text{CC}$
14			1501	1467			1501	1467	1500	1466	56 $\beta\text{CH}_3$ ; 17/14 $\beta\text{CCH}_3$ ; 10 $\beta\text{CH}$
15			1488	1454	1461w		1490	1456	1489	1455	79/70 $\beta\text{CH}_3$ ; 18 $\beta\text{CCH}_3$
16	1441 s		1463	1429	1443 w		1463	1430	1462	1428	33/39 $\nu\text{CC}$ ; 27/25 $\beta\text{CH}$ ; 15 $\beta\text{CH}_3$ ; 14/11 $\beta\text{NH}_2$
17		1380 m	1417	1385	1379 vw	1380 m	1420	1388	1418	1386	95/91 $\beta\text{CH}_3$
18	1324 m	1324 w	1359	1328	1327 vw	1327 m	1365	1334	1365	1333	61/60 $\beta\text{CH}$ ; 17 $\beta\text{NH}_2$ ; 12 $\nu\text{CC}$
19		1281 m	1333	1302	1296 vw	1296 vw	1337	1306	1334	1304	54/59 $\nu\text{CC}$ ; 15/18 $\beta\text{NH}_2$ ; 12/11 $\beta\text{CH}$
20	1267 vs	1271 m	1301	1271	1236 w,sh		1263	1234	1246	1217	45/41 $\nu\text{CN}$ ; 21 $\nu\text{CC}$ ; 23/21 $\beta\text{CH}$
21		1218 m	1235	1207	1221 m	1212vs	1234	1206	1234	1205	63/67 $\nu\text{CC}$ ; 27/21 $\beta\text{CH}$
22	1176 s	1179 m	1207	1179	1182 vw	1183 m	1211	1184	1210	1183	74 $\beta\text{CH}$ ; 16/20 $\nu\text{CC}$
23	1120 s		1153	1127	1120 m,sh	1131 vw	1161	1135	1161	1134	45 $\beta\text{CH}$ ; 25/23 $\beta\text{NH}_2$ (rock.); 11/15 $\nu\text{CC}$
24	1074 m		1092	1067	1072 vs	1081 s	1126	1101	1122	1096	40/42 $\beta\text{NH}_2$ (rock.); 12/17 $\nu\text{CC}$ ; 17/14 $\beta\text{CH}$ ; 14 $\beta\text{CH}_3$
25	1044 m		1064	1040		1067 s	1067	1042	1067	1042	75/69 $\gamma\text{CCH}_3$ ; 17/13 $\gamma\text{CH}$
26	983 w		1034	1010			1040	1016	1038	1014	70/60 $\beta\text{CCC}$ ; 15/20 $\beta\text{CH}$
27	953 w		1002	979	956 w	939 vw	1008	985	1008	985	52/54 $\beta\text{CCH}_3$ ; 17/22 $\beta\text{CH}_3$ ; 15/10 $\beta\text{CH}$ ; 10 $\beta\text{CNH}_2$
28			933	912			969	947	951	929	76/83 $\gamma\text{CH}$ ; 21/12 $\gamma\text{CCC}$

Table 4.12 cont.

p-toluidine					ZnBr <sub>2</sub> (p-tol) <sub>2</sub>						
No	IR	Exp.*	B3LYP/def2-TZVP		IR	Exp.**	B3LYP/def2-TZVP				PED (%) Assignments
		Ra	Calc.	Scaled		Ra	Calc.	Scaled	Calc.	Scaled	
29	931 w		931	910			944	922	942	920	72/69 $\gamma$ CH; 20 $\gamma$ CNH <sub>2</sub>
30		844 s	854	834		836 s	846	827	845	826	64/58 $\nu$ CC+ $\nu$ CN; 23/30 $\beta$ CCC
31	812 vs		830	811	812 vs	816 s	847	828	833	814	69/57 $\gamma$ CH; 15/18 $\gamma$ CNH <sub>2</sub>
32			821	802			833	814	826	807	89/80 $\gamma$ CH
33	720 m		752	735	735 m	738 w	745	728	743	726	36/37 $\nu$ CC; 30/27 $\nu$ CN; 18/29 $\beta$ CCC
34			724	707	704 m	705 vw	727	710	724	708	64/72 $\gamma$ CCC; 16 $\gamma$ CNH <sub>2</sub> ; 11 $\gamma$ CH
35		645 s	661	646	661 s	647 s	661	646	661	646	76/70 $\beta$ CCC; 10/11 $\beta$ CNH <sub>2</sub> (wag.)
36			591	577			1053	1029	967	945	77/67 $\gamma$ NH <sub>2</sub> (wag.); 10/19 $\gamma$ CCC
37	504 vs		510	498	522 vs	521 w	532	520	527	515	77/82 $\gamma$ CCC+ $\gamma$ NH <sub>2</sub> (wag.)
38	470	466 s	470	459	473 w	472 s	478	467	474	463	48/49 $\beta$ CCC; 42/44 $\nu$ CN+ $\nu$ CC
39		409 w	420	410	401 m	407	421	411	419	409	76/75 $\gamma$ CCC; 18/14 $\gamma$ CH
40			410	401	360 m	364	397	388	384	375	71/68 $\beta$ CCH <sub>3</sub> + $\beta$ CNH <sub>2</sub> ; 25 $\beta$ CCC
41		335 m	323	316	300 s	303 s	380	372	364	356	73 $\gamma$ CNH <sub>2</sub> + $\gamma$ CCH <sub>3</sub> ; 25/23 $\gamma$ CCC
42			300	293	280 w,sh		303	296	292	285	70/81 $\beta$ CNH <sub>2</sub> + $\beta$ CCH <sub>3</sub> ; 10 $\nu$ MBr
43			278	272	633 s	628 w	591	577	561	548	87 $\gamma$ NH <sub>2</sub> (twist.)
					246 s		280	273			57 $\nu$ MBr; 23 $\beta$ CCC+ $\beta$ CNH <sub>2</sub>
					228 m,sh		260	254	242	236	58/59 $\nu$ MN; 26/23 $\gamma$ CCH <sub>3</sub> + $\gamma$ CNH <sub>2</sub>
					207 s	204 s	198	193			93 $\nu$ MBr
44		121 vs	140	137			136	133	123	120	52/56 $\gamma$ CCH <sub>3</sub> + $\gamma$ CNH <sub>2</sub> ; 20/25 $\nu$ MN
							90	88	82	80	64/67 $\nu$ MN; 22 $\tau$ CNMN
							77	75	67	66	65/59 $\gamma$ NMBr; 24/28 $\tau$ CCNM
							53	52			86 $\gamma$ NMN+ $\gamma$ BrMBr
							40	39	26	26	53/56 $\tau$ CCNM; 26 $\gamma$ NMBr; 0/11 $\gamma$ CH <sub>3</sub>
45			20	20			38	37	37	36	76/86 $\gamma$ CH <sub>3</sub> (torsion)
							24	23	16	16	41 $\tau$ CCNM; 10/22 $\gamma$ NMBr; 39/40 $\gamma$ CH <sub>3</sub>
							18	17			69 $\gamma$ NMN; 29 $\tau$ CCNM
							10	10			77/76 $\tau$ CNMN; 21 $\gamma$ NMBr

\*Experimental data is taken from Ref. [144], \*\*Experimental data is taken from Ref. [26].

Table 4.13 Experimental and calculated vibrational frequencies (in  $\text{cm}^{-1}$ ) of free p-toluidine and  $\text{CdBr}_2(\text{p-tol})_2$ .

p-toluidine					$\text{CdBr}_2(\text{p-tol})_2$						
Exp.*			B3LYP/def2-TZVP		Exp.**		B3LYP/def2-TZVP				PED (%) Assignments
No	IR	Ra	Calc.	Scaled	IR	Ra	Calc.	Scaled	Calc.	Scaled	
1	3416 s	3418 w	3647	3470	3301 m	3307 w	3585	3411	3564	3391	100 $\nu\text{NH}_2$ (asym.)
2	3333 s	3337 w	3552	3379	3251 s	3247 m	3499	3329	3489	3319	100 $\nu\text{NH}_2$
3	3056 w	3054 s	3171	3017	3053 w	3051 s	3182	3027	3180	3025	98 $\nu\text{CH}$
4	3020m,sh	3032 s	3168	3014	3026 m	3017 m	3180	3025	3177	3023	97/98 $\nu\text{CH}$ (asym.)
5	3008 m	3013 s	3152	2999	3007 w		3165	3011	3163	3009	94/98 $\nu\text{CH}$
6			3152	2999			3164	3011	3162	3009	95/99 $\nu\text{CH}$
7	2912 m	2917 s	3097	2946	2921 m	2918 s	3107	2956	3106	2955	99 $\nu\text{CH}_3$ (asym.)
8	2859 m	2861m	3070	2921	2861 w	2858 w	3080	2930	3079	2929	99 $\nu\text{CH}_3$ (asym.)
9	2737 w	2738 w	3019	2872	2730 w	2722 w	3028	2880	3026	2879	99 $\nu\text{CH}_3$
10	1621 vs	1617 s	1667	1629		1599 m	1655	1617	1643	1605	58/79 $\beta\text{NH}_2$ (sciss.); 11/18 $\beta\text{CNH}_2$ ; 18/0 $\nu\text{CC}$
11			1654	1616	1617 m	1619 s	1661	1623	1660	1622	42/58 $\nu\text{CC}$ ; 21/15 $\beta\text{NH}_2$ (sciss.); 20 $\beta\text{CH}$
12	1582 s, sh	1581 m	1621	1584	1577 s	1565 m	1633	1596	1627	1590	65/66 $\nu\text{CC}$ ; 15/14 $\beta\text{NH}_2$ ; 10 $\beta\text{CH}$ ; 10 $\beta\text{CCH}_3$
13	1514 vs		1555	1519	1515 vs		1553	1518	1553	1517	63 $\beta\text{CH}$ ; 15/17 $\beta\text{CCC}$ ; 12/14 $\nu\text{CC}$
14			1501	1467	1461 w		1501	1466	1500	1466	69/70 $\beta\text{CH}_3$ ; 12/11 $\beta\text{CH}$
15			1488	1454			1490	1456	1489	1455	72/75 $\beta\text{CH}_3$ ; 23/22 $\beta\text{CCH}_3$
16	1441 s		1463	1429	1444 w		1463	1429	1462	1428	31/32 $\beta\text{CH}$ ; 28/20 $\nu\text{CC}$ ; 13/12 $\beta\text{CH}_3$ ; 12 $\beta\text{NH}_2$
17		1380 m	1417	1385	1379 w	1380 m	1419	1387	1418	1386	96/91 $\beta\text{CH}_3$
18	1324 m	1324 w	1359	1328	1322 vw	1317 vw	1364	1333	1363	1332	64/67 $\beta\text{CH}$ ; 14/10 $\beta\text{NH}_2$ ; 11 $\nu\text{CC}$
19		1281 m	1333	1302	1295 vw	1280 vw	1335	1304	1333	1303	61/60 $\nu\text{CC}$ ; 13/11 $\beta\text{CH}$ ; 10 $\beta\text{NH}_2$
20	1267 vs	1271 m	1301	1271	1237 s	1236 m	1268	1239	1253	1225	41/49 $\nu\text{CN}$ ; 36/35 $\nu\text{CC}$ ; 12/10 $\beta\text{CH}$
21		1218 m	1235	1207	1226 s	1224m	1234	1206	1234	1205	57/61 $\nu\text{CC}$ ; 30/31 $\beta\text{CH}$
22	1176 s	1179 m	1207	1179	1182 w	1181 m	1210	1183	1210	1182	75/73 $\beta\text{CH}$ ; 12/13 $\nu\text{CC}$
23	1120 s		1153	1127	1115 w	1112m,sh	1159	1133	1158	1132	53/47 $\beta\text{CH}$ ; 19/20 $\beta\text{NH}_2$ (rock.); 16/12 $\nu\text{CC}$
24	1074 m		1092	1067	1096 w	1091 m	1119	1094	1116	1090	42/41 $\beta\text{NH}_2$ (rock.); 12/13 $\beta\text{CH}_3$ ; 10 $\beta\text{CH}$ ; 11 $\nu\text{CC}$
25	1044 m		1064	1040	1043 vs	1044 s	1067	1042	1067	1042	81/79 $\gamma\text{CCH}_3$ ; 16/19 $\gamma\text{CH}$
26	983 w		1034	1010			1039	1016	1038	1014	78/85 $\beta\text{CCC}$ ; 18/15 $\beta\text{CH}$
27	953 w		1002	979			1006	983	1006	983	55/57 $\beta\text{CCH}_3$ ; 15/14 $\beta\text{CH}_3$ ; 11 $\beta\text{CH}$ ; 10/11 $\beta\text{CNH}_2$
28			933	912			967	945	952	930	78/83 $\gamma\text{CH}$ ; 20/11 $\gamma\text{CCC}$

Table 4.13 cont.

p-toluidine					CdBr <sub>2</sub> (p-tol) <sub>2</sub>						
Exp.*		B3LYP/def2-TZVP		Exp.**		B3LYP/def2-TZVP				PED (%) Assignments	
No	IR	Ra	Calc.	Scaled	IR	Ra	Calc.	Scaled	Calc.		Scaled
29	931 w		931	910	930 m	933 vw	956	934	942	921	73/83 $\gamma$ CH; 17/12 $\gamma$ CNH <sub>2</sub>
30		844 s	854	834	834 m	836 m	846	826	845	825	45/47 $\nu$ CC; 25 $\nu$ CN; 21/19 $\beta$ CCC
31	812 vs		830	811	806 s	809 m	828	809	824	805	65/71 $\gamma$ CH; 11 $\gamma$ CNH <sub>2</sub>
32			821	802			845	826	833	814	88/85 $\gamma$ CH
33	720 m		752	735		738 w	745	727	743	726	37/35 $\nu$ CC; 24 $\nu$ CN; 29/28 $\beta$ CCC
34			724	707	705 m	708 w	728	711	724	707	72/59 $\gamma$ CCC; 13/20 $\gamma$ CNH <sub>2</sub> ; 15/10 $\gamma$ CCH <sub>3</sub>
35		645 s	661	646	647 vw	643 m	661	646	660	645	81/80 $\beta$ CCC; 13 $\nu$ CC
36			591	577			991	968	901	881	74/76 $\gamma$ NH <sub>2</sub> (wag.); 16/14 $\gamma$ CCC
37	504 vs		510	498	507 s	514 vw	527	515	523	511	80/79 $\gamma$ CCC+ $\gamma$ CNH <sub>2</sub> (wag.)
38	470	466 s	470	459	474 w	472 m	474	463	472	461	55/43 $\beta$ CCC; 43/46 $\nu$ CN+ $\nu$ CC
39		409 w	420	410	411 m	407 m	421	411	417	407	76 $\gamma$ CCC; 19/15 $\gamma$ CH
40			410	401	394 m	370 m	395	386	386	377	74/79 $\beta$ CCH <sub>3</sub> + $\beta$ CNH <sub>2</sub> ; 21/17 $\beta$ CCC
41		335 m	323	316	302 s	303 s	358	350	351	343	68/79 $\gamma$ CNH <sub>2</sub> + $\gamma$ CCH <sub>3</sub> ; 21/13 $\gamma$ CCC
42			300	293	279 w		299	292	292	286	88/85 $\beta$ CNH <sub>2</sub> + $\beta$ CCH <sub>3</sub>
43			278	272	568 s	562 w	541	529	515	503	88 $\gamma$ NH <sub>2</sub> (twist.)
					245 s	246 s	247	241	172	168	96/94 $\nu$ MBr
44		121 vs	140	137	227 m		229	224	210	206	64/65 $\gamma$ CCH <sub>3</sub> + $\gamma$ CNH <sub>2</sub> ; 27/29 $\nu$ MN
						139m,sh	113	110	109	107	55/53 $\nu$ MN; 28/27 $\gamma$ CNH <sub>2</sub> + $\gamma$ CCH <sub>3</sub>
							69	68	65	63	57/64 $\tau$ CCNM; 22 $\gamma$ NMBr
							68	67	61	59	66/68 $\nu$ MN; 16/10 $\gamma$ BrMBr
							44	43	33	32	61/54 $\gamma$ CNM; 23/20 $\gamma$ BrMBr
							35	34	20	20	68/71 $\tau$ CNMN; 15/10 $\gamma$ NMBr
45			20	20			22	22	15	15	89/78 $\gamma$ CH <sub>3</sub> (torsion)
							16	16			52 $\tau$ CNMN; 18 $\tau$ CCNM; 16 $\gamma$ CCH <sub>3</sub>
							16	15			60 $\tau$ CNMN; 23 $\gamma$ CCH <sub>3</sub>
							9	9			80 $\tau$ CNMN; 20 $\gamma$ NMBr

\*Experimental data is taken from Ref. [144], \*\*Experimental data is taken from Ref. [26].

Table 4.14 Experimental and calculated vibrational frequencies (in  $\text{cm}^{-1}$ ) of free p-toluidine and  $\text{HgBr}_2(\text{p-tol})_2$ .

p-toluidine					$\text{HgBr}_2(\text{p-tol})_2$						
Exp.*			B3LYP/def2-TZVP		Exp.**		B3LYP/def2-TZVP				PED (%) Assignments
No	IR	Ra	Calc.	Scaled	IR	Ra	Calc.	Scaled	Calc.	Scaled	
1	3416 s	3418 w	3647	3470	3300 m	3002vw	3618	3442	3587	3413	100/99 $\nu\text{NH}_2$ (asym.)
2	3333 s	3337 w	3552	3379	3243 s	3247 vs	3526	3354	3503	3333	100/99 $\nu\text{NH}_2$
3	3056 w	3054 s	3171	3017	3053 w	3058 vs	3180	3025	3178	3023	95/97 $\nu\text{CH}$
4	3020m, sh	3032 s	3168	3014	3033 w	3038 s	3176	3021	3175	3021	97/95 $\nu\text{CH}$ (asym.)
5	3008 m	3013 s	3152	2999	3008 w	3014 s	3161	3007	3160	3007	91/89 $\nu\text{CH}$
6			3152	2999			3160	3006	3160	3006	90/91 $\nu\text{CH}$
7	2912 m	2917 s	3097	2946	2913vw	2915 vs	3104	2954	3103	2952	98 $\nu\text{CH}_3$ (asym.)
8	2859 m	2861m	3070	2921	2857vw	2858 vs	3077	2928	3075	2925	98 $\nu\text{CH}_3$ (asym.)
9	2737 w	2738 w	3019	2872		2732 w	3025	2878	3024	2877	99 $\nu\text{CH}_3$
10	1621 vs	1617 s	1667	1629		1593 m	1654	1616	1651	1613	54/69 $\beta\text{NH}_2$ (sciss.); 17/11 $\beta\text{CNH}_2$ ; 15/14 $\nu\text{CC}$
11			1654	1616	1612 s	1611 vs	1663	1625	1661	1623	45/58 $\nu\text{CC}$ ; 26 $\beta\text{NH}_2$ (sciss.); 18/12 $\beta\text{CH}$
12	1582 s, sh	1581 m	1621	1584	1575 vs	1570vw	1628	1591	1624	1587	58/46 $\nu\text{CC}$ ; 12/19 $\beta\text{CCC}$ ; 15/17 $\beta\text{CCH}_3$ ; 14/19 $\beta\text{NH}_2$
13	1514 vs		1555	1519	1512 vs	1512 w	1554	1518	1553	1517	59/57 $\beta\text{CH}$ ; 21/23 $\beta\text{CCC}$ ; 16 $\nu\text{CC}$
14			1501	1467			1501	1466	1500	1466	67/71 $\beta\text{CH}_3$ ; 13/10 $\beta\text{CH}$
15			1488	1454			1489	1455	1489	1455	73/67 $\beta\text{CH}_3$ ; 22/23 $\beta\text{CCH}_3$
16	1441 s		1463	1429			1463	1429	1462	1428	37/34 $\nu\text{CC}$ ; 23/16 $\beta\text{CH}$ ; 17 $\beta\text{CH}_3$ ; 11/13 $\beta\text{NH}_2$
17		1380 m	1417	1385	1373 w	1375 s	1419	1386	1417	1385	92/91 $\beta\text{CH}_3$
18	1324 m	1324 w	1359	1328		1327vw	1362	1331	1362	1331	66/61 $\beta\text{CH}$ ; 16/13 $\beta\text{NH}_2$ ; 12/15 $\nu\text{CC}$
19		1281 m	1333	1302	1295vw	1298vw	1334	1304	1333	1302	65/55 $\nu\text{CC}$ ; 15/13 $\beta\text{CH}$ ; 10/15 $\beta\text{NH}_2$
20	1267 vs	1271 m	1301	1271	1242 s	1236 m	1284	1255	1272	1243	46/49 $\nu\text{CN}$ ; 30/28 $\nu\text{CC}$ ; 19/18 $\beta\text{CH}$
21		1218 m	1235	1207	1219 s	1212 vs	1234	1206	1234	1206	63/60 $\nu\text{CC}$ ; 24/29 $\beta\text{CH}$
22	1176 s	1179 m	1207	1179	1206 s	1186 s	1209	1181	1208	1181	73/74 $\beta\text{CH}$ ; 13/19 $\nu\text{CC}$
23	1120 s		1153	1127	1116 w		1157	1131	1156	1129	45/52 $\beta\text{CH}$ ; 18/14 $\beta\text{NH}_2$ (rock.); 21/15 $\nu\text{CC}$
24	1074 m		1092	1067	1098 m	1090 vs	1113	1088	1105	1080	45/52 $\beta\text{NH}_2$ (rock.); 24/11 $\nu\text{CC}$ ; 14/12 $\beta\text{CH}$
25	1044 m		1064	1040	1041 vs	1045 m	1067	1042	1065	1041	84/74 $\gamma\text{CCH}_3$ ; 15/17 $\gamma\text{CH}$
26	983 w		1034	1010			1038	1014	1037	1013	76/75 $\beta\text{CCC}$ ; 18/16 $\beta\text{CH}$
27	953 w		1002	979	990 m	980 vw	1005	982	1005	982	51/43 $\beta\text{CCH}_3$ ; 16/22 $\beta\text{CH}_3$ ; 10/12 $\beta\text{CH}$ ; 11/13 $\beta\text{CNH}_2$
28			933	912			964	942	946	924	74/81 $\gamma\text{CH}$ ; 22/12 $\gamma\text{CCC}$

Table 4.14 cont.

p-toluidine					HgBr <sub>2</sub> (p-tol) <sub>2</sub>						
Exp.*			B3LYP/def2-TZVP		Exp.**		B3LYP/def2-TZVP				PED (%) Assignments
No	IR	Ra	Calc.	Scaled	IR	Ra	Calc.	Scaled	Calc.	Scaled	
29	931 w		931	910	938 s	931 vw	951	929	942	920	69 $\gamma$ CH; 15/13 $\gamma$ CCC; 13/15 $\gamma$ CNH <sub>2</sub>
30		844 s	854	834	835 m	838 s	856	836	844	825	41/47 $\nu$ CC; 23/21 $\nu$ CN; 13/10 $\beta$ CH; 10 $\beta$ CCC
31	812 vs		830	811		817 m	841	822	818	799	61/56 $\gamma$ CH; 14/35 $\gamma$ CNH <sub>2</sub>
32			821	802	810 vs		838	819	832	813	85/95 $\gamma$ CH
33	720 m		752	735	733 s	740 m	768	750	743	726	37/39 $\nu$ CC; 21 $\nu$ CN; 31/22 $\beta$ CCC
34			724	707	705 s	709 vw	733	716	724	708	52/60 $\gamma$ CCC; 27/17 $\gamma$ CNH <sub>2</sub> ; 16 $\gamma$ CCH <sub>3</sub>
35		645 s	661	646	650 s	645 vw	661	646	661	646	76/82 $\beta$ CCC; 12/10 $\beta$ CNH <sub>2</sub>
36			591	577			888	868	720	704	73/67 $\gamma$ CNH <sub>2</sub> (wag.); 11/15 $\gamma$ CH
37	504 vs		510	498	524 vs	518 vw	524	512	522	510	69/78 $\gamma$ CCC+ $\gamma$ CNH <sub>2</sub> ; 22/17 $\gamma$ CCH <sub>3</sub>
38	470	466 s	470	459			472	461	471	460	46/42 $\beta$ CCC; 45 $\nu$ CN+ $\nu$ CC
39		409 w	420	410	415 m,sh		421	411	417	408	67/81 $\gamma$ CCC; 19/14 $\gamma$ CH
40			410	401	399 m	400 s	388	379	384	376	58/52 $\beta$ CNH <sub>2</sub> ; 30 $\beta$ CCH <sub>3</sub> ; 11/10 $\beta$ CCC
41		335 m	323	316	318 vw		344	336	337	329	63/77 $\gamma$ CCH <sub>3</sub> + $\gamma$ CNH <sub>2</sub> ; 30/23 $\gamma$ CCC
42			300	293	297 s	280 vs	299	292	296	289	83/87 $\beta$ CNH <sub>2</sub> + $\beta$ CCH <sub>3</sub>
43			278	272	471 w	469 m	485	474	455	445	80/87 $\gamma$ NH <sub>2</sub> (twist.); 10 $\gamma$ CCC
					241 m		245	239			98 $\nu$ MBr
						196s	197	192			51 $\nu$ MN; 21 $\nu$ MBr; 31 $\gamma$ CNH <sub>2</sub> + $\gamma$ CCH <sub>3</sub>
44		121 vs	140	137		160 s	179	175	164	160	74/75 $\gamma$ CCH <sub>3</sub> + $\gamma$ CNH <sub>2</sub> ; 11 $\nu$ MN
							86	84	83	81	57/63 $\nu$ MN; 31/25 $\gamma$ CCH <sub>3</sub>
							61	60			54 $\gamma$ NMBr; 41 $\gamma$ BrMBr
							60	59	59	57	53/62 $\tau$ CCNM; 35/31 $\gamma$ NMBr
							55	53	32	31	48/56 $\gamma$ NMBr; 28/29 $\tau$ CCNM
							40	39			76 $\gamma$ NMBr+ $\gamma$ NMN
							30	29	16	16	66/84 $\tau$ CNMN; 20/12 $\gamma$ NMBr
45			20	20			28	28	21	20	85/81 $\gamma$ CCH <sub>3</sub> (torsion)
							25	24			34 $\tau$ CCNM; 26 $\gamma$ NMBr; 21 $\gamma$ CCH <sub>3</sub>
							17	16	8	8	69/75 $\tau$ CNMN; 22/25 $\gamma$ NMBr

\*Experimental data is taken from Ref. [144], \*\*Experimental data is taken from Ref. [26].

### 4.3.3 Vibrational Frequencies of the Metal Iodide Complexes of P-toluidine

Detailed vibrational analysis of Ni, Zn and Cd iodide complexes of p-toluidine are performed in this part by providing theoretical vibrational spectra of the title compounds with corresponding infrared and Raman intensities (Figures 4.14 and 4.15) and giving observed and theoretical vibrational frequencies with the PED(%) assignments of each complex in Tables 4.15-4.17.

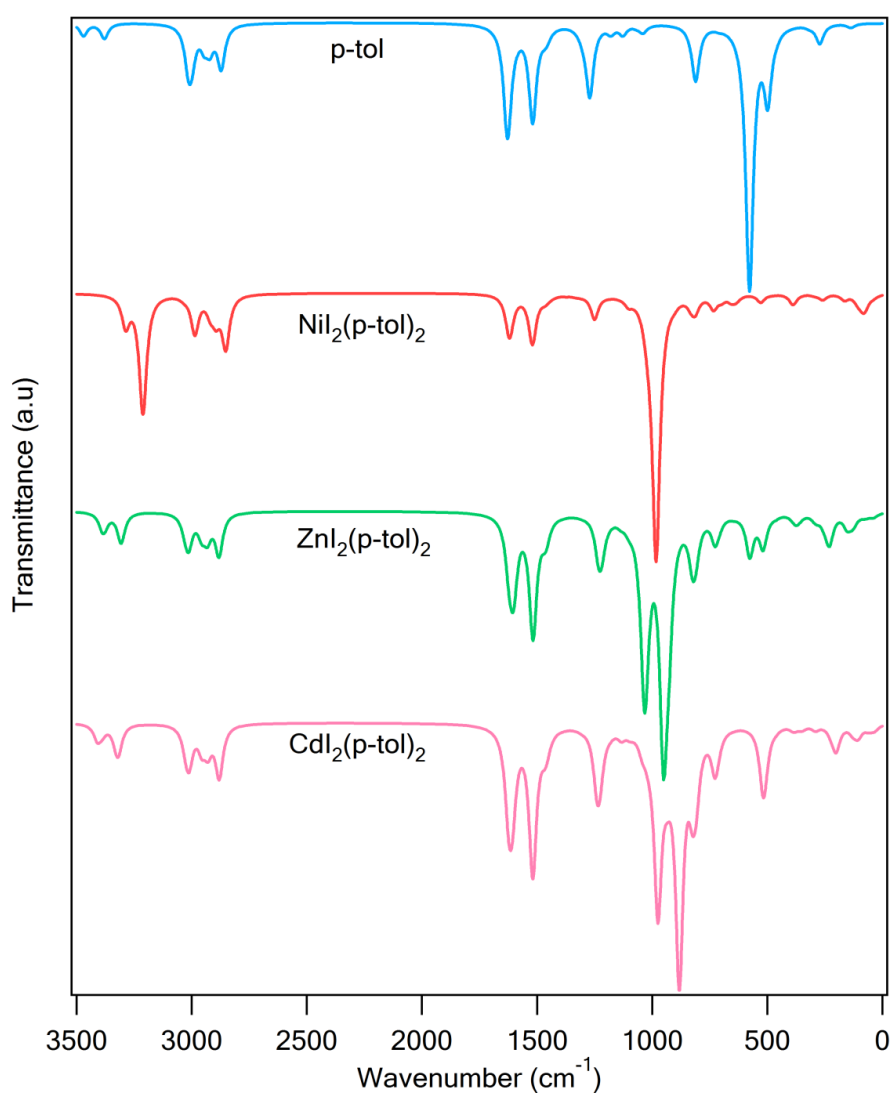


Figure 4.14 Theoretical IR spectra of p-toluidine and its iodide complexes.

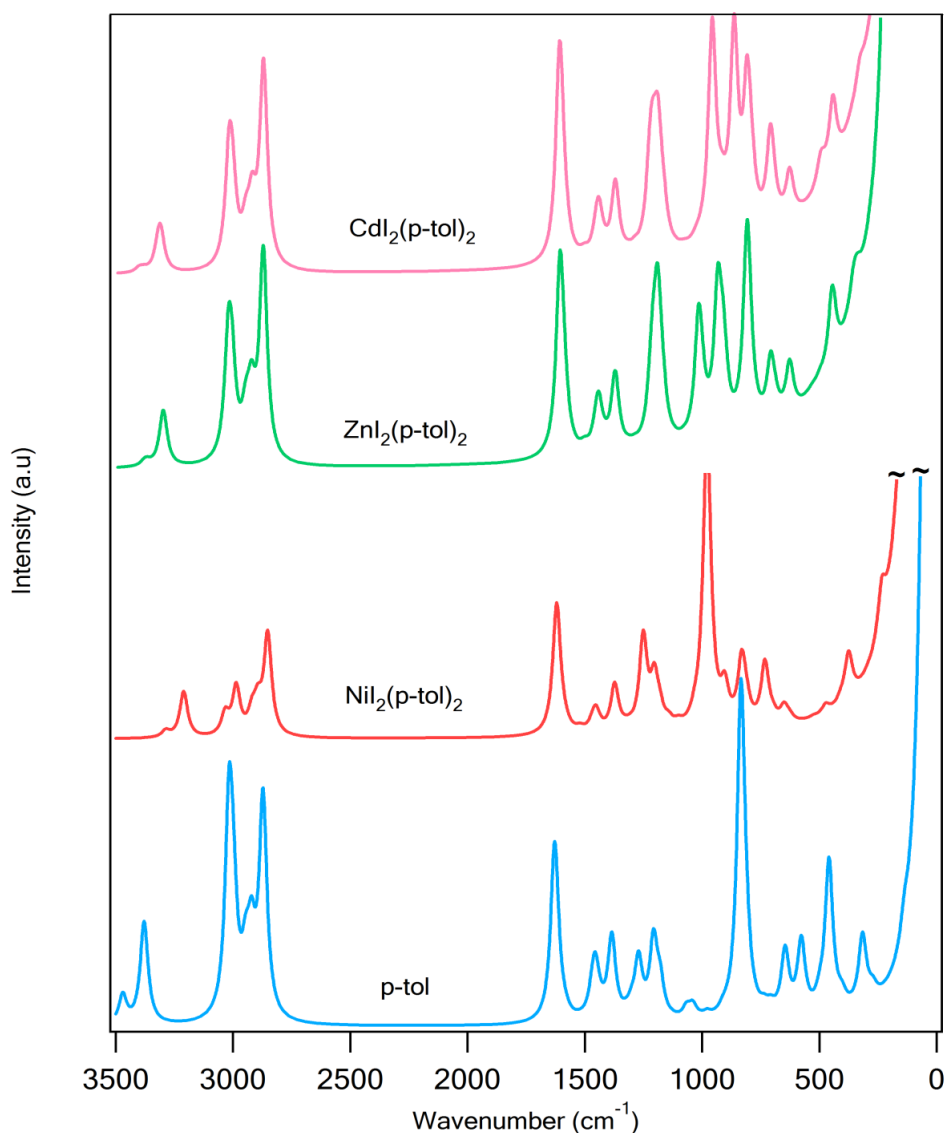


Figure 4.15 Theoretical Raman spectra of p-toluidine and its iodide complexes.

#### 4.3.3.1 3500-2700 $\text{cm}^{-1}$ Region

This spectral region starts with the N-H stretching vibrations of the amino group. The asymmetric and symmetric  $\nu_{\text{NH}}$  band of free ligand is observed respectively at  $3416 \text{ cm}^{-1}$  (strong IR) /  $3418 \text{ cm}^{-1}$  (weak Raman) and  $3333 \text{ cm}^{-1}$  (strong IR) /  $3337$  (weak Raman). However this band is observed at lower frequencies in the complexes, such as  $3344 \text{ cm}^{-1}$  (strong IR) and  $3276 \text{ cm}^{-1}$  (strong IR and very strong Ra) for Ni



complex,  $3287\text{ cm}^{-1}$  (strong IR) /  $3289$  (medium Raman) and  $3219\text{ cm}^{-1}$  (strong IR) /  $3222\text{ cm}^{-1}$  (strong Raman) for Zn complex, and finally  $3312\text{ cm}^{-1}$  (medium IR) /  $3313\text{ cm}^{-1}$  (weak Raman) and  $3250\text{ cm}^{-1}$  (strong IR) /  $3253\text{ cm}^{-1}$  (medium Raman) for the Cd complex. This downward shift of N-H stretching band in the complexes prove the coordination occur via nitrogen atom of the free p-toluidine.

Present calculations predict C-H stretching vibrations of the benzene ring between  $3056\text{-}3008\text{ cm}^{-1}$  region for the free p-toluidine. Being almost same with the previous assignments from similar studies [22, 55] and the free ligand, these vibrations are determined in the  $3055\text{-}3007\text{ cm}^{-1}$  range for the related complexes. So, it can be said that  $\nu\text{CH}$  bands of the benzene ring is not affected due to the coordination.

Similarly methyl group stretching vibrations, i.e.  $\nu\text{CH}_3$  are observed between  $2917\text{-}2737\text{ cm}^{-1}$  in the free p-toluidine and this band is between  $2921\text{-}2732\text{ cm}^{-1}$  in the Ni, Zn, and Cd complexes, being very good agreement with the studies in the literature [21-26, 144, 152, 153]. Since methyl group is the farthest group of atoms to the coordination, these vibrations are not affected from the complexation as expected.

#### **4.3.3.2 1700-600 $\text{cm}^{-1}$ Region**

$\text{NH}_2$  scissoring vibrations of the free ligand are seen in the lower frequencies in the corresponding complexes in these types of studies. This is because, the reduction of HNH angle of p-toluidine leads to decrease in scissoring force constant and the reduced mass increase upon coordination [21-26], and this, downshifts  $\text{NH}_2$  scissoring frequency. In our study, in the free p-toluidine HNH angle is  $111.9^\circ$ , whereas it is  $108.7^\circ$ ,  $108.5^\circ$ , and  $108.9^\circ$  in the Ni, Zn, and Cd complexes, respectively, so the vibrations are also observed in the lower frequencies compared with the free ligand.

Methyl group in plane bending vibrations, i.e.  $\beta\text{CH}_3$  are not affected from coordination as in the case of methyl group stretching vibrations. Significant  $\beta\text{CH}_3$  vibrations at  $1467\text{ cm}^{-1}$  and  $1454\text{ cm}^{-1}$  (scaled def2-TZVP frequencies) for the p-toluidine are not observed experimentally, as well as in the complexes. These vibrations are computed as  $1467\text{ cm}^{-1}$  and  $1455\text{ cm}^{-1}$  for the Cd complex,  $1467\text{ cm}^{-1}$  and  $1456\text{ cm}^{-1}$  for the Zn complex, and  $1467\text{ cm}^{-1}$  and  $1452\text{ cm}^{-1}$  for the Ni complex.  $\beta\text{CH}_3$  vibration is

observed at  $1380\text{ cm}^{-1}$  (medium Raman) with a PED  $\sim 92\%$  in the free p-toluidine and in the Ni, Zn, and Cd complexes it is in the almost same band as expected.

C-N stretching vibration is one of the significant band of this region is observed at  $1267\text{ cm}^{-1}$  (very strong IR) /  $1271\text{ cm}^{-1}$  (medium Raman) in the p-toluidine. In the corresponding complexes this band downshifts  $24\text{ cm}^{-1}$  (IR) /  $35\text{ cm}^{-1}$  (Raman) in the Ni complex,  $24\text{ cm}^{-1}$  (IR) in the Zn complex, and finally  $31\text{ cm}^{-1}$  (IR) /  $34\text{ cm}^{-1}$  (Raman) in the Cd complex upon complexation of the nitrogen atom.

Although  $\text{NH}_2$  wagging and twisting vibrations of p-toluidine are found below  $600\text{ cm}^{-1}$  (are not observed experimentally), these bands are found to be in higher wavenumbers in the title complexes because of coordination [18-26]. For instance computed (scaled) frequency of p-toluidine for  $\text{NH}_2$  wagging is  $577\text{ cm}^{-1}$ , whereas it is  $983\text{ cm}^{-1}$ ,  $1032\text{ cm}^{-1}$  and  $975\text{ cm}^{-1}$  in Ni, Zn and Cd complexes respectively. In the same manner, the scaled  $\text{NH}_2$  twisting vibration is determined at  $272\text{ cm}^{-1}$  in the free p-toluidine, and this vibration is determined at  $656\text{ cm}^{-1}$ ,  $576\text{ cm}^{-1}$ , and  $520\text{ cm}^{-1}$  in the Ni, Zn and Cd complexes respectively.

#### 4.3.3.3 Below $600\text{ cm}^{-1}$

Metal-ligand and metal-halogen vibrations of transition metal complexes are generally observed below  $600\text{ cm}^{-1}$  as in the bromide complexes of p-toluidine. Consistent with this, in our study  $\nu\text{MN}$  vibrations occur at  $217\text{ cm}^{-1}$  (medium IR) and  $142\text{ cm}^{-1}$  (strong Raman) for the Ni complex,  $274\text{ cm}^{-1}$  (medium IR) and  $141\text{ cm}^{-1}$  (very strong Raman) for the Zn complex, and  $150\text{ cm}^{-1}$  for the Cd complex. Metal-halogen, i.e.  $\nu\text{MI}$  vibrations are observed for the Ni complex at  $211\text{ cm}^{-1}$  (medium IR) /  $206\text{ cm}^{-1}$  (very weak Raman) and  $111\text{ cm}^{-1}$  (very strong Raman), for the Zn complex at  $218\text{ cm}^{-1}$  (weak IR) and for the Cd complex  $220\text{ cm}^{-1}$  (very weak IR) /  $130\text{ cm}^{-1}$  (strong Raman). Therefore, two  $\nu\text{MN}$  and two  $\nu\text{MI}$  vibrations are determined for the Ni complex, two  $\nu\text{MN}$  and one  $\nu\text{MI}$  vibrations for the Zn complex, and one  $\nu\text{MN}$  and one  $\nu\text{MI}$  vibrations for the Cd complex. Below  $200\text{ cm}^{-1}$ ,  $\text{CH}_3$  torsion is the only ligand vibration and  $\tau\text{CNMN}$ ,  $\gamma\text{NMI}$ ,  $\tau\text{CCNM}$  are the mostly observed metal vibrations in the present study, as in the literature [54, 57, 61].



Table 4.15 cont.

p-toluidine				NiI <sub>2</sub> (p-tol) <sub>2</sub>							
Exp.*		B3LYP/def2-TZVP		Exp.**		B3LYP/def2-TZVP				PED (%) Assignments	
IR	Ra	Calc.	Scaled	IR	Ra	Calc.	Scaled	Calc.	Scaled		
31	812 vs		830	811	810 vs		832	813	831	812	74/70 γCH; 14/16 γCCH <sub>3</sub> +γCNH <sub>2</sub>
32			821	802	740 s	740 m	826	807	825	807	93/95 γCH
33	720 m		752	735	708 s	709 vw	750	733	749	732	38/45 υCN; 30/36 υCC; 19/10 βCCC
34			724	707	646 m	645 vw	715	698	714	698	76/71 γCCC+γNH <sub>2</sub> (wag.); 16 γCCH <sub>3</sub>
35		645 s	661	646	520 vs	518 vw	666	650	651	636	50/47 βCCC; 43 βCNH <sub>2</sub>
36			591	577			1006	983	1001	979	87/81 γNH <sub>2</sub> (wag.)
37	504 vs		510	498			540	528	537	525	63/62 γCCC; 25/30 γCNH <sub>2</sub>
38	470	466 s	470	459	474 vw	474 w	487	476	484	473	58/61 βCCC; 33/32 υCC+ υCN
39		409 w	420	410	408 vw		420	410	420	410	67/69 γCCC; 22 γCH
40			410	401	387 m	379 w	399	390			62 βCCH <sub>3</sub> + βCNH <sub>2</sub> ; 23 βCCC
41		335 m	323	316	300 m	296 vw	397	388	396	387	37/38 γCCH <sub>3</sub> ; 27/26 γCNH <sub>2</sub> ; 20/24 γCCC
42			300	293	274 m		301	294	299	292	88/87 βCCH <sub>3</sub> + βCNH <sub>2</sub>
43			278	272	608 vs	613 vw	672	656	639	625	87/90 γNH <sub>2</sub> (twist)
44		121 vs	140	137	279 m,sh	285 vw	384	375	239	234	71/72 γCNH <sub>2</sub> + γCCH <sub>3</sub> ; 13 γCCC
					217 m		265	259	168	164	60/75 υMN; 34/12 γCNH <sub>2</sub> + γCCH <sub>3</sub>
					211 m	206 vw	118	115			45 υMI; 44 τCNMN
						142 sh	113	110			45 υMN; 24 υMI; 13 γCCC+γCNH <sub>2</sub>
						111 vs	110	108	106	104	66/47 υMI; 22/33 τCNMN
							94	92			55 υMN; 25 τCNMN; 18 γNMI
							89	87	83	81	67/60 υMI; 25/26 γNMI
							75	73			68 γNMI; 21 τCNMN
45			20	20			61	59	57	56	77/81 γCH <sub>3</sub> (torsion); 10/12 τCCNM
							59	58	56	55	65/67 τCCNM; 31/32 γCH <sub>3</sub> (torsion)
							55	54	50	49	61/60 γNMI; 37 τCCNM
							46	45	42	41	56 τCNMN; 37/38 γNMI
							35	34			47 γCNM; 41 γNMI
							34	34	31	30	56/50 τCNMN; 35/41 γNMI
							23	22			71 τCNMN; 13 γCCH <sub>3</sub>
							17	16	13	12	57/66 τCNMN; 37/21 γNMI

\*Experimental data is taken from Ref. [144], \*\*Experimental data is taken from Ref. [22].



Table 4.16 cont.

p-toluidine					ZnI <sub>2</sub> (p-tol) <sub>2</sub>						PED (%) Assignments
Exp.*	B3LYP/def2-TZVP				Exp.**	B3LYP/def2-TZVP					
No	IR	Ra	Calc.	Scaled	IR	Ra	Calc.	Scaled	Calc.	Scaled	
29	931 w		931	910	936 w	939 vw	949	928	943	922	56/71 $\gamma$ CH; 25/10 $\gamma$ CNH <sub>2</sub> ; 13/12 $\gamma$ CCC
30		844 s	854	834	833 s	836 s	846	827	845	826	65/67 $\nu$ CC+ $\nu$ CN; 17/13 $\beta$ CCC
31	812 vs		830	811	817 vs	816 s	836	817	827	808	76/70 $\gamma$ CH; 20/22 $\gamma$ CCH <sub>3</sub> + $\gamma$ CNH <sub>2</sub>
32			821	802			849	830	835	815	98/96 $\gamma$ CH
33	720 m		752	735	735 s	738 w	744	727	743	726	40/36 $\beta$ CCC; 30/27 $\nu$ CC; 20/21 $\nu$ CN
34			724	707	704 m	705 vw	730	713	724	707	62/61 $\gamma$ CCC; 13/10 $\gamma$ CNH <sub>2</sub> ; 10 $\gamma$ CCH <sub>3</sub>
35		645 s	661	646	648 s	647 s	662	646	661	646	80/74 $\beta$ CCC; 14/11 $\beta$ CNH <sub>2</sub>
36			591	577	1079 vs	1091 s	1056	1032	973	951	76/80 $\gamma$ NH <sub>2</sub> (wag.); 14/12 $\gamma$ CCC
37	504 vs		510	498	518 vs	521 w	532	520	527	515	66/68 $\gamma$ CCC+ $\gamma$ CNH <sub>2</sub> (wag.); 29/26 $\gamma$ CCH <sub>3</sub>
38	470	466 s	470	459	473 m	474 m	478	467	474	463	60/66 $\beta$ CCC; 17 $\nu$ CC; 16 $\nu$ CN
39		409 w	420	410	426 m	429 m	423	413	420	411	77/78 $\gamma$ CCC; 20/13 $\gamma$ CH
40			410	401	377 m	377 s	397	388	386	378	72/67 $\beta$ CNH <sub>2</sub> + $\beta$ CCH <sub>3</sub> ; 23/27 $\beta$ CCC
41		335 m	323	316	311 m	314 s	382	373	366	357	40/38 $\gamma$ CNH <sub>2</sub> ; 25/23 $\gamma$ CCH <sub>3</sub> ; 21/25 $\gamma$ CCC
42			300	293	280 m,sh	277 m	300	293	291	285	82/83 $\beta$ CNH <sub>2</sub> + $\beta$ CCH <sub>3</sub>
43			278	272	604 s	606 w	590	576	564	551	89/88 $\gamma$ NH <sub>2</sub> (twist.)
					274 m		256	251	239	233	68/77 $\nu$ MN; 24/21 $\gamma$ CCH <sub>3</sub>
					218 w		234	229	156	153	90/82 $\nu$ MI
						141 vs	133	130	86	84	44/51 $\nu$ MN; 30/33 $\gamma$ NMN; 16/10 $\gamma$ CNH <sub>2</sub> + $\gamma$ CCH <sub>3</sub>
44		121 vs	140	137		113 vs	119	116			67 $\gamma$ CCC + $\gamma$ CCH <sub>3</sub> ; 21 $\gamma$ CNH <sub>2</sub>
							78	77	63	62	40/48 $\tau$ CCNM; 44/27 $\gamma$ CNM
							74	72			47 $\gamma$ NMI; 27 $\tau$ CNMN; 21 $\gamma$ IMI
45			20	20			52	51	43	42	87/90 $\gamma$ CH <sub>3</sub> (torsion)
							45	44			73 $\gamma$ NMI+ $\gamma$ NMN; 15 $\gamma$ IMI
							37	36	36	35	76/65 $\tau$ CCNM; 11/14 $\gamma$ CCC+ $\gamma$ CNH <sub>2</sub>
							34	34			75 $\gamma$ NMN; 21 $\tau$ CNMN
							19	19			70 $\gamma$ NMN; 12 $\gamma$ CCH <sub>3</sub>
							16	16	12	12	89/85 $\tau$ CNMN; 10/12 $\gamma$ NMI

\*Experimental data is taken from Ref. [144], \*\*Experimental data is taken from Ref. [22].

Table 4.17 Experimental and calculated vibrational frequencies (in  $\text{cm}^{-1}$ ) of free p-toluidine and  $\text{CdI}_2(\text{p-tol})_2$ .

p-toluidine					$\text{CdI}_2(\text{p-tol})_2$						
Exp.*			B3LYP/def2-TZVP		Exp.**		B3LYP/def2-TZVP				
No	IR	Ra	Calc.	Scaled	IR	Ra	Calc.	Scaled	Calc.	Scaled	PED (%) Assignments
1	3416 s	3418 w	3647	3470	3312 m	3313 w	3584	3409	3561	3388	100 $\nu\text{NH}_2$ (asym.)
2	3333 s	3337 w	3552	3379	3250 s	3253 m	3497	3327	3487	3317	100 $\nu\text{NH}_2$
3	3056 w	3054 s	3171	3017	3054 w	3058 s	3183	3028	3180	3025	95/98 $\nu\text{CH}$
4	3020m,sh	3032 s	3168	3014	3030 w	3040 m	3181	3026	3177	3023	93/97 $\nu\text{CH}$ (asym.)
5	3008 m	3013 s	3152	2999	3007 w	3014 m	3167	3013	3163	3010	97/99 $\nu\text{CH}$
6			3152	2999			3165	3011	3162	3009	95/98 $\nu\text{CH}$
7	2912 m	2917 s	3097	2946	2918 m	2921 s	3107	2956	3107	2956	93/92 $\nu\text{CH}_3$ (asym.)
8	2859 m	2861m	3070	2921	2857 w	2863 w	3080	2930	3078	2928	95/94 $\nu\text{CH}_3$ (asym.)
9	2737 w	2738 w	3019	2872	2737 w	2741 w	3028	2881	3027	2880	97/99 $\nu\text{CH}_3$
10	1621 vs	1617 s	1667	1629	1583 vs	1594 m	1634	1596	1627	1590	59/60 $\nu\text{CC}$ ; 15 $\beta\text{NH}_2$ (rock.); 14/12 $\beta\text{CH}$ ; 11 $\beta\text{CCH}_3$
11			1654	1616	1612 m	1613 m	1656	1618	1644	1607	56/64 $\beta\text{NH}_2$ (sciss.); 21/10 $\nu\text{CC}$ ; 12/15 $\beta\text{CNH}_2$
12	1582s,sh	1581 m	1621	1584			1662	1624	1661	1623	42/54 $\nu\text{CC}$ ; 28/12 $\beta\text{NH}_2$ (sciss.); 12/21 $\beta\text{CH}$
13	1514 vs		1555	1519	1518 vs		1554	1519	1553	1518	48 $\beta\text{CH}$ ; 25/24 $\nu\text{CC}$ ; 18/12 $\beta\text{CCC}$
14			1501	1467	1509 vs		1502	1467	1500	1466	54/56 $\beta\text{CH}_3$ ; 15/12 $\beta\text{CCH}_3$ ; 11/12 $\beta\text{CH}$
15			1488	1454	1458 w		1489	1455	1489	1455	76/75 $\beta\text{CH}_3$ ; 20/13 $\beta\text{CCH}_3$
16	1441 s		1463	1429	1450 w		1464	1430	1462	1429	38/37 $\nu\text{CC}$ ; 15/27 $\beta\text{CH}$ ; 17/13 $\beta\text{CH}_3$ ; 10 $\beta\text{NH}_2$ (rock.)
17		1380 m	1417	1385	1379 w	1380 m	1419	1387	1419	1386	95/92 $\beta\text{CH}_3$
18	1324 m	1324 w	1359	1328	1327vw	1326 vw	1365	1334	1365	1333	66/67 $\beta\text{CH}$ ; 16/17 $\beta\text{CCC}$ ; 14/13 $\beta\text{NH}_2$ (rock.)
19		1281 m	1333	1302		1298 vw	1336	1306	1334	1303	47/49 $\nu\text{CC}$ ; 19/20 $\beta\text{CCH}_3$ ; 16 $\beta\text{NH}_2$ (rock.); 12/10 $\beta\text{CH}$
20	1267 vs	1271 m	1301	1271	1236 s	1237 w,sh	1269	1240	1255	1227	55 $\nu\text{CN}$ ; 20/22 $\nu\text{CC}$ ; 15/20 $\beta\text{CH}$
21		1218 m	1235	1207	1214 m	1214 s	1234	1206	1234	1206	58/48 $\nu\text{CC}$ ; 14/20 $\beta\text{CCC}$ ; 10/14 $\beta\text{CH}$
22	1176 s	1179 m	1207	1179	1179 w		1211	1183	1210	1182	74/75 $\beta\text{CH}$ ; 14/17 $\nu\text{CC}$
23	1120 s		1153	1127	1115 w		1161	1134	1159	1132	45/53 $\beta\text{CH}$ ; 24/21 $\beta\text{NH}_2$ (rock.); 21/14 $\nu\text{CC}$
24	1074 m		1092	1067	1099 m		1124	1098	1118	1093	48/53 $\beta\text{NH}_2$ (rock.); 18/15 $\beta\text{CH}$ ; 22/20 $\beta\text{CCH}_3$ ; 13/10 $\nu\text{CC}$
25	1044 m		1064	1040	1026 vs	1027 m	1067	1042	1067	1042	62/55 $\gamma\text{CCH}_3$ ; 19/16 $\gamma\text{CH}_3$ ; 11/15 $\gamma\text{CH}$
26	983 w		1034	1010	1011 vs	1014 s	1041	1017	1038	1014	63/74 $\beta\text{CCC}$ ; 17/12 $\beta\text{CH}$
27	953 w		1002	979	952 vw		1008	985	1007	983	49/56 $\beta\text{CCH}_3$ ; 18 $\beta\text{CH}_3$ ; 13/12 $\beta\text{CNH}_2$ ; 13/11 $\beta\text{CH}$
28			933	912			969	946	952	930	80/83 $\gamma\text{CH}$ ; 17/13 $\gamma\text{CCC}$

Table 4.17 cont.

p-toluidine				CdI <sub>2</sub> (p-tol) <sub>2</sub>								
Exp.*			B3LYP/def2-TZVP		Exp.**			B3LYP/def2-TZVP				PED (%) Assignments
No	IR	Ra	Calc.	Scaled	IR	Ra	Calc.	Scaled	Calc.	Scaled		
29	931 w		931	910	934 vw	933 vw	957	935	942	921	73 $\gamma$ CH; 13/10 $\gamma$ CCC; 10 $\gamma$ CNH <sub>2</sub>	
30		844 s	854	834	834 s	836 m	846	827	845	825	64/60 $\nu$ CC+CN; 21/22 $\beta$ CCC	
31	812 vs		830	811	819 s		845	826	834	815	87/85 $\gamma$ CH; 11 $\gamma$ CCC	
32			821	802	808 vs	810 m	829	810	824	806	69/73 $\gamma$ CH; 21/11 $\gamma$ CNH <sub>2</sub>	
33	720 m		752	735	737 s	738 w	745	728	743	726	43 $\beta$ CCC; 27/26 $\nu$ CC; 27 $\nu$ CN	
34			724	707	702 m	708 w	729	712	725	708	71/60 $\gamma$ CCC+ $\gamma$ CNH <sub>2</sub> ; 17/20 $\gamma$ CCH <sub>3</sub>	
35		645 s	661	646	644 m	643 m	661	646	661	646	73/74 $\beta$ CCC; 10 $\nu$ CC 13/12 $\beta$ NH <sub>2</sub>	
36			591	577	960 w		998	975	903	882	83/72 $\gamma$ NH <sub>2</sub> (wag.); 12/18 $\gamma$ CH	
37	504 vs		510	498	515 vs	514 vw	527	515	525	513	73/84 $\gamma$ CCC+ $\gamma$ CNH <sub>2</sub> (wag.)	
38	470	466 s	470	459	470 vw	470 w	474	464	472	461	54/52 $\beta$ CCC; 41/47 $\nu$ CN+ $\nu$ CC	
39		409 w	420	410	393 m,sh	395 m,sh	422	413	418	408	77/79 $\gamma$ CCC; 17/14 $\gamma$ CH	
40			410	401	387 m	387 m	395	386	389	380	65/74 $\beta$ CNH <sub>2</sub> + $\beta$ CCH <sub>3</sub> ; 21/15 $\beta$ CCC	
41		335 m	323	316	303 w	305 vw	360	351	350	342	71/83 $\gamma$ CNH <sub>2</sub> + $\gamma$ CCH <sub>3</sub> ; 17/13 $\gamma$ CCC	
42			300	293	279 w	271 m	299	292	296	289	78/74 $\beta$ CNH <sub>2</sub> (twist.) + $\beta$ CCH <sub>3</sub> ; 14/12 $\nu$ CC	
43			278	272	582 s		532	520	512	500	83/85 $\gamma$ NH <sub>2</sub> (twist.)	
44		121 vs	140	137	235 vw		225	220	204	199	74/73 $\gamma$ CNH <sub>2</sub> + $\gamma$ CCH <sub>3</sub> ; 11 $\gamma$ CCC	
					220 vw	130 s	205	201	131	128	96/95 $\nu$ MI	
						150 m	113	110	106	104	37/44 $\nu$ MN; 36/27 $\tau$ CCCN; 13/10 $\gamma$ CCH <sub>3</sub>	
							72	70	67	65	63/73 $\tau$ CNMN; 13/10 $\gamma$ NMI	
							66	64			78 $\tau$ CNMN; 14 $\gamma$ IMI	
							54	52	38	37	51/42 $\gamma$ IMI; 29/41 $\tau$ CNMN	
							35	34	32	31	54/44 $\tau$ CCNM; 16 $\gamma$ NMI; 10 $\gamma$ CCH <sub>3</sub>	
							31	31			44 $\tau$ CCNM; 23 $\gamma$ CCH <sub>3</sub> ; 15 $\gamma$ NMI	
45			20	20			27	27	26	25	92/81 $\gamma$ CH <sub>3</sub> (torsion)	
							19	19	13	12	60/65 $\tau$ CNMN; 25 $\gamma$ NMI	
							18	17			80 $\tau$ CNMN	

\*Experimental data is taken from Ref. [144], \*\*Experimental data is taken from Ref. [22].



#### 4.3.4 Vibrational Frequencies of the Metal Bromide Complexes of M-toluidine

In this part, vibrational assignments and frequencies of Mn, Co, Ni, Cu, Zn, Cd and Hg bromide complexes of m-toluidine and the shifts of ligand vibrations upon coordination are explained. In the Tables 4.18-4.24 (given at the end of this section), ligand and complex vibrations are provided both experimentally and theoretically with the PED (%) assignments. Theoretical infrared and Raman spectra of the complexes as well as spectra of free ligand are given in Figures 4.16 and 4.17.

##### 4.3.4.1 3500-2700 $\text{cm}^{-1}$ Region

As in the case of metal bromide and iodide complexes of p-toluidine, in the metal bromide complexes of m-toluidine complexation occurs via nitrogen atom of the free ligand too. Thus, shifts in the nitrogen containing vibrations are inevitable. First example to this is the  $\nu\text{NH}$  stretching vibrations of the amino group. These asymmetric and symmetric N-H stretching vibrations are observed at 3435  $\text{cm}^{-1}$  (strong IR) and 3354  $\text{cm}^{-1}$  (strong IR) / 3353  $\text{cm}^{-1}$  (medium Raman) in the free m-toluidine, respectively. For the asymmetric  $\nu\text{NH}$  vibrations, observed downward shifts in the IR spectra of the complexes are 107  $\text{cm}^{-1}$  (Mn complex), 171  $\text{cm}^{-1}$  (Co complex), 118  $\text{cm}^{-1}$  (Ni complex), 139  $\text{cm}^{-1}$  (Cu complex), 170  $\text{cm}^{-1}$  (Zn complex), 130  $\text{cm}^{-1}$  (Cd complex) and 143  $\text{cm}^{-1}$  (Hg complex). And for the symmetric vibrations, downward shifts in the experimental IR and Raman spectra of the complexes are, respectively 58  $\text{cm}^{-1}$  / 56  $\text{cm}^{-1}$  (Mn complex), 139  $\text{cm}^{-1}$  (Co complex), 118  $\text{cm}^{-1}$  / 118  $\text{cm}^{-1}$  (Ni complex), 133  $\text{cm}^{-1}$  (Cu complex), 136  $\text{cm}^{-1}$  / 134  $\text{cm}^{-1}$  (Zn complex), 106  $\text{cm}^{-1}$  / 107  $\text{cm}^{-1}$  (Cd complex) and finally 132  $\text{cm}^{-1}$  / 119  $\text{cm}^{-1}$  (Hg complex).

C-H stretching vibrations of the benzene rings and methyl groups are not affected so much from the coordination. As mentioned above,  $\nu\text{CH}$  vibrations are generally observed in the 3100-3000  $\text{cm}^{-1}$  in the aromatic benzene rings [150], and also in this study, ring these vibrations are found at 3034-2975  $\text{cm}^{-1}$  in the free m-toluidine, and similar in the complexes (~3060-2966  $\text{cm}^{-1}$ ). Methyl group stretching vibrations, i.e.  $\nu\text{CH}_3$  are observed between 2946-2857  $\text{cm}^{-1}$  in the title complexes and in the free m-toluidine as well, being in good agreement with the previous studies [145, 152].

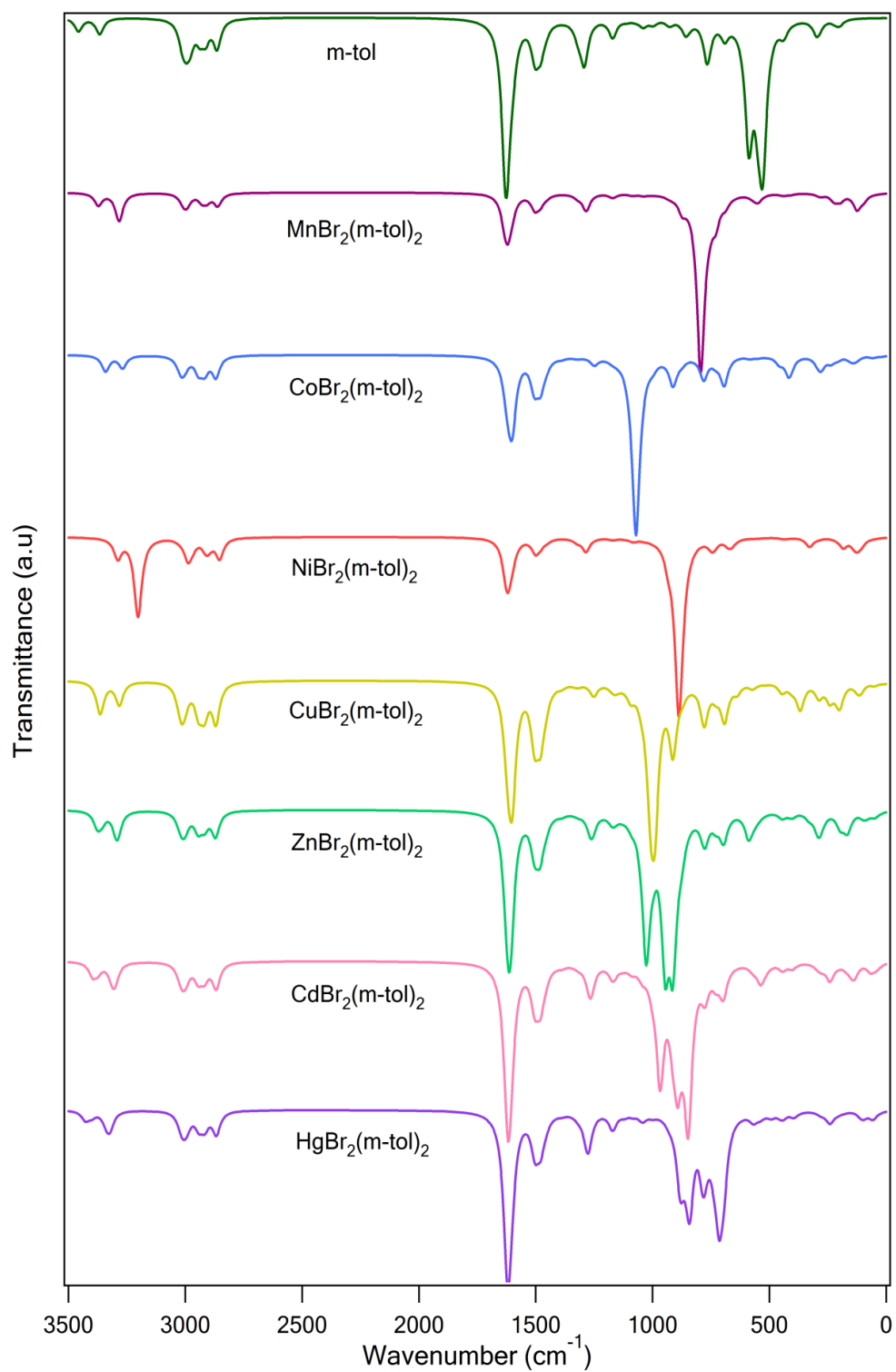


Figure 4.16 Theoretical IR spectra of m-toluidine and its bromide complexes.

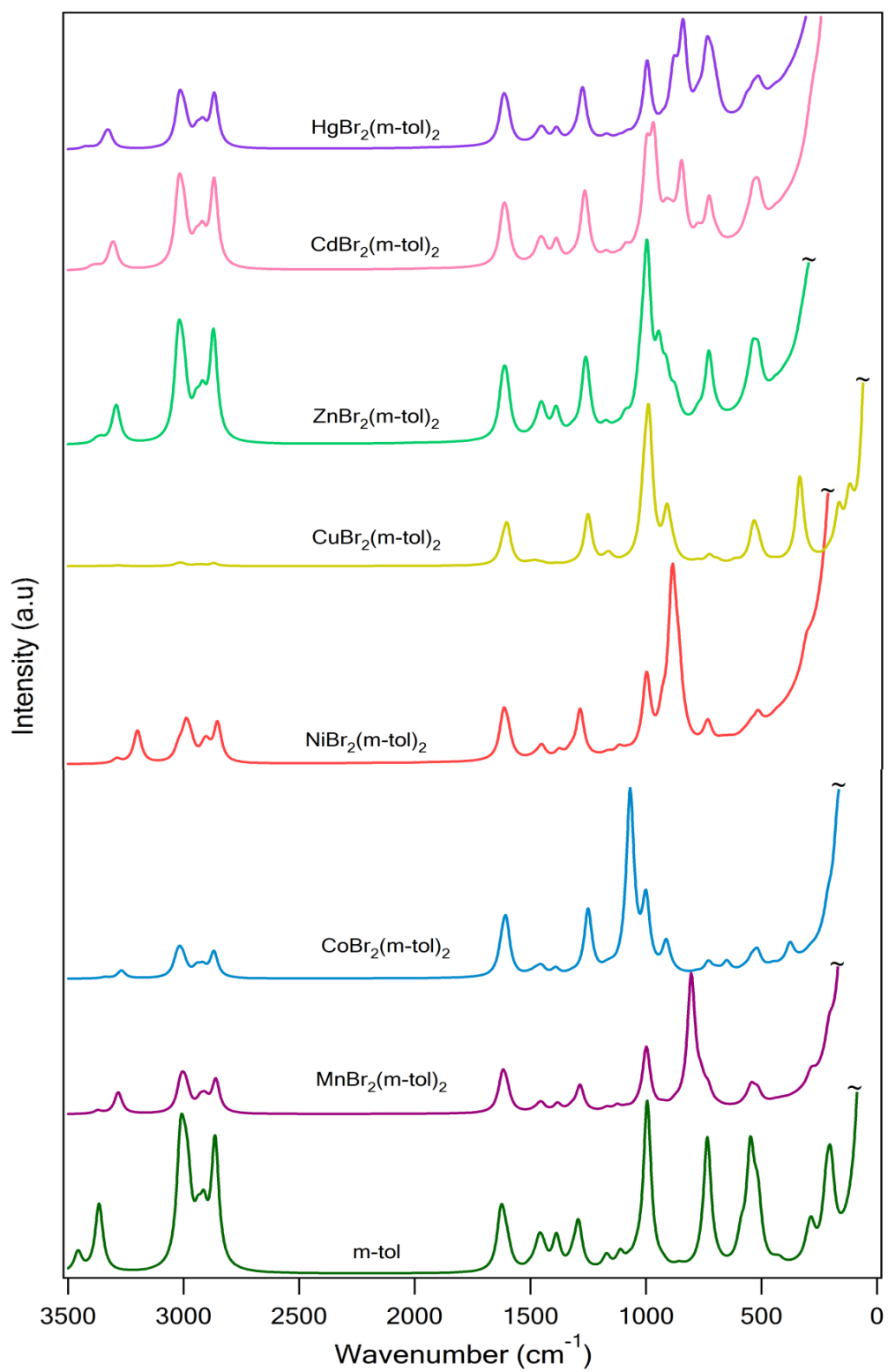


Figure 4.17 Theoretical Raman spectra of m-toluidine and its bromide complexes.

#### 4.3.4.2 1700-600 $\text{cm}^{-1}$ Region

In the previous studies downward shift was observed in the  $\text{NH}_2$  scissoring frequency for the title metal bromide complexes of m-toluidine [23-25]. However, our calculations found a small downward shift in the frequencies of Co, Cu, and Zn complexes, whereas for the Mn, Ni, Cd and Hg complexes this band is found in the similar places ( $\sim 8 \text{ cm}^{-1}$  difference) with free m-toluidine as seen from Fig. 4.16 and 4.17.

C-C stretching and  $\beta\text{CH}$  vibrations of the title complexes generally are not affected much from the coordination, and these vibrations are mostly seen in the  $\sim 1600\text{-}1100 \text{ cm}^{-1}$  region, as in the literature [54-57]. Since the  $\text{CH}_3$  is the most distant to the coordination, related vibrations to methyl groups generally found in the same place with the free ligand. Out of plane CH vibrations, i.e.  $\gamma\text{CH}$  are observed between  $926 \text{ cm}^{-1}$  and  $775 \text{ cm}^{-1}$  in the m-toluidine and its corresponding complexes. Therefore  $\nu\text{CC}$ ,  $\beta/\gamma\text{CH}$ ,  $\beta/\gamma\text{CH}_3$  vibration bands are generally found in the same places both in the ligand and complexes.

Silverstein determined the C-N stretching band between  $1360\text{-}1080 \text{ cm}^{-1}$  in the amines [150]. In our study,  $\nu\text{CN}$  stretching is observed at  $1293 \text{ cm}^{-1}$  in both IR and Raman spectra of the m-toluidine, and this band is found in lower frequencies (between  $1284\text{-}1253 \text{ cm}^{-1}$ ) in all of the complexes, consistent with the literature range. Maximum shift is observed in the Hg complex and this may be due to the metal-ligand bond length of Hg complex ( $2.79 \text{ \AA}$ ) is longer than other six complexes (with an average  $2.25 \text{ \AA}$ ).

$\text{NH}_2$  wagging and twisting vibrations of m-toluidine are found in the higher wavenumbers in the complexes as in the metal bromides and iodides of p-toluidine. In the previous studies,  $\text{NH}_2$  wagging vibrations (IR) of Mn, Co, Ni, Cu, Zn, Cd and Hg complexes are assigned, respectively at  $1022 \text{ cm}^{-1}$ ,  $1035 \text{ cm}^{-1}$ ,  $1043 \text{ cm}^{-1}$ ,  $1084 \text{ cm}^{-1}$ ,  $1100 \text{ cm}^{-1}$ ,  $1050 \text{ cm}^{-1}$ , and  $1040 \text{ cm}^{-1}$  [23-25]. However, according to the present calculations this band is not observed in the experimental spectra of the complexes, except Co ( $1094 \text{ cm}^{-1}$ ) and Ni ( $919 \text{ cm}^{-1}$ ) complexes. Corresponding computed (scaled) frequencies for the title complexes are  $804/794 \text{ cm}^{-1}$  (Mn complex),  $1010/1009 \text{ cm}^{-1}$  (Cu complex),  $1027/946 \text{ cm}^{-1}$  (Zn complex),  $968/847 \text{ cm}^{-1}$  (Cd complex), and  $841/715 \text{ cm}^{-1}$  (Hg complex). Similarly,  $\text{NH}_2$  twisting vibration of the m-toluidine determined at  $294 \text{ cm}^{-1}$  (medium

Raman) in the observed spectrum, and this vibration is found in the pretty higher wavenumbers in the spectral data of the complexes, such as  $557\text{ cm}^{-1}$  for the Mn complex,  $652\text{ cm}^{-1}$  for the Co complex,  $618\text{ cm}^{-1}$  for the Ni complex,  $670\text{ cm}^{-1}$  for the Cu complex,  $646\text{ cm}^{-1}$  for the Zn complex,  $523\text{ cm}^{-1}$  in the Cd complex, and  $442\text{ cm}^{-1}$  in the Hg complex. On the other hand, in the previous experimental studies [24-26]  $\text{NH}_2$  twisting vibration were not determined correctly, except Co, Ni, and Cu complexes. Since the density functional calculations for these complexes are not performed before, these types of errors can be found in the experimental only studies.

#### **4.3.4.3 Below $600\text{ cm}^{-1}$**

Although some ligand vibrations present in this spectral region, we will focus on metal-ligand and metal-bromine stretching vibrations in this subsection. In the previous experimental studies, metal-ligand stretching vibrations generally observed between  $600\text{--}400\text{ cm}^{-1}$  region[19-26]. However, computations predict these vibrations in the lower bands of the spectrum. Starting with metal-ligand stretching vibrations, i.e.  $\nu_{\text{MN}}$ , it is observed at  $285\text{ cm}^{-1}$  (medium IR)/ $284\text{ cm}^{-1}$  (medium Raman) and  $167\text{ cm}^{-1}$  (medium Raman) for the Mn complex, at  $234\text{ cm}^{-1}$  (strong IR) and  $210\text{ cm}^{-1}$  (strong IR) for the Co complex, at  $194\text{ cm}^{-1}$  (strong Raman) for the Ni complex, at  $202\text{ cm}^{-1}$  (medium IR) for the Cu complex, at  $154\text{ cm}^{-1}$  (medium Raman) for the Cd complex. For the Zn and Hg complexes observed spectral data for the metal-ligand stretching vibrations are not found in our study, but computations predict Zn complex at  $170\text{ cm}^{-1}/163\text{ cm}^{-1}$  and  $99\text{ cm}^{-1}/86\text{ cm}^{-1}$  and Hg complex at  $106\text{ cm}^{-1}/94\text{ cm}^{-1}$ .

According to our calculations  $\nu_{\text{MBr}}$  is found at  $240\text{ cm}^{-1}$  (medium IR) and  $192\text{ cm}^{-1}$  (medium Raman) for the Mn complex, at  $246\text{ cm}^{-1}$  (strong IR) for the Co complex, at  $152\text{ cm}^{-1}$  (medium Raman) for the Ni complex, at  $237\text{ cm}^{-1}$  (medium IR) /  $245\text{ cm}^{-1}$  (weak Raman) for the Cu complex, at  $293\text{ cm}^{-1}$  (strong IR) /  $296\text{ cm}^{-1}$  (medium Raman) and  $205\text{ cm}^{-1}$  (medium IR) /  $197\text{ cm}^{-1}$  (very strong Raman) for the Zn complex, at  $183\text{ cm}^{-1}$  (very strong Raman) for the Cd complex, and at  $241\text{ cm}^{-1}$  (medium IR) and  $186\text{ cm}^{-1}$  (very strong Raman) in the Hg complex. Therefore all metal vibrations are found below  $600\text{ cm}^{-1}$ , as in the related transition metal complex studies [56,57, 59-61], but at different wavenumbers compared with the experimental only studies [23-25].

Table 4.18 Experimental and calculated vibrational frequencies (in  $\text{cm}^{-1}$ ) of free m-toluidine and  $\text{MnBr}_2(\text{m-tol})_2$ .

m-toluidine					$\text{MnBr}_2(\text{m-tol})_2$						
Exp.*		B3LYP/def2-TZVP			Exp.**		B3LYP/def2-TZVP				PED (%) Assignments
No	IR	Ra	Calc.	Scaled	IR	Ra	Calc.	Scaled	Calc.	Scaled	
1	3435 s		3652	3457	3328 m	3330 w	3563	3372	3561	3371	99 $\nu\text{NH}_2$ (asym.)
2	3354 s	3353 m,br	3556	3366	3296 m	3297 w	3469	3283	3469	3283	96 $\nu\text{NH}_2$
3	3034 m	3046s	3184	3014	3028 w, sh	3046 s	3184	3014	3184	3014	93 $\nu\text{CH}$
4	3015m,sh	3012 s	3169	2999	3012 w, sh	3014 m,sh	3170	3000	3170	3000	96 $\nu\text{CH}$
5			3158	2989			3160	2991	3160	2991	98 $\nu\text{CH}$
6	2975m,sh	2974 m	3147	2979		2976 w	3154	2985	3154	2985	91 $\nu\text{CH}$
7	2946m,sh		3104	2938		2951 w, sh	3093	2928	3093	2928	95 $\nu\text{CH}_3$ (asym.)
8	2919 m	2919 s	3078	2913	2914 w	2917 s	3071	2907	3071	2907	94/95 $\nu\text{CH}_3$ (asym.)
9	2857 w	2857m,sh	3026	2864	2858 w	2860 w	3022	2861	3022	2861	97/99 $\nu\text{CH}_3$
10	1622 vs		1661	1629	1616 s	1614 s	1665	1632	1665	1632	83/84 $\beta\text{NH}_2$ (sciss.); 10 $\nu\text{CC}$
11			1649	1617	1598 s	1598 s	1652	1619	1651	1618	51/40 $\nu\text{CC}$ ; 29/30 $\beta\text{NH}_2$ ; 10 $\beta\text{CH}$ ; 10 $\beta\text{CCC}$
12	1591 vs	1590 m	1630	1598	1572 s		1634	1601	1633	1601	40/50 $\nu\text{CC}$ ; 21 $\beta\text{CCC}$ ; 21/16 $\beta\text{NH}_2$
13			1533	1503	1516 vw,sh		1534	1504	1534	1504	51/47 $\beta\text{CH}$ ; 16/24 $\beta\text{CCC}$ ; 12/13 $\beta\text{NH}_2$
14	1493 vs	1493 w	1510	1480	1494 vs	1494 w	1511	1481	1511	1481	63/66 $\beta\text{CH}_3$ ; 13/10 $\beta\text{CH}$ ; 10/11 $\nu\text{CC}$ ; 10 $\beta\text{NH}_2$
15	1469 s		1490	1461	1466 s	1463 vw	1488	1458	1488	1458	67/61 $\beta\text{CH}_3$ ; 20/22 $\beta\text{CCH}_3$
16	1443m,sh	1447w,br	1473	1444		1440 w, br	1477	1448	1477	1447	47/45 $\beta\text{CH}_3$ ; 23/24 $\beta\text{CH}$ ; 20/21 $\beta\text{NH}_2$
17	1381 w	1378 m	1415	1387	1374 w	1378 s	1410	1382	1410	1382	87/90 $\beta\text{CH}_3$
18			1354	1327	1313 vw	1312 w	1355	1328	1355	1328	61/58 $\beta\text{CH}$ ; 20/23 $\nu\text{CC}$
19	1314 m	1313m,sh	1342	1315	1264 m	1278 m, sh	1345	1318	1345	1318	40/43 $\nu\text{CC}$ ; 21 $\beta\text{CH}$ ; 16/15 $\beta\text{CNH}_2$ ; 12/10 $\beta\text{CCH}_3$
20	1293 s	1293 m	1319	1292		1268 s	1311	1285	1310	1284	35/41 $\nu\text{CN}$ ; 21/20 $\nu\text{CC}$ ; 17/14 $\beta\text{CH}$ ; 12 $\beta\text{CCC}$
21	1170 s	1166 m	1195	1171	1170 m	1170 m	1194	1171	1194	1171	44/48 $\beta\text{CH}$ ; 30/28 $\nu\text{CC}$ ; 18/16 $\nu\text{CN}$
22			1194	1170		1146 vw	1191	1167	1190	1167	65/66 $\beta\text{CH}$ ; 21/27 $\nu\text{CC}$
23		1106 w	1133	1111			1148	1125	1146	1123	39/44 $\beta\text{NH}_2$ (rock.); 24/20 $\nu\text{CC}$ ; 22/21 $\beta\text{CH}$
24	1077 w	1075 w	1094	1072	1086 m	1085 vw	1107	1085	1106	1085	40/43 $\beta\text{NH}_2$ (rock.);20/16 $\nu\text{CC}$ ;14/15 $\beta\text{CH}$ ; 10 $\beta\text{CCH}_3$
25	1038 w		1061	1040			1060	1039	1060	1039	62 $\gamma\text{CCH}_3$ ; 17/15 $\gamma\text{CH}_3$ ; 16/18 $\gamma\text{CH}$
26			1021	1001	1022 vs	1025 m	1023	1003	1023	1003	55/53 $\beta\text{CCH}_3$ ; 25/27 $\beta\text{CNH}_2$ ; 11/14 $\beta\text{CCC}$
27	996 m	996 vs	1014	994	990 vs	1000 vs	1017	997	1017	997	62/67 $\nu\text{CC}$ ; 22/23 $\beta\text{CCC}$
28	965 vw		946	927			946	927	946	927	33/39 $\beta\text{CCC}$ ; 22/21 $\nu\text{CN}$ ; 23/21 $\nu\text{CC}$

Table 4.18 cont.

m-toluidine					MnBr <sub>2</sub> (m-tol) <sub>2</sub>						
Exp.*		B3LYP/def2-TZVP		Exp.**		B3LYP/def2-TZVP				PED (%) Assignments	
No	IR	Ra	Calc.	Scaled	IR	Ra	Calc.	Scaled	Calc.		Scaled
29	926 m	928 vw	943	924	918 vs	919 w	931	913	931	913	79/78 $\gamma$ CH; 19 $\gamma$ CCC
30	870 m		875	858	882 s	886 w	892	874	890	873	69/77 $\gamma$ CH; 17/13 $\gamma$ CCC
31	855 m		856	839	854 m	866 w	867	850	867	850	79/86 $\gamma$ CH; 15/11 $\gamma$ CCC
32	775 vs	784 w	782	766	776 vs	778 w	776	761	775	760	70/66 $\gamma$ CH; 14/15 $\gamma$ CCC; 12 $\gamma$ CNH <sub>2</sub>
33		738 s	749	734	730 m	728 s	746	731	744	730	44/53 $\beta$ CCC; 22/18 $\nu$ CC; 20/22 $\nu$ CN (breath.)
34	691 vs		705	691	690 vs		702	688	702	688	48/42 $\gamma$ CCC; 25 $\gamma$ CH; 13/15 $\gamma$ NH <sub>2</sub> (wag.)
35			600	588			820	804	810	794	60/53 $\gamma$ NH <sub>2</sub> (wag.); 27/30 $\gamma$ CCC; 11 $\gamma$ CCH <sub>3</sub>
36	557 m		559	548	570 s	574 m	585	573	584	573	39/40 $\gamma$ CNH <sub>2</sub> ; 35/33 $\gamma$ CCH <sub>3</sub> ; 21/22 $\gamma$ CCC
37	538 m	543 m	539	528	543 m	545 s	554	543	552	541	31/30 $\beta$ CCC; 36/34 $\beta$ NH <sub>2</sub> ; 16/14 $\nu$ CC; 15/17 $\nu$ CN
38		518 m	526	515	518 vw,sh	520 s	528	517	528	517	68/58 $\beta$ CCC; 24/30 $\nu$ CC
39		431 w	449	440	441 s	441 vw	450	441	450	441	73/60 $\gamma$ CCC; 18/30 $\gamma$ CH
40			431	422	412 s	419 w	421	412	419	411	74/71 $\beta$ CCH <sub>3</sub> + $\beta$ CNH <sub>2</sub> ; 16/13 $\beta$ CCC
41		294 m	304	298	557 s		566	555	557	546	75/73 $\beta$ NH <sub>2</sub> (twist.); 17/15 $\beta$ CCC
42		234 m	289	284	296 m	293 m	292	287	292	286	80 $\beta$ CCH <sub>3</sub> + $\beta$ CNH <sub>2</sub>
					285 m	284 m	282	276			63 $\nu$ MN; 31 $\beta$ CCH <sub>3</sub> + $\beta$ CNH <sub>2</sub>
43		218 m	223	219	257 m		279	273			81 $\gamma$ CCC + $\gamma$ CNH <sub>2</sub>
					240 m		227	223			79 $\nu$ MBr; 17 $\gamma$ CCC
44			204	200	221 m	221 s	211	207	210	206	61/52 $\gamma$ CCH <sub>3</sub> ; 26/30 $\gamma$ CCC; 11/10 $\gamma$ CNH <sub>2</sub>
						192 m	199	195	148	146	87 $\nu$ MBr
						167 m	128	125	104	102	71/55 $\nu$ MN; 13/22 $\gamma$ CCC+ $\gamma$ CCH <sub>3</sub>
							99	97			66 $\gamma$ NMBr; 20 $\gamma$ BrMBr
							90	89	87	86	56/57 $\tau$ CNMN; 20/25 $\gamma$ NMBr; 16/14 $\gamma$ BrMBr
							80	78	66	65	36/33 $\tau$ CNMN; 30/28 $\gamma$ NMBr; 24/26 $\gamma$ BrMBr
45			27	26			61	60	56	55	94/95 $\gamma$ CH <sub>3</sub> (torsion)
							44	43	43	42	46/23 $\gamma$ NMBr; 25/29 $\gamma$ BrMBr; 15/30 $\tau$ CNMN
							32	31	28	28	50 $\tau$ CCNM; 16/14 $\gamma$ NMBr; 12/15 $\gamma$ BrMBr
							23	23	17	17	60/51 $\tau$ CCNM; 21/36 $\gamma$ NMBr
							15	15	12	12	75/81 $\tau$ CNMN; 12/17 $\gamma$ CCH <sub>3</sub>

\*Experimental data is taken from Ref. [145], \*\*Experimental data is taken from Ref. [24].

Table 4.19 Experimental and calculated vibrational frequencies (in cm<sup>-1</sup>) of free m-toluidine and CoBr<sub>2</sub>(m-tol)<sub>2</sub>.

m-toluidine					CoBr <sub>2</sub> (m-tol) <sub>2</sub>					PED (%) Assignments
Exp.*		B3LYP/def2-TZVP		Exp.**		B3LYP/def2-TZVP		Calc.	Scaled	
No	IR	Ra	Calc.	Scaled	IR	Calc.	Scaled			
1	3435 s		3652	3457	3264 s	3530	3341	3530	3341	100 νNH <sub>2</sub> (asym.)
2	3354 s	3353 m,br	3556	3366	3215 s	3454	3269	3453	3268	100 νNH <sub>2</sub>
3	3034 m	3046s	3184	3014	3033 m	3201	3030	3201	3030	97 νCH
4	3015 m,sh	3012 s	3169	2999		3186	3016	3186	3016	96 νCH
5			3158	2989		3180	3010	3179	3009	97 νCH
6	2975 m,sh	2974 m	3147	2979		3169	2999	3169	2999	96 νCH
7	2946 m,sh		3104	2938		3109	2943	3109	2943	99 νCH <sub>3</sub> (asym.)
8	2919 m	2919 s	3078	2913	2918 m	3082	2917	3082	2917	99 νCH <sub>3</sub> (asym.)
9	2857 w	2857 m, sh	3026	2864	2855 vw	3031	2869	3031	2869	99 νCH <sub>3</sub>
10	1622 vs		1661	1629	1572 vs	1634	1602	1631	1599	89/87 βNH <sub>2</sub> (sciss.)
11			1649	1617	1615 s	1656	1623	1655	1622	64/69 νCC; 21/23 βNH <sub>2</sub> (sciss.)
12	1591 vs	1590 m	1630	1598	1596 s	1637	1605	1637	1605	56/59 νCC; 22/20 βNH <sub>2</sub> (rock.); 15/11 βCH
13			1533	1503	1517 vw	1536	1506	1536	1506	54/52 βCH; 21/24 νCC; 13/14 βNH <sub>2</sub> (rock.)
14	1493 vs	1493 w	1510	1480	1492 vs	1511	1481	1510	1480	64 βCH <sub>3</sub> ; 18 βCH; 11/12 νCC
15	1469 s		1490	1461	1470 s	1489	1460	1489	1460	76/74 βCH <sub>3</sub> ; 16 βCCH <sub>3</sub>
16	1443 m,sh	1447 w, br	1473	1444	1436 m, sh	1476	1447	1476	1447	48 βCH <sub>3</sub> ; 30 βCH; 10/12 βNH <sub>2</sub>
17	1381 w	1378 m	1415	1387	1374 w	1418	1390	1418	1390	92/93 βCH <sub>3</sub>
18			1354	1327		1358	1331	1358	1331	68/66 βCH; 22 νCC
19	1314 m	1313 m, sh	1342	1315		1345	1318	1344	1317	50 νCC; 18/17 βCH; 16 βCNH <sub>2</sub> ; 12 βCCH <sub>3</sub>
20	1293 s	1293 m	1319	1292	1277 w	1275	1250	1274	1249	48/50 νCN; 26 νCC; 14/12 βCCC
21	1170 s	1166 m	1195	1171	1167 w	1185	1162	1184	1161	58 βCH; 36/38 νCC+νCN
22			1194	1170	1257 s	1201	1177	1200	1176	76 βCH; 14/13 νCC
23		1106 w	1133	1111	1144 w	1172	1149	1169	1146	50/51 βNH <sub>2</sub> (rock.); 28 νCC; 18/17 βCH
24	1077 w	1075 w	1094	1072		1118	1096	1117	1095	40/38 νCC; 36 βNH <sub>2</sub> (rock.); 22/24 βCH
25	1038 w		1061	1040	1035 w	1065	1044	1065	1044	72 γCCH <sub>3</sub> ; 15/16 γCH <sub>3</sub> ; 10 γCH
26			1021	1001		1024	1004	1024	1004	52 βCCH <sub>3</sub> ; 24 βCCC; 18/20 βCNH <sub>2</sub>
27	996 m	996 vs	1014	994	996 m, sh	1019	999	1019	999	58/56 νCC; 28/30 βCCC; 12 βCCH <sub>3</sub>
28	965 vw		946	927	916 m	931	913	930	912	30 βCCC; 27 βCH; 21 νCN; 18/20 νCC



Table 4.19 cont.

m-toluidine					CoBr <sub>2</sub> (m-tol) <sub>2</sub>					PED (%) Assignments
Exp.*		B3LYP/def2-TZVP		Exp.**		B3LYP/def2-TZVP				
No	IR	Ra	Calc.	Scaled	IR	Calc.	Scaled	Calc.	Scaled	
29	926 m	928 vw	943	924		971	952	971	952	82/79 $\gamma$ CH; 10/11 $\gamma$ CCC
30	870 m		875	858	889 m	913	895	912	894	76 $\gamma$ CH; 18 $\gamma$ CCC
31	855 m		856	839	867 m	894	876	893	875	76 $\gamma$ CH; 18/19 $\gamma$ CCC
32	775 vs	784 w	782	766	780 vs	797	781	797	781	80/82 $\gamma$ CH; 12 $\gamma$ CCC
33		738 s	749	734	729 m	745	730	744	729	56/60 $\nu$ CC+ $\nu$ CN; 38/36 $\beta$ CCC (breath.)
34	691 vs		705	691	688 vs	709	695	708	694	40 $\gamma$ CCC; 38/40 $\gamma$ CH; 14/13 $\gamma$ CNH <sub>2</sub> (wag.)
35			600	588	1094 vs	1093	1071	1090	1068	74/76 $\gamma$ NH <sub>2</sub> (wag.); 11/12 $\gamma$ CCC
36	557 m		559	548	568 m	596	584	586	574	36 $\gamma$ CNH <sub>2</sub> ; 34 $\gamma$ CCH <sub>3</sub> ; 28/26 $\gamma$ CCC
37	538 m	543 m	539	528	546 w	563	552	553	542	38 $\beta$ NH <sub>2</sub> (wag.); 45/41 $\nu$ CC+ $\nu$ CN; 15 $\beta$ CCC
38		518 m	526	515	518 vw	529	519	528	518	68/70 $\beta$ CCC; 12 $\nu$ CC
39		431 w	449	440	445 m	466	457	457	448	72 $\gamma$ CCC; 18/16 $\gamma$ CH
40			431	422	399 m	413	405	408	400	80/81 $\beta$ CCH <sub>3</sub> + $\beta$ NH <sub>2</sub> (twist.)
41		294 m	304	298	652 m	707	693	663	650	70/84 $\beta$ NH <sub>2</sub> (twist.); 18/10 $\beta$ CH
42		234 m	289	284	292 s	300	294	291	285	84 $\beta$ CCH <sub>3</sub> + $\beta$ NH <sub>2</sub> (twist.)
43		218 m	223	219	420 m	425	417	384	376	76/82 $\gamma$ CCC + $\gamma$ NH <sub>2</sub> (twist.); 14/10 $\nu$ MN
					246 s	285	279			96 $\nu$ MBr
					234 s	242	237			68 $\nu$ MN; 30 $\gamma$ NMBr
44			204	200	219 m	217	213	213	209	60/58 $\gamma$ CCH <sub>3</sub> ; 26 $\gamma$ CCC; 10 $\gamma$ CNH <sub>2</sub>
					210 s	177	173	159	156	80 $\nu$ MN
						159	156	132	129	54/49 $\gamma$ NMBr; 41/47 $\tau$ CNMN
						146	143	126	124	80/72 $\tau$ CNMN; 14/26 $\gamma$ NMBr
						65	64	56	55	46/44 $\tau$ CNMN; 40/45 $\gamma$ BrMBr
						61	60	39	38	82/79 $\tau$ CNMN
45			27	26		30	29	29	28	92 $\gamma$ CH <sub>3</sub> (torsion)
						18	18			88 $\tau$ CNMN
						16	16	13	13	85/76 $\tau$ CNMN; 10/22 $\gamma$ NMBr

\*Experimental data is taken from Ref. [145], \*\*Experimental data is taken from Ref. [24].

Table 4.20 Experimental and calculated vibrational frequencies (in cm<sup>-1</sup>) of free m-toluidine and NiBr<sub>2</sub>(m-tol)<sub>2</sub>.

m-toluidine					NiBr <sub>2</sub> (m-tol) <sub>2</sub>						
Exp.*		B3LYP/def2-TZVP		Exp.**		B3LYP/def2-TZVP				PED (%) Assignments	
No	IR	Ra	Calc.	Scaled	IR	Ra	Calc.	Scaled	Calc.		Scaled
1	3435 s		3652	3457	3317 s	3316 w	3475	3289	3474	3288	94/95 υNH <sub>2</sub> (asym.)
2	3354 s	3353 m,br	3556	3366	3236 s	3235 s	3383	3202	3380	3199	90 υNH <sub>2</sub>
3	3034 m	3046s	3184	3014	3034 w	3053 s	3193	3022	3193	3022	91/92 υCH
4	3015 m,sh	3012 s	3169	2999			3177	3007	3176	3007	92/88 υCH
5			3158	2989			3157	2988	3157	2988	92/90 υCH
6	2975 m,sh	2974 m	3147	2979	2966 vw	2977 w	3136	2968	3136	2968	89/87 υCH
7	2946 m,sh		3104	2938		2947 w	3077	2912	3077	2912	96 υCH <sub>3</sub> (asym.)
8	2919 m	2919 s	3078	2913	2919 w	2917 s	3062	2898	3062	2898	94/91 υCH <sub>3</sub> (asym.)
9	2857 w	2857m,sh	3026	2864	2855 vw	2852 w,sh	3014	2853	3014	2853	89 υCH <sub>3</sub>
10	1622 vs		1661	1629	1617 s	1614 m,sh	1658	1626	1656	1624	82/83 βNH <sub>2</sub> (sciss.)
11			1649	1617	1594 m,sh	1597 s	1648	1615	1647	1614	62/60 υCC; 30/31 βNH <sub>2</sub> (sciss.)
12	1591 vs	1590 m	1630	1598	1573 s		1630	1597	1629	1597	48/50 υCC; 22/20 βCH; 16 βNH <sub>2</sub> (rock.)
13			1533	1503	1516 vw		1532	1501	1531	1501	48 βCH; 26/25 υCC; 18/20 βCCC
14	1493 vs	1493 w	1510	1480	1496 vs		1509	1479	1509	1479	52/57 βCH <sub>3</sub> ; 18/17 βCH; 12/10 βNH <sub>2</sub>
15	1469 s		1490	1461	1467 s	1472 m	1483	1454	1483	1454	82/83 βCH <sub>3</sub>
16	1443m,sh	1447 w,br	1473	1444	1437 m,sh	1440 w,br	1478	1448	1477	1448	44 βCH <sub>3</sub> ; 36/38 βCH; 14/16 βNH <sub>2</sub>
17	1381 w	1378 m	1415	1387	1374 w	1382 m	1405	1377	1405	1377	90/91 βCH <sub>3</sub>
18			1354	1327			1356	1329	1356	1329	56/60 βCH; 26/23 υCC
19	1314 m	1313m,sh	1342	1315	1309 vw	1313 vw	1346	1319	1345	1319	38/41 υCC; 32/30 βCH; 14/12 βCNH <sub>2</sub> ; 13 βCCH <sub>3</sub>
20	1293 s	1293 m	1319	1292	1282 vw	1284 wsh	1312	1286	1311	1285	50/49 υCN; 22/20 υCC; 20/21 βCCC
21	1170 s	1166 m	1195	1171	1262 m	1261 s	1195	1171	1195	1171	48/50 βCH; 30 υCC; 12/10 υCN
22			1194	1170	1170 m	1168 m	1187	1164	1187	1164	77/74 βCH; 11/14 υCC
23		1106 w	1133	1111	1143 w	1139 vw	1141	1119	1140	1117	42/43 βCH; 30 βNH <sub>2</sub> (rock.); 15/16 υCC
24	1077 w	1075 w	1094	1072	1087 m	1087 m	1105	1083	1104	1082	36/38 βNH <sub>2</sub> (rock.); 28/30 υCC; 26/24 βCH
25	1038 w		1061	1040	1043 vs	1058 s	1056	1035	1056	1035	72/68 γCCH <sub>3</sub> ; 16/19 γCH <sub>3</sub> ; 10 γCH
26			1021	1001			1024	1003	1023	1003	52/51 βCCH <sub>3</sub> ; 24/22 βCNH <sub>2</sub> ; 20/23 βCCC
27	996 m	996 vs	1014	994	999 m	1000 vs	1017	997	1017	997	62 βCCC; 28/25 υCC
28	965 vw		946	927			950	932	950	931	32/35 βCCC; 31/34 βCH; 33/30 υCN+υCC
29	926 m	928 vw	943	924	886 w	889 w	904	886	902	884	62/60 γCH; 36 γCNH <sub>2</sub>

Table 4.20 cont.

m-toluidine					NiBr <sub>2</sub> (m-tol) <sub>2</sub>						PED (%) Assignments
No	Exp.*		B3LYP/def2-TZVP		IR	Exp.**		B3LYP/def2-TZVP			
	IR	Ra	Calc.	Scaled		Ra	Calc.	Scaled	Calc.	Scaled	
30	870 m		875	858	862 w		881	864	877	860	63/61 $\gamma$ CH; 34/35 $\gamma$ CNH <sub>2</sub>
31	855 m		856	839	773 vs		849	832	849	832	82/83 $\gamma$ CH; 10 $\gamma$ CCC
32	775 vs	784 w	782	766	733 m	733 s	761	746	761	746	64/70 $\gamma$ CH; 15/12 $\gamma$ CCC
33		738 s	749	734			748	734	748	734	56/40 $\beta$ CCC; 22/23 $\nu$ CN; 14/30 $\nu$ CC (breath.)
34	691 vs		705	691	690 s	690 m	689	675	689	675	41/45 $\gamma$ CCC; 38 $\gamma$ CH; 13/11 $\gamma$ CNH <sub>2</sub> (wag.)
35			600	588	919 m	920 m	909	891	908	890	60 $\gamma$ NH <sub>2</sub> (wag.); 21/20 $\gamma$ CCC; 16 $\gamma$ CH
36	557 m		559	548	575 w	575 vw	589	577	587	575	62/63 $\gamma$ CCC; 26/24 $\gamma$ NH <sub>2</sub> (wag.)
37	538 m	543 m	539	528	549 w	549 m	560	549	558	547	60 $\nu$ CC+ $\nu$ CN; 27/28 $\beta$ CCC
38		518 m	526	515		518 s	529	518	529	518	56/49 $\beta$ CCC; 32/40 $\nu$ CC
39		431 w	449	440	445 m	450 w	448	439	447	438	62/64 $\gamma$ CCC; 18/17 $\gamma$ CH
40			431	422	415 s	417 vw	427	418	426	418	81/84 $\beta$ CCCH <sub>3</sub> + $\beta$ CNH <sub>2</sub>
41		294 m	304	298	618 s	608 m	673	660	656	643	83 $\beta$ NH <sub>2</sub> (twist.)
42		234 m	289	284	297 s	297 m	296	290	294	289	83/88 $\beta$ CCCH <sub>3</sub> + $\beta$ NH <sub>2</sub> (twist.)
43		218 m	223	219	354 m, br	357 m, br	335	328	315	309	81 $\gamma$ CCC+ $\gamma$ NH <sub>2</sub>
44			204	200	215 s	220 s	218	214	215	211	63/66 $\gamma$ CCH <sub>3</sub> ; 18/16 $\gamma$ CCC; 11/10 $\gamma$ CNH <sub>2</sub>
						194 s	188	184	147	144	87/80 $\nu$ MN
						152m	140	137	125	123	93/91 $\nu$ MBr
							118	115	117	114	63/59 $\tau$ CNMN; 22/27 $\gamma$ NMBr
							107	105	103	101	60 $\tau$ CNMN; 36 $\gamma$ NMBr
							106	104			78 $\tau$ CNMN; 13 $\gamma$ NMBr
							78	77	72	71	72/68 $\gamma$ BrMBr; 20/21 $\tau$ CNMN
							68	67	64	63	48/52 $\gamma$ BrMBr; 44/42 $\tau$ CNMN
							55	54			54 $\gamma$ NMBr; 21 $\gamma$ CH <sub>3</sub> (torsion); 16 $\tau$ CNMN
45			27	26			51	50	50	49	94/95 $\gamma$ CH <sub>3</sub> (torsion)
							42	41	39	39	58/67 $\gamma$ BrMBr; 33/24 $\tau$ CNMN
							33	32	24	24	51/50 $\tau$ CNMN; 42 $\gamma$ NMBr
							17	17	7	7	82/80 $\tau$ CCNM; 15/16 $\gamma$ BrMBr
							7	7			91 $\tau$ CNMN

\*Experimental data is taken from Ref. [145], \*\*Experimental data is taken from Ref. [24].

Table 4.21 Experimental and calculated vibrational frequencies (in cm<sup>-1</sup>) of free m-toluidine and CuBr<sub>2</sub>(m-tol)<sub>2</sub>.

m-toluidine					CuBr <sub>2</sub> (m-tol) <sub>2</sub>						PED (%) Assignments
Exp.*		B3LYP/def2-TZVP		Exp.**		B3LYP/def2-TZVP					
No	IR	Ra	Calc.	Scaled	IR	Ra	Calc.	Scaled	Calc.	Scaled	
1	3435 s		3652	3457	3296 s		3554	3364	3554	3364	100 νNH <sub>2</sub> (asym.)
2	3354 s	3353 m,br	3556	3366	3353 m	3220 w	3469	3283	3468	3282	100 νNH <sub>2</sub>
3	3034 m	3046s	3184	3014	3060 w	3062 w	3199	3028	3199	3028	98 νCH
4	3015 m,sh	3012 s	3169	2999	3020 w		3185	3015	3185	3015	98 νCH
5			3158	2989	2920 m	2913 w	3178	3008	3178	3008	99/98 νCH
6	2975 m, sh	2974 m	3147	2979	2857 w	2856 w	3169	2999	3169	2999	99/98 νCH
7	2946 m, sh		3104	2938			3109	2943	3109	2943	100 νCH <sub>3</sub> (asym.)
8	2919 m	2919 s	3078	2913			3083	2918	3083	2918	100 νCH <sub>3</sub> (asym.)
9	2857 w	2857 m, sh	3026	2864			3031	2869	3031	2869	99 νCH <sub>3</sub>
10	1622 vs		1661	1629	1558 s	1561 vw	1635	1603	1631	1599	72/78 βNH <sub>2</sub> (sciss.); 14 βCNH <sub>2</sub>
11			1649	1617			1653	1621	1653	1620	60/62 νCC; 16/14 βCH; 14 βNH <sub>2</sub> (rock.)
12	1591 vs	1590 m	1630	1598	1592 m	1596 m	1635	1603	1634	1601	52/50 νCC; 32 βNH <sub>2</sub> (sciss.); 16 βCH
13			1533	1503			1536	1505	1536	1505	48/50 βCH; 22/23 νCC; 14 βNH <sub>2</sub> (rock.)
14	1493 vs	1493 w	1510	1480	1491 s	1487 w	1510	1480	1510	1480	60 βCH <sub>3</sub> ; 24/23 νCC; 12 βNH <sub>2</sub>
15	1469 s		1490	1461	1463 s		1489	1460	1489	1460	76/80 βCH <sub>3</sub> ; 18/16 βCCH <sub>3</sub>
16	1443 m, sh	1447 w, br	1473	1444		1445 m	1476	1447	1476	1447	48/46 βCH <sub>3</sub> ; 38/40 βCH; 11/10 βNH <sub>2</sub>
17	1381 w	1378 m	1415	1387	1374 m		1418	1390	1418	1390	90 βCH <sub>3</sub>
18			1354	1327			1358	1331	1358	1331	72/74 βCH; 19/21 νCC
19	1314 m	1313 m, sh	1342	1315	1312 w		1345	1318	1344	1318	50/52 νCC; 18 βCH; 18 βCNH <sub>2</sub>
20	1293 s	1293 m	1319	1292	1254 m	1256 m	1277	1252	1277	1252	46/44 νCN; 30/28 βCCC; 20/21 νCC
21	1170 s	1166 m	1195	1171			1185	1162	1185	1161	51/50 βCH; 42 νCC+νCN
22			1194	1170	1230 vw	1232 m	1200	1176	1200	1176	78 βCH; 10/13 νCC
23		1106 w	1133	1111	1130 vw	1122 w	1165	1142	1163	1140	52 βNH <sub>2</sub> (rock.); 20/17 βCH; 14/20 νCC
24	1077 w	1075 w	1094	1072	1084 vs	1085 s	1116	1094	1116	1094	40/38 νCC; 32 βNH <sub>2</sub> (rock.); 19/20 βCH
25	1038 w		1061	1040	1032 w		1065	1044	1065	1044	65/66 γCCH <sub>3</sub> ; 22 γCH <sub>3</sub> ; 10 γCH
26			1021	1001	920 m		931	913	929	911	46/49 βCCH <sub>3</sub> ; 23/24 βCNH <sub>2</sub> ; 19/18 βCCC
27	996 m	996 vs	1014	994			1024	1004	1024	1003	46/43 βCCC; 30 βCCH <sub>3</sub> ; 20/22 νCC
28	965 vw		946	927	1000 w	998 m	1010	990	1009	989	42/40 νCC+νCN; 28/26 βCCC; 28/32 βNH <sub>2</sub>

Table 4.21 cont.

m-toluidine					CuBr <sub>2</sub> (m-tol) <sub>2</sub>						
Exp.*			B3LYP/def2-TZVP		Exp.**			B3LYP/def2-TZVP			PED (%) Assignments
No	IR	Ra	Calc.	Scaled	IR	Ra	Calc.	Scaled	Calc.	Scaled	
29	926 m	928 vw	943	924			970	951	970	951	80 $\gamma$ CH; 12 $\gamma$ CCC
30	870 m		875	858			908	890	907	889	78 $\gamma$ CH; 11/15 $\gamma$ CCC
31	855 m		856	839	878 m		890	873	889	872	73 $\gamma$ CH; 23/21 $\gamma$ CCC
32	775 vs	784 w	782	766	780 vs		795	779	795	779	76/78 $\gamma$ CH; 12/10 $\gamma$ CCC
33		738 s	749	734	724 m		744	729	743	728	36/40 $\beta$ CCC; 26 $\nu$ CC; 24 $\nu$ CN
34	691 vs		705	691	693 s	692 w	707	693	706	692	51 $\gamma$ CCC; 29/30 $\gamma$ CH; 12 $\gamma$ NH <sub>2</sub> (wag.)
35			600	588			1030	1010	1030	1009	72/74 $\gamma$ NH <sub>2</sub> (wag.); 14 $\gamma$ CCC
36	557 m		559	548			584	572	580	569	37/38 $\gamma$ CNH <sub>2</sub> ; 30 $\gamma$ CCH <sub>3</sub> ; 31/30 $\gamma$ CCC
37	538 m	543 m	539	528	537 m	549 vw	553	542	548	537	45/40 $\nu$ CC+ $\nu$ CN; 33 $\beta$ NH <sub>2</sub> (wag.); 16/20 $\beta$ CCC
38		518 m	526	515	474 w	466 m, b	527	517	527	516	58/60 $\beta$ CCC; 26/22 $\nu$ CC
39		431 w	449	440	440 m		455	446	453	444	66/67 $\gamma$ CCC; 24/23 $\gamma$ CH
40			431	422	389 w	360 m, b	412	404	408	400	80/85 $\beta$ CCH <sub>3</sub> + $\beta$ CNH <sub>2</sub>
41		294 m	304	298	670 s	645 m, b	651	638	630	617	84/86 $\beta$ NH <sub>2</sub> (twist.)
42		234 m	289	284	306 w	305 w	294	288	287	282	82 $\beta$ CCH <sub>3</sub> + $\beta$ NH <sub>2</sub> (twist.)
43		218 m	223	219	322 s		375	368	344	337	83/80 $\gamma$ CCC+ $\gamma$ NH <sub>2</sub>
					237 m	245 w	247	242	138	135	93/88 $\nu$ MBr
44			204	200	218 s	224 m, b	220	215	215	211	60/62 $\gamma$ CCH <sub>3</sub> ; 25/27 $\gamma$ CCC
					202 m		203	199	173	169	88/83 $\nu$ MN
							127	124			61 $\nu$ MN; 30 $\gamma$ NMBr
							124	122	118	115	80/76 $\tau$ CNMN; 10/13 $\gamma$ NMBr
							111	109			68 $\gamma$ BrMBr; 30 $\tau$ CNMN
							59	57	50	49	56/54 $\tau$ CNMN; 40/43 $\gamma$ NMBr
45			27	26			55	54	35	35	61/40 $\tau$ CNMN; 32/58 $\tau$ CCNM
							28	27	27	26	94 $\gamma$ CH <sub>3</sub> (torsion)
							16	16			86 $\tau$ CNMN; 12 $\gamma$ CH <sub>3</sub> (torsion)
							14	13	6	6	62/68 $\tau$ CNMN; 32/30 $\gamma$ NMBr

\*Experimental data is taken from Ref. [145], \*\*Experimental data is taken from Ref. [25].

Table 4.22 Experimental and calculated vibrational frequencies (in  $\text{cm}^{-1}$ ) of free m-toluidine and  $\text{ZnBr}_2(\text{m-tol})_2$ .

m-toluidine					$\text{ZnBr}_2(\text{m-tol})_2$					PED (%) Assignments	
Exp.*		B3LYP/def2-TZVP		Exp.**		B3LYP/def2-TZVP		Calc.	Scaled		
No	IR	Ra	Calc.	Scaled	IR	Ra	Calc.				Scaled
1	3435 s		3652	3457	3265s	3271 m	3567	3376	3547	3357	100 $\nu\text{NH}_2$ (asym.)
2	3354 s	3353 m,br	3556	3366	3218 s	3219 m	3482	3296	3473	3288	100/99 $\nu\text{NH}_2$
3	3034 m	3046s	3184	3014	3032 w, sh	3048 s	3195	3024	3192	3022	98/99 $\nu\text{CH}$
4	3015m,sh	3012 s	3169	2999	3012 w, sh	3017 w,sh	3180	3010	3177	3007	94/99 $\nu\text{CH}$
5			3158	2989			3171	3001	3169	3000	93/98 $\nu\text{CH}$
6	2975m,sh	2974 m	3147	2979	2978 w	2980 w	3168	2998	3161	2992	99 $\nu\text{CH}$
7	2946m,sh		3104	2938	2949 w	2951 w,sh	3112	2945	3111	2945	97/99 $\nu\text{CH}_3$ (asym.)
8	2919 m	2919 s	3078	2913	2916 m	2920 s	3084	2919	3081	2916	96/100 $\nu\text{CH}_3$ (asym.)
9	2857 w	2857m,sh	3026	2864	2851 w	2859 m	3033	2871	3032	2870	99/98 $\nu\text{CH}_3$
10	1622 vs		1661	1629	1597 s	1599 s	1655	1622	1641	1608	89/83 $\beta\text{NH}_2$ (sciss.); 10 $\nu\text{CC}$
11			1649	1617	1615 s	1617 s	1657	1624	1652	1619	64/62 $\nu\text{CC}$ ; 21/22 $\beta\text{NH}_2$ (rock.); 13/11 $\beta\text{CH}$
12	1591 vs	1590 m	1630	1598	1574 s	1575 w	1636	1604	1634	1602	57/53 $\nu\text{CC}$ ; 17/23 $\beta\text{NH}_2$ (rock.); 12/13 $\beta\text{CH}_3$
13			1533	1503	1509 vw		1536	1506	1535	1504	53/49 $\beta\text{CH}$ ; 34 $\nu\text{CC}$ ; 11 $\beta\text{CCC}$
14	1493 vs	1493 w	1510	1480	1494 vs	1495 w	1512	1482	1511	1481	61/57 $\beta\text{CH}_3$ ; 14 $\nu\text{CC}$ ; 10/11 $\beta\text{NH}_2$
15	1469 s		1490	1461	1470 s	1472 vw	1490	1460	1488	1458	70/73 $\beta\text{CH}_3$ ; 11/22 $\beta\text{CCH}_3$
16	1443m,sh	1447w, br	1473	1444	1442 m,sh	1436 w,br	1478	1449	1474	1445	55 $\beta\text{CH}_3$ ; 21 $\nu\text{CC}$ ; 10 $\beta\text{NH}_2$
17	1381 w	1378 m	1415	1387	1376 w	1378 s	1419	1391	1417	1389	86/94 $\beta\text{CH}_3$
18			1354	1327			1357	1330	1356	1329	67/71 $\beta\text{CH}$ ; 23/16 $\nu\text{CC}$
19	1314 m	1313m,sh	1342	1315	1306 vw	1312 m	1342	1316	1341	1314	47/46 $\nu\text{CC}$ ; 18/20 $\beta\text{CH}$ ; 16 $\beta\text{CNH}_2$ ; 14/17 $\beta\text{CCH}_3$
20	1293 s	1293 m	1319	1292	1276 w	1275 w	1291	1266	1282	1256	46/49 $\nu\text{CN}$ ; 31 $\nu\text{CC}$ ; 14/12 $\beta\text{CH}$
21	1170 s	1166 m	1195	1171	1170 m	1170 s	1191	1167	1185	1161	50/48 $\beta\text{CH}$ ; 35/41 $\nu\text{CC}+\nu\text{CN}$
22			1194	1170	1256 m	1258 s	1200	1176	1199	1175	72 $\beta\text{CH}$ ; 13/11 $\nu\text{CC}$
23		1106 w	1133	1111	1146 m	1144 m	1156	1134	1152	1129	45/44 $\beta\text{NH}_2$ (rock.); 24/21 $\nu\text{CC}$ ; 17/20 $\beta\text{CH}$
24	1077 w	1075 w	1094	1072	1100 vs	1105 m	1114	1092	1111	1089	41/42 $\beta\text{NH}_2$ (rock.); 29/35 $\nu\text{CC}$ ; 18/17 $\beta\text{CH}$
25	1038 w		1061	1040	1040	1038 vw	1065	1044	1065	1044	82/77 $\gamma\text{CCH}_3$ ; 11/12 $\gamma\text{CH}$
26			1021	1001			1027	1007	1025	1005	50/46 $\beta\text{CCH}_3$ ; 22 $\nu\text{CC}$ ; 10/15 $\beta\text{CNH}_2$
27	996 m	996 vs	1014	994	996 m	1001 vs	1017	997	1015	995	58/61 $\nu\text{CC}$ ; 25/23 $\beta\text{CCC}$ ; 12/13 $\beta\text{CCH}_3$
28	965 vw		946	927			933	915	930	912	55/61 $\beta\text{CCC}$ ; 30/24 $\nu\text{CC}+\nu\text{CN}$

Table 4.22 cont.

m-toluidine					ZnBr <sub>2</sub> (m-tol) <sub>2</sub>					PED (%) Assignments	
Exp.*		B3LYP/def2-TZVP		Exp.**		B3LYP/def2-TZVP		Calc.	Scaled		
No	IR	Ra	Calc.	Scaled	IR	Ra	Calc.				Scaled
29	926 m	928 vw	943	924	916 s	919 m	977	958	964	945	84/77 $\gamma$ CH; 12/15 $\gamma$ CCC
30	870 m		875	858	890 s	886 w	898	880	894	877	60/58 $\gamma$ CH; 31/37 $\gamma$ CCC+ $\gamma$ CNH <sub>2</sub>
31	855 m		856	839	868 s	868 w	887	870	874	857	75/87 $\gamma$ CH; 14/10 $\gamma$ CCC
32	775 vs	784 w	782	766	780 vs	778 w	797	781	789	774	85/74 $\gamma$ CH; 10/20 $\gamma$ CCC
33		738 s	749	734	728 m	732 s	744	730	744	729	52/48 $\beta$ CCC; 41/47 $\nu$ CC+ $\nu$ CN
34	691 vs		705	691	688 vs	689 vw	713	699	706	692	62/55 $\gamma$ CCC; 11/25 $\gamma$ CH; 16/10 $\gamma$ CNH <sub>2</sub> (wag.)
35			600	588			1048	1027	965	946	77/75 $\gamma$ NH <sub>2</sub> (wag.); 10/11 $\gamma$ CH
36	557 m		559	548	570 m	572 m	583	572	578	566	40/42 $\gamma$ CNH <sub>2</sub> ; 31/28 $\gamma$ CCH <sub>3</sub> ; 11 $\gamma$ CCC
37	538 m	543 m	539	528	544 m	542 m	553	542	552	541	54/48 $\beta$ CCC; 26/30 $\nu$ CN+ $\nu$ CC; 18/20 $\beta$ CNH <sub>2</sub>
38		518 m	526	515	520 vw	519 s	528	518	527	516	66/67 $\beta$ CCC; 20/27 $\nu$ CC
39		431 w	449	440	443 m	445 w	456	447	451	442	68/80 $\gamma$ CCC; 16/11 $\gamma$ CH
40			431	422	416 m	419 w	415	407	405	397	78/73 $\beta$ CCH <sub>3</sub> + $\beta$ CNH <sub>2</sub> ; 10/17 $\beta$ CCC
41		294 m	304	298	646 m		601	589	572	560	84/75 $\beta$ NH <sub>2</sub> (twist.); 10/12 $\beta$ CCC
42		234 m	289	284	226 m	227 m	284	278	275	269	76/81 $\beta$ CCH <sub>3</sub> + $\beta$ NH <sub>2</sub> (twist.); 13/15 $\nu$ MBr
43		218 m	223	219	386 m	384 m	338	331	312	305	80/72 $\gamma$ CCC + $\gamma$ NH <sub>2</sub> (twist.); 10/14 $\nu$ MN
44			204	200	293 s	296 m	295	289			62 $\nu$ MBr; 25 $\beta$ CCC+ $\gamma$ NH <sub>2</sub> (twist.)
					205 m	197 vs	216	211	214	210	42/55 $\gamma$ CCH <sub>3</sub> ; 21/15 $\gamma$ CCC; 12 $\gamma$ CNH <sub>2</sub> ; 10 $\gamma$ NMBr
							200	196			88 $\nu$ MBr
							173	170	166	163	67/76 $\nu$ MN; 28/20 $\gamma$ CCC+ $\gamma$ CCH <sub>3</sub>
							101	99	88	86	61/68 $\nu$ MN; 20/16 $\gamma$ BrMBr
							79	78	67	65	67/66 $\tau$ CNMN; 24/28 $\gamma$ NMBr
45			27	26			57	56	52	51	84/91 $\gamma$ CH <sub>3</sub> (torsion)
							54	53	43	42	37/20 $\gamma$ BrMBr; 37/50 $\gamma$ NMBr; 24/30 $\tau$ CNMN
							31	30	23	22	59/49 $\tau$ CCNM; 27/39 $\gamma$ NMBr
							24	23			69 $\tau$ CCNM; 30 $\gamma$ NMN
							16	16	12	11	82/88 $\tau$ CNMN

\*Experimental data is taken from Ref. [145], \*\*Experimental data is taken from Ref. [23].

Table 4.23 Experimental and calculated vibrational frequencies (in cm<sup>-1</sup>) of free m-toluidine and CdBr<sub>2</sub>(m-tol)<sub>2</sub>.

m-toluidine			CdBr <sub>2</sub> (m-tol) <sub>2</sub>								
Exp.*			B3LYP/def2-TZVP		Exp.**		B3LYP/def2-TZVP				PED (%) Assignments
No	IR	Ra	Calc.	Scaled	IR	Ra	Calc.	Scaled	Calc.	Scaled	
1	3435 s		3652	3457	3305 s	3306 m	3588	3396	3563	3373	100 υNH <sub>2</sub> (asym.)
2	3354 s	3353 m,br	3556	3366	3248	3246	3500	3313	3487	3300	100/99 υNH <sub>2</sub>
3	3034 m	3046s	3184	3014	3050 w	3051 s	3193	3022	3191	3021	99/98 υCH
4	3015 m,sh	3012 s	3169	2999	3030 m	3019m,sh	3177	3007	3177	3007	99/98 υCH
5			3158	2989			3169	3000	3168	2999	99/98 υCH
6	2975 m,sh	2974 m	3147	2979		2980w,sh	3164	2994	3159	2990	99 υCH
7	2946 m,sh		3104	2938	2945 vw		3112	2945	3112	2945	100/96 υCH <sub>3</sub> (asym.)
8	2919 m	2919 s	3078	2913	2918 m	2919 s	3084	2919	3083	2918	99/95 υCH <sub>3</sub> (asym.)
9	2857 w	2857m,sh	3026	2864	2854 w	2859 w	3031	2869	3030	2867	99 υCH <sub>3</sub>
10	1622 vs		1661	1629	1616 s	1617 m	1657	1624	1647	1614	76/70 βNH <sub>2</sub> (sciss.); 15/16 βCNH <sub>2</sub> ; 10/12 υCC
11			1649	1617	1598 s	1598 m	1655	1622	1650	1618	46/49 υCC; 22/20 βNH <sub>2</sub> (sciss.); 13/10 βCH
12	1591 vs	1590 m	1630	1598	1572 s	1568 vw	1636	1604	1634	1602	48/49 υCC; 30 βNH <sub>2</sub> (sciss.); 11/10 βCH; 10 βCCC
13			1533	1503	1508 vw		1536	1505	1534	1504	53/50 βCH; 11/14 βCCC; 14/15 βNH <sub>2</sub> ; 11/12 βCH <sub>3</sub>
14	1493 vs	1493 w	1510	1480	1492 vs	1497 w	1511	1481	1510	1480	64/65 βCH <sub>3</sub> ; 23/24 βCH; 12 υCC
15	1469 s		1490	1461	1471 s	1478 vw	1492	1462	1491	1461	71/70 βCH <sub>3</sub> ; 23/21 βCCH <sub>3</sub>
16	1443 m,sh	1447 w,br	1473	1444	1440 m, br	1436w,br	1475	1446	1474	1445	52/59 βCH <sub>3</sub> ; 20/17 βCH; 14/11 βNH <sub>2</sub>
17	1381 w	1378 m	1415	1387	1376 w	1381 m	1417	1389	1417	1389	92/89 βCH <sub>3</sub>
18			1354	1327			1357	1330	1356	1330	73/67 βCH; 19/23 υCC
19	1314 m	1313m,sh	1342	1315	1316 vw	1313 w	1342	1315	1340	1314	52/53 υCC; 14/16 βCH; 17/15 βCNH <sub>2</sub>
20	1293 s	1293 m	1319	1292	1276 w	1279 m,sh	1296	1270	1287	1262	48/46 υCN; 26/34 υCC; 12/13 βCCC
21	1170 s	1166 m	1195	1171			1191	1167	1187	1164	58/57 βCH; 39/34 υCC+υCN
22			1194	1170	1170 m	1172 m	1199	1175	1198	1175	69/75 βCH; 21/10 υCC
23		1106 w	1133	1111			1152	1129	1148	1126	47/44 βNH <sub>2</sub> (rock.); 12/20 βCH; 21/17 υCC
24	1077 w	1075 w	1094	1072	1088 m	1090 m	1112	1090	1109	1087	39/35 υCC; 33/39 βNH <sub>2</sub> (rock.); 21/22 βCH
25	1038 w		1061	1040	1050 vs	1047 s	1066	1044	1064	1043	61/62 γCCH <sub>3</sub> ; 19 γCH <sub>3</sub> ; 12/11 γCH
26			1021	1001			1026	1005	1024	1004	44/49 βCCH <sub>3</sub> ; 26/20 βCCC; 19/17 βCNH <sub>2</sub>
27	996 m	996 vs	1014	994	998 m, sh	1001 vs	1022	1002	1018	997	74/44 βCCC; 11/36 υCC
28	965 vw		946	927	920 s	921 w	946	927	931	913	32/38 υCC+υCN; 34/30 βCCC; 22 βNH <sub>2</sub> (wag.)



Table 4.23. cont.

m-toluidine			CdBr <sub>2</sub> (m-tol) <sub>2</sub>								
Exp.*			B3LYP/def2-TZVP		Exp.**		B3LYP/def2-TZVP				PED (%) Assignments
No	IR	Ra	Calc.	Scaled	IR	Ra	Calc.	Scaled	Calc.	Scaled	
29	926 m	928 vw	943	924			976	957	964	945	78/82 $\gamma$ CH; 16/10 $\gamma$ CCC
30	870 m		875	858	888 s	888 vw	911	893	892	874	76/78 $\gamma$ CH; 18/20 $\gamma$ CNH <sub>2</sub>
31	855 m		856	839	866 m	868 vw	888	870	877	859	81/77 $\gamma$ CH; 10/13 $\gamma$ CCC
32	775 vs	784 w	782	766	778 vs	776 m	794	779	789	773	71/81 $\gamma$ CH; 23/12 $\gamma$ CCC
33		738 s	749	734	732 m	734 s	744	729	743	729	40/41 $\beta$ CCC; 24/27 $\nu$ CC; 19/23 $\nu$ CN
34	691 vs		705	691	688 vs	687 vw	714	700	708	694	54/60 $\gamma$ CCC; 29/15 $\gamma$ CH; 13 $\gamma$ NH <sub>2</sub> (wag.)
35			600	588			988	968	864	847	72/68 $\gamma$ NH <sub>2</sub> (wag.); 12/20 $\gamma$ CCC; 10/11 $\gamma$ CH
36	557 m		559	548	570 m	570 m	582	571	577	566	34/43 $\gamma$ CNH <sub>2</sub> (wag.); 36 $\gamma$ CCC; 29/19 $\gamma$ CCH <sub>3</sub>
37	538 m	543 m	539	528	548 m	546 m	551	541	551	540	56/34 $\beta$ CCC; 30/33 $\beta$ NH <sub>2</sub> (wag.); 12/22 $\nu$ CC+ $\nu$ CN
38		518 m	526	515	444 m		527	517	527	516	63/62 $\beta$ CCC; 33/20 $\nu$ CC
39		431 w	449	440	418 m		454	445	451	442	69/76 $\gamma$ CCC; 17/13 $\gamma$ CH
40			431	422		350 m	411	403	407	399	78/70 $\beta$ CCH <sub>3</sub> + $\beta$ CNH <sub>2</sub> ; 21/27 $\beta$ CCC
41		294 m	304	298		523 s	547	536	522	512	81/87 $\beta$ NH <sub>2</sub> (twist.)
42		234 m	289	284	285 s	283 m	288	282	283	278	85/81 $\beta$ CCH <sub>3</sub> + $\beta$ NH <sub>2</sub> (twist.)
43		218 m	223	219			302	296	277	271	71/60 $\gamma$ CCC + $\gamma$ NH <sub>2</sub> (twist.); 16/21 $\nu$ MN
						183 vs	246	241	175	171	94 $\nu$ MBr
44			204	200	214 m	217 m	213	209	213	208	59/51 $\gamma$ CCH <sub>3</sub> ; 23/25 $\gamma$ CCC; 10 $\gamma$ CNH <sub>2</sub>
						154 m	151	148	138	135	80/87 $\nu$ MN
							71	70			48 $\gamma$ BrMBr; 33 $\gamma$ NMN; 17 $\gamma$ CH <sub>3</sub> (torsion)
45			27	26			69	67	58	57	93/94 $\gamma$ CH <sub>3</sub> (torsion)
							65	64			41 $\nu$ MN; 30 $\tau$ CNMN; 13 $\gamma$ NMBr; 14 $\gamma$ CCH <sub>3</sub>
							62	61	57	56	66/57 $\tau$ CCNM; 32/34 $\gamma$ NMBr
							43	42	37	36	37/45 $\gamma$ NMN; 45/33 $\gamma$ BrMBr
							29	28	24	23	67/45 $\tau$ CCNM; 30/42 $\gamma$ NMBr
							19	19	11	11	66/72 $\tau$ CNMN; 23 $\gamma$ NMBr
							14	14			88 $\tau$ CNMN

\*Experimental data is taken from Ref. [145], \*\*Experimental data is taken from Ref. [23].

Table 4.24 Experimental and calculated vibrational frequencies (in  $\text{cm}^{-1}$ ) of free m-toluidine and  $\text{HgBr}_2(\text{m-tol})_2$ .

m-toluidine					$\text{HgBr}_2(\text{m-tol})_2$						PED (%) Assignments
Exp.*		B3LYP/def2-TZVP		Exp.**		B3LYP/def2-TZVP					
No	IR	Ra	Calc.	Scaled	IR	Ra	Calc.	Scaled	Calc.	Scaled	
1	3435 s		3652	3457	3292 s	3291 w	3620	3427	3592	3400	100 $\nu\text{NH}_2$ (asym.)
2	3354 s	3353 m,br	3556	3366	3222 s	3234 m	3527	3338	3510	3322	100 $\nu\text{NH}_2$
3	3034 m	3046s	3184	3014	3028 w	3053 s	3190	3019	3189	3019	92/96 $\nu\text{CH}$
4	3015 m,sh	3012 s	3169	2999		3013 w	3176	3006	3174	3005	100/99 $\nu\text{CH}$
5			3158	2989			3166	2997	3166	2996	85/98 $\nu\text{CH}$
6	2975 m,sh	2974 m	3147	2979	2973 vw	2977 w	3160	2991	3157	2988	99 $\nu\text{CH}$
7	2946 m,sh		3104	2938		2947 w	3108	2942	3107	2941	95/98 $\nu\text{CH}_3$ (asym.)
8	2919 m	2919 s	3078	2913	2917 w	2914 s	3082	2917	3081	2916	95/97 $\nu\text{CH}_3$ (asym.)
9	2857 w	2857m,sh	3026	2864	2851 w	2857 w	3030	2867	3029	2867	97/98 $\nu\text{CH}_3$
10	1622 vs		1661	1629	1613 s	1612 m, sh	1658	1625	1649	1616	74/62 $\beta\text{NH}_2$ (sciss.); 11/10 $\beta\text{CNH}_2$ ; 10/14 $\nu\text{CC}$
11			1649	1617	1598 m,sh	1597 s	1653	1620	1648	1615	56/43 $\nu\text{CC}$ ; 21/28 $\beta\text{NH}_2$ (sciss.) 15/10 $\beta\text{CH}$
12	1591 vs	1590 m	1630	1598	1568 s	1566 vw,br	1634	1602	1631	1599	65/67 $\nu\text{CC}$ ; 17/14 $\beta\text{NH}_2$ (rock.); 14/12 $\beta\text{CCC}$
13			1533	1503	1509 vw	1515 vw	1534	1504	1533	1503	49/40 $\beta\text{CH}$ ; 25/31 $\nu\text{CC}$ ; 11 $\beta\text{NH}_2$ ;10 $\beta\text{CH}_3$
14	1493 vs	1493 w	1510	1480	1492 vs	1497 vw	1510	1480	1509	1479	56/40 $\beta\text{CH}_3$ ; 20/36 $\nu\text{CC}$ ; 11/10 $\beta\text{NH}_2$
15	1469 s		1490	1461	1472 s	1473 vw	1490	1461	1489	1459	73/70 $\beta\text{CH}_3$ ; 23/21 $\beta\text{CCH}_3$
16	1443m,sh	1447 w,br	1473	1444	1437 m	1438 w, br	1475	1445	1473	1444	51/56 $\beta\text{CH}_3$ ; 27/24 $\beta\text{CH}$ ; 12 $\beta\text{NH}_2$
17	1381 w	1378 m	1415	1387	1378 m	1375 m	1417	1389	1416	1388	90/93 $\beta\text{CH}_3$
18			1354	1327			1355	1328	1355	1328	64/61 $\beta\text{CH}$ ; 22/23 $\nu\text{CC}$
19	1314 m	1313m,sh	1342	1315		1313 w	1341	1315	1340	1313	58/45 $\nu\text{CC}$ ; 19/25 $\beta\text{CNH}_2$ ; 12 $\beta\text{CCH}_3$ ; 10/14 $\beta\text{CH}$
20	1293 s	1293 m	1319	1292	1256 w	1253 s	1306	1281	1298	1273	36/39 $\nu\text{CN}$ ; 27/22 $\nu\text{CC}$ ; 22 $\beta\text{CCC}$
21	1170 s	1166 m	1195	1171			1194	1171	1191	1167	57/52 $\beta\text{CH}$ ; 39/32 $\nu\text{CC} + \nu\text{CN}$
22			1194	1170	1168 m	1171	1197	1173	1196	1173	74/72 $\beta\text{CH}$ ; 14/15 $\nu\text{CC}$
23		1106 w	1133	1111			1145	1122	1139	1117	42/31 $\beta\text{NH}_2$ (rock.); 26/32 $\nu\text{CC}$ ; 20/21 $\beta\text{CH}$
24	1077 w	1075 w	1094	1072			1106	1085	1102	1080	39/44 $\beta\text{NH}_2$ (rock.); 32/21 $\nu\text{CC}$ ; 13/16 $\beta\text{CCH}_3$
25	1038 w		1061	1040	1040 vs	1058 s	1064	1043	1063	1042	68/66 $\gamma\text{CCH}_3$ ; 18/17 $\gamma\text{CH}_3$ ; 12 $\gamma\text{CH}$
26			1021	1001			1023	1003	1022	1001	55/56 $\beta\text{CCH}_3$ ; 17 $\beta\text{CNH}_2$ ; 19/20 $\beta\text{CCC}$
27	996 m	996 vs	1014	994	996 m, sh	1000 vs	1018	998	1015	995	65/56 $\beta\text{CCC}$ ; 31/37 $\nu\text{CC}$
28	965 vw		946	927	916 s	918 m	946	928	945	926	48/47 $\beta\text{CCC}$ ; 37/36 $\nu\text{CC} + \nu\text{CN}$ ; 12/15 $\beta\text{CH}$

Table 4.24 cont.

m-toluidine					HgBr <sub>2</sub> (m-tol) <sub>2</sub>						
Exp.*			B3LYP/def2-TZVP		Exp.**		B3LYP/def2-TZVP				PED (%) Assignments
No	IR	Ra	Calc.	Scaled	IR	Ra	Calc.	Scaled	Calc.	Scaled	
29	926 m	928 vw	943	924			969	950	956	937	75/87 $\gamma$ CH; 19/11 $\gamma$ CCC
30	870 m		875	858	890	897 w	901	884	894	877	67/68 $\gamma$ CH; 21/20 $\gamma$ CCC
31	855 m		856	839	868	870 vw	878	860	872	854	85/79 $\gamma$ CH; 11/14 $\gamma$ CCC
32	775 vs	784 w	782	766	778 vs	779 w	800	784	785	770	72/74 $\gamma$ CH; 18/14 $\gamma$ CCC
33		738 s	749	734	730 m	734 m	755	740	744	729	44/46 $\beta$ CCC; 21/22 $\nu$ CC; 21/26 $\nu$ CN
34	691 vs		705	691	688 vs	690 m	710	696	707	693	64/74 $\gamma$ CCC; 26/22 $\gamma$ CH
35			600	588			858	841	729	715	58/56 $\gamma$ NH <sub>2</sub> (wag.); 18 $\gamma$ CH; 14/17 $\gamma$ CCC
36	557 m		559	548	574 w		579	568	579	567	41/47 $\gamma$ CCC; 26/29 $\gamma$ CNH <sub>2</sub> (wag.); 25/21 $\gamma$ CCH <sub>3</sub>
37	538 m	543 m	539	528	542 w		550	539	550	539	43/34 $\beta$ CCC; 33/36 $\nu$ CC+ $\nu$ CN; 24 $\beta$ NH <sub>2</sub> (wag.)
38		518 m	526	515			527	516	526	515	59/68 $\beta$ CCC; 28/21 $\nu$ CC
39		431 w	449	440	414 w	414 w	452	443	450	441	66/67 $\gamma$ CCC; 20 $\gamma$ CH
40			431	422	376 w, br	361 s	405	397	398	390	70/68 $\beta$ CCH <sub>3</sub> + $\beta$ CNH <sub>2</sub> ; 20/23 $\beta$ CCC
41		294 m	304	298	442 m	444 w	502	492	465	456	84/75 $\beta$ NH <sub>2</sub> (twist.); 11/20 $\beta$ CCC
42		234 m	289	284	288 w	287 m	287	281	286	280	87/88 $\beta$ CCH <sub>3</sub> + $\beta$ NH <sub>2</sub> (twist.)
43		218 m	223	219	247 s		264	258	245	240	79 $\gamma$ CCC+ $\gamma$ CNH <sub>2</sub> ; 13/14 $\nu$ MN
					241 m		245	240			82 $\nu$ MBr
44			204	200			212	208	211	207	88/80 $\gamma$ CCC+ $\gamma$ CCH <sub>3</sub>
						186 vs	184	181			95 $\nu$ MBr
							109	106	96	94	80/89 $\nu$ MN
							62	60	58	56	77/75 $\gamma$ BrMBr; 20 $\gamma$ NMBr
							54	53	52	51	66/67 $\tau$ CCNM; 21/17 $\gamma$ NMBr
							41	40			70 $\tau$ CNMN; 22 $\gamma$ NMBr
45			27	26			33	33	28	27	86/80 $\gamma$ CH <sub>3</sub> (torsion)
							31	30	25	24	60/65 $\tau$ CNMN; 39/33 $\gamma$ CH <sub>3</sub> (torsion)
							23	22			45 $\gamma$ NMBr; 32 $\tau$ CCNM; 17 $\gamma$ CH <sub>3</sub> (torsion)
							17	17	13	13	70/72 $\tau$ CNMN; 12/14 $\gamma$ CH <sub>3</sub> (torsion)
							7	7			68 $\tau$ CNMN; 21 $\gamma$ CH <sub>3</sub> (torsion)

\*Experimental data is taken from Ref. [145], \*\*Experimental data is taken from Ref. [23].

### 4.3.5 Vibrational Frequencies of the Metal Iodide Complexes of M-toluidine

Vibrational frequencies of Ni, Zn and Cd iodide complexes of m-toluidine are investigated in this section. Theoretical vibrational spectra of the title compounds; scaled frequencies versus infrared and Raman intensities are given in Figures 4.18 and 4.19. Furthermore, observed and theoretical vibrational frequencies with the PED (%) assignments of each complex are provided at the end of this section in Tables 4.24-4.26.

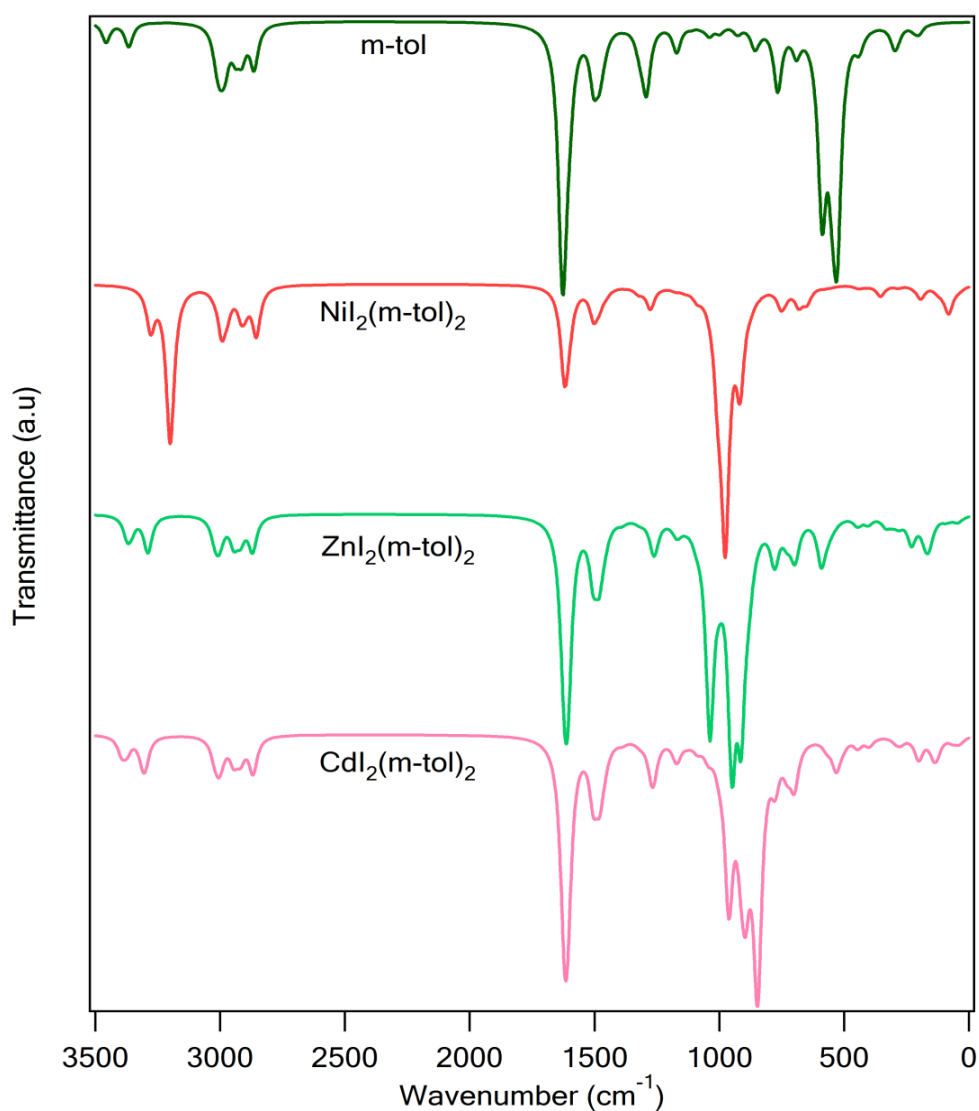


Figure 4.18 Theoretical IR spectra of m-toluidine and its iodide complexes.

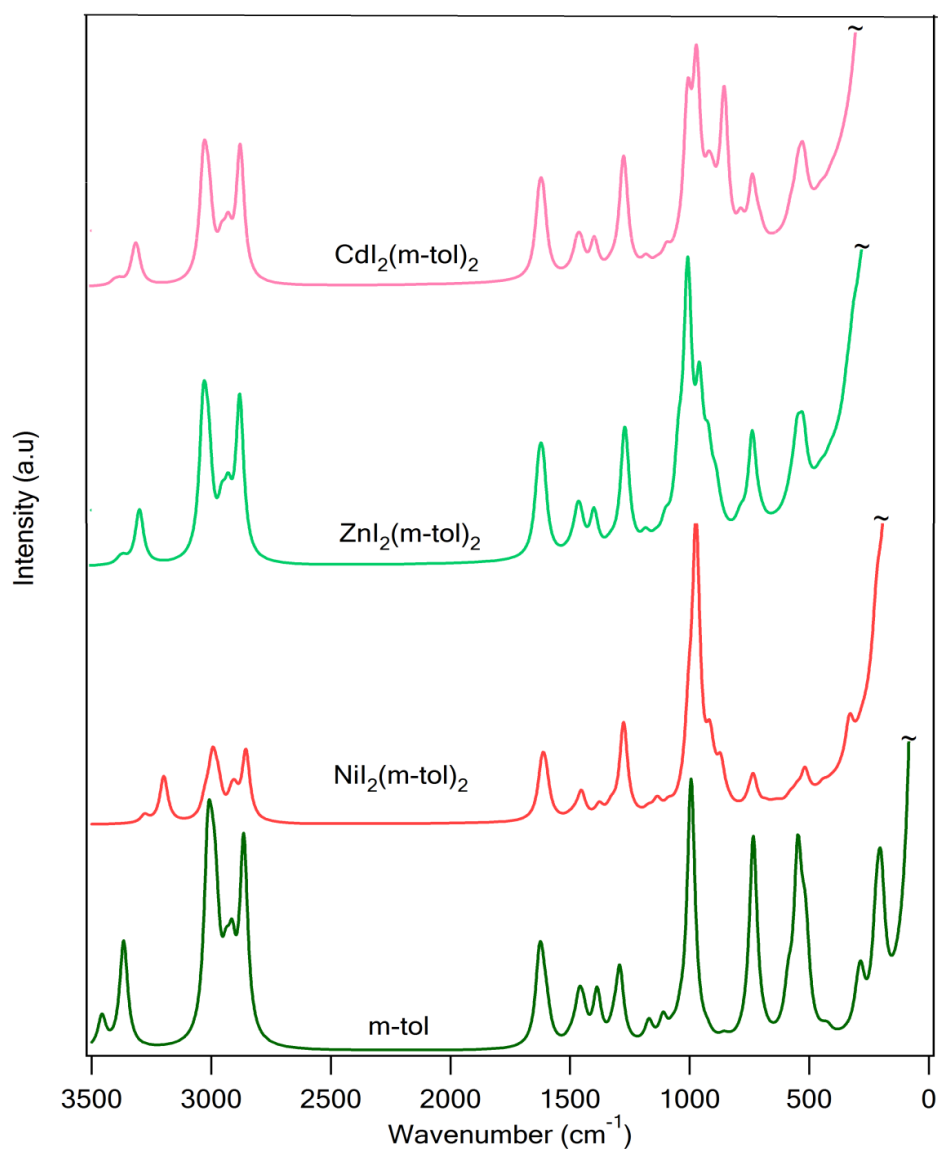


Figure 4.19 Theoretical Raman spectra of m-toluidine and its iodide complexes.

#### 4.3.5.1 3500-2700 $\text{cm}^{-1}$ Region

Consistent with the previous studies, in our computations 3435-3354  $\text{cm}^{-1}$  range is determined for the asymmetric and symmetric NH stretching vibration ( $\nu_{\text{NH}}$ ) of  $\text{NH}_2$  for the free m-toluidine [20, 67, 145]. It is already well known that when the nitrogen atom is involved in coordination, vibrational frequencies of the amino group shift to upper or lower wavenumbers. And in this study, asymmetric  $\nu_{\text{NH}}$  band of free ligand is lowered in the complexes by 92  $\text{cm}^{-1}$  in the Ni complex, 165  $\text{cm}^{-1}$  in the Zn complex,

and  $133\text{ cm}^{-1}$  in the Cd complex. Symmetric  $\nu\text{NH}$  band is also shifted downward  $78\text{ cm}^{-1}$  in the Ni complex,  $137\text{ cm}^{-1}$  in the Zn complex, and  $113\text{ cm}^{-1}$  in the Cd complex. This significant negative shift for the  $\nu\text{NH}$  band of complexes, attributed to the coordination occurs through nitrogen atom of the free m-toluidine.

CH stretching vibrations of aromatic benzene ring and methyl group are also seen in this spectral group [151, 160]. Both of the vibrations are not affected from coordination, benzene ring and methyl group  $\nu\text{CH}$  vibrations of the m-toluidine and its corresponding complexes are determined respectively in the  $3034\text{-}2975\text{ cm}^{-1}$  and  $2950\text{-}2850\text{ cm}^{-1}$  regions.

#### 4.3.5.2 1700-600 $\text{cm}^{-1}$ Region

$\text{NH}_2$  scissoring vibrations are generally seen at  $1600\text{-}1650\text{ cm}^{-1}$  region [18-26, 57, 60, 156, 161]. Similarly, in this study  $\text{NH}_2$  scissoring vibration of the free ligand is found at  $1622\text{ cm}^{-1}$  (very strong IR), and it is lowered in the Ni, Zn, and Cd complexes by  $8\text{ cm}^{-1}$ ,  $23\text{ cm}^{-1}$ , and  $8\text{ cm}^{-1}$  respectively. Negative shift in the  $\text{NH}_2$  scissoring band is quite small, when compared with the stretching frequencies.

On the other hand, drastic changes are observed in the vibrational bands of in the  $\text{NH}_2$  wagging and twisting vibrations when compared with free ligand. Since the experimental wavenumber of m-toluidine for the  $\text{NH}_2$  wagging is missing, we provide computed (scaled) frequencies both for the ligand and complexes. This band is  $588\text{ cm}^{-1}$  for the m-toluidine and shifted upward to  $976\text{ cm}^{-1}/973\text{ cm}^{-1}$  in the Ni complex,  $1037\text{ cm}^{-1}/949\text{ cm}^{-1}$  in the Zn complex, and  $962\text{ cm}^{-1}/846\text{ cm}^{-1}$  in the Cd complex. And present calculations assign Ni complex at  $985\text{ cm}^{-1}$  (very strong IR), and Cd complex at  $963\text{ cm}^{-1}$  (strong IR) different from the work of Altun et. al. (these vibrations were assigned at  $1008\text{ cm}^{-1}$  (very strong IR),  $1040\text{ cm}^{-1}$  (strong IR),  $1030\text{ cm}^{-1}$  (strong IR) for the Ni, Zn and Cd complexes respectively) [21].

In a similar manner  $\text{NH}_2$  twisting vibrations of the m-toluidine is found in quite higher frequencies in the complexes. It is  $294\text{ cm}^{-1}$  (medium Raman) for the m-toluidine and  $615\text{ cm}^{-1}$  (strong IR) for the Ni complex,  $543\text{ cm}^{-1}$  (medium IR) /  $545\text{ cm}^{-1}$  (medium Raman) for the Cd complex, and  $634\text{ cm}^{-1}$  (very strong IR) /  $635\text{ cm}^{-1}$  (very weak

Raman) the Zn complex. Thus this band is shifted upward  $321\text{ cm}^{-1}$  for the Ni complex,  $251\text{ cm}^{-1}$  for the Cd complex, and  $341\text{ cm}^{-1}$  for the Zn complex.

CN stretching is one of the significant bands of this region also affected by coordination. Computations predict the place of this band at  $1293\text{ cm}^{-1}$  (strong IR) /  $1293\text{ cm}^{-1}$  (medium Raman) for the m-toluidine and it is lowered by  $11\text{ cm}^{-1}$  (Ni complex),  $17\text{ cm}^{-1}$  (Cd complex), and  $38\text{ cm}^{-1}$  (Zn complex) consistent with the previous study [21].

CC stretching, CH,  $\text{CH}_3$ , CCC bending are also mostly seen vibrations of this spectral region and are not affected from the complex formations, with a few exception. These exceptions occur with the contribution of the amino group vibrations to these bands.

#### **4.3.5.3 Below $600\text{ cm}^{-1}$**

Although some ligand vibrations (10 of total 45) are also observed below  $600\text{ cm}^{-1}$ , metal modes are the remarkable vibrational bands of this region [18-26, 56, 63]. Frequently observed metal modes are the metal-ligand and metal-halogen stretchings, ligand-metal-ligand or ligand-metal-iodine deformations, and  $\tau\text{CNMN}$  torsional vibrations.

Metal ligand stretching vibrations ( $\nu\text{MN}$ ) are found at  $206\text{ cm}^{-1}$  (medium IR) and  $177\text{ cm}^{-1}$  (medium Raman) for the Ni complex,  $159\text{ cm}^{-1}$  (very strong Raman) for the Zn complex, and  $180\text{ cm}^{-1}$  (very strong Raman) for the Cd complex. On the other hand, in the experimental only study of m-toluidine iodide complexes, these vibrations determined around  $400\text{ cm}^{-1}$  [21].

Metal halogen stretching, i.e.  $\nu\text{MI}$  vibrations are observed at  $107\text{ cm}^{-1}$  (very strong Raman) for the Ni complex,  $223\text{ cm}^{-1}$  (weak IR) /  $221\text{ cm}^{-1}$  (strong Raman) for the Zn complex, and  $209\text{ cm}^{-1}$  (weak IR) for the Cd complex. Therefore this study predicts 2 metal-ligand and 1 metal-halogen for the Ni complex, 1 metal-ligand and 2 metal-halogen for the Zn complex, and finally 1 metal-ligand and 1 metal-halogen stretching vibrations for the Cd complex.

Table 4.25 Experimental and calculated vibrational frequencies (in  $\text{cm}^{-1}$ ) of free m-toluidine and  $\text{NiI}_2(\text{m-tol})_2$ .

m-toluidine					$\text{NiI}_2(\text{m-tol})_2$						PED (%) Assignments
Exp.*		B3LYP/def2-TZVP		Exp.**		B3LYP/def2-TZVP					
No	IR	Ra	Calc.	Scaled	IR	Ra	Calc.	Scaled	Calc.	Scaled	
1	3435 s		3652	3457	3343 m		3465	3280	3461	3276	93/94 $\nu\text{NH}_2$ (asym.)
2	3354 s	3353m,br	3556	3366	3276 s	3278 m	3381	3200	3379	3198	88 $\nu\text{NH}_2$
3	3034 m	3046s	3184	3014	3036 w	3044 s	3197	3026	3196	3025	94 $\nu\text{CH}$
4	3015m,sh	3012 s	3169	2999	3015vw,sh	3015 w	3179	3009	3177	3007	99 $\nu\text{CH}$
5			3158	2989			3162	2993	3162	2993	94 $\nu\text{CH}$
6	2975m,sh	2974 m	3147	2979	2983vw	2982 m	3139	2971	3139	2971	99 $\nu\text{CH}$
7	2946m,sh		3104	2938	2936vw,sh		3080	2915	3080	2915	94/96 $\nu\text{CH}_3$ (asym.)
8	2919 m	2919 s	3078	2913	2915 m	2918 m	3065	2901	3064	2900	97/96 $\nu\text{CH}_3$ (asym.)
9	2857 w	2857m,sh	3026	2864	2854 w		3016	2855	3016	2855	96/95 $\nu\text{CH}_3$
10	1622 vs		1661	1629	1614 vs	1613 m	1653	1620	1652	1619	78/75 $\beta\text{NH}_2$ (sciss.); 20/22 $\nu\text{CC}$
11			1649	1617	1560 vs		1633	1601	1633	1601	66 $\nu\text{CC}$ ; 20 $\beta\text{CCC}$ ; 12 $\beta\text{NH}_2$ (rock.)
12	1591 vs	1590 m	1630	1598	1594 vs	1594 m	1648	1615	1646	1613	40/39 $\beta\text{NH}_2$ (sciss.); 36/37 $\nu\text{CC}$
13			1533	1503			1534	1503	1533	1503	59/52 $\beta\text{CH}$ ; 12 $\nu\text{CC}$ ; 14/15 $\beta\text{NH}_2$ ; 10/11 $\beta\text{CH}_3$
14	1493 vs	1493 w	1510	1480	1495 vs		1510	1480	1509	1480	66/57 $\beta\text{CH}_3$ ; 12/14 $\beta\text{CC}$ ; 11/13 $\beta\text{NH}_2$
15	1469 s		1490	1461	1466 s		1483	1454	1483	1454	73/75 $\beta\text{CH}_3$ ; 18/17 $\beta\text{CCH}_3$
16	1443m,sh	1447w,br	1473	1444	1458 s		1479	1450	1479	1450	51/48 $\beta\text{CH}_3$ ; 20/27 $\beta\text{CH}$ ; 13/12 $\beta\text{NH}_2$
17	1381 w	1378 m	1415	1387	1377 s	1376 w	1406	1378	1406	1378	88/92 $\beta\text{CH}_3$
18			1354	1327			1357	1330	1357	1330	62/64 $\beta\text{CH}$ ; 21 $\nu\text{CC}$
19	1314 m	1313m,sh	1342	1315	1317 w		1348	1321	1348	1321	45/46 $\nu\text{CC}$ ; 18 $\beta\text{CNH}_2$ ; 17/18 $\beta\text{CCH}_3$ ; 11 $\beta\text{CH}$
20	1293 s	1293 m	1319	1292	1282 w		1302	1276	1301	1276	44/50 $\nu\text{CN}$ ; 26/20 $\nu\text{CC}$ ; 22/24 $\beta\text{CH}$
21	1170 s	1166 m	1195	1171	1170 s	1170vw	1198	1175	1198	1174	50/49 $\beta\text{CH}$ ; 21/24 $\nu\text{CC}$ ; 11 $\nu\text{CN}$
22			1194	1170			1189	1166	1189	1165	65/68 $\beta\text{CH}$ ; 21/20 $\nu\text{CC}$
23		1106 w	1133	1111			1160	1138	1157	1134	49/41 $\beta\text{NH}_2$ (rock.); 22/30 $\nu\text{CC}$ ; 18/20 $\beta\text{CH}$
24	1077 w	1075 w	1094	1072	1085 m		1111	1089	1111	1089	40/41 $\beta\text{NH}_2$ (rock.); 33/29 $\nu\text{CC}$ ; 18/21 $\beta\text{CH}$
25	1038 w		1061	1040			1058	1037	1057	1036	65/63 $\gamma\text{CCH}_3$ ; 19/20 $\gamma\text{CH}_3$ ; 11/12 $\gamma\text{CH}$
26			1021	1001	1008 vs		1027	1006	1026	1005	44/54 $\beta\text{CCH}_3$ ; 24/21 $\beta\text{CNH}_2$ ; 16/15 $\beta\text{CCC}$
27	996 m	996 vs	1014	994		994 s	1025	1004	1024	1004	57/61 $\beta\text{CCC}$ ; 35/30 $\nu\text{CC}$
28	965 vw		946	927			935	917	935	916	33/36 $\beta\text{CCC}$ ; 20 $\beta\text{CH}$ ; 23/20 $\nu\text{CN}$ ; 20/22 $\nu\text{CC}$
29	926 m	928vw	943	924	917 vs	917vw	917	899	916	898	72/77 $\gamma\text{CH}$ ; 18/14 $\gamma\text{CCC}$



Table 4.25 cont.

m-toluidine					NiI <sub>2</sub> (m-tol) <sub>2</sub>					PED (%) Assignments	
Exp.*		B3LYP/def2-TZVP		Exp.**		B3LYP/def2-TZVP					
No	IR	Ra	Calc.	Scaled	IR	Ra	Calc.	Scaled	Calc.		Scaled
30	870 m		875	858	889 s		889	872	888	870	71/74 $\gamma$ CH; 22/23 $\gamma$ CCC
31	855 m		856	839	866 s		858	841	857	840	84/81 $\gamma$ CH; 10/12 $\gamma$ CCC
32	775 vs	784 w	782	766	787 vs	786 w	767	752	767	751	79 $\gamma$ CH; 12/11 $\gamma$ CCC
33		738 s	749	734	731 s	732 m	749	734	748	734	65 $\beta$ CCC; 30/35 $\nu$ CC+ $\nu$ CN
34	691 vs		705	691	694 vs		696	682	695	681	60/55 $\gamma$ CCC; 20 $\gamma$ CH; 10/12 $\gamma$ CNH <sub>2</sub> (wag.)
35			600	588	985 vs		996	976	993	973	56/60 $\gamma$ NH <sub>2</sub> (wag.); 24/21 $\gamma$ CCC; 11/12 $\gamma$ CCH <sub>3</sub>
36	557 m		559	548	576 m		592	580	589	578	40/49 $\gamma$ CCC 30/20 $\gamma$ CNH <sub>2</sub> ; 26/14 $\gamma$ CCH <sub>3</sub>
37	538 m	543 m	539	528	548 m	549 vw	564	553	561	550	36/38 $\beta$ NH <sub>2</sub> (wag.); 35/37 $\nu$ CC+ $\nu$ CN; 20/22 $\beta$ CCC
38		518 m	526	515	519 w	521 vw	529	519	529	518	68 $\beta$ CCC; 22/21 $\nu$ CC
39		431 w	449	440	445 m		451	442	450	441	66/76 $\gamma$ CCC; 20/12 $\gamma$ CH
40			431	422	408 m		418	410	418	410	85/86 $\beta$ CCH <sub>3</sub> + $\beta$ CNH <sub>2</sub>
41		294 m	304	298	615 s		663	650	646	633	83/80 $\beta$ NH <sub>2</sub> (twist.)
42		234 m	289	284	291 s		289	284	288	282	88/89 $\beta$ CCH <sub>3</sub> + $\beta$ NH <sub>2</sub> (twist.)
43		218 m	223	219	376/346 m		361	354	339	332	72/78 $\gamma$ CCC + $\gamma$ NH <sub>2</sub> (twist.) 14/16 $\nu$ MN
44			204	200	227 w		223	219	220	215	75/81 $\gamma$ CCC+ $\gamma$ CCH <sub>3</sub> ; 10 $\nu$ MN
					206 m		197	193			84 $\nu$ MN
						177 m	148	145			86 $\nu$ MN
						107 vs	128	125	84	82	74/84 $\nu$ MI; 12 $\gamma$ NMI
							113	111	108	106	61/53 $\tau$ CNMN; 21/32 $\nu$ MN
							92	90	90	88	55/51 $\nu$ MN; 31 $\tau$ CNMN
							79	78			76 $\nu$ MI; 14 $\nu$ MN
45			27	26			60	59	59	58	82/88 $\gamma$ CH <sub>3</sub> (torsion)
							55	54	52	51	62 $\gamma$ NMI; 12/14 $\tau$ CCNM; 11/13 $\gamma$ CH <sub>3</sub> (torsion)
							50	49	45	44	80/73 $\tau$ CCNM; 20/24 $\gamma$ CH <sub>3</sub> (torsion)
							50	49	33	33	30/51 $\gamma$ NMI; 53/30 $\tau$ CNMN
							43	42	36	36	53/51 $\gamma$ NMI; 33/32 $\tau$ CNMN
							30	29	26	25	55/65 $\tau$ CNMN; 45/22 $\gamma$ NMI
							13	13	10	10	53/40 $\tau$ CNMN; 47/42 $\gamma$ NMI

\*Experimental data is taken from Ref. [145], \*\*Experimental data is taken from Ref. [21].

Table 4.26 Experimental and calculated vibrational frequencies (in  $\text{cm}^{-1}$ ) of free m-toluidine and  $\text{ZnI}_2(\text{m-tol})_2$ .

m-toluidine				$\text{ZnI}_2(\text{m-tol})_2$							
Exp.*		B3LYP/def2-TZVP		Exp.**		B3LYP/def2-TZVP					
No	IR	Ra	Calc.	Scaled	IR	Ra	Calc.	Scaled	Calc.	Scaled	PED (%) Assignments
1	3435 s		3652	3457	3270 vs	3272 m	3562	3372	3546	3356	100 $\nu\text{NH}_2$ (asym.)
2	3354 s	3353m,br	3556	3366	3217 vs	3218 s	3478	3292	3473	3287	100 $\nu\text{NH}_2$
3	3034 m	3046s	3184	3014	3046 m	3052 s	3195	3024	3192	3022	97/99 $\nu\text{CH}$
4	3015m,sh	3012 s	3169	2999	3015 w	3015 s	3181	3011	3177	3007	91/99 $\nu\text{CH}$
5			3158	2989			3172	3002	3169	3000	90/99 $\nu\text{CH}$
6	2975 m,sh	2974 m	3147	2979	2979 vw	2981 m	3166	2997	3164	2995	99 $\nu\text{CH}$
7	2946 m,sh		3104	2938	2948 vw		3112	2946	3111	2944	93/99 $\nu\text{CH}_3$ (asym.)
8	2919 m	2919 s	3078	2913	2917 m	2919 s	3085	2920	3081	2916	93/98 $\nu\text{CH}_3$ (asym.)
9	2857 w	2857m,sh	3026	2864	2854 w	2860 m	3033	2870	3032	2870	99/98 $\nu\text{CH}_3$
10	1622 vs		1661	1629	1599 vs	1602 m	1654	1621	1640	1608	76/65 $\beta\text{NH}_2$ (sciss.); 13/11 $\beta\text{CNH}_2$ ; 10/14 $\nu\text{CC}$
11			1649	1617	1564 vs	1563 w	1637	1604	1634	1601	54/51 $\nu\text{CC}$ ; 30/37 $\beta\text{NH}_2$ (sciss.); 12 $\beta\text{CH}$
12	1591 vs	1590 m	1630	1598	1614 vs	1615 m	1657	1625	1651	1619	63/50 $\nu\text{CC}$ ; 13/17 $\beta\text{NH}_2$ (rock.); 11/15 $\beta\text{CCC}$
13			1533	1503			1536	1506	1534	1504	51/50 $\beta\text{CH}$ ; 20/23 $\beta\text{CCC}$ ; 16/14 $\nu\text{CC}$
14	1493 vs	1493 w	1510	1480	1494 vs		1511	1482	1510	1480	64/58 $\beta\text{CH}_3$ ; 18/14 $\beta\text{CH}$ ; 12/15 $\beta\text{NH}_2$
15	1469 s		1490	1461	1469 s		1490	1461	1488	1458	70 $\beta\text{CH}_3$ ; 20/22 $\beta\text{CCH}_3$
16	1443m,sh	1447 w,br	1473	1444	1457 s		1478	1449	1474	1445	46/51 $\beta\text{CH}_3$ ; 21/20 $\beta\text{CH}$ ; 17/13 $\beta\text{NH}_2$
17	1381 w	1378 m	1415	1387	1377 m	1378 m	1419	1390	1418	1390	88/84 $\beta\text{CH}_3$
18			1354	1327			1357	1330	1356	1330	83/81 $\beta\text{CH}$
19	1314 m	1313m,sh	1342	1315	1316 vw		1342	1316	1341	1314	54/48 $\nu\text{CC}$ ; 16/20 $\beta\text{CH}$ ; 12/14 $\beta\text{CNH}_2$ ; 14 $\beta\text{CCH}_3$
20	1293 s	1293 m	1319	1292	1255 s	1257 s	1291	1265	1281	1256	41/49 $\nu\text{CN}$ ; 24/21 $\nu\text{CC}$ ; 23/21 $\beta\text{CH}$
21	1170 s	1166 m	1195	1171	1162 vw,sh		1190	1166	1185	1161	48 $\beta\text{CH}$ ; 31/30 $\nu\text{CN}$ ; 20 $\nu\text{CC}$
22			1194	1170	1170 m	1174 m	1201	1177	1199	1175	71 $\beta\text{CH}$ ; 17/11 $\nu\text{CC}$
23		1106 w	1133	1111	1144 m	1147 w	1160	1137	1152	1129	48/50 $\beta\text{NH}_2$ (rock.); 28/27 $\nu\text{CC}$ ; 15/22 $\beta\text{CH}$
24	1077 w	1075 w	1094	1072	1090 vs	1095 s	1116	1094	1111	1089	40/38 $\nu\text{CC}$ ; 33/39 $\beta\text{NH}_2$ (rock.); 21/19 $\beta\text{CH}$
25	1038 w		1061	1040	1040 s		1065	1044	1065	1044	67/72 $\gamma\text{CCH}_3$ ; 19/20 $\gamma\text{CH}_3$
26			1021	1001	1001 m	1000 vs	1028	1008	1025	1004	49/52 $\beta\text{CCH}_3$ ; 23/21 $\beta\text{CNH}_2$ ; 20/23 $\nu\text{CC}$
27	996 m	996 vs	1014	994	997 m		1018	998	1017	997	42/41 $\nu\text{CC}$ ; 34/38 $\beta\text{CCC}$ ; 17/10 $\beta\text{CCH}_3$
28	965vw		946	927	914 vs	916 vw	933	914	930	912	52/53 $\nu\text{CC}+\nu\text{CN}$ ; 35/30 $\beta\text{CCC}$

Table 4.26 cont.

m-toluidine			ZnI <sub>2</sub> (m-tol) <sub>2</sub>								
Exp.*			B3LYP/def2-TZVP		Exp.**		B3LYP/def2-TZVP				PED (%) Assignments
No	IR	Ra	Calc.	Scaled	IR	Ra	Calc.	Scaled	Calc.	Scaled	
29	926 m	928 vw	943	924	966 m		979	959	965	946	73/82 $\gamma$ CH; 17/10 $\gamma$ CCC
30	870 m		875	858	890 s	892 vw	901	883	897	879	72/71 $\gamma$ CH; 15/17 $\gamma$ CCC
31	855 m		856	839	868 vs	872 vw	890	872	873	856	86/84 $\gamma$ CH
32	775 vs	784 w	782	766	772 vs		798	782	791	775	74/77 $\gamma$ CH; 10/14 $\gamma$ CCC
33		738 s	749	734	728 s	732 s	744	729	744	729	54/57 $\beta$ CCC; 40/41 $\nu$ CC+ $\nu$ CN
34	691 vs		705	691	689 vs	693 vw	715	701	706	692	49/53 $\gamma$ CCC; 30/20 $\gamma$ CH; 10/12 $\gamma$ CNH <sub>2</sub> (wag.)
35			600	588			1058	1037	968	949	86/72 $\gamma$ NH <sub>2</sub> (wag.); 10/19 $\gamma$ CCC
36	557 m		559	548	568 m	571 m	585	573	579	567	47/41 $\gamma$ CNH <sub>2</sub> ; 26/24 $\gamma$ CCH <sub>3</sub> ; 20/24 $\gamma$ CCC
37	538 m	543 m	539	528	542 m	543 m	553	542	552	541	37/41 $\beta$ NH <sub>2</sub> (wag.); 25/21 $\nu$ CC; 20 $\beta$ CCC; 10 $\nu$ CN
38		518 m	526	515	520 vw	520 m	529	518	527	516	58/61 $\beta$ CCC; 27/32 $\nu$ CC
39		431 w	449	440	441 m	447 w	456	447	452	443	76/70 $\gamma$ CCC; 12/17 $\gamma$ CH
40			431	422	411 m	415 m	414	406	406	398	83/85 $\beta$ CCH <sub>3</sub> + $\beta$ CNH <sub>2</sub>
41		294 m	304	298	634 vs	635 vw	603	591	573	562	86/80 $\beta$ NH <sub>2</sub> (twist.)
42		234 m	289	284	287 vs	288 m	287	282	282	277	85/87 $\beta$ CCH <sub>3</sub> + $\beta$ NH <sub>2</sub> (twist.)
43		218 m	223	219	340 vw	307 w	338	332	312	306	78/72 $\gamma$ CCC + $\gamma$ NH <sub>2</sub> (twist.); 21/10 $\nu$ MN
					223 w	221 s	235	230	149	146	89/74 $\nu$ MI; 10/18 $\tau$ CNMN
44			204	200	216 w		216	211	215	210	63/51 $\gamma$ CCH <sub>3</sub> ; 20 $\gamma$ CCC; 10/23 $\gamma$ CNH <sub>2</sub>
						159 vs	180	176	164	161	75/84 $\nu$ MN; 15/13 $\gamma$ CCC+ $\gamma$ CNH <sub>2</sub>
							97	95	80	79	71/55 $\nu$ MN; 30/42 $\tau$ CNMN
							75	73	67	66	61/55 $\tau$ CNMN; 25/31 $\gamma$ NMI
45			27	26			50	49	37	36	91/94 $\gamma$ CH <sub>3</sub> (torsion)
							48	47	41	40	59/41 $\gamma$ NMI; 33/44 $\tau$ CNMN
							32	31	28	27	68/64 $\tau$ CCNM; 16/22 $\gamma$ NMI
							21	20	16	16	53/52 $\tau$ CNMN; 38/30 $\tau$ CCNM
							13	13			73 $\tau$ CNMN; 23 $\gamma$ NMI

\*Experimental data is taken from Ref. [145], \*\*Experimental data is taken from Ref. [21].

Table 4.27 Experimental and calculated vibrational frequencies (in  $\text{cm}^{-1}$ ) of free m-toluidine and  $\text{CdI}_2(\text{m-tol})_2$ .

m-toluidine			$\text{CdI}_2(\text{m-tol})_2$								
Exp.*		B3LYP/def2-TZVP		Exp.**		B3LYP/def2-TZVP				PED (%) Assignments	
No	IR	Ra	Calc.	Scaled	IR	Ra	Calc.	Scaled	Calc.		Scaled
1	3435 s		3652	3457	3302 m	3305 m	3586	3394	3563	3373	100 $\nu\text{NH}_2$ (asym.)
2	3354 s	3353 mbr	3556	3366	3241 m	3243 s	3498	3311	3486	3300	100 $\nu\text{NH}_2$
3	3034 m	3046s	3184	3014	3045 w	3046 s	3193	3022	3192	3021	99/98 $\nu\text{CH}$
4	3015 m,sh	3012 s	3169	2999	3014 w	3015 m	3177	3007	3176	3006	99 $\nu\text{CH}$
5			3158	2989			3169	2999	3169	2999	98/99 $\nu\text{CH}$
6	2975m,sh	2974 m	3147	2979	2967 vw	2976 w	3166	2996	3162	2993	99 $\nu\text{CH}$
7	2946m,sh		3104	2938	2939 vw		3112	2946	3111	2945	99/95 $\nu\text{CH}_3$ (asym.)
8	2919 m	2919 s	3078	2913	2914 w	2917 s	3085	2920	3082	2917	98/94 $\nu\text{CH}_3$ (asym.)
9	2857 w	2857m,sh	3026	2864	2854 w	2859 m, sh	3032	2869	3029	2867	99 $\nu\text{CH}_3$
10	1622 vs		1661	1629	1614 vs	1616 s	1656	1623	1643	1610	76/64 $\beta\text{NH}_2$ (sciss.); 14/15 $\beta\text{CNH}_2$
11			1649	1617	1596 vs	1596 s	1654	1622	1650	1617	59/53 $\nu\text{CC}$ ; 21 $\beta\text{NH}_2$ (sciss.); 12/10 $\beta\text{CH}$
12	1591 vs	1590 m	1630	1598	1565 vs		1636	1603	1632	1600	58/55 $\nu\text{CC}$ ; 12 $\beta\text{CH}$ ; 15/17 $\beta\text{NH}_2$ (rock.)
13			1533	1503			1535	1505	1534	1504	49/42 $\beta\text{CH}$ ; 27/30 $\nu\text{CC}$ ; 12/10 $\beta\text{CCC}$
14	1493 vs	1493 w	1510	1480	1492 vs	1494 w	1510	1480	1509	1479	56/51 $\beta\text{CH}_3$ ; 21 $\beta\text{CH}$ ; 12 $\nu\text{CC}$
15	1469 s		1490	1461	1467 s	1470 w	1492	1462	1490	1460	73/71 $\beta\text{CH}_3$ ; 20/18 $\beta\text{CCH}_3$
16	1443m,sh	1447 w, br	1473	1444	1438 m	1443 w	1475	1446	1473	1444	56/48 $\beta\text{CH}_3$ ; 26/30 $\nu\text{CC}$ ; 11 $\beta\text{NH}_2$
17	1381 w	1378 m	1415	1387	1374 m	1382 m	1418	1390	1417	1388	93/92 $\beta\text{CH}_3$
18			1354	1327			1357	1330	1356	1329	75/71 $\beta\text{CH}$ ; 12 $\nu\text{CC}$
19	1314 m	1313 m, sh	1342	1315	1315 m	1317 w	1341	1315	1340	1314	48/49 $\nu\text{CC}$ ; 22 $\beta\text{CH}$ ; 14/11 $\beta\text{CNH}_2$ ; 12/13 $\beta\text{CCH}_3$
20	1293 s	1293 m	1319	1292	1276 m	1278 m	1296	1271	1287	1262	37/40 $\nu\text{CN}$ ; 24/23 $\nu\text{CC}$ ; 18/13 $\beta\text{CCC}$ ; 13/10 $\beta\text{CH}$
21	1170 s	1166 m	1195	1171	1171 s	1172 m	1199	1175	1199	1175	70/68 $\beta\text{CH}$ ; 10/15 $\nu\text{CC}$ ; 11/10 $\nu\text{CN}$
22			1194	1170	1160 m	1163 w,sh	1192	1169	1188	1164	48/45 $\beta\text{CH}$ ; 40/49 $\nu\text{CC}+\nu\text{CN}$
23		1106 w	1133	1111		1106 w	1151	1128	1148	1125	44/48 $\beta\text{NH}_2$ (rock.); 20/31 $\beta\text{CH}$ ; 23/13 $\nu\text{CC}$
24	1077 w	1075 w	1094	1072	1087 s	1087 m	1111	1089	1108	1086	40/42 $\beta\text{NH}_2$ (rock.); 28/26 $\nu\text{CC}$ ; 20/22 $\beta\text{CH}$
25	1038 w		1061	1040	1030 vs	1030 s	1065	1044	1065	1044	60/65 $\gamma\text{CCH}_3$ ; 21/15 $\gamma\text{CH}_3$ ; 10/11 $\gamma\text{CH}$
26			1021	1001			1025	1005	1024	1004	49/47 $\beta\text{CCH}_3$ ; 27 $\beta\text{CCC}$ ; 17/20 $\beta\text{CNH}_2$
27	996 m	996 vs	1014	994	998 vs	1000 vs	1021	1001	1017	997	62/57 $\beta\text{CCC}$ ; 29/33 $\nu\text{CC}$
28	965 vw		946	927	919 vs	921 m	947	928	930	912	45/46 $\nu\text{CC}+\nu\text{CN}$ ; 30/31 $\beta\text{CCC}$ ; 10 $\beta\text{CNH}_2$

Table 4.27 cont.

m-toluidine			CdI <sub>2</sub> (m-tol) <sub>2</sub>								
Exp.*		B3LYP/def2-TZVP		Exp.**		B3LYP/def2-TZVP				PED (%) Assignments	
No	IR	Ra	Calc.	Scaled	IR	Ra	Calc.	Scaled	Calc.		Scaled
29	926 m	928 vw	943	924			976	957	964	945	72/79 $\gamma$ CH; 17/12 $\gamma$ CCC+ $\gamma$ CNH <sub>2</sub>
30	870 m		875	858	888 vs	885 m	913	895	891	873	72/76 $\gamma$ CH; 21/15 $\gamma$ CCC+ $\gamma$ CNH <sub>2</sub>
31	855 m		856	839	867 s	870 vw	890	872	874	857	75/69 $\gamma$ CH; 21/25 $\gamma$ CCC+ $\gamma$ CNH <sub>2</sub>
32	775 vs	784 w	782	766	777 vs	777 m	795	779	790	774	67/74 $\gamma$ CH; 30/23 $\gamma$ CCC+ $\gamma$ CNH <sub>2</sub>
33		738 s	749	734	730 s	734 s	744	729	743	728	59/52 $\nu$ CC+ $\nu$ CN; 31/40 $\beta$ CCC
34	691 vs		705	691	689 vs		716	702	709	695	62/55 $\gamma$ CCC; 10/25 $\gamma$ CH; 10/11 $\gamma$ CNH <sub>2</sub> (wag.)
35			600	588	963 s		981	962	863	846	67/69 $\gamma$ NH <sub>2</sub> (wag.); 23 $\gamma$ CCC
36	557 m		559	548	583 vs		582	570	578	567	76/73 $\gamma$ CCC+ $\gamma$ CNH <sub>2</sub> ; 20/23 $\gamma$ CCH <sub>3</sub>
37	538 m	543 m	539	528	556 vs	567 m	552	541	551	540	50/42 $\beta$ CCC; 23/30 $\nu$ CC+ $\nu$ CN; 12/14 $\beta$ NH <sub>2</sub>
38		518 m	526	515	518 w	522 s	527	517	526	516	64/65 $\beta$ CCC; 23/24 $\nu$ CC
39		431 w	449	440	444 m	446 m	455	446	452	443	69/70 $\gamma$ CCC; 17/16 $\gamma$ CH
40			431	422	415 m	418 m	410	401	402	394	81/86 $\beta$ CCH <sub>3</sub> + $\beta$ CNH <sub>2</sub>
41		294 m	304	298	543 m	545 m	541	530	516	505	79/72 $\beta$ NH <sub>2</sub> (twist.); 12/15 $\beta$ CCC
42		234 m	289	284	283 m	285 m	287	281	277	272	89/81 $\beta$ CCH <sub>3</sub> + $\beta$ CNH <sub>2</sub>
43		218 m	223	219		341 m	299	293	276	270	67/72 $\gamma$ CCC + $\gamma$ CNH <sub>2</sub> ; 15/11 $\nu$ MN
44			204	200	219 m	221 s	214	210	213	209	49/54 $\gamma$ CCH <sub>3</sub> ; 23 $\gamma$ CCC; 17 $\gamma$ CNH <sub>2</sub>
					209 w		204	200			92 $\nu$ MI
						180 vs	146	143	139	136	69/75 $\nu$ MN; 18/14 $\gamma$ CNH <sub>2</sub> + $\gamma$ CCH <sub>3</sub>
						122 vs	128	126			87 $\gamma$ NMI+ $\gamma$ IMI
							69	68	62	61	64/44 $\tau$ CNMN; 31/25 $\gamma$ NMI; 0/30 $\gamma$ CH <sub>3</sub> (torsion)
45			27	26			61	59	16	16	89/87 $\gamma$ CH <sub>3</sub> (torsion)
							57	56	45	44	59/68 $\tau$ CCNM; 22/14 $\gamma$ NMI
							39	39	34	34	44/29 $\gamma$ IMI; 20/31 $\tau$ CNMN; 20/23 $\gamma$ NMI
							28	28	23	23	57/53 $\tau$ CCNM; 38/33 $\gamma$ NMI
							20	20	15	15	57/41 $\tau$ CNMN; 21/10 $\tau$ CCNM; 17/31 $\gamma$ CH <sub>3</sub> (torsion)
							10	10			84 $\tau$ CNMN

\*Experimental data is taken from Ref. [145], \*\*Experimental data is taken from Ref. [21].

### 4.3.6 Comparison Between Computed Vibrational Frequencies and the Observed Frequencies in the Title Compounds

As mentioned in Chapter 3, DFT calculations generally neglect anharmonicity and overestimate the experimental frequencies. In this section we compare experimental and computed vibrational frequencies for all our twenty transition metal complexes by means of mean absolute errors (MAE), and linear correlation coefficients ( $R^2$ ). As it is well known, obtaining smaller MAE values and finding  $R^2$  values very close to 1 mean our systematic computational study is in agreement with the experimental data. Therefore, we try to find an answer to this question: Which transition metal halide complex(es) can be more accurately estimated by B3LYP/def2-TZVP method in terms of their vibrational frequencies?

Table 4.28 The MAE and the  $R^2$  values for the title complexes.

	Unscaled Frequencies			Scaled Frequencies		
	MAE	MAE*	$R^2$	MAE	MAE*	$R^2$
MnBr <sub>2</sub> (p-tol) <sub>2</sub>	59.05	25.44	0.9980	21.82	14.84	0.9989
CoBr <sub>2</sub> (p-tol) <sub>2</sub>	64.05	25.77	0.9977	23.29	13.97	0.9987
NiBr <sub>2</sub> (p-tol) <sub>2</sub>	50.88	22.16	0.9984	19.38	16.78	0.9991
CuBr <sub>2</sub> (p-tol) <sub>2</sub>	61.28	28.38	0.9982	23.40	17.02	0.9991
ZnBr <sub>2</sub> (p-tol) <sub>2</sub>	65.97	29.32	0.9978	25.92	14.00	0.9984
CdBr <sub>2</sub> (p-tol) <sub>2</sub>	63.47	26.56	0.9979	23.12	10.70	0.9985
HgBr <sub>2</sub> (p-tol) <sub>2</sub>	63.92	25.11	0.9977	24.87	9.49	0.9983
NiI <sub>2</sub> (p-tol) <sub>2</sub>	65.04	42.14	0.9978	28.94	26.11	0.9979
ZnI <sub>2</sub> (p-tol) <sub>2</sub>	61.81	24.96	0.9979	22.26	13.09	0.9989
CdI <sub>2</sub> (p-tol) <sub>2</sub>	61.14	28.22	0.9978	21.61	13.43	0.9988
MnBr <sub>2</sub> (m-tol) <sub>2</sub>	49.68	21.66	0.9992	11.72	10.53	0.9997
CoBr <sub>2</sub> (m-tol) <sub>2</sub>	48.21	24.09	0.9978	15.26	12.97	0.9993
NiBr <sub>2</sub> (m-tol) <sub>2</sub>	45.10	22.75	0.9988	16.16	15.28	0.9994
CuBr <sub>2</sub> (m-tol) <sub>2</sub>	58.31	24.96	0.9974	23.23	13.26	0.9984
ZnBr <sub>2</sub> (m-tol) <sub>2</sub>	60.89	25.71	0.9977	17.64	14.21	0.9990
CdBr <sub>2</sub> (m-tol) <sub>2</sub>	62.50	27.30	0.9985	15.69	12.10	0.9994
HgBr <sub>2</sub> (m-tol) <sub>2</sub>	65.44	25.99	0.9981	18.48	12.68	0.9991
NiI <sub>2</sub> (m-tol) <sub>2</sub>	45.75	20.18	0.9992	15.30	12.52	0.9996
ZnI <sub>2</sub> (m-tol) <sub>2</sub>	55.48	21.76	0.9984	12.58	8.42	0.9995
CdI <sub>2</sub> (m-tol) <sub>2</sub>	56.48	22.89	0.9986	14.01	10.17	0.9995

\*; Mean Absolute Error for the vibrations below 1700 cm<sup>-1</sup>.

In Table 4.28 we provide a comparison for calculated and scaled frequencies and give linear correlation coefficients for both of them. MAE values are also provided for all vibrations and for the vibrations below  $1700\text{ cm}^{-1}$ . In addition to this, in order to follow the table easily, we have underlined some results with specific colors, such as best result is painted with pink and second best with yellow, whereas the worst result is painted with green and the second worst result with blue.

As seen from the table, all  $R^2$  values are close to 1, but in  $\text{MnBr}_2(\text{m-tol})_2$  it is very close, being greater than 0,999 for both scaled and unscaled frequencies. If we look at the MAE values, we see that  $\text{NiBr}_2(\text{m-tol})_2$  gives the best result for the unscaled frequencies, and after a scaling procedure, this time  $\text{MnBr}_2(\text{m-tol})_2$  gives best result. For the frequencies below  $1700\text{ cm}^{-1}$ , the results of  $\text{NiI}_2(\text{m-tol})_2$  (for the unscaled) and  $\text{ZnI}_2(\text{m-tol})_2$  (for the scaled frequencies) are in very good agreement with the experimental data. For the unscaled frequencies, the worst result is obtained in  $\text{ZnBr}_2(\text{p-tol})_2$  with a MAE value  $65.97\text{ cm}^{-1}$ , and for the scaled frequencies  $\text{NiI}_2(\text{p-tol})_2$  has the biggest MAE value as  $28.94\text{ cm}^{-1}$ .

Thus according to the table, computed frequencies for the transition metal complexes of m-toluidine are better than p-toluidine complexes. And for all complexes, the overall average shift with respect to the experimental data is  $\sim 58\text{ cm}^{-1}$  for the unscaled frequencies, and after a scaling procedure this shift is lowered to  $\sim 19\text{ cm}^{-1}$ . Furthermore, below  $1700\text{ cm}^{-1}$ , this result is better; for the unscaled frequencies shift is  $25\text{ cm}^{-1}$  and for the scaled frequencies, it is  $13\text{ cm}^{-1}$ , being in a good agreement with the experimental frequencies.

## CHAPTER 5

### CONCLUDING REMARKS

A systematic DFT study on twenty different transition metal complexes have been performed and molecular structures, charge, spin distributions and vibrational frequencies of these complexes are elucidated. Significant results are summarized below.

Cobalt, copper, zinc, cadmium and mercury complexes are found to have tetra-coordinate structures. Among these,  $\text{CoBr}_2(\text{m-tol})_2$ ,  $\text{CuBr}_2(\text{p-tol})_2$ , and  $\text{CuBr}_2(\text{m-tol})_2$  have square planar geometries, whilst others have distorted tetrahedral structures. In addition to this, nickel complexes have octahedral coordination around the Ni atom, by sharing two Br/I atoms of the neighboring complexes; however manganese complexes have 5-coordinate polymeric bridged structure around the Mn atom, by sharing one Br atom of the neighbor complex.

Spin analysis is only performed for the open-shell complexes, and the complexes generally have high spins, except cobalt bromide complex of m-toluidine. DFT calculations predict Mn complexes as sextet ( $S=5/2$ ), Ni complexes as triplet ( $S=1$ ), Co complex of p-toluidine as quartet ( $S=3/2$ ) and Co complex of m-toluidine as doublet ( $S=1/2$ ), and also Cu complexes as doublet ( $S=1/2$ ). The unpaired spins are mostly accumulated on metal atoms as expected, and the remaining amount is generally located on halogen atoms.

As for the charge distribution, Mulliken, NBO and APT charge analysis methods are performed. According to the calculations NBO results are not reliable for our metal iodide complexes, and also for the cadmium and mercury bromide complexes. That is, natural charge results fail in heavy atoms at B3LYP/def2-TZVP level.



Most probably pseudopotential/ECP which is utilized in the def2-TZVP basis set for the heavy atoms caused this unfavourable result. Mulliken method also has some deficiencies, e.g. in copper and cobalt complexes. Therefore, it can be said that, in terms of having physically most meaningful results, APT method is more trustworthy by showing the most positive charges on metal atoms, and the most negative charges on the nitrogen atoms and halogens.

In the vibrational spectra of experimental-only studies some assignments were not determined correctly. However, we provide a full vibrational assignment (with PED %) of the title complexes for the first time, by means of density functional calculations. To give an example, although metal-ligand stretching vibrations, i.e.  $\nu_{MN}$  were generally assigned in the 600-400  $\text{cm}^{-1}$  region in the experimental only studies, present computations predict these bands in lower wavenumbers for all of the title complexes. Therefore, the present study allows accurate assignments of the vibrational bands, which otherwise assigned tentatively in experimental-only studies.

As an evidence of complex formation between metal (II) halides and the ligands p-toluidine and m-toluidine, some modes originating from ligands show substantial shifts in the vibrational frequencies of complexes. These modes are generally amino group frequencies, shift lower or higher wavenumbers, which show coordination occurs via nitrogen atom of the free ligands.

Additionally, if the computed frequencies of the complexes compared with the experimental data, one can explicitly see that computed vibrational frequencies of m-toluidine complexes are compatible than the p-toluidine complexes. Mn and Ni complexes of m-toluidine provide best vibrational frequency results with the B3LYP/def2-TZVP method, among the twenty transition metal complexes.

As a final comment, density functional theory finds a good compromise in terms of accuracy and the computational cost. Nevertheless, despite the B3LYP/def2-TZVP level calculations for the molecular structures and vibrational frequencies of the transition metal complexes are feasible, this study can be extended with different functionals and basis sets for investigating various molecular properties of the analogous transition metal systems.

## REFERENCES

- [1] Dirac, P. A., "Quantum mechanics of many-electron systems", *Proceedings of the Royal Society of London A: Mathematical, Physical and Engineering Sciences*, Vol. 123(792), pp. 714-733, 1929.
- [2] Diaz-Acosta, I., Baker, J., Cordes, W., Pulay, P., "Calculated and experimental geometries and infrared spectra of metal tris-acetylacetonates: Vibrational spectroscopy as a probe of molecular structure for ionic complexes. Part I" *The Journal of Physical Chemistry A*, Vol. 105(1), pp. 238-244, 2001.
- [3] Williams, T. G., & Wilson, A. K., "Importance of the quality of metal and ligand basis sets in transition metal species", *The Journal of Chemical Physics*, Vol. 129(5), pp. 054108 (1-10), 2008.
- [4] Luo, S., Averkiev, B., Yang, K. R., Xu, X., & Truhlar, D. G., "Density Functional Theory of Open-Shell Systems. The 3d-Series Transition-Metal Atoms and Their Cations" *Journal of Chemical Theory and Computation*, Vol. 10(1), pp. 102-121, 2013.
- [5] Neese, F., "Prediction of molecular properties and molecular spectroscopy with density functional theory: From fundamental theory to exchange-coupling", *Coordination Chemistry Reviews*, Vol. 253(5), 526-563, 2009.
- [6] Cramer, C. J., & Truhlar, D. G., "Density functional theory for transition metals and transition metal chemistry", *Physical Chemistry Chemical Physics*, Vol. 11(46), pp. 10757-10816, 2009.
- [7] Neese, F., & Solomon, E. I., "Detailed spectroscopic and theoretical studies on [Fe(EDTA)(O<sub>2</sub>)]<sup>3-</sup>: electronic structure of the side-on ferric-peroxide bond and its relevance to reactivity", *Journal of the American Chemical Society*, Vol. 120(49), pp. 12829-12848, 1998.

- [8] Atkins, P. W., & Friedman, R. S., *Molecular Quantum Mechanics*, Oxford University Press, New York, 2005.
- [9] Neese, F., *Applying Computational Chemistry to Transition Metal Complexes*, 2013.  
<http://dirac.ups-tlse.fr/bast/esqc/static/lectures/ESQC13-Neese-TransitionMetals-final.pdf>
- [10] Whysner, J., Verna, L., Williams, G. M., “Benzidine mechanistic data and risk assessment: species-and organ-specific metabolic activation”, *Pharmacology & Therapeutics* Vol. 71(1), 107-126, 1996.
- [11] Santos, L., Martinez, E., Ballesteros, B., Sanchez, J., “Molecular structures and vibrations of m-methylaniline in the S 0 and S 1 states studied by laser induced fluorescence spectroscopy and ab initio calculations”, *Spectrochimica Acta Part A: Molecular and Biomolecular Spectroscopy*, Vol. 56(10), pp. 1905-1915, 2000.
- [12] Vaschetto, M. E., Retamal, B. A., Monkman, A. P., “Density functional studies of aniline and substituted anilines”, *Journal of Molecular Structure: Theochem*, Vol. 468(3), pp. 209-221, 1999.
- [13] Shao, D., Hu, J., Chen, C., Sheng, G., Ren, X., Wang, X., “Polyaniline multiwalled carbon nanotube magnetic composite prepared by plasma-induced graft technique and its application for removal of aniline and phenol”, *The Journal of Physical Chemistry C*, Vol. 114(49), pp. 21524-21530, 2010.
- [14] Prevost, V., Petit, A., Pla, F., “Studies on chemical oxidative copolymerization of aniline and o-alkoxysulfonated anilines: Synthesis and characterization of novel self-doped polyanilines” *Synthetic Metals*, Vol. 104(2), pp. 79-87, 1999.
- [15] Raffa, D., Leung, K. T., Battaglini, F., “A microelectrochemical enzyme transistor based on an N-alkylated poly (aniline) and its application to determine hydrogen peroxide at neutral pH” *Analytical Chemistry*, Vol. 75(19), pp. 4983-4987, 2003.
- [16] Cardoso, M. J. R., Lima, M. F. S., Lenz, D. M., “Polyaniline synthesized with functionalized sulfonic acids for blends manufacture”, *Materials Research*, Vol. 10(4), pp. 425-429, 2007.

- [17] Allan, J. R., & Paton, A. D., "Preparation, structural characterisation, thermal and electrical studies of complexes of cobalt, nickel and copper with m-toluidine", *Thermochimica Acta*, Vol. 214(2), pp. 235-241, 1993.
- [18] Akyüz, S., & Davies, J. E. D., "Solid-state vibrational spectroscopy: Part 11. An infrared and raman vibrational spectroscopic study of metal (II) halide aniline complexes", *Journal of Molecular Structure*, Vol. 95, pp. 157-168, 1983.
- [19] Engelter, C., & Thornton, D. A., "Infrared spectra of bis (aniline) and bis (p-toluidine) metal (II) isothiocyanate complexes", *Journal of Molecular Structure*, Vol. 33(1), pp. 119-126, 1976.
- [20] Engelter, C., Thornton, D. A., Ziman, M. R., "Infrared spectra of o-toluidine and m-toluidine complexes of Co (II), Ni (II), Cu (II) and Zn (II) halides", *Journal of Molecular Structure*, Vol. 49(1), pp. 7-15, 1978.
- [21] Altun, A., Gölcük, K., Kumru, M., "Vibrational and thermal studies of metal (II)[Ni (II), Zn (II) and Cd (II)] iodide m-methylaniline complexes", *Vibrational Spectroscopy*, Vol. 31(2), pp. 215-225, 2003.
- [22] Altun, A., Gölcük, K., Kumru, M., "Vibrational and thermal studies of p-methylaniline complexes with Ni (II), Zn (II) and Cd (II) iodides", *Vibrational Spectroscopy*, Vol. 33(1), pp. 63-74, 2003.
- [23] Golcuk, K., Altun, A., Kumru, M., "Thermal studies and vibrational analyses of m-methylaniline complexes of Zn (II), Cd (II) and Hg (II) bromides" *Spectrochimica Acta Part A: Molecular and Biomolecular Spectroscopy*, Vol. 59(8), pp. 1841-1847, 2003.
- [24] Golcuk, K., Altun, A., Kumru, M., "Spectroscopic and thermal studies of Mn (II), Co (II) and Ni (II) bromide m-methylaniline complexes", *Journal of Molecular Structure*, Vol. 657(1), pp. 385-393, 2003.
- [25] Golcuk, K., Altun, A., Guner, S., Kumru, M., Aktas, B., "Thermal, vibrational and EPR studies of Cu (II) bromide bis (p-methylaniline) and bis (m-methylaniline) complexes", *Spectrochimica Acta Part A: Molecular and Biomolecular Spectroscopy*, Vol. 60(1), pp. 303-309, 2004.

- [26] Golcuk, K., Altun, A., Somer, M., Kumru, M., “Vibrational and thermal studies of [MBr<sub>2</sub>(p-methylaniline)<sub>2</sub>](M: Zn<sup>2+</sup>, Cd<sup>2+</sup> and Hg<sup>2+</sup>) complexes” *Vibrational Spectroscopy*, Vol. 39(1), pp. 68-73, 2005.
- [27] Bowman-James, K., “Alfred Werner revisited: the coordination chemistry of anions” *Accounts of Chemical Research*, Vol. 38(8), pp. 671-678, 2005.
- [28] Hao, X., Zhu, N., Gschneidner, T., Jonsson, E. Ö., Zhang, J., Moth-Poulsen, K., ... & Chi, Q., “Direct measurement and modulation of single-molecule coordinative bonding forces in a transition metal complex”, *Nature Communications*, Vol. 4, pp. 1-10. 2013.
- [29] Gispert, J. R., *Coordination Chemistry*. Vol. 483. Wiley-VCH, Weinheim, 2008.
- [30] Henson, N. J., Hay, P. J., Redondo, A., “Density functional theory studies of the binding of molecular oxygen with Schiff's base complexes of cobalt”, *Inorganic Chemistry*, Vol. 38(7), pp. 1618-1626, 1999.
- [31] Waters, T., Woo, H. K., Wang, X. B., Wang, L. S., “Probing the Intrinsic Electronic Structure of the Bis (dithiolene) Anions [M(mnt)<sub>2</sub>]<sup>2-</sup> and [M(mnt)<sub>2</sub>]<sup>1-</sup> (M= Ni, Pd, Pt; mnt= 1, 2-S<sub>2</sub>C<sub>2</sub>(CN)<sub>2</sub>) in the Gas Phase by Photoelectron Spectroscopy”, *Journal of the American Chemical Society*, Vol. 128(13), pp. 4282-4291. (2006).
- [32] Robertson, N., & Cronin, L., “Metal bis-1, 2-dithiolene complexes in conducting or magnetic crystalline assemblies”, *Coordination Chemistry Reviews*, Vol. 227(1), 93-127, 2002.
- [33] Karlin, K. D., & Stiefel, E. I., *Dithiolene Chemistry: Synthesis, Properties and Applications*, Vol. 52, Wiley, New York, 2003.
- [34] Farrel, N., *Transition Metal Complexes as Drugs and Chemotherapeutic Agents*, Kluwer Academic Publishers, Dordrecht, 1989.
- [35] Krishnan, G., & Suprabha, S., “Antitumour and Antimicrobial Studies of a Series of Mn (II) and Ni (II) Complexes derived from N-Amidino-N1-Naphthylthiourea”, *International Journal of ChemTech Research*, Vol. 4(2), pp. 484-492, 2012.

- [36] Rafique, S., Idrees, M., Nasim, A., Akbar, H., Athar, A., "Transition metal complexes as potential therapeutic agents", *Biotechnology and Molecular Biology Reviews*, Vol. 5(2), pp. 38-45, 2010.
- [37] Desoize, B., "Metals and metal compounds in cancer treatment", *Anticancer Research*, Vol. 24 (3A), pp. 1529-1544, 2004.
- [38] Ibrahim, M., Haider, A., Lan, Y., Bassil, B. S., Carey, A. M., Liu, R., ... & Kortz, U., "Multinuclear Cobalt (II)-Containing Heteropolytungstates: Structure, Magnetism, and Electrochemistry", *Inorganic Chemistry*, Vol. 53(10), pp. 5179-5188, 2014.
- [39] Clark, R. J., & Williams, C. S., "The far-infrared spectra of metal-halide complexes of pyridine and related ligands", *Inorganic Chemistry*, Vol. 4(3), pp. 350-357, 1965.
- [40] Ahuja, I. S., Brown, D. H., Nuttall, R. H., Sharp, D. W. A., "The preparation and spectroscopic properties of some aniline complexes of transition metal halides", *Journal of Inorganic and Nuclear Chemistry*, Vol. 27(5), pp. 1105-1110, 1965.
- [41] Allen, J. R., Brown, D. H., Nuttall, R. H., Sharp, D. W. A., "The thermal decomposition of metal complexes-V. The decomposition of some pyridine and substituted-pyridine complexes of manganese (II) halides", *Journal of Inorganic and Nuclear Chemistry*, Vol. 27(8), pp. 1865-1867, 1965.
- [42] Brown, D. H., Nuttall, R. N., Sharp, D. W. A., "The thermal decomposition of metal complexes-II: The decomposition of some bisquinoline metal (II) halides" *Journal of Inorganic and Nuclear Chemistry*, Vol. 26(7), pp. 1151-1156, 1964.
- [43] Beech, G., Marr, G., Ashcroft, S. J., "The thermochemistry of some acetonitrile and benzonitrile complexes of transition-metal halides", *Journal of the Chemical Society A: Inorganic, Physical, Theoretical*, pp. 2903-2906, 1970.
- [44] Coucouvanis, D., Baenziger, N. C., Johnson, S. M., "Metal complexes as ligands. II. Synthesis, structure determination, and bonding characteristic of certain tin (IV) halide adducts of the nickel (II) and palladium (II) dithiooxalato complexes", *Journal of the American Chemical Society*, Vol. 95(12), pp. 3875-3886, 1973.

- [45] Brown, D. H., & Richardson, R. T., "The preparation, thermal decomposition, visible and infrared spectra of some chromium (III) halide complexes", *Journal of Inorganic and Nuclear Chemistry*, Vol. 35(3), pp. 755-759, 1973.
- [46] Karayannis, N. M., Pytlewski, L. L., Mikulski, C. M., "Metal complexes of aromatic amine N-oxides", *Coordination Chemistry Reviews*, Vol. 11(2), pp. 93-159, 1973.
- [47] Venkappayya, D., & Brown, D. H., "Some metal halide complexes of morpholine-4-thiocarbonic acid anilide", *Journal of Inorganic and Nuclear Chemistry*, Vol. 36(5), pp. 1023-1030, 1974.
- [48] Ahrland, S., Blauenstein, P., Tagesson, B., Tuhtar, D., "Metal Halide and Pseudohalide Complexes in Dimethylsulfoxide Solution. VII. Thermodynamics of Copper (I) Halide and Copper (II) Bromide Complex Formation". *Acta Chemica Scandinavica A*, Vol. 34(4), pp. 265-272, 1980.
- [49] Ahrland, S., Persson, I., Portanova, R., "Metal Halide and Pseudohalide Complexes in Dimethylsulfoxide Solution. IX. Equilibrium and Enthalpy Measurements on the Mercury (II) Chloride, Bromide, Iodide and Thiocyanate Systems", *Acta Chemica Scandinavica A*, Vol. 35(1), pp. 49-60, 1981.
- [50] Cseh, L., Csunderlik, C., Pantenburg, I., Meyer, G., Costisor, O., "Synthesis, Crystal Structure, and Spectral Properties of a Cobalt (II) Complex with N-Salicylidene-p-Toluidine" *Zeitschrift für Anorganische und Allgemeine Chemie*, Vol. 629(6), pp. 985-988, 2003.
- [51] Henderson, W., & Evans, C., "Electrospray mass spectrometric analysis of transition-metal halide complexes", *Inorganica chimica acta*, Vol. 294(2), pp. 183-192, 1999.
- [52] Yurdakul, Ş., Ataç, A., Şahin, E., Ide, S., "Synthesis, spectroscopic and structural studies on metal halide complexes of isonicotinamide", *Vibrational spectroscopy*, Vol. 31(1), pp. 41-49, 2003.

- [53] Wu, G., Wang, X. F., Okamura, T. A., Sun, W. Y., Ueyama, N., “Syntheses, structures, and photoluminescence properties of metal (II) halide complexes with pyridine-containing flexible tripodal ligands”, *Inorganic chemistry*, Vol. 45(21), pp. 8523-8532, 2006.
- [54] Ozel, A. E., Kecel, S., Akyuz, S., “FT-IR and Raman spectroscopic and quantum chemical studies of zinc halide complexes with 2, 2'-biquinoline”, *Vibrational Spectroscopy*, Vol. 48(2), pp. 238-245, 2008.
- [55] Ozel, A. E., Celik, S., Akyuz, S., Kecel, S., “Infrared and Raman spectroscopic and quantum chemical investigations of zinc halide complexes of 3-aminoquinoline”, *Vibrational Spectroscopy*, Vol. 53(1), pp. 151-157, 2010.
- [56] Yurdakul, Ş., Badoğlu, S., Güleşçi, Y., “Experimental and theoretical study on free 5-nitroquinoline, 5-nitroisoquinoline, and their zinc (II) halide complexes” *Spectrochimica Acta Part A: Molecular and Biomolecular Spectroscopy*, Vol. 137, pp. 945-956, 2015.
- [57] Akalin, E., & Akyuz, S., “FT-IR and Raman spectroscopic and DFT theoretical investigations on Zn (II) halide complexes of 2-aminopyrimidine”, *Vibrational Spectroscopy*, Vol. 53(1), 140-145, 2010.
- [58] Sabounchei, S. J., Dadrass, A., Akhlaghi, F., Nojini, Z. B., Khavasi, H. R., “Synthesis of a new carbbenzyloxymethylenetriphenylphosphorane ylide and the study of its reaction with mercury (II) halides: Spectral and structural characterization” *Polyhedron*, Vol. 27(8), 1963-1968, 2008.
- [59] Erdogdu, Y., Güllüoğlu, M. T., Kurt, M., Yurdakul, Ş., “Theoretical and experimental study on metal (II) halide complexes of 1, 3-bis (4-pyridyl) propane”, *Journal of Inclusion Phenomena and Macrocyclic Chemistry*, Vol. 64(3-4), pp. 341-355, 2009.
- [60] Keşan, G., Bağlayan, Ö., Parlak, C., Alver, Ö., Şenyel, M., “FT-IR and Raman spectroscopic and quantum chemical investigations of some metal halide complexes of 1-phenylpiperazine”, *Spectrochimica Acta Part A: Molecular and Biomolecular Spectroscopy*, Vol. 88, pp. 144-155, 2012.



- [61] Gökce, H., & Bahçeli, S., “A study of molecular structure and vibrational spectra of copper (II) halide complex of 2-(2'-thienyl) pyridine”, *Spectrochimica Acta Part A: Molecular and Biomolecular Spectroscopy*, Vol. 96, pp. 139-147, 2012.
- [62] Tyagi, P., Chandra, S., Saraswat, B. S., Yadav, D., “Design, spectral characterization, thermal, DFT studies and anticancer cell line activities of Co (II), Ni (II) and Cu (II) complexes of Schiff bases derived from 4-amino-5-(pyridin-4-yl)-4H-1, 2, 4-triazole-3-thiol”, *Spectrochimica Acta Part A: Molecular and Biomolecular Spectroscopy*, Vol. 145, pp. 155-164, 2015.
- [63] Eryürek, M., Bayarı, S. H., Yüksel, D., Hanhan, M. E., “Density functional investigation of the molecular structures, vibrational spectra and molecular properties of sulfonated pyridyl imine ligands and their palladium complexes”, *Computational and Theoretical Chemistry*, Vol. 1013, pp. 109-115, 2013.
- [64] Ozbek, O., Özalp-Yaman, Ş., Ozkan, I., Önal, A. M., Isci, H., “Spectroelectrochemical investigations of pyrimidine-2-thionato-bridged binuclear platinum (III) complexes”, *Polyhedron*, Vol. 74, pp. 122-128, 2014.
- [65] Mansour, A. M., “Synthesis, spectroscopic, electrochemical, DFT and SAR studies of nifuroxazide complexes with Pd (II), Pt (II) and Ru (II)” *Polyhedron*, Vol. 78, pp. 10-17, 2014.
- [66] Bardakçı, T., Kumru, M., Güner, S., “Molecular structure, vibrational and EPR spectra of Cu (II) chloride complex of 4-amino-1-methylbenzene combined with quantum chemical calculations” *Journal of Molecular Structure*, Vol. 1054, pp. 76-82, 2013.
- [67] Kumru, M., Bardakçı, T., & Güner, S., “DFT calculations and experimental FT-IR, dispersive-Raman and EPR spectral studies of Copper (II) chloride complex with 3-amino-1-methylbenzene”, *Spectrochimica Acta Part A: Molecular and Biomolecular Spectroscopy*, Vol. 123, pp. 187-193, 2014.
- [68] Furche, F., & Perdew, J. P., “The performance of semilocal and hybrid density functionals in 3d transition-metal chemistry”, *The Journal of Chemical Physics*, Vol. 124(4), pp. 044103(1-27), 2006.

- [69] Riley, K. E., & Merz, K. M., "Assessment of density functional theory methods for the computation of heats of formation and ionization potentials of systems containing third row transition metals", *The Journal of Physical Chemistry A*, Vol. 111(27), pp. 6044-6053, 2007.
- [70] Yang, Y., Weaver, M. N., & Merz Jr, K. M., "Assessment of the "6-31+ G\*\*+ LANL2DZ" Mixed Basis Set Coupled with Density Functional Theory Methods and the Effective Core Potential: Prediction of Heats of Formation and Ionization Potentials for First-Row-Transition-Metal Complexes", *The Journal of Physical Chemistry A*, Vol. 113(36), pp. 9843-9851, 2009.
- [71] Tekarli, S. M., Drummond, M. L., Williams, T. G., Cundari, T. R., Wilson, A. K., "Performance of Density Functional Theory for 3d Transition Metal-Containing Complexes: Utilization of the Correlation Consistent Basis Sets", *The Journal of Physical Chemistry A*, Vol. 113(30), pp. 8607-8614, 2009.
- [72] Ye, S., & Neese, F., "Accurate modeling of spin-state energetics in spin-crossover systems with modern density functional theory", *Inorganic Chemistry*, Vol. 49(3), pp. 772-774, 2010.
- [73] Matczak, P., "Assessment of B3LYP combined with various ECP basis sets for systems containing Pd, Sn, and Pb", *Computational and Theoretical Chemistry*, Vol. 983, pp. 25-30, 2012.
- [74] O Dohn, A., B Moller, K., PA Sauer, S., "Optimizing the structure of Tetracyanoplatinate (II): a comparison of relativistic density functional theory methods" *Current Inorganic Chemistry*, Vol. 3(3), pp. 213-219, 2013.
- [75] Warra, A. A., "Transition metal complexes and their application in drugs and cosmetics-A Review", *Journal of Chemical and Pharmaceutical Research*, Vol. 3(4), pp. 951-958, 2011.
- [76] Záliš, S., Ben Amor, N., Daniel, C., "Influence of the Halogen Ligand on the Near-UV-Visible Spectrum of [Ru (X)(Me)(CO) 2 ( $\alpha$ -diimine)](X= Cl, I;  $\alpha$ -Diimine= Me-DAB, iPr-DAB; DAB= 1, 4-Diaza-1, 3-butadiene): An ab Initio and TD-DFT Analysis", *Inorganic Chemistry*, Vol. 43(25), pp. 7978-7985, 2004.

- [77] Wang, T. H., Wang, I. T., Lin, S. H., Huang, L. Y., Chen, S. K., “Structures, frontier molecular orbitals and UV–vis spectra of RuX (PPh<sub>3</sub>)(NH<sub>2</sub>Ph)<sub>2</sub> L (X= Tp and Cp\*; L= Cl and N<sub>3</sub>): A DFT study”, *Journal of Organometallic Chemistry*, Vol. 757, pp. 36-41, 2014.
- [78] Mukuta, T., Fukazawa, N., Murata, K., Inagaki, A., Akita, M., Tanaka, S. I., Koshihara S., Onda, K., “Infrared vibrational spectroscopy of [Ru (bpy)<sub>2</sub> (bpm)]<sup>2+</sup> and [Ru (bpy)<sub>3</sub>]<sup>2+</sup> in the excited triplet state” *Inorganic Chemistry*, Vol. 53(5), pp. 2481-2490, 2014.
- [79] Vlček, A., & Zálíš, S., “Modeling of charge-transfer transitions and excited states in d<sup>6</sup> transition metal complexes by DFT techniques” *Coordination Chemistry Reviews*, Vol. 251(3), pp. 258-287, 2007.
- [80] Schrödinger, E., “Quantization as an eigenvalue problem”, *Annalen der Physik*, Vol. 79(4), pp. 361-376, 1926.
- [81] Born, M., & Oppenheimer, J. R., “Zur quantentheorie der molekeln”, *Annalen der Physik*, Vol. 389(20), pp. 457-484, 1927.
- [82] Parr, R. G., & Yang, R. G. P. W., *Density-Functional Theory of Atoms and Molecules*. Oxford university press, 1989.
- [83] Hartree, D. R., “The wave mechanics of an atom with a non-Coulomb central field. Part I. Theory and methods”, *Mathematical Proceedings of the Cambridge Philosophical Society*, Vol. 24(01), pp. 89-110, 1928.
- [84] Fock, V., “Näherungsmethode zur Lösung des Quantenmechanischen Mehrkör per problems”, *Zeitschrift für Physik*, Vol. 61(1-2), pp. 126-148, 1930.
- [85] Slater, J. C., “Note on Hartree's method”, *Physical Review*, Vol. 35(2), p. 210, 1930.
- [86] Szabo, A., & Ostlund, N. S., *Modern Quantum Chemistry: Introduction to Advanced Electronic Structure Theory*, Dover Press, New York, 1989.

- [87] Orio, M., Pantazis, D. A., & Neese, F., "Density functional theory", *Photosynthesis research*, Vol. 102(2-3), pp. 443-453, 2009.
- [88] Koch, W., Holthausen, M. C., Holthausen, M. C., *A Chemist's Guide to Density Functional Theory*, Second Edition, Wiley-VCH, Weinheim, 2001.
- [89] Jensen, F., *Introduction to Computational Chemistry*, John Wiley & Sons, West Sussex, 2007.
- [90] Thomas, L. H., "The calculation of atomic fields", *Mathematical Proceedings of the Cambridge Philosophical Society*, Vol. 23(05), pp. 542-548, 1927.
- [91] Fermi, E., "Application of statistical gas methods to electronic systems" *Accad. Lincei. Atti.*, Vol. 6, pp. 602-607, 1927.
- [92] Eschrig, H., *The fundamentals of DFT*, Teubner, Stuttgart, 1996.
- [93] Hohenberg, P., & Kohn, W., "Inhomogeneous electron gas", *Physical Review*, Vol. 136(3B), pp. B864-B871, 1964.
- [94] Kohn, W., & Sham, L. J., "Self-consistent equations including exchange and correlation effects", *Physical Review*, Vol. 140(4A), pp. A1133-A1138, 1965.
- [95] Lewars, E., *Computational Chemistry: Introduction to the Theory and Applications of Molecular and Quantum Mechanics*. Kluwer Academic Publishers, Dordrecht, 2003.
- [96] Cramer, C. J., *Essentials of Computational Chemistry: Theories and Models*, John Wiley & Sons, West Sussex, 2004.
- [97] Corminboeuf, C., Tran, F., Weber, J., "The role of density functional theory in chemistry: Some historical landmarks and applications to zeolites", *Journal of Molecular Structure: Theochem*, Vol. 762(1), pp. 1-7, 2006.
- [98] Argaman, N., & Makov, G., "Density functional theory: An introduction", *American Journal of Physics*, Vol. 68(1), pp. 69-79, 2000.
- [99] Slater, J. C., "A simplification of the Hartree-Fock method", *Physical Review*, Vol. 81(3), 385, 1951.

- [100] Yin, Z., *Microscopic Mechanisms of Magnetism and Superconductivity Studied from First Principle Calculations*, Ph.D. Thesis, University of California Davis, 2009.
- [101] Perdew, J. P., Burke, K., Ernzerhof, M., “Generalized gradient approximation made simple”, *Physical Review Letters*, Vol. 77(18), pp. 3865-68, 1996.
- [102] Perdew, J. P., Burke, K., Ernzerhof, M., “Errata: Generalized gradient approximation made simple”, *Physical Review Letters*, Vol. 78, p. 1396, 1997.
- [103] Becke, A. D., “Density-functional exchange-energy approximation with correct asymptotic behavior”, *Physical Review A*, Vol. 38(6), pp. 3098-100, 1988.
- [104] Perdew, J. P., “Density-functional approximation for the correlation energy of the inhomogeneous electron gas”, *Physical Review B*, Vol 33(12), pp. 8822-24, 1986.
- [105] Tao, J., Perdew, J. P., Staroverov, V. N., Scuseria, G. E., “Climbing the density functional ladder: Nonempirical meta-generalized gradient approximation designed for molecules and solids”, *Physical Review Letters*, Vol. 91(14), pp. 146401-4, 2003.
- [106] Hao, P., Sun, J., Xiao, B., Ruzsinszky, A., Csonka, G. I., Tao, J., Glindmeyer, S., Perdew, J. P., “Performance of meta-GGA Functionals on General Main Group Thermochemistry, Kinetics, and Noncovalent Interactions”, *Journal of Chemical Theory and Computation*, Vol. 9(1), pp. 355-363, 2012.
- [107] Becke, A. D., “A new mixing of Hartree-Fock and local density-functional theories”, *The Journal of Chemical Physics*, Vol. 98(2), pp. 1372-77, 1993.
- [108] Lee, C., Yang, W., Parr, R. G., “Development of the Colle-Salvetti correlation-energy formula into a functional of the electron density”, *Physical Review B*, Vol. 37(2), pp. 785-789, 1988.
- [109] Miehlich, B., Savin, A., Stoll, H., Preuss, H., “Results obtained with the correlation energy density functionals of Becke and Lee, Yang and Parr”, *Chemical Physics Letters*, Vol. 157(3), pp. 200-206, 1989.

- [110] Siegbahn, P. E., "The performance of hybrid DFT for mechanisms involving transition metal complexes in enzymes." *JBIC Journal of Biological Inorganic Chemistry*, Vol. 11(6), pp. 695-701, 2006.
- [111] Davidson, E. R., & Feller, D., "Basis set selection for molecular calculations", *Chemical Reviews*, Vol. 86(4), pp. 681-696, 1986.
- [112] Hehre, W. J., Stewart, R. F., & Pople, J. A., "Self-consistent molecular-orbital methods. 1. Use of gaussian expansions of slater-type atomic orbitals" *The Journal of Chemical Physics*, Vol. 51(6), pp. 2657-2664, 1969.
- [113] Collins, J. B., Schleyer, P. V. R., Binkley, J. S., Pople, J. A., "Self-consistent molecular orbital methods. XVII. Geometries and binding energies of second-row molecules. A comparison of three basis sets" *The Journal of Chemical Physics*, Vol. 64(12), pp. 5142-51, 1976.
- [114] Binkley, J. S., Pople, J. A., Hehre, W. J., "Self-consistent molecular orbital methods. 21. Small split-valence basis sets for first-row elements" *Journal of the American Chemical Society*, Vol. 102(3), pp. 939-947, 1980.
- [115] Gordon, M. S., Binkley, J. S., Pople, J. A., Pietro, W. J., Hehre, W. J., "Self-consistent molecular-orbital methods. 22 Small split-valence basis sets for second-row elements", *Journal of the American Chemical Society*, Vol. 104(10), pp. 2797-2803, 1982.
- [116] Ditchfield, R., Hehre, W. J., Pople, J.A., "Self-Consistent Molecular Orbital Methods. 9. Extended Gaussian-type basis for molecular-orbital studies of organic molecules" *Journal of Chemical Physics*, Vol. 54(2), p. 724, 1971.
- [117] Rassolov, V. A., Ratner, M. A., Pople, J. A., Redfern, P. C., Curtiss, L. A. "6-31G\* Basis Set for Third-Row Atoms", *Journal of Computational Chemistry*, Vol. 22(9), pp. 976-984, 2001.
- [118] McLean, A. D., & Chandler, G. S., "Contracted Gaussian basis sets for molecular calculations. I. Second row atoms, Z= 11-18", *The Journal of Chemical Physics*, Vol. 72, pp. 5639-5648, 1980.

- [119] Raghavachari, K., Binkley, J. S., Seeger, R., Pople, J. A., "Self-Consistent Molecular Orbital Methods. 20. Basis set for correlated wave-functions," *The Journal of Chemical Physics*, Vol. 72, pp. 650-54, 1980.
- [120] Dunning Jr, T. H., "Gaussian basis sets for use in correlated molecular calculations. I. The atoms boron through neon and hydrogen", *The Journal of Chemical Physics*, Vol. 90(2), pp. 1007-1023, 1989.
- [121] Schäfer, A., Horn, H., Ahlrichs, R., "Fully optimized contracted Gaussian basis sets for atoms Li to Kr", *The Journal of Chemical Physics*, Vol. 97(4), pp. 2571-2577, 1992.
- [122] Schäfer, A., Huber, C., Ahlrichs, R., "Fully optimized contracted Gaussian basis sets of triple zeta valence quality for atoms Li to Kr", *The Journal of Chemical Physics*, Vol. 100(8), pp. 5829-5835, 1994.
- [123] Gulde, R., Pollak, P., Weigend, F., "Error-Balanced Segmented Contracted Basis Sets of Double- $\zeta$  to Quadruple- $\zeta$  Valence Quality for the Lanthanides", *Journal of Chemical Theory and Computation*, Vol. 8(11), pp. 4062-4068, 2012.
- [124] Weigend, F., & Ahlrichs, R., "Balanced basis sets of split valence, triple zeta valence and quadruple zeta valence quality for H to Rn: Design and assessment of accuracy", *Physical Chemistry Chemical Physics*, Vol. 7(18), pp. 3297-3305, 2005.
- [125] Hill, J. G., "Gaussian basis sets for molecular applications", *International Journal of Quantum Chemistry*, Vol. 113(1), pp. 21-34, 2013.
- [126] The International Genetically Engineered Machine (iGEM), 2013.  
<http://2013.igem.org/Team:Freiburg/Project/modeling>
- [127] Ingle, J.D. Crouch, S.R, *Spectrochemical Analysis*, Printice Hall, Inc. New Jersey 1988.
- [128] Chang, R., *Basic Principles of Spectroscopy*, Mc Graw-Hill, New York, 1971.
- [129] Straughan, B. P., & Walker, S., *Spectroscopy, Vol. 2*. Wiley, New York, 1976.

- [130] Banwell, C. N., *Fundamentals of Molecular Spectroscopy*, Mc Graw-Hill, London, 1983.
- [131] Larkin, P., *Infrared and Raman Spectroscopy; Principles and Spectral Interpretation*. Elsevier, Waltham, 2011.
- [132] Frisch, A. (Ed.), *Gaussian 03*, Gaussian Inc., Wallingford CT, 2004.
- [133] Dennington, I. I. R, Keith T, Millam J, *GaussView, Version 4.1*, Semichem Inc., Shawnee Mission, KS, 2007.
- [134] Allouche, A. R., “Gabedit—A graphical user interface for computational chemistry softwares”, *Journal of Computational Chemistry*, Vol. 32(1), pp. 174-182, 2011.
- [135] Jamroz, M. H., Vibrational energy distribution analysis VEDA 4, 2004.
- [136] Jamróz, M. H., “Vibrational energy distribution analysis (VEDA): Scopes and limitations”, *Spectrochimica Acta Part A: Molecular and Biomolecular Spectroscopy*, Vol. 114, pp. 220-230, 2013.
- [137] Bohr, H. G., Jalkanen, K. J., Elstner, M., Frimand, K., & Suhai, S., “A comparative study of MP2, B3LYP, RHF and SCC-DFTB force fields in predicting the vibrational spectra of N-acetyl-L-alanine-N'-methyl amide: VA and VCD spectra” *Chemical physics*, Vol. 246(1), pp. 13-36, 1999.
- [138] Altun, A., & Thiel, W., “Combined quantum mechanical/molecular mechanical study on the pentacoordinated ferric and ferrous cytochrome P450cam complexes”, *The Journal of Physical Chemistry B*, Vol. 109(3), pp. 1268-1280, 2005.
- [139] Ebrahimi, H. P., Hadi, J. S., Abdalnabi, Z. A., Bolandnazar, Z., “Spectroscopic, thermal analysis and DFT computational studies of salen-type Schiff base complexes”, *Spectrochimica Acta Part A: Molecular and Biomolecular Spectroscopy*, Vol. 117, pp. 485-492, 2014.
- [140] Altun, A., Breidung, J., Neese, F., Thiel, W., “Correlated Ab Initio and Density Functional Studies on H<sub>2</sub> Activation by FeO<sup>+</sup>”, *Journal of Chemical Theory and Computation*, Vol. 10(9), pp. 3807-3820, 2014.



[141] EMSL Basis Set Exchange, 2015.

<https://bse.pnl.gov/bse/portal>

[142] Scott, A. P., & Radom, L., "Harmonic vibrational frequencies: an evaluation of Hartree-Fock, Møller-Plesset, quadratic configuration interaction, density functional theory, and semiempirical scale factors", *The Journal of Physical Chemistry*, Vol. 100(41), pp. 16502-13, 1996.

[143] Keresztury, G., *Raman Spectroscopy: Theory-Handbook of vibrational spectroscopy*, John Wiley & Sons, New York, 2002.

[144] Altun, A., Gölcük, K., Kumru, M., "Structure and vibrational spectra of p-methylaniline: Hartree-Fock, MP2 and density functional theory studies", *Journal of Molecular Structure: Theochem*, Vol. 637(1), pp. 155-169, 2003.

[145] Altun, A., Gölcük, K., Kumru, M., "Theoretical and experimental studies of the vibrational spectra of m-methylaniline", *Journal of Molecular Structure: Theochem*, Vol. 625(1), pp. 17-24, 2003.

[146] Tzeng, W. B., & Narayanan, K., "Structures and vibrations of p-methylaniline in the S 0 and S 1 states studied by ab initio calculations and resonant two-photon ionization spectroscopy", *Journal of molecular structure*, Vol. 446(1), pp. 93-102, 1998.

[147] Gross, K. C., Seybold, P. G., Hadad, C. M., "Comparison of different atomic charge schemes for predicting pKa variations in substituted anilines and phenols\*. *International Journal of Quantum Chemistry*, Vol. 90(1), pp. 445-458, 2002.

[148] Reed, A. E., Weinstock, R. B., Weinhold, F., "Natural population analysis", *The Journal of Chemical Physics*, Vol. 83(2), pp. 735-746, 1985.

[149] Milani, A., Tommasini, M., Castiglioni, C., "Atomic charges from IR intensity parameters: theory, implementation and application", *Theoretical Chemistry Accounts*, Vol. 131(3), pp. 1-17, 2012.

[150] Silverstein, R. M., Bassler, G. C., Morrill, T. C., *Spectrometric Identification of Organic Compounds*, Wiley, New York, 1981.

- [151] Karabacak, M., Karagöz, D., & Kurt, M., “FT-IR, FT-Raman vibrational spectra and molecular structure investigation of 2-chloro-4-methylaniline: A combined experimental and theoretical study”, *Spectrochimica Acta Part A: Molecular and Biomolecular Spectroscopy*, Vol. 72(5), pp. 1076-1083, 2009.
- [152] Ismael, A., Paixão, J. A., Fausto, R., Cristiano, M. L. S., “Molecular structure of nitrogen-linked methyltetrazole-saccharinates”, *Journal of Molecular Structure*, Vol. 1023, pp. 128-142, 2012.
- [153] Shoba, D., Periandi, S., Boomadevi, S., Ramalingam, S., Fereyduni, E., “FT-IR, FT-Raman, UV, NMR spectra, molecular structure, ESP, NBO and HOMO–LUMO investigation of 2-methylpyridine 1-oxide: A combined experimental and DFT study”, *Spectrochimica Acta Part A: Molecular and Biomolecular Spectroscopy*, Vol. 118, pp. 438-447, 2014.
- [154] Altun, A., & Aghatabay, N. M., “X-ray, vibrational spectra and density functional studies on cynacure” *Vibrational Spectroscopy*, Vol. 64, pp. 68-77, 2013.
- [155] Sas, E. B., Kurt, M., Karabacak, M., Poiyamozi, A., Sundaraganesan, N., “FT-IR, FT-Raman, dispersive Raman, NMR spectroscopic studies and NBO analysis of 2-Bromo-1H-Benzimidazol by density functional method” *Journal of Molecular Structure*, Vol. 1081, pp. 506-518, 2015.
- [156] Ataç, A., Yurdakul, Ş., Berber, S., “Synthesis, spectroscopy, and characterization of some bis-nicotinamide metal (II) dihalide complexes” *Spectrochimica Acta Part A: Molecular and Biomolecular Spectroscopy*, Vol. 81(1), pp. 684-689, 2011.
- [157] Sert, Y., Uçun, F., & Büyükata, M., “Conformational and vibrational analysis of 2-, 3-and 4-trifluoromethylbenzaldehyde by ab initio Hartree–Fock, density functional theory and Moller–Plesset perturbation theory calculations”, *Journal of Molecular Structure: Theocem*, Vol. 861(1), pp. 122-130, 2008.
- [158] Balachandran, V., Karpagam, V., Santhi, G., Revathi, B., Ilango, G., Kavimani, M., “Conformational stability, vibrational (FT-IR and FT-Raman) spectra and computational analysis of m-trifluoromethyl benzoic acid”, *Spectrochimica Acta Part A: Molecular and Biomolecular Spectroscopy*, Vol. 137, pp. 165-175, 2015.

[159] Bardakçı, T., Altun, A., Gölcük, K., Kumru, M., “Synthesis, structural, spectral (FT-IR, FT-Ra and UV-Vis), thermal and density functional studies on p-methylaniline complexes of Mn(II), Co(II), and Ni(II) bromides.” *Journal of Molecular Structure*, Vol. 1100, pp. 475-485, 2015.

[160] Soliman, S. M., & Massoud, R. A., “Theoretical studies of molecular structure and vibrational spectra of free, H-bonded and coordinated nicotinamide” *Computational and Theoretical Chemistry*, Vol. 988, pp. 27-33, 2012.

[161] Sundaraganesan, N., Ilakiamani, S., Joshua, B. D., “FT-Raman and FT-IR spectra, ab initio and density functional studies of 2-amino-4, 5-difluorobenzoic acid”, *Spectrochimica Acta Part A: Molecular and Biomolecular Spectroscopy*, Vol. 67(2), pp. 287-297, 2007.

## **APPENDIX A**

### **DECLARATION STATEMENT FOR THE ORIGINALITY OF THE THESIS, FURTHER STUDIES AND PUBLICATIONS FROM THESIS WORK**

#### **A.1 DECLARATION STATEMENT FOR THE ORIGINALITY OF THE THESIS**

I hereby declare that this thesis comprises my original work. No material in this thesis has been previously published and written by another person, except where due reference is made in the text of the thesis. I further declare that this thesis contains no material which has been submitted for a degree or diploma or other qualifications at any other university.

Signature:

Date: June 2, 2015

#### **A.2 FURTHER STUDIES**

Further studies related to this thesis work can be done in the following areas:

- (a) Providing a reference for future theoretical studies on transition metal-based drugs or large systems such as metalloproteins.
- (b) Development of new functionals and basis sets.

### A.3 PUBLICATIONS FROM THESIS WORK

#### Academic Journals

- Tayyibe Bardakçı, Ahmet Altun, Kurtuluş Gölcük, Mustafa Kumru “Synthesis, structural, spectral (FT-IR, FT-Ra and UV-Vis), thermal and density functional studies on p-methylaniline complexes of Mn(II), Co(II), and Ni(II) bromides.” *Journal of Molecular Structure*, Vol. 1100, pp. 475-485, 2015.
- Tayyibe Bardakçı, Mustafa Kumru, Ahmet Altun, “Molecular structures, charge distributions, and vibrational analyses of the tetracoordinate Cu(II), Zn(II), Cd(II), and Hg(II) bromide complexes of p-toluidine investigated by density functional theory in comparison with experiments” (**submitted.**)

## CURRICULUM VITAE

### CONTACT INFORMATION

Tayyibe Bardakçı

Şehremini Mah. Deniz Abdal Çeşmesi Sk. Özde Apt. No: 15/4 Fatih, İstanbul.

Email: [tayyibe.b@gmail.com](mailto:tayyibe.b@gmail.com)

Phone: +90-212-632-2811

### EDUCATION

- Ph.D., Fatih University - The Graduate School of Sciences and Engineering, Physics, 2010- June, 2015, Istanbul, Turkey.  
Thesis: *Density Functional Theory Studies on Molecular Structures and Vibrational Spectra of Transition Metal Complexes of Aniline Derivatives.*
- M.S., Fatih University - The Graduate School of Sciences and Engineering, Physics, 2007-2010, Istanbul, Turkey.  
Thesis: *Structural and Spectroscopic Investigation of Some Copper (II) Compounds.*
- Integrated B.S & M.S, Bogazici University, Physics Teaching, 2001-2007 Istanbul, Turkey.

### PROFESSIONAL EXPERIENCE

- Research Assistant, Department of Physics, Fatih University, Istanbul, Turkey, 2007-2015.
- Student Assistant, Department of Physics, Bogazici University, Istanbul, Turkey, 2004-2006.

### PUBLICATIONS

#### Academic Journals

- Tayyibe Bardakçı, Ahmet Altun, Kurtuluş Gölcük, Mustafa Kumru “Synthesis, structural, spectral (FT-IR, FT-Ra and UV-Vis), thermal and density functional studies on p-methylaniline complexes of Mn(II), Co(II), and Ni(II) bromides.” *Journal of Molecular Structure*, Vol. 1100, pp. 475-485, 2015.
- Mustafa Kumru, Tayyibe Bardakçı, Sadık Güner, "DFT calculations and experimental FT-IR, dispersive-Raman and EPR spectral studies of Copper (II) chloride complex with 3-amino-1-methylbenzene", *Spectrochimica Acta Part A: Molecular and Biomolecular Spectroscopy*, Vol. 123, pp. 187-193, 2014

- Tayyibe Bardakçı, Mustafa Kumru, Sadık Güner, "Molecular structure, vibrational and EPR spectra of Cu(II) chloride complex of 4-amino-1-methylbenzene combined with quantum chemical calculations", *Journal of Molecular Structure*, Vol. 1054-1055, pp. 76-82, 2013.
- Mustafa Kumru, Vesile Küçük, Tayyibe Bardakçı, "Theoretical and experimental studies on the vibrational spectra of 3-quinolinecarboxaldehyde", *Spectrochimica Acta Part A*, Vol. 90, pp. 28-34, 2012.

### **Conference Proceedings**

- Mustafa Kumru, Mustafa Kocademir, Tayyibe Bardakçı, "Combined experimental and theoretical studies on the vibrational and electronic spectra of 5-Quinolinecarboxaldehyde", 70th International Symposium on Molecular Spectroscopy, Champaign-Urbana, Illinois-USA Jun. 2015.
- Tayyibe Bardakçı, Mustafa Kumru, "Density Functional Calculations and Experimental Vibrational Spectral Studies of Free *m*-toluidine and its Copper(II) Chloride Complex", International Turkish Congress on Molecular Spectroscopy (TURCMOS 2013), Istanbul, Turkey, Sep. 2013,
- Mustafa Kumru, Mustafa Kocademir, Tayyibe Bardakçı, "Determination of structural and vibrational properties of 5-Quinolinecarboxaldehyde using experimental FT-IR, FT-Raman techniques and theoretical HF and DFT methods", 68th International Symposium on Molecular Spectroscopy, Columbus, Ohio, U.S.A, Jun. 2013,
- Tayyibe Bardakçı, Mustafa Kumru, "Experimental FT-IR, Dispersive Raman and Theoretical DFT Calculations on Cu(II) Chloride Complex of *P*-Toluidine", 68th International Symposium on Molecular Spectroscopy, Columbus, Ohio, U.S.A., Jun. 2013.
- Mustafa Kumru, Tayyibe Bardakçı, Levent Sarı, "Density functional theory study on molecular structure and vibrational spectra of *m*-methylaniline". 13th National Liquid Phase Physics Symposium, Tuzla, Istanbul, Turkey, Oct. 2009.

### **RESEARCH PROJECTS**

- "Investigations of Molecular Properties of Some  $ML_2X_2$  (M: Metal, L: Ligand, X: Halogen) Types Transition Metal Complexes Using DFT and Comparing with Experimental Results", University Research Fund, May 2014 – May 2015, Researcher, Amount: 7,500 TL.
- "Vibration analysis and molecular structure determination of quinoline derivatives via FT-IR, FT-Ra and dispersive Ra techniques", University Research Fund, Nov 2010-Jul 2012, Researcher, Amount: 15,000 TL.

### **REVIEWING ACTIVITIES**

- Spectrochimica Acta Part A: Molecular and Biomolecular Spectroscopy

**CERTIFICATES**

- Summer Course on “Molecular Dynamics Simulations of Proteins: Fundamentals and Applications”, TOBB University of Economics & Technology, June 22 – July 2, 2015, Ankara, Turkey.

**LANGUAGES**

- Turkish (Native)
- English (Fluent)

**TECHNICAL SKILLS**

- Operating systems: Windows, Linux, Mac OS X.
- Scientific Softwares: Gaussian 03, Gaussview, VEDA, Gabedit, IGOR.
- Performing parallel computations using linux clustered computers.
- Experience in laboratory processes and equipments including Infrared and Raman spectroscopy techniques.